Investigation of the Roles of Cullin-RING Ubiquitin Ligases in Polyglutamine Diseases

WONG, Kam Yan

A Thesis Submitted in Partial Fulfillment
of the Requirements for the Degree of
Doctor of Philosophy
in
Molecular Biotechnology

The Chinese University of Hong Kong
September 2010

ProQuest LLC
789 East Eisenhower Parkway
P.O. Box 1346
Ann Arbor, MI 48106-1346

Thesis/ Assessment Committee

Professor SHAW, Pang Chui (Chair)

Professor CHAN, Ho Yin Edwin (Thesis Supervisor)

Professor WAN, Chi Cheong (Committee Member)

Professor WONG, Ricky Ngok Shun (External Examiner)

DECLARATION

I declare that this thesis is entirely my own work except where otherwise stated, either in the form of citation of published work, or acknowledgement of the source of any unpublished materials.

Signed 

WONG, Kam Yan

ABSTRACT

Abstract of thesis entitled:

Investigation of the Roles of Cullin–RING Ubiquitin Ligases in Polyglutamine Diseases

Submitted by WONG, Kam Yan

for the degree of Doctor of Philosophy
at The Chinese University of Hong Kong in September 2010

Polyglutamine (polyQ) diseases describe a group of late-onset progressive neurodegenerative disorders which are caused by the *CAG* triplet repeat expansion in the coding region of disease genes. Such expansions result in expanded polyQ tracts in the disease proteins which confer neurotoxicity. To date, nine such diseases are reported including Huntington's disease and several types of spinocerebellar ataxias. Misfolding of polyQ proteins and formation of intracellular SDS-insoluble protein aggregates are closely associated with the toxicity of these diseases. In particular, impairment of the ubiquitin-proteasome system (UPS) which is responsible for protein degradation has been observed in polyQ diseases. Recently, ubiquitin ligases, which govern substrate specificity of the UPS, have gained huge attention in polyQ disease pathogenesis studies. In humans, cullin (Cul) proteins, including Cul1, 2, 3, 4 & 5, are integral components of a group of ubiquitin ligases called cullin-RING ubiquitin ligases (CRLs). Each CRL displays distinct substrate specificity through specific substrate receptors. Cullin proteins are evolutionarily conserved and *Cul* orthologues are found in the *Drosophila* genome. In the present study, it was found

that individual Culs displayed distinct effects on polyQ pathogenesis in *Drosophila* polyQ models. Particularly, it was found that Cul1 modulated polyQ-induced toxic phenotype. This modification was accompanied with an alteration in the ubiquitination level and SDS-solubility properties of expanded polyQ protein. Through genetic interaction studies and biochemical analyses, it is suggested that Cul1-based CRL specifically targets SDS-insoluble species of expanded polyQ protein for ubiquitination via selective recognition by CG2010 substrate receptor. On the other hand, it was found that expanded polyQ protein induced accumulation of CRL substrates in cells. Current data support a hypothesis that polyQ protein would impair the ubiquitin ligase activity of CRLs upon expansion of the polyQ domain, through interfering with neddylation of cullin and other uncharacterized mechanisms. Taken together, the present study identifies Cul1-CRL as a novel E3 ligase that modifies polyQ toxicity through modulating ubiquitination of expanded polyQ protein, and demonstrates a pathological mechanism by expanded polyQ protein through impairing CRL activity. These findings would lead to a better understanding of polyQ pathogenesis and give insights on developing treatments against polyQ diseases.

ABSTRACT (CHINESE VERSION)

多聚谷氨酰胺病描述一群於致病基因譯碼區內發生 *CAG* 三聯核酸重複序列擴增而引起的持發型、逐進神經退化性疾病。此序列擴增令致病蛋白帶有神經毒性。至今，已經有九種多聚谷氨酰胺病被發現，當中包括亨丁頓舞蹈症及個別類型的脊髓小腦共濟失調症。多聚谷氨酰胺延伸蛋白的錯誤摺疊及其於細胞內的聚集，與此病的毒性有密切的關係。特別是，負責蛋白質降解的泛蛋白－蛋白酶體系統，被發現在此病中出現障礙。最近，於泛蛋白－蛋白酶體系統（Ubiquitin Proteasome System）中負責操控受質選擇專一性的泛素黏合酶，在多聚谷氨酰胺病的病理機制研究中獲得重大的注目。人類 Cullin（Cul）蛋白（包括 Cul1、2、3、4 及 5）是 Cullin-RING 泛素黏合酶（CRL）的主要組成部分。每一種 CRL 透過特異的受質受體去展示不同的受質選擇專一性。Cullin 蛋白在進化過程中高度保守，在果蠅（*Drosophila*）的基因組內也有 *Cul* 的同源基因。此研究發現，個別的 Cul 蛋白對多聚谷氨酰胺病產生獨特的影響。尤其是，Cul1 蛋白調變多聚谷氨酰胺蛋白引發的病徵，而此修改與多聚谷氨酰胺延伸蛋白的泛素化程度的變動和其於十二烷基硫酸鈉（Sodium Dodecyl Sulfate）的溶解度特性的變動，一同出現。透過基因的交互作用考察和生物化學的分析，此研究揭示 Cul1-類 CRL 透過 CG2010 受質受體的選擇性識別，特異地泛素化多聚谷氨酰胺延伸蛋白的不溶解於十二烷基硫酸鈉的種類。另一方面，此研究發現，多聚谷氨酰胺延伸蛋白引致 CRL 受質累積於細胞內。現有的數據暗示多聚谷氨酰胺延伸蛋白，會透過干擾 Cullin 蛋白的 Nedd8 類泛素分子轉譯

後修飾及其他尚未被考究的機制，而妨害 CRL 的泛素黏合活動。總括而言，此研究發現，Cul1-類 CRL 是一種新的透過調變多聚谷氨酰胺延伸蛋白的泛素化而去修改多聚谷氨酰胺蛋白毒性的泛素黏合酶，以及演示了一種多聚谷氨酰胺延伸蛋白透過妨害 CRL 泛素黏合活動而致病的機制。這些發現會增加對多聚谷氨酰胺病的了解及幫助發展治療方法。

ACKNOWLEDGEMENTS

I would like express my deepest gratitude to my supervisor Dr. H. Y. Edwin Chan for his continuous support and patient guidance in completing this project and writing up the thesis.

Besides, I would like to express my gratefulness to all members of the Laboratory of *Drosophila* Research, CUHK, especially Dr. Priscilla W. M. Chan, Dr. Philip Y. Lam, Mr. Alan S. L. Wong, Ms. Gigi C. G. Choi, Ms. Angel Y. W. Lee, Mr. Eric C. M. Chan, Mr. Steve T. W. Lo, Ms. Shirley Chan, Ms. Aurora H. Y. Chan, Ms. Joyce Lau, Mr. Martin T. S. Fung, Mr. Koel Ko, Mr. T. C. Cheng, Mr. Y. P. Cheng, Ms. Teresa Fung, Mr. Frankie H. Tosi, Mr. C. C. Wu, Mr. Eric H. W. Luk. and all labmates at MMW509, in particular Dr. Wayne J. W. Zhou, Ms. Christine Tung, Ms. Peggy P. Y. Law, Mr. M. Y. Liu, Ms. Sheila S. K. Li for their technical assistance, helpful suggestions and kindness encouragement throughout my Ph.D. study.

Last but not least, special thanks are addressed to my family and friends whose warmest care and support strengthen me in completing this study.

LIST OF ABBREVIATIONS

Abbreviation	Term
AD	Alzheimer's Disease
Ago	Archipelago
ALS	Amyotrophic Lateral Sclerosis
APS	Ammonium Persulfate
ARtr	truncated Antrogen Receptor
bp	base-pair
Ca^{2+}	Calcium ion
cDNA	complementary Deoxyribonucleic Acid
CDS	coding sequence
CHIP	C-terminus of Hsp70 Interacting Protein
Ci	Cubitus interruptus
co-IP	co-immunoprecipitation
CRL	Cullin-RING Ubiquitin Ligase
CSN	COP9 signalosome
Cul	Cullin
CycE	Cyclin E
DA	dopaminergic
ddc	*dopa decarboxylase*
DEPC	Diethyl Pyrocarbonate
DM1	dorsomedial 1

DMEM	Dulbecco's Modified Eagle's Medium
DNA	Deoxyribonucleic acid
DNase	Deoxyribonuclease
dNTPs	Deoxynucleoside Triphosphates
dpe	days post-eclosion
dpi	days post-induction
DRPLA	Dentatorubropallidoluysian Atrophy
dsRNA	double-stranded RNA
DTT	Dithiothreitol
ECL	Enhanced Chemiluminescent
EDTA	Ethylenediaminetetraacetic Acid
eGFP	enhanced Green Fluorescent Protein
$GAL80^{ts}$	Temperature-sensitive GAL80
GFP	Green Fluorescent Protein
gmr	*glass multiple reporter*
H_2O	water
HA	Hemagglutinin
HCl	Hydrochloric Acid
HD	Huntington's Disease
HECT	homologous to E6-AP C-terminus
HEK	Human Embryonic Kidney
HEPES	4-(2-hydroxyethyl)-1-piperazineethanesulfonic acid
hpt	hours post-transfection
HRP	Horseradish Peroxidase

Hsp	Heat shock protein
IgG	Immunoglobulin G
KCl	Potassium Chloride
Keap1	Kelch-like ECH-associated protein 1
KH_2PO_4	Dipotassium Hydrogen Phosphate
LB	Luria-Bertani
LBA	Luria-Bertani-ampicillin
LD	Light-Dark
LRR	leucine-rich repeat
$MgCl_2$	Magnesium Chloride
$MgCl_2.6H_2O$	Magnesium Chloride Hexahydrate
MJD	Machado-Joseph Disease
Na_2HPO_4	Disodium Hydrogen Phosphate
NaCl	Sodium Chloride
NaF	Sodium Fluoride
Nedd8	Neural precursor cell expressed developmentally downregulated 8
Neh2	Nrf2-ECH homology 2
NIG	National Institute of Genetics
NP-40	Nonidet P-40
Nrf2	NF-E2-related factor-2
nt	nucleotide
PBS	Phosphate-Buffered Saline
PD	Parkinson's Disease

PolyQ	Polyglutamine
PVDF	Polyvinylidene Fluoride
Roc1	Regulator of cullins 1
RNA	Ribonucleic Acid
RNAi	RNA interference
RNase	Ribonuclease
RNI	RNase inhibitor
RT-PCR	Reverse Transcription-Polymerase Chain Reaction
S.E.M.	Standard Error of the Mean
SBMA	Spinobulbar Muscular Atrophy
SCA	Spinocerebellar Ataxia
SCA3fl	full-length ataxin-3
SCA3tr	truncated ataxin-3
SCOP	Structural Classification of Proteins
SDS	Sodium Dodecyl Sulfate
SDS-PAGE	Sodium Dodecyl Sulfate-Polyacylamide Gel Electrophoresis
siRNA	small interfering RNA
Slmb	Slimb
Taq	*Thermus aquaticus*
TBE	Tris-Borate-EDTA
TBS	Tris-Buffered Saline
TBST	Tris-Buffered Saline-Tween-20
TEMED	N,N,N',N'-Di-(dimethylamino)ethane
tim	*timeless*

UAS	Upstream Activation Sequence
Ub^{WT}	wild-type ubiquitin
UPS	Ubiquitin proteasome system
VDRC	Vienna *Drosophila* RNAi Center
YFP	Yellow Fluorescent Protein
α-synuclein^{WT}	wild-type alpha-synuclein
β-cat	beta-catenin
β-TrCP	beta-Transducin repeat Containing Protein

LIST OF TABLES

LIST OF FIGURES

TABLE OF CONTENTS

Chapter 1 Introduction

1.1 Neurodegenerative diseases

Neurodegenerative diseases are neurological diseases involving neurodegeneration [1, 2]. Common neurodegenerative diseases include Alzheimer's disease (AD) [3], Parkinson's disease (PD) [4], amyotrophic lateral sclerosis (ALS) [5], prion disease [6] and several types of triplet repeat expansion diseases [7] including polyglutamine (polyQ) diseases. Neurodegenerative diseases are progressive in nature and strike most often after midlife [8]. In terms of diagnosis, despite of the distinctive pathological conditions in different neurodegenerative diseases, cognitive impairment and loss of mobility are two major symptoms in neurodegenerative diseases patients [1]. In terms of neuropathology, neurodegenerative diseases are highly associated with deposition of proteinaceous aggregates in neurons and neuronal deterioration in selective areas of the brain [9, 10]. Mechanisms of neuronal deterioration include impairment of the protein degradation system [11], mitochondrial dysfunction [12] and dysregulation of axonal transport [13].

1.2 Polyglutamine diseases

Polyglutamine diseases describe a group of neurodegenerative diseases caused by expansion of *CAG* triplet repeats beyond a certain threshold in the coding region

of the disease genes [14]. Such expansions result in expanded polyQ tracts in the disease proteins [14]. Expanded polyQ proteins are misfolded and prone to aggregate [14]. To-date, nine neurodegenerative diseases are known to be caused by such expansions, namely Huntington's disease (HD), dentatorubral pallidoluysian atrophy (DRPLA), spinal and bulbar muscular atrophy (SBMA), and spinocerebellar ataxia (SCA) types 1, 2, 3, 6, 7 and 17 (Table 1) [14-16]. SCA3 is also named as Machado-Joseph Disease (MJD).

Table 1. Polyglutamine diseases currently identified and their respective characteristics

Disease	Gene locus	Protein product	Normal range of *CAG* repeat	Expanded range of *CAG* repeat	Protein subcellular localization	Brain regions affected
HD	4p16.3	Huntingtin	6-34	36-121	Cytoplasm	Striatum, cerebral cortex
SBMA	Xq11-12	Androgen receptor	9-36	38-62	Nuclear and cytoplasm	Anterior horn and bulbar neurons, dorsal root ganglia
DRPLA	12q	Atrophin-1	6-36	49-84	Cytoplasm	Cerebellum, cerebral cortex, basal ganglia, Luys body
SCA1	6p22-23	Ataxin-1	6-44	39-82	Nuclear	Cerebellar Purkinje cells, dentate nucleus, brain stem
SCA2	12q23-24	Ataxin-2	15-31	36-63	Cytoplasm	Cerebellar Purkinje cells, brain stem, fronto-temporal lobe
SCA3/ MJD	14q24.3-31	Ataxin-3	12-41	62-84	Cytoplasm	Cerebellar dentate neurons, basal ganglia, brain stem, spinal cord
SCA6	19p13	Ataxin-6	4-18	21-33	Cell membrane	Cerebellar Purkinje cells, dentate nucleus, inferior olive
SCA7	3p12-p21.1	Ataxin-7	4-35	37-306	Nuclear	Cerebellum, brain stem, macula, visual cortex
SCA17	6q27	Ataxin-17	25-42	47-63	Nuclear	Cerebellar Purkinje cells

(Modified from [15, 17].)

Similar to other neurodegenerative diseases, polyQ diseases are adult-onset and progressive in nature [14, 15]. There are accumulation of disease protein aggregates and neuronal dysfunction [14, 15]. All polyQ diseases, except for SBMA, are autosomal dominantly inherited [14, 15]. It is interesting to note that the number of *CAG* repeat, once beyond the threshold, is proportional to the severity of the disease and inversely proportional to the age-of-onset [15]. For the majority of polyQ diseases, the threshold of *CAG* repeat for disease development is around 40 (Table 1) [15].

The molecular pathogenesis of polyQ diseases can be illustrated by both the loss-of-function and the gain-of-function mechanisms [18]. Regarding the loss-of-function mechanism, polyQ proteins have intrinsic function in cells [19]. It is hypothesized that expansion of the polyQ domains would abolish the normal functions of polyQ proteins [19] . In particular, it was found that the function of huntingtin, the disease protein of HD, is related to neuronal survival and brain development [20]. Upon expansion of the polyQ domain, the activity of huntingtin was reduced to 50% [21, 22].

Remarkably though, merely loss-of-function cannot explain the common cellular pathologies, such as protein aggregation and neuronal dysfunction, observed among different polyQ diseases. Indeed, by comparative studies between various polyQ diseases [15], by removing the non-polyQ region of the polyQ proteins [23, 24]

and the use of irrelevant proteins fused to polyQ domains [25-27], it was demonstrated that expansion of polyQ domain confers polyQ proteins a gain-of-function toxicity [28]. The pathological mechanisms involve polyQ protein conformational change and aggregation [29, 30], aberrant interactions with and recruitment of important cellular proteins to aggregates [31, 32], interference with transcription [33, 34], mitochondrial dysfunction [35], impairment of protein degradation machineries [11], intervention with axonal transport [36], activation of caspases, disturbance of intracellular Ca^{2+} homeostasis [37] and genotoxic stress [28, 38, 39].

Not until recently, it is suggested the *CAG* repeats in the non-coding region of RNA of the disease genes also contributes to toxicity in polyQ diseases [40-42]. Investigations on the pathological mechanisms of this RNA toxicity are under intense investigations.

1.3 Protein quality control in polyglutamine diseases

The presence of intraneuronal inclusion bodies is a major hallmark of polyQ diseases, and they are mainly composed of the corresponding disease proteins [15, 43]. Expanded polyQ proteins have been demonstrated to undergo intracellular aggregation in transfected cells, transgenic animal models and polyQ diseases patients' neuronal tissues [10]. It is suggested that expansion of the polyQ domain triggers a conformational transition in the polyQ proteins and results in a β-sheet-rich

structure [44]. Expanded polyQ proteins with this misfolded conformation are prone to aggregate into amyloid-like fibrils and thus accumulate as microscopic-visible inclusion bodies in neurons [45]. These inclusion bodies are heterogeneous and dynamic in the sense that the composing expanded polyQ proteins are undergoing conformational transition from monomers, oligomers, fibrils to aggregates along disease development [46, 47] (Figure 1.1). It is generally believed that certain expanded polyQ protein species are toxic [48-51] (Figure 1.1). Previously, our laboratory identified a toxic role of SDS-insoluble expanded polyQ protein oligomers in polyQ pathogenesis [52]. No matter what the true toxic species are, preventing misfolding of expanded polyQ proteins and eliminating misfolded expanded polyQ proteins have been general accepted to help reduce polyQ toxicity [53].

In response to misfolded proteins, the neuron has two protein quality control systems (Figure 1.2). First, the cell attempts to refold misfolded proteins by molecular chaperones [54, 55]. Heat shock protein (Hsp) 70 is a well-known example of molecular chaperones. Besides assisting folding of newly synthesized unfolded polypeptides, Hsp70 also binds to misfolded proteins and keeps them in soluble conformation. Its protein folding activity is further enhanced by co-chaperone Hsp40. Both chaperones and co-chaperones including the Hsp70/Hsp40 pairs were found in polyQ protein aggregates reflecting their efforts in counteracting polyQ protein aggregation [56-58]. Besides, overexpression of *Hsp70* was reported to enhance polyQ protein solubility, reduce aggregation and suppress

Figure 1.1

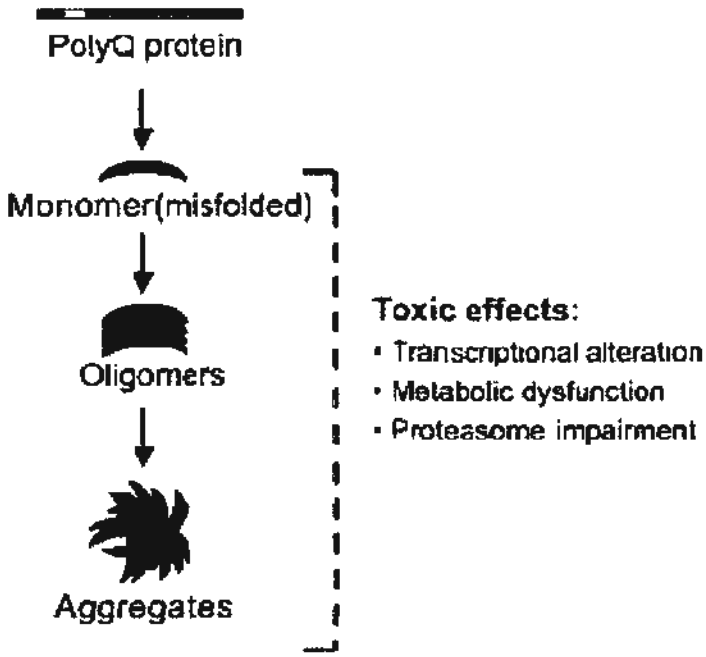

Figure 1.1. The conformational transition of expanded polyQ proteins.

Expanded polyQ proteins undergo conformational transition from monomers, oligomers to aggregates. Some of these species are suggested to cause cytotoxicity. Yellow box: the expanded polyQ domain; red object: the expanded polyQ protein (adapted from [28]).

Figure 1.2

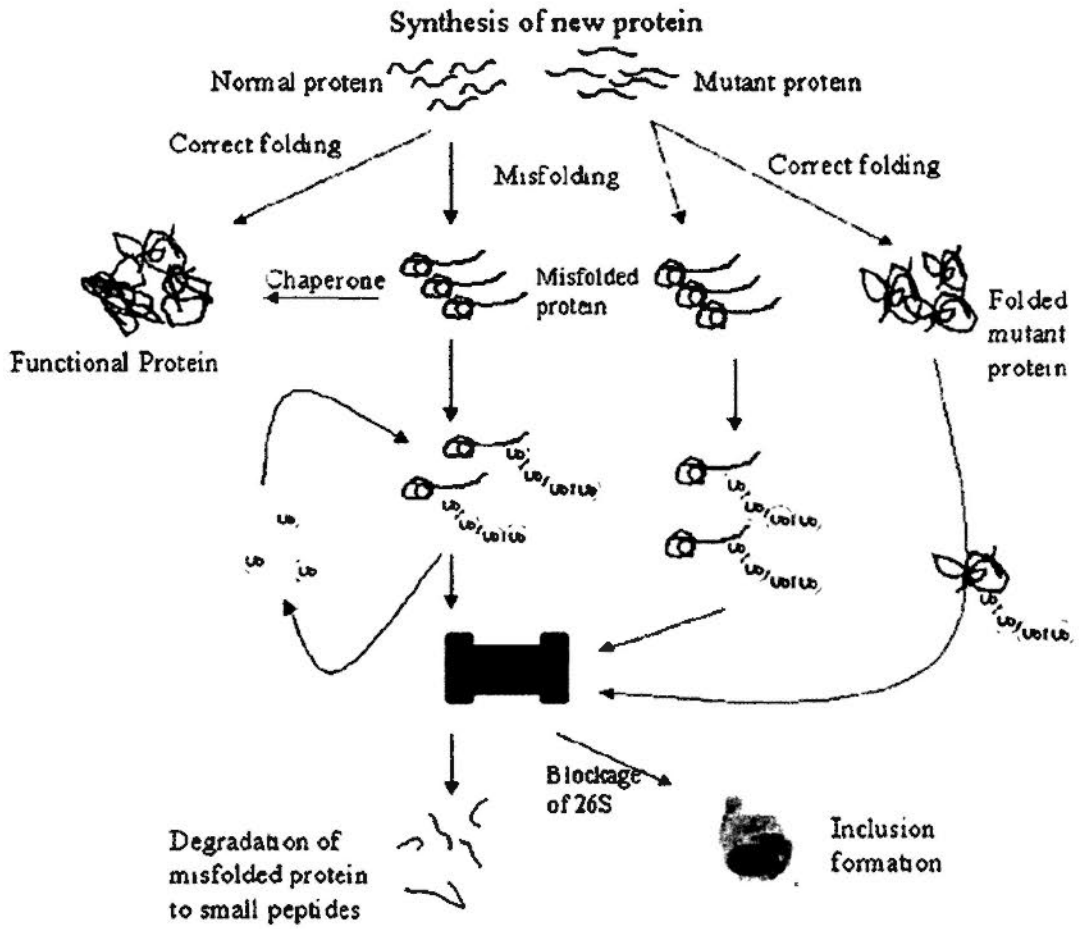

Figure 1.2. Refolding and proteasomal degradation of misfolded expanded proteins.

Misfolded expanded polyQ proteins are either refolded by chaperones or degraded by the 26S proteasome. Failure of the above would lead to accumulation of aggregates as inclusion bodies in cells. Abbreviation: Ub: ubiquitin (adapted from [59]).

polyQ toxicity in mammalian cultured cells and various transgenic animal polyQ models [23, 60, 61].

Failure of refolding misfolded proteins would trigger the second control system or the protein degradation pathways. The ubiquitin proteasome system (UPS) is the major protein destruction machinery in most cells including neurons [59, 62]. The UPS helps in maintaining cellular homeostasis by selective degradation of targeted misfolded proteins in both cytoplasm and nucleus [63]. It involves the covalent attachment of ubiquitin, a small (76 amino acids in length) and highly conserved protein [64], to substrate proteins to act as a signal for targeted degradation (Figure 1.3). Initially, an E1 ubiquitin-activating enzyme activates the C-terminal carboxyl group of ubiquitin. Next, E2 ubiquitin-conjugating enzyme transfers the activated ubiquitin to the substrate protein. This substrate protein is previously bound specifically by the E3 ubiquitin ligase which controls substrate specificity in the UPS. Then E3 ubiquitin ligase catalyzes the final covalent attachment of the ubiquitin to the lysine residue of the substrate protein. These steps repeat until a polyubiquitin chain is formed on the substrate protein, which is then recognized and finally degraded by the proteasome [65, 66]. In various polyQ diseases studies, the presence of UPS components in polyQ protein aggregates suggests that the UPS has attempted to degrade misfolded polyQ proteins. However, the degradation of misfolded polyQ proteins is inefficient for some reasons and so UPS components themselves also accumulate in the aggregates [67].

Figure 1.3

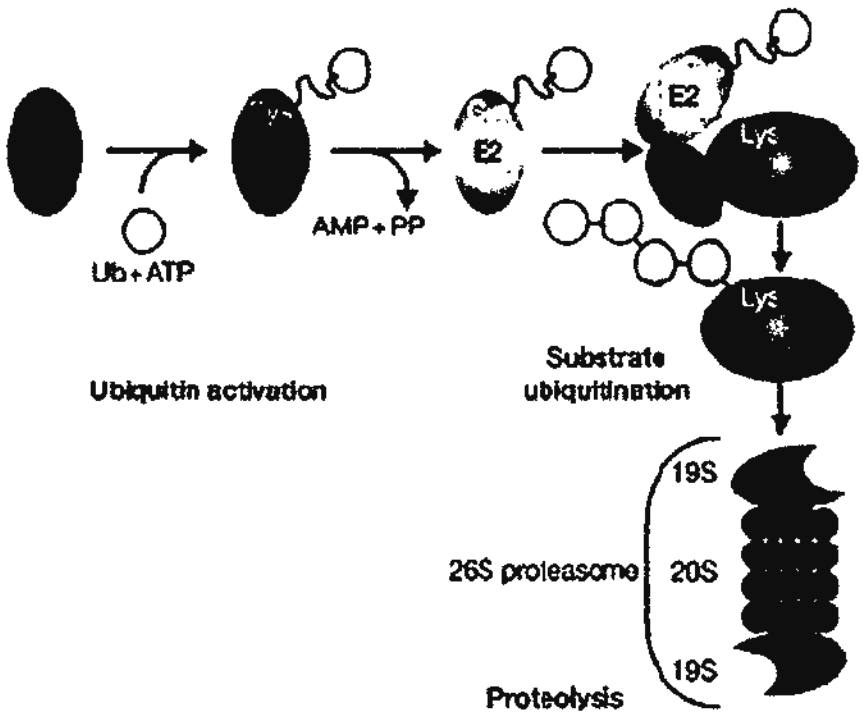

Figure 1.3. A typical UPS pathway.

In UPS, ubiquitin (in yellow) is first activated by E1 activation enzyme (in blue). Activated ubiquitin is then transferred to the E2 conjugation enzyme (in orange). E3 ubiquitin ligase (in green) recruits the specific substrate protein (in dark brown) to the ubiquitin-loaded E2 and facilitates the conjugation of ubiquitin to a lysine residue on the substrate protein. This process repeats resulting in a polyubiquitin chain attached to the substrate protein. The ubiquitinated substrate protein is then recognized and degraded by the 26S proteasome. Abbreviations: ATP: adenosine triphosphate; AMP: adenosine monophosphate; PP: inorganic phosphate; Ub: ubiquitin; Cys: cysteine; Lys: lysine (adapted from [68]).

1.4 Implication of E3 ubiquitin ligases on polyQ diseases

It becomes crucial to figure out why polyQ proteins are not degraded efficiently. The most obvious clue lines in the substrate recognition machinery of UPS. Among all the UPS components, E3 ligases play key roles in conferring substrate specificity, as they bind the target proteins specifically and serve as recognition elements for the proteasome [65]. Recently, E3 ubiquitin ligases have gained huge implication in neurodegenerative diseases involving misfolded proteins including polyQ diseases [69].

Based on their protein-interacting domains, E3 ubiquitin ligases can be categorized into three groups, and they are the U-box E3s, homologous to E6-AP C-terminus(HECT)-domain E3s and the RING-finger E3s [65]. Members of each group have been implicated in polyQ diseases. The C-terminus of Hsp70 interacting protein (CHIP) is an example from the U-box E3s. It has dual functions as both a co-chaperone with the N-terminal Hsp70/Hsp90 interacting domain and an E3 ligase with the C-terminal U-box domain [70-73]. It was found that, in transfected cells and a fly model of SCA1, overexpression of *CHIP* promoted ubiquitination and degradation of polyQ protein and suppressed toxicity [74]. HD transgenic mice that were deficient in CHIP displayed enhanced disease phenotype [75]. E6-AP is the founding member of HECT-domain E3 ubiquitin ligases [65, 76]. It has been demonstrated, in cultured cells and transgenic mice model, that E6-AP promoted degradation of polyQ protein, and suppressed polyQ protein aggregation and

polyQ-induced cell death [77]. Parkin is categorized as a RING-finger E3 ubiquitin ligase by the existence of two RING-finger motifs at its C-terminus [78, 79]. It was shown that Parkin induced ubiquitination and degradation of an expanded polyQ protein, reduced aggregation and cytotoxicity mediated by this expanded polyQ protein in cultured cells [80].

1.5 Cullin-RING ubiquitin ligases

Cullin-RING ubiquitin ligases (CRLs) is a subgroup of the RING-finger E3 ubiquitin ligases [81, 82]. CRLs are modular in structure with cullin proteins acting as scaffolds for the complex assembly [81, 82] (Figure 1.4). In a typical CRL complex, the N-terminus of cullin binds with an adaptor protein which in turn binds with a substrate receptor that recruits the protein substrate [81, 82]. Meanwhile, the C-terminus of cullin interacts with the RING-domain protein named Regulator of cullins 1 (Roc1) that recruits the ubiquitin-loaded-E2 [81, 82]. The resulting close proximity between substrate protein and ubiquitin-loaded-E2 hence promotes substrate ubiquitination [81, 82].

The ubiquitin ligase activity of CRLs is regulated by neddylation and deneddylation of cullins [81, 83, 84]. In neddylation, the neural precursor cell expressed developmentally downregulated 8 (Nedd8) [85] is conjugated to the conserved lysine residue on cullins. This potentiates the recruitment of activated E2s through Roc1 to form active CRLs [86]. Mutation of this conserved lysine residue

Figure 1.4

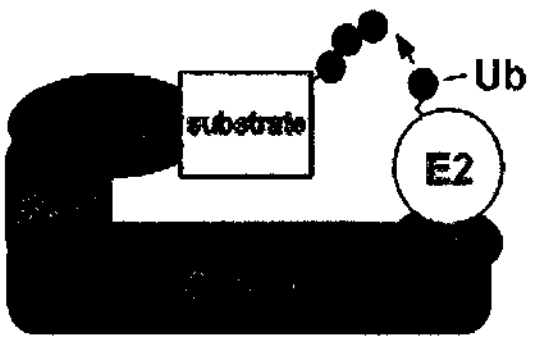

Figure 1.4. Schematic diagram showing a Cul1-based CRL.

Cul1 (in green) acts as the scaffold of Cul1-based CRL. N-terminus of Cul1 binds to Skp1 adaptor protein (in blue) which in turn binds to an F-box substrate receptor (in pink). C-terminus of Cul1 binds to Rbx1/Roc1 RING protein (in red) which in turn binds to an ubiquitin (in purple)-loaded E2 (in orange; adapted from [87]).

has been shown to inhibit the formation of active CRLs [86]. However, neddylated cullins are unstable and short-lived [86]. Deneddylation serves to detach the conjugated Nedd8 from cullins and recycle the unstable neddylated cullins into stable unneddylated ones [86, 88]. Besides, it is found that substrate receptors often undergo autoubiquitination and subsequent proteasomal degradation [89, 90]. Deneddylation also serves to prevent autoubiquitination of substrate receptors and therefore stabilizes the CRL complex [91]. Deneddylation is carried out by COP9 signalosome (CSN), in which the CSN5 subunit possess isopeptidase activity which is responsible for the cleavage of conjugated Nedd8 [92].

In metazoans, there are five main cullins (Cul1-5) which are conserved from *Drosophila* to humans [93]. Different cullins bind with different adaptor proteins which in turn associate with different groups of substrate receptors [81]. The number of substrate receptors is large [81]. So far, about 600 putative substrate receptors have been identified in humans [81]. This large figure confers diversity and substrate specificity to CRLs. Indeed, by selective degradation of specific substrate, CRLs are involved in many cellular pathways [81]. These include but are not limited to cell cycle, signal transduction, transcription, protein quality control, DNA replication, viral modulation and circadian rhythm [81].

Given the large number of substrate receptors present in cells, there is a possibility that certain substrate receptors could recognize expanded polyQ proteins

and target them to ubiquitination through CRLs. In line with this postulation, it was demonstrated that overexpression of a substrate receptor of Cul1-based CRL named *FBXO25* reduced aggregation of expanded polyQ protein [94]. More recently, it was reported that knock-down the expression of *cul-1* and *cul-2*, the worm homologs of *Cul1* and *Cul2* respectively, enhanced polyQ degenerative phenotypes in *Caenorhabditis elegans* [95]. These findings suggest that certain CRLs are involved in polyQ protein aggregation and toxicity.

On the other hand, it was observed that Nedd8 accumulated in polyQ protein aggregates [96, 97]. This might affect neddylation of cullins, limit formation of active CRLs and in turn disturb CRLs-mediated proteolysis. Moreover, according to the previous findings from cultured cells in our laboratory, by the use of degron reporters which mimicked specific endogenous substrates of individual CRLs [98, 99], it was found that polyQ protein caused accumulation of Cul1- and Cul3-based CRLs degron reporters upon expansion of polyQ domain (C. C. Wu and H. Y. E. Chan, unpublished observations). This suggests that expanded polyQ proteins impair the activity of Cul1- and Cul3-based CRLs. This impairment may eventually disturb the numerous cellular pathways regulated by Cul1- and Cul3-based CRLs.

1.6 Modeling polyglutamine diseases in *Drosophila*

For a decade, various models from cultured cells, transgenic *Caenorhabditis elegans, Drosophila melanogaster* to mouse models have been used to reveal the

pathological mechanisms of polyQ diseases [100, 101]. Among all, *Drosophila melanogaster*, or fruit fly, stands out as one excellent model for a number of reasons [102-108]. Firstly, the short generation cycle (around 10 days at 25°C) and the large number of progeny allow large-scale genetic analysis and screening. Secondly, well-studied physiology and anatomy enable detailed examinations of degenerative phenotypes. Moreover, amenability to genetic manipulations and availability of genome-wide collections of transgenic fly stocks facilitate extensive genetic studies [109, 110]. The most important is that the fundamental biology of neurodegeneration is conserved from fly to humans [111, 112]. Over 60 percent of human disease genes have homologs in fly [113]. All these make *Drosophila* a desirable model for the studies of polyQ diseases.

Although the disease proteins in polyQ diseases are expressed in every cell-type, tissue-specific degenerative phenotypes are observed in polyQ patients. To mimic the tissue-specific nature of the pathological conditions in polyQ patients, restricted regional expression of disease transgenes is preferred. This spatial control of transgene expression is conducted by *GAL4/UAS* bipartite system [114-116] (Figure 1.5). In this system, there are two types of transgenic fly line. One line, referred as the *GAL4* driver line, bears the yeast transcriptional activator gene *GAL4* gene placed downstream of a tissue-specific promoter [114-116]. The other line, referred as the *UAS* line, carries the transgene placed downstream of the yeast *upstream activator sequence* (*UAS*) binding site [114-116]. After crossing the *GAL4* line and the *UAS*

Figure 1.5

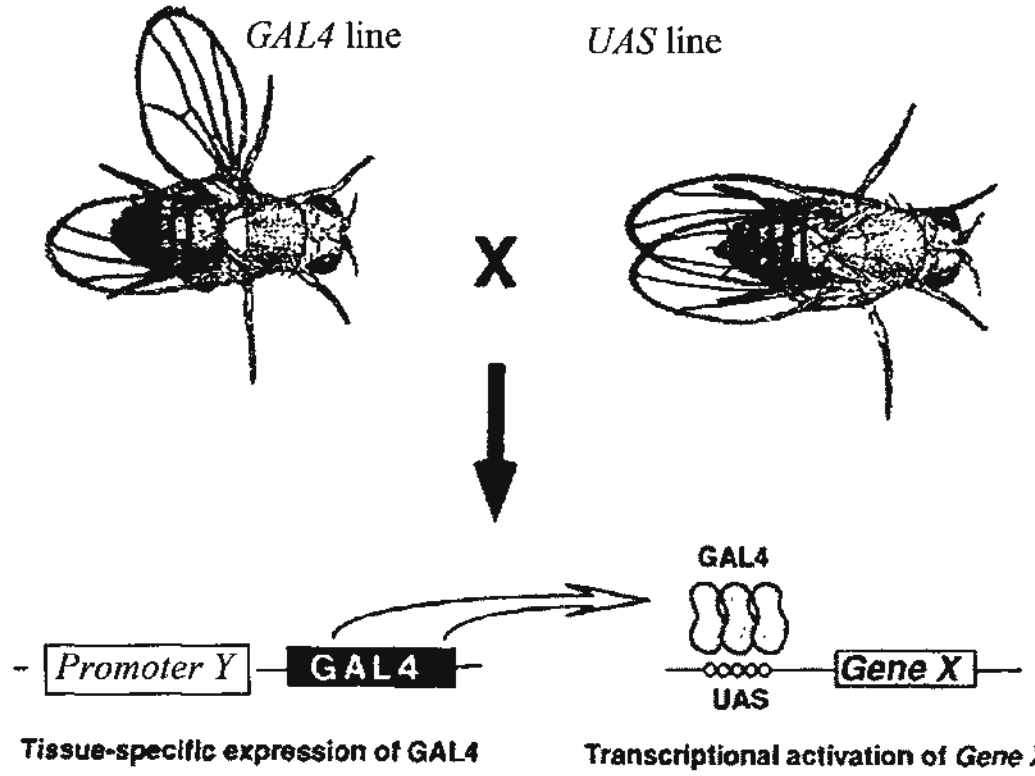

Figure 1.5. Directed expression of transgene in specific tissue by *GAL4/UAS* bipartite system.

When the *GAL4* line is crossed with the *UAS* line, the progeny expresses the GAL4 protein (in grey) in the specific tissue under the control of the promoter (*Promoter Y*). The GAL4 protein then activates expression of the transgene under *UAS* control (*Gene X*; adapted from [114]).

line together, transcriptional activator *GAL4* gene is expressed in designated tissues in the progeny [114-116]. The resulting transcriptional activator GAL4 protein then binds to the *UAS* binding site and directs the expression of the downstream transgene in the corresponding tissues [114-116].

This *GAL4/UAS* bipartite system has been extensively used to express transgenes of polyQ diseases in designated tissues for studying polyQ degenerative phenotypes in *Drosophila*. For example, SCA3 was first modeled in *Drosophila* by expressing a transgene encoding for a truncated form of ataxin-3 using *glass-multiple reporter* (*gmr*)-*GAL4* driver [117]. In *gmr-GAL4* driver line, multiple copies of *glass* gene promoter sequence were placed upstream of the *GAL4* gene. This driver line directs the expression of *truncated ataxin-3* transgene in eye cells posterior to the morphogenetic furrow including the photoreceptor neurons and the eye pigment cells [118]. The expression of the expanded *truncated ataxin-3* in the fly eyes induced late-onset, progressive degenerative phenotypes such as collapse of internal retinal morphology and loss of pigmentation [117]. Expanded truncated ataxin-3 protein forms microscopic visible aggregates in both nucleus and cytoplasm [117]. The severity of degenerative phenotypes and the earliness of onset of protein aggregation positively associate with the length of polyQ repeats and the expression level of expanded polyQ protein [117]. Besides SCA3, other polyQ diseases have also been modeled in *Drosophila*. These include HD [119], DRPLA [120], SBMA [24, 121], SCA1 [122], SCA2 [123], SCA7 [124] and SCA8 [125].

In short, due to the nature of the model, the conservation in neurobiology between humans and *Drosophila*, and the recapitulation of polyQ degenerative phenotypes upon expression of polyQ disease genes, *Drosophila* has emerged as an attractive model for studying polyQ diseases.

1.7 Hypothesis and aims of study

Quality control systems which deal with misfolded proteins including polyQ proteins are essential for cell survival. Therefore, it is believed that multiple E3 ubiquitin ligases are involved in the ubiquitination and subsequent degradation of the misfolded polyQ proteins [69]. The findings on CHIP, E6-AP and Parkin well support this hypothesis. Therefore, it is imperative to explore more E3 ubiquitin ligases which are possibly involved in polyQ diseases.

In the present study, it is hypothesized that certain CRLs are involved in the degradation of polyQ protein and would modify polyQ toxicity. On the other hand, as CRLs regulate numerous cellular pathways, it is hypothesized that expanded polyQ protein interferes with the cellular pathways involving CRLs and thus confer toxicity.

This project aimed to investigate the roles of CRLs in polyQ pathogenesis using

Drosophila polyQ models. Particularly, there are three specific aims:

1. to study the involvement of CRLs in polyQ toxicity (Chapters 3 - 5);
2. to study the involvement of CRLs in the biochemical properties of expanded polyQ protein (Chapters 3 - 5);
3. to study the effect of expanded polyQ protein on CRLs activity (Chapter 6)

1.8 Long-term significance

PolyQ diseases are a group of neurodegenerative diseases in which protein misfolding is a central issue. In the past decade, E3 ubiquitin ligases have gained large respect in the studies of this type of diseases. Increasing E3 ubiquitin ligases are identified to be involved in polyQ diseases. Through this project, the roles of CRLs in polyQ pathogenesis were revealed in depth. The results provide insights on how the cellular protein quality control systems involving E3 ubiquitin ligases such as CRLs target misfolded polyQ proteins, and enhance our understanding on the possible mechanisms of polyQ pathogenesis including the dysregulation of CRLs activity. Moreover, these findings may open up a new attractive therapeutic avenue for polyQ diseases. Therefore, in the long run, this study lays a solid foundation on the understanding of the physiology of polyQ diseases and an economic significance in developing therapeutic potentials.

Chapter 2 Materials and Methods

2.1 Maintenance of *Drosophila* culture

Fly stocks and genetic crosses were raised on standard cornmeal medium supplemented with dry yeast (section 2.14.1) in cotton-plugged plastic vials and kept in incubators (LMS Ltd., UK) maintained at 18°C, 21°C or 25°C as specified. To collect virgin females for genetic crosses, adult flies were first removed from the vials and virgin females were collected within 8 hr at 25°C or 16 hr at 18°C. For each genetic cross, approximately 6 virgin females and 4 males of the desired genotypes were put in the same vial.

2.2 Phenotypic assays for toxicity in fly

2.2.1 Examination of adult external eye depigmentation

The eyes of adult fly with specified age and genotype were examined under an Olympus SZX-12 stereomicroscope (Olympus, Japan). External eye images were captured using a SPOT Insight CCD camera (Diagnostic Instruments Inc., USA) operated with the SPOT Advanced software (version 4.1; Diagnostic Instruments Inc., USA).

2.2.2 Deep pseudopupil assay of adult retinal degeneration

Adult flies with specified age and genotype were decapitated. The heads were put on a glass slide with the antennae facing upward and the ocelli facing forward and immersed in a drop of immersion oil (Nikon Instruments Inc., USA). To prepare the glass slide, two glass cover-slips were placed side-by-side with a space in

between where fly heads were put. Another glass cover-slip was then placed on top of the heads. Ommatidia were examined under an Olympus CX31 light microscope (Olympus, Japan) using a 60X oil objective. Ommatidia images were captured using a SPOT Insight CCD camera (Diagnostic Instruments Inc., USA) operated with the SPOT Advanced software (version 4.1; Diagnostic Instruments Inc., USA).

2.2.3 Locomotor activity assay

Sixteen adult male flies with specified age and genotype were collected and individually transferred to cotton-plugged small glass tubes (Trikinetics Inc., USA) containing sucrose medium (section 2.14.1). The diameter of the glass tube was just slightly larger than the size of an adult fly. The glass tubes were loaded horizontally onto the Trikinetics *Drosophila* Activity Monitors (Trikinetics Inc., USA) [126]. The flies were maintained at 25°C in light-dark (LD) cycle with light on from 06:00 to 17:59 and light off from 18:00 to 05:59. Each time when the fly walked across the glass tube, a signal was generated and recorded by a signal-processing box (Trikinetics Inc., USA). The locomotor activity data were collected and analyzed by the DAM system (Trikinetics Inc., USA). This system expressed the data in terms of the number of events of walking across the glass tube within one min for each fly. The total locomotor activity within 30 min was summed up throughout 24 hr for each fly. An average locomotor activity within 30 min time period throughout 24 hr was then obtained from 16 flies. The averaged locomotor activity of each 30 min time period throughout 24 hr was then averaged from 3 consecutive days to get the circadian locomotor activity rhythm.

2.2.4 Counting of adult brain dopaminergic neurons

Adult flies with specified genotype were raised at 25°C for 25 days. The brains were dissected out carefully according to [127] with minor modifications in 1X phosphate buffered saline (PBS) (section 2.14.4). They were then fixed in 4% (v/v) formaldehyde (Sigma, USA) at room temperature for 15 min and then washed with 1X PBS (section 2.14.4) for 5 min for 3 times. After that, the brains were mounted on a glass slide with Fluorescence Mounting Medium (Dako, USA) and then subjected to confocal microscopy (Leica SP5; Leica Microsystems, Germany). To prepare the glass slide, two glass cover-slips were placed side-by-side with a space in between where the brains were put. Another glass cover-slip was then placed on top of the brains. Optical sections with a Z-step of 2 μm distance under a 40X dry lens were taken through the whole-mount brain transversely. The sections were overlapped and the total number of Green Fluorescent Protein (GFP)-positive dopaminergic (DA) neurons in the dorsomedial 1 (DM1) clusters were counted.

2.3 Semi-quantitative Reverse Transcription-Polymerase Chain Reaction

2.3.1 Ribonucleic acid extraction from adult *Drosophila* heads

Heads of 16 adult flies with specified age and genotype were homogenized in 800 μL of chilled TRIZOL reagent (Invitrogen, USA) using a motorized plastic pestle (Kontes, USA). The homogenate was incubated at room temperature for 5 min. It was then mixed with 160 μL of chloroform and incubated at room temperature for 3 min. The mixture was centrifuged at 12,000 x *g* at 4°C for 15 min. The upper aqueous phase containing the RNA was transferred to a new tube. The sample was mixed with 400 μL of isopropanol and incubated at -20°C overnight to precipitate the

RNA. It was then centrifuged at 12,000 x *g* at 4°C for 10 min. The supernatant was discarded and the pellet was washed with 1 mL of 70% ethanol. The sample was centrifuged again at 12,000 x *g* at 4°C for 10 min. The supernatant was discarded and the pellet was air-dried at room temperature. The dried pellet was resuspended with 50 µL of diethyl pyrocarbonate (DEPC)-treated water (section 2.14.2). The quality and the concentration of the extracted ribonucleic acid (RNA) were determined by spectrophotometry (Eppendorf BioPhotometer; Eppendorf, Germany).

2.3.2 Deoxyribonuclease treatment of extracted ribonucleic acid

To remove any residual deoxyribonucleic acid (DNA) left in the extracted RNA, the following reaction mixture was set up and incubated at room temperature for 15 min.

Table 2.1. Reaction mixture for deoxyribonuclease (DNase) treatment of extracted RNA

Reagent	Volume (µL)
Extracted RNA	50
Ribonuclease (RNase)-free DNase (Promega, USA)	3
10X DNase buffer (Promega, USA)	6
DEPC-treated water	1
Total	60

The mixture was added with 6 µL of DNase stop solution (Promega, USA) and

incubated at 65°C for 10 min to stop the reaction. To precipitate RNA, the sample was mixed with 8 µL of sodium acetate, 6 µL of DEPC-treated water and subsequently 160 µL of 70% ethanol. After incubating at -80°C overnight, the mixture was then centrifuged at 12,000 x *g* at 4°C for 15 min. The supernatant was discarded and the pellet was washed with 1 mL of 70% ethanol. The sample was centrifuged again at 12,000 x *g* at 4°C for 10 min. The supernatant was discarded and the pellet was air-dried at room temperature. The dried pellet was resuspended with 50 µL of DEPC-treated water. The quality and the concentration of RNA in the sample were determined by spectrometry (Eppendorf BioPhotometer; Eppendorf, Germany).

2.3.3 Reverse Transcription-Polymerase Chain Reaction

The following reactions were performed using a thermocycler (i-Cycler; Bio-Rad Laboratories, USA).

A reaction mixture consisting of 4 µL of RNA (containing 2 µg of RNA) and 1 µL of oligo dT primer (10 µM) (section 2.14.2) was incubated at 70°C for 5 min to denature the RNA. The mixture was chilled at 4°C for 5 min. It was then added with the following reagents and subjected to reverse transcription-polymerase chain reaction (RT-PCR) according to the following conditions:

Table 2.2. RT-PCR reaction mixture

Reagent	Volume (µL)
5X RT reaction buffer (Promega, USA)	4

Magnesium chloride ($MgCl_2$; 25mM; Promega, USA)	2.4
deoxynucleoside triphosphates mixture (dNTPs) (20mM; GE Healthcare, UK)	0.5
RNaseOUT™ (Invitrogen, USA)	0.5
Reverse Transcriptase (Promega, USA)	1
DEPC-treated water	6.6
Total	15

Table 2.3. RT-PCR conditions

Step	Time
25℃	5 min
42℃	60 min
70℃	15 min

The synthesized first strand complementary DNA (cDNA) was used as the template for PCR amplification of target transcripts. In general, the PCR reaction mixtures contained the following components and the PCR conditions were as follows:

Table 2.4. PCR reaction mixture for amplification of target transcript

Reagent	Volume (μL)
10X PCR reaction buffer (Promega, USA)	2.5
dNTPs (20 mM; GE Healthcare, UK)	0.3

$MgCl_2$ (25 mM; Promega, USA)	1.5
Target transcript forward primer (10 μM) (section 2.14.2)	0.5
Target transcript reverse primer (10 μM) (section 2.14.2)	0.5
Thermus aquaticus (*Taq*) DNA polymerase (GeneSys Limited, UK)	0.2
cDNA	2
Autoclaved double distilled water	17.5
Total	25

Table 2.5. PCR conditions for amplification of target transcript

Step		Time
Initial denaturation: 95℃		5 min
25 cycles	Denaturation: 95℃	30 sec
	Annealing: 56℃	30 sec
	Extension: 72℃	30 sec
Final extension: 72℃		10 min
Storage: 4℃		Infinity

2.3.4 Agarose gel electrophoresis

Ten microlitres of PCR product was mixed with 2 μL of 6X DNA loading dye (section 2.14.2). The mixture was loaded onto a 1% agarose gel (section 2.14.2). Two microlitres of DNA ladder (section 2.14.2) was loaded as a molecular weight marker. Electrophoresis was performed in 1X Tris-Borate-Ethylenediaminetetraacetic acid

(TBE) buffer (section 2.14.2) in the wide-mini-sub cell GT system (Bio-Rad Laboratories, USA) at a constant voltage of 120 V. It was ended when the dye front reached an appropriate position. Gel photo was taken by the Gel Documentation System (500MZ; Tech Dragon Ltd., China). The band intensity was quantified by the AlphaEaseFC software (version 3.1.2; Alpha Innotech Corporation, USA).

2.4 Construction of human *myc-Cul1*^{N252} mammalian expression plasmid

The fragment containing the N-terminal *myc* tag and the first 756 nucleotides (nt) of the human *Cul1* (*myc-hCul1*^{N252}) was amplified from the *pcDNA3.1/neo(+)-myc-hCul1* plasmid (F. T. Liang and H. Y. E. Chan, unpublished observations) by PCR using the conditions shown below. Additional *Kpn*I (New England Biolabs, USA) and *Xho*I (New England Biolabs, USA) restriction sites were added to the 5' and 3' ends of the amplified *myc-hCul1*^{N252} fragment respectively for subsequent cloning into the vector.

Table 2.6. PCR reaction mixture for amplification of *myc-hCul1*^{N252} fragment

Reagent	Volume (μL)
5X Phusion™ HF buffer (Finnzymes, Finland)	10
dNTPs (20 mM; GE Healthcare, UK)	1
*Kpn*I-*myc-hCul1*^{N252} forward primer (10 μM; section 2.14.2)	2.5
*Xho*I-*hCul1*^{N252} reverse primer (10 μM; section 2.14.2)	2.5
pcDNA3.1/neo(+)-myc-hCul1 plasmid	0.5
Phusion™ DNA polymerase (Finnzymes, Finland)	0.5

Autoclaved double distilled water	33
Total	50

Table 2.7. PCR conditions for amplification of *myc-hCul1*^{N252} fragment

Step		Time
Initial denaturation: 98℃		30 sec
35 cycles	Denaturation: 98℃	10 sec
	Annealing: 56℃	15 sec
	Extension: 72℃	15 sec
Final extension: 72℃		5 min
Storage: 4℃		infinity

The PCR product was resolved on a 1% agarose gel (section 2.14.2) by electrophoresis and purified by the QIAquick Gel Extraction Kit (QIAGEN, Germany). The purified *myc-hCul1*^{N252} fragment and the mammalian expression vector, *pcDNA3.1/neo(+)* (Invitrogen, USA), were respectively subjected to restriction digestion with *Kpn*I (New England Biolabs, USA) and *Xho*I (New England Biolabs, USA) at 37℃ overnight.

Table 2.8. Reaction mixture for restriction digestion of *myc-hCul1*^{N252} fragment and *pcDNA3.1/neo(+)* vector

Reagent	Volume/ Amount
10X NEB buffer 1 (New England Biolabs, USA)	3 μL

100X BSA (New England Biolabs, USA)	0.3 µL
*Kpn*I (New England Biolabs, USA)	0.5 µL
*Xho*I (New England Biolabs, USA)	0.5 µL
Purified *myc-hCul1*^{N252} fragment or *pcDNA3.1/neo(+)* vector (Invitrogen, USA)	1 µg
Autoclaved double distilled water	Make up to final volume
Total	30 µL

The digested *myc-hCul1*^{N252} fragment and vector were respectively resolved on a 1% agarose gel (section 2.14.2) by electrophoresis and purified by the QIAquick Gel Extraction Kit (QIAGEN, Germany).

Ligation reaction between the purified digested *myc-hCul1*^{N252} fragment and the purified linearized *pcDNA3.1/neo(+)* vector was set up as follows and incubated at 16℃ overnight.

Table 2.9. Reaction mixture for ligation between *myc-hCul1*^{N252} and *pcDNA3.1/neo(+)*

Reagent	**Volume (µL)**
10X ligation buffer (New England BioLabs, USA)	1
T4 DNA ligase (New England BioLabs, USA)	0.5
*Kpn*I and *Xho*I digested *myc-hCul1*^{N252}	7.5
*Kpn*I and *Xho*I digested *pcDNA3.1/neo(+)*	1

Total	10

The entire ligation product was used to transform competent *Escherichia coli (E. coli)* strain *DH5α*. After mixing the ligation product with *DH5α* cells, the mixture was allowed to stand on ice for 15 min. After that, the mixture was heat shocked at 42℃ for 2 min and then chilled on ice for another 2 min. For recovery, the mixture was added with 800 µL of Luria-Bertani (LB) medium (section 2.14.3) and incubated at 37℃ for 30 min with gentle shaking. After recovery, the cells were collected by centrifugation at 5,000 x *g* for 5 min. The supernatant was discarded and the cell pellet was resuspended in 100 µL of LB medium. The cell suspension was then spread over a LB-ampicillin (LBA) agar plate (50 µg/mL ampicillin) and incubated at 37 ℃ overnight. Colonies grown on plate were selected and checked by PCR amplification for the presence of the *myc-hCul1*^{N252} insert according to the following conditions:

Table 2.10. PCR reaction mixture for checking of *pcDNA3.1/neo(+)-myc-hCul1*^{N252} positive clones

Reagent	Volume (µL)
10X PCR reaction buffer (Promega, USA)	1.5
dNTPs (20 mM; GE Healthcare, UK)	0.18
$MgCl_2$ (25 mM; Promega, USA)	0.9
*Kpn*I-*myc-hCul1*^{N252} forward primer (10 µM; section 2.14.2)	0.3
BGH reverse primer (10 µM; section 2.14.2)	0.3

Taq DNA polymerase (GeneSys Limited, UK)	0.12
Bacterial colony on LBA plate	a trace amount
Autoclaved double distilled water	11.7
Total	15

Table 2.11 PCR conditions for checking of *pcDNA3.1/neo(+)-myc-hCul1*^{N252} positive clones

Step			Time
Initial denaturation: 95℃			5 min
30 cycles	{	Denaturation: 95℃	30 sec
		Annealing: 56℃	30 sec
		Extension: 72℃	50 sec
Final extension: 72℃			10 min
Storage: 4℃			infinity

A positive clone was cultured in 5 mL of LB medium freshly added with ampicillin (50 μg/mL final) at 37℃ overnight. The plasmid DNA was harvested by the DNA-Spin™ Plasmid DNA Extraction Kit (Tech Dragon Ltd., China). The identity of the plasmid was further checked by *Kpn*I and *Xho*I double restriction digestion at 37℃ for 1 hr. Finally, the sequence of the insert in the plasmid was confirmed by DNA sequencing analysis (Tech Dragon Ltd., China).

Table 2.12. Reaction mixture for restriction digestion of

***pcDNA3.1/neo(+)-myc-hCul1^{N252}* positive clones**

Reagent	Volume (μL) / Amount (μg)
10X NEB buffer 1 (New England Biolabs, USA)	1 μL
100X BSA (New England Biolabs, USA)	0.1 μL
*Kpn*I (New England Biolabs, USA)	0.5 μL
*Xho*I (New England Biolabs, USA)	0.5 μL
pcDNA3.1/neo(+)-myc-hCul1^{N252} plasmid	0.5 μg
Autoclaved double distilled water	Make up to final volume
Total	10 μL

2.5 Maintenance of Human Embryonic Kidney 293FT cells

The human embryonic kidney (HEK) 293FT cells (Invitrogen, USA) were a generous gift from Dr. F. S. Y. Tsang (The Biochemistry Department, The Chinese University of Hong Kong, China). The cells were maintained in complete high glucose Dulbecco's Modified Eagle's Medium (DMEM) (section 2.14.4) in a 37°C humidified incubator supplemented with 5% CO_2. For sub-culturing, trypsin-EDTA (0.05%) solution (Invitrogen, USA) was applied to detach the cells from culture flasks.

2.6 Transient transfection of Human Embryonic Kidney 293FT cells

For transfection of plasmid DNA, cells with specified density were seeded on either 24- or 6-well plate one day prior to transfection. Transfection was carried out using FuGENE® HD transfection reagent (Roche, Germany). Specified amount of DNA was made up to a specified total volume by serum-free DMEM (section 2.14.4).

The diluted DNA was added with specified amount of FuGENE® HD and incubated at room temperature for 15 min. The DNA-transfection reagent mixture was applied over the cells. After incubating at 37°C for 24 hr, the medium was replaced with fresh complete DMEM. The cells were harvested at specified time point. For *pcDNA3.1/neo(+)-eGFP*, *eGFP-Q27* and *eGFP-Q75* constructs, 0.4 μg or 1 μg of plasmid DNA was used for each transfection in a 24- or 6-well plate. For *pcDNA3.1/neo(+)-myc-hCul1* and *myc-hCul1*^{N252} constructs, 0.2 μg or 1 μg of plasmid DNA was used for each transfection in a 24- or 6-well plate. The total plasmid DNA for each transfection was made up with *pcDNA3.1/neo(+)* empty vector to a specified amount.

Table 2.13. Transfection mixture for HEK 293FT cells

	24-well plate	**6-well plate**
Cell density	0.5 x 10^5	2 x 10^5
Total plasmid DNA (μg)	1	2
FuGENE® HD (μL)	2	4
Total volume of DNA diluted with serum-free DMEM (μL)	50	100
Experiments	immunoblotting, filter retardation assay	co-immunoprecipitation

For small interfering RNA (siRNA) transfection before transfection of plasmid DNA, 0.5 x 10^5 cells were seeded in 24-well plate one day prior to transfecion.

Transfection of siRNA was performed with Lipofectamine 2000 (Invitrogen, USA). Five or fifty picomoles of siRNA and 1 μL of Lipofectamine 2000 were respectively diluted with serum-free DMEM (section 2.14.4) to a final volume of 25 μL. They were then mixed and incubated at room temperature for 20 min. After that, the mixture was applied over the cells. After incubating at 37°C for 24 hr, the cells were subsequently transfected with plasmid DNA as described above.

2.7 Immunoblotting

2.7.1 Protein extraction

For fly experiments, heads of 6 adult flies with specified age and genotype were homogenized in 30 μL of chilled 6X SDS sample buffer (section 2.14.5) with a motorized plastic pestle (Kontes, USA). The homogenate was centrifuged at 16,000 x *g* for 1 min to remove any debris. A volume of 20 μL of homogenate (equivalent to 4 heads) was then heated at 99°C for 5 min to denature the proteins and stored at -20°C until use.

For experiments on HEK 293FT cells, transfected cells were harvested at specified time point and lysed with 100 μL of chilled lysis buffer (section 2.14.5). The lysate was centrifuged at 16,000 x *g* for 1 min to remove any debris. Protein quantification was performed on the lysate by DC Protein Assay (Bio-Rad Laboratories, USA). An aliquot of lysate containing 5 μg proteins was made up to a final volume of 10 μL with lysis buffer (section 2.14.5). The sample was mixed with 2 μL of 6X SDS sample buffer (section 2.14.5), heated at 99°C for 5 min and stored at -20°C until use.

2.7.2 Sodium Dodecyl Sulfate-Polyacrylamide Gel Electrophoresis

Sodium dodecyl sulfate-polyacrylamide gel electrophoresis (SDS-PAGE) was performed using the Mini-PROTEAN III electrophoresis cell (Bio-Rad Laboratories, USA). A short glass plate and a 1.5 mm spacer glass plate were inserted into the gel cassette. Running gel solution (section 2.14.5) was added into the assembled gel cassette with isopropanol on the top so as to remove any air bubbles and to keep the running gel out of reach of the atmospheric oxygen. When the polymerization in the running gel completed, the isopropanol was rinsed away with double distilled water. Stacking gel solution (section 2.14.5) was added on top of the running gel. A 1.5 mm thick comb with either a 10- or 15-well mold was inserted on top of the stacking gel. When the polymerization in the stacking gel completed, the gel cassette was placed into the electrophoresis cell. Both the inner and the outer cell chambers were filled up with 1X electrophoresis buffer (section 2.14.5). The comb was removed and the wells were rinsed with 1X electrophoresis buffer (section 2.14.5) to remove any residual stacking gel solution.

Fly or cell protein samples were denatured at 99°C for 5 min. They were loaded into the wells. Five microlitres of broad-range pre-stained protein standard (Bio-Rad Laboratories, USA) was used as a molecular weight marker. Electrophoresis was carried out at a constant voltage of 80 V and then 120 V when the protein samples entered the running gel. It was ended when the dye front reached an appropriate position.

2.7.3 Transfer

The gel was removed from the gel cassette and rinsed with double distilled water. A polyvinylidene fluoride (PVDF) membrane (PALL, USA) was activated by immersing in methanol for 15 sec. The gel, the activated membrane, 4 pieces of filter paper (Whatman, USA) and 4 pieces of filter pad (Bio-Rad Laboratories, USA) were equilibrated with 1X transfer buffer (section 2.14.5) at room temperature for 1 min. They were assembled into a transfer cassette in the following order: 2 pieces of filter pad on the cathode (black) side of the transfer cassette, 2 pieces of filter paper, the gel, the membrane, another 2 pieces of filer paper and finally another 2 pieces of filter pad. Before closing the transfer cassette, a glass rod was used to roll over the transfer stack so as to expel any trapped air bubbles. The transfer cassette was placed into the transfer tank together with the Bio-Ice cooling unit. The tank was filled up with freshly prepared 1X transfer buffer (section 2.14.5). Transfer was performed at a constant voltage of 80 V on ice for 2 hr.

2.7.4 Immunodetection

The membrane was removed from the transfer cassette and washed with 1X Tris-buffered saline (TBS) (section 2.14.5) at room temperature for 5 min with shaking. It was then blocked with blocking solution (section 2.14.5) at room temperature for 1 hr with shaking. After that, the membrane was incubated with primary antibody diluted in blocking solution in a plastic vial at 4°C overnight with rotation. The immunoblot was then washed with 1X TBS-Tween-20 (TBST) (section 2.14.5) at room temperature for 15 min with shaking for 4 times. Later, it was incubated with secondary antibody diluted in blocking solution in a new plastic vial

at room temperature for 2 hr. The immunoblot was washed again with 1X TBST (section 2.14.5) at room temperature for 15 min with shaking for 4 times.

Home-made enhanced chemiluminescent (ECL) reagents (section 2.14.5) were used to detect signal from the immunoblot. Equal volumes of ECL reagent A (section 2.14.5) and ECL reagent B (section 2.14.5) were mixed and spread over the immunoblot. After 2 min of incubation at room temperature, the immunoblot was wrapped with a piece of cling film and exposed to an X-ray film (FUJI super RX, Japan) for the desired time period. The exposed film was developed by an X-ray film processor (Kodak, Japan).

To reprobe the immunoblot with another antibody, the immunoblot was incubated with stripping solution (Pierce, USA) at room temperature for 10 min with shaking. It was then washed with 1X TBST (section 2.14.5) at room temperature for 5 min with shaking twice. After that, the immunoblot was incubated with another primary antibody and the corresponding secondary antibody as described above.

Primary antibodies used were rabbit anti-hemagglutinin (HA) (1:250; Zymed, USA), rabbit anti-Cul1 (1:250; Invitrogen, USA), rabbit anti-myc (71D10; 1:1,000; Cell Signaling Technology, USA), mouse anti-myc (9B11; 1:1,000; Cell Signaling Technology, USA), mouse anti-GFP (JL-8; 1:3,000; Clontech, USA), mouse anti-ubiquitin (P4D1; 1:500; Cell Signaling Technology, USA) and mouse anti-β-tubulin E7 (1:5,000; Developmental Studies Hybridoma Bank, University of Iowa, USA). The secondary antibodies used were affinity purified goat anti-rabbit

immunoglobulin (IgG) (H + L) antibody conjugated to horseradish peroxidase (HRP) (1:2,500; Cell Signaling Technology, USA) and goat anti-mouse IgG (H + L) conjugated to HRP (1:2,500; Chemicon, USA). The band intensity was quantified by the AlphaEaseFC software (version 3.1.2; Alpha Innotech Corporation, USA).

2.8 Formic acid treatment

Heads of 6 adult flies with specified age and genotype were homogenized in 30 µL of chilled 2% SDS sample buffer (section 2.14.6) with a motorized plastic pestle (Kontes, USA). The homogenate was centrifuged at 16,000 x *g* for 1 min to remove any debris. A volume of 20 µL of homogenate (equivalent to 4 heads) was added to 180 µL of 100% formic acid (Sigma, USA) and incubated at 37°C for 0.5 hr. Formic acid in the sample was removed by SpeedVac (Savant, USA) at low drying rate for 2 hr. The resulting pellet was resuspended with 10 µL of 6X SDS sample buffer (section 2.14.5). Ten microlitres of 1M Tris-hydrochloride acid (HCl) (pH 8.8; USB, USA) was added to neutralize any residual formic acid left in the sample. The sample was heated at 99°C for 5 min and stored at -20°C until being subjected to immunoblotting (sections 2.7.2 – 2.7.4).

2.9 SDS-insoluble protein isolation by ultracentrifugation

Heads of 35 adult flies with specified age and genotype were homogenized in 100 µL of chilled 2% SDS sample buffer (section 2.14.6) with a motorized plastic pestle (Kontes, USA). The homogenate was centrifuged at 16,000 x *g* for 1 min to remove any debris. It was then subjected to ultracentrifuge at 100,000 rpm (434,513 x *g*; TLA120.2 rotor; TLX-120; Beckman Coulter, USA). The supernatant was

discarded. The pellet was resuspended with 80 μL of 100% formic acid (Sigma, USA) and incubated at 37°C for 30 min. Formic acid in the sample was removed by SpeedVac (Savant, USA) at low drying rate for 1 hr. The resulting pellet was resuspended with 10 μL of 6X SDS sample buffer (section 2.14.5). Ten microlitres of 1M Tris-hydrochloric acid (Tris-HCl; pH 8.8; USB, USA) was added to neutralize any residual formic acid left in the sample. The sample was heated at 99°C for 5 min and stored at -20°C until being subjected to immunoblotting (sections 2.7.2 – 2.7.4).

2.10 Filter retardation assay

For fly experiments, heads of 10 adult flies with specified age and genotype were homogenized in 100 μL of chilled 2% SDS solution (section 2.14.7) with a motorized plastic pestle (Kontes, USA). The homogenate was centrifuged at 16,000 x *g* for 1 min to remove any debris. A volume of 70 μL of homogenate (equivalent to 7 heads) was made up to a final volume of 200 μL by 2% SDS solution (section 2.14.7). It was then heated at 99°C for 5 min and stored at -20°C until use.

For experiments on HEK 293FT cells, transfected cells were harvested at specified time point and lysed with 100 μL of chilled 2% SDS solution (section 2.14.7). The lysate was centrifuged at 16,000 x *g* for 1 min to remove any debris. Protein quantification was performed on the lysate by DC Protein Assay (Bio-Rad Laboratories, USA). An aliquot of lysate containing 10 μg of protein was made up to a final volume of 200 μL by 2% SDS solution (section 2.14.7). It was then heated at 99°C for 5 min and stored at -20°C until use.

The Slot Blot Manifold blot apparatus (GE Healthcare, UK) was assembled with a cellulose acetate membrane of 0.22 μm pore size (Sartorius, Germany) sandwiched in between. The apparatus was connected to a vacuum pump. Upon vacuum pumping, the membrane was wetted with double distilled water, equilibrated with 0.01% SDS solution (section 2.14.7) and then 2% SDS solution (section 2.14.7). The fly or cell protein samples were then loaded onto the slots. Each slot was washed with 300 μL of 2% SDS solution (section 2.14.7). After 15 min of vacuum pumping, the membrane was removed from the blot apparatus. Immunodetection was then performed as described in section 2.7.4.

2.11 Co-immunoprecipitation

For fly experiments, heads of 45 adult flies with specified age and genotype were homogenized in 225 μL of chilled co-immunoprecipitation (co-IP) buffer (section 2.14.8) with a motorized plastic pestle (Kontes, USA). The homogenate was centrifuged at 16,000 x *g* at 4°C for 10 min to remove any debris. A volume of 30 μL of homogenate (equivalent to 6 heads) was saved as the input. It was mixed with 6 μL of 6X SDS sample buffer (section 2.14.5), heated at 99°C for 5 min and then stored at -20°C until use. Another aliquot of 150 μL of homogenate (equivalent to 30 heads) was added with co-IP buffer (section 2.14.8) to a final volume of 500 μL.

For experiments on HEK 293FT cells, transfected cells were harvested at specified time points and lysed with 200 μL of chilled Cul1 IP buffer (section 2.14.8). The lysate was sonicated on ice for 5 sec twice by Ultrasonic Processor (A. Daigger, USA). The lysate was centrifuged at 16,000 x *g* at 4°C for 10 min to remove any

debris. Protein quantification was performed on the lysate by DC Protein Assay (Bio-Rad Laboratories, USA). An aliquot of lysate containing 5 μg of proteins was saved as the input. It was added with co-IP buffer (section 2.14.7) to a final volume of 10 μL, mixed with 2 μL of 6X SDS sample buffer (section 2.14.5), heated at 99°C for 5 min and then stored at -20°C until use. Another aliquot of lysate containing 150 μg of proteins was added with co-IP buffer (section 2.14.8) to a final volume of 200 μL.

One microlitre of mouse anti-myc (9B11; 1:1,000; Cell Signaling Technology, USA) was added to the fly or cell protein samples except the "no antibody" control. The samples were incubated at 4°C overnight with rotation. A volume of 20 μL of Protein A agarose beads suspension (P3476; Sigma, USA) was washed with 500 μL of 1X PBS (section 2.14.4) for 3 times and added to each sample. After 2 hr of incubation at 4°C, the samples were centrifuged at 16,000 x *g* for 30 sec to remove the supernatant. The remaining beads were washed with 500 μL of co-IP buffer (section 2.14.8) for 4 times. A volume of 20 μL of 6X SDS sample buffer (section 2.14.5) was added to the beads. The samples were heated at 99°C for 5 min and stored at -20°C until being subjected to immunoblotting (sections 2.7.2 – 2.7.4).

2.12 *In vivo* ubiquitination assay

2.12.1 *In vivo* ubiquitination assay on soluble protein

Heads of 120 adult flies with specified age and genotype were homogenized in 600 μL of chilled ubiquitination assay buffer (section 2.14.9) with a motorized plastic pestle (Kontes, USA). The homogenate was centrifuged at 16,000 x *g* at 4°C

for 10 min to remove any debris. A volume of 30 μL of homogenate (equivalent to 6 heads) was saved as the input. It was mixed with 6 μL of 6X SDS sample buffer (section 2.14.5), heated at 99°C for 5 min and then stored at -20°C until use.

A volume of 500 μL of homogenate (equivalent to 100 heads) was added with 1 μL of rabbit anti-myc (71D10; 1:1,000; Cell Signaling Technology, USA) except the "no antibody" control. The samples were incubated at 4°C overnight with rotation. A volume of 20 μL of Protein A agarose beads suspension (P3476; Sigma, USA) was washed with 500 μL of 1X PBS (section 2.14.4) for 3 times and added to each sample. After 2 hr of incubation at 4°C, the samples were centrifuged at 16,000 x *g* for 30 sec to remove the supernatant. The remaining beads were washed with 500 μL of ubiquitination assay buffer (section 2.14.9) for 4 times. A volume of 20 μL of 6X SDS sample buffer (section 2.14.5) was added to the beads. The samples were heated at 99°C for 5 min and stored at -20°C until being subjected to immunoblotting (sections 2.7.2 – 2.7.4).

2.12.2 *In vivo* ubiquitination assay followed by filter retardation assay

Heads of 280 adult flies with specified age and genotype were homogenized in 1,400 μL of chilled ubiquitination assay buffer (section 2.14.9) with a motorized plastic pestle (Kontes, USA). The homogenate was centrifuged at 16,000 x *g* at 4°C for 10 min to remove any debris. A volume of 60 μL of homogenate (equivalent to 12 heads) was saved as the input. It was made up to a final volume of 400 μL by 2% SDS solution (section 2.14.7), heated at 99°C for 5 min and then stored at -20°C until use.

A volume of 1,250 μL of homogenate (equivalent to 250 heads) was added with 1 μL of rabbit anti-myc (71D10; 1:1,000; Cell Signaling Technology, USA) except the "no antibody" control. The samples were incubated at 4°C overnight with rotation. A volume of 20 μL of Protein A agarose beads suspension (P3476; Sigma, USA) was washed with 500 μL of 1X PBS (section 2.14.4) for 3 times and added to the each sample. After 2 hr of incubation at 4°C, the samples were centrifuged at 16,000 x *g* for 30 sec to remove the supernatant. The remaining beads were washed with 1,250 μL of ubiquitination assay buffer (section 2.14.9) for 4 times. A volume of 400 μL of 2% SDS solution (section 2.14.7) was added to the beads. The samples were heated at 99°C for 5 min. The eluate was then collected from each sample, divided into two equal halves and stored at -20°C until being subjected to filter retardation assay (section 2.10).

2.12.3 *In vivo* ubiquitination assay on SDS-insoluble protein isolated by ultracentrifugation

Heads of 220 adult flies with specified age and genotype were homogenized in 1,100 μL of chilled ubiquitination assay buffer (section 2.14.9) with a motorized plastic pestle (Kontes, USA). The homogenate was centrifuged at 16,000 x *g* at 4°C for 10 min to remove any debris.

A volume of 1,000 μL of homogenate (equivalent to 200 heads) was added with 1 μL of mouse anti-myc (9B11; 1:1,000; Cell Signaling Technology, USA) except the "no antibody" control. The samples were incubated at 4°C overnight with rotation. A

volume of 20 μL of Protein A agarose beads suspension (P3476; Sigma, USA) was washed with 500 μL of 1X PBS (section 2.14.4) for 3 times and added to each sample. After 2 hr of incubation at 4°C, the samples were centrifuged at 16,000 x *g* for 30 sec to remove the supernatant. The remaining beads were washed with 1,000 μL of ubiquitination assay buffer (section 2.14.9) for 4 times. A volume of 100 μL of 2% SDS sample buffer (section 2.14.6) was added to the beads. The samples were heated at 99°C for 10 min. After vortexing for 10 sec, the samples were centrifuged at 16,000 x *g* at 4°C for 1 min to collect the eluates. The eluates were then subjected to ultracentrifugation (section 2.9) and subsequent immunoblotting (section 2.7.2 – 2.7.4).

2.13 Statistics

For the counting of adult brain DA neurons, semi-quantitative RT-PCR and immunoblotting experiments, the difference in the mean value between samples was compared using two-tailed unpaired Student's t-test (Microsoft Office Excel 2003, USA). Statistical significance was denoted by a *p*-value of less than 0.05.

For the deep pseudopupil assay experiments, the difference in the mean value between samples was compared using Mann-Whitney Rank Sum Test (SigmaStat, USA). Statistical significance was denoted by a *p*-value of less than 0.05.

2.14 Reagents and buffers

2.14.1 *Drosophila* culture

***Drosophila* strains**

The fly lines used are listed in Tables 2.14 and 2.15.

Table 2.14. Transgenic fly lines used in this study

Transgenic line	Genotype	Reference
gmr-GAL4	*w*; *gmr-GAL4*;	[118]
gmr-GAL4 UAS-HA-SCA3tr-Q27	*w*; *gmr-GAL4 UAS-HA-SCA3tr-Q27/CyO*;	[128]
gmr-GAL4 UAS-HA-SCA3tr-Q78(w)	*w*; *gmr-GAL4 UAS-HA-SCA3tr-Q78(w)/CyOTb*;	[128]
gmr-GAL4 UAS-HA-SCA3tr-Q78(s)	*w*; *gmr-GAL4 UAS-HA-SCA3tr-Q78(s)/CyO*;	[128]
gmr-GAL4 UAS-ARtr-Q16	*w*; *gmr-GAL4/CyO*; *UAS-ARtr-Q16/MKRS*	[24]
gmr-GAL4 UAS-ARtr-Q112(w)	*w*; *gmr-GAL4/CyO*; *UAS-ARtr-Q112(w)/MKRS*	[24]
gmr-GAL4 UAS-eGFP-Q76-FLAG	*w*; *gmr-GAL4/CyO*; *UAS-eGFP-Q76/MKRS*	[25]
gmr-GAL4 UAS-myc-SCA3fl-Q27	*w*; *gmr-GAL4 UAS-myc-SCA3fl-Q27#46.2/CyO*;	[129]
gmr-GAL4 UAS-myc-SCA3fl-Q84	*w*; *gmr-GAL4/CyO*; *UAS-myc-SCA3fl-Q84#7.2/MKRS*	[129]
gmr-GAL4 UAS-α-synuclein^{WT}	*w*; *gmr-GAL4/CyO*; *UAS-α-synuclein^{WT}/MKRS*	[130]
gmr-GAL4 UAS-myc-SCA3fl-Q84 UAS-Cul1$^{RNAi\ (VDRC42445)}$	*w*; *gmr-GAL4/CyO*; *UAS-myc-SCA3fl-Q84 UAS-Cul1$^{RNAi\ (VDRC42445)}$/MKRS*	The present study
UAS-HA-Ub^{WT}	*w*;; *UAS-HA-Ub^{WT}/MKRS*	[130]
UAS-Cul1$^{5-1}$	*w*; *UAS-Cul1$^{5-1}$/CyO*;	[131]
UAS-Cul1$^{11-1}$	*w*; *UAS-Cul1$^{11-1}$/CyO*;	[131]
UAS-FLAG-Cul1	*w*; *UAS-FLAG-Cul1/CyO*;	[86]
UAS-FLAG-Cul1^{KR}	*w*;; *UAS-FLAG-Cul1^{KR}/TM6B*	[86]
UAS-Roc1a^{R127}	*w*; *P{pUAST-Roc1a} #9.1*;	[132]
UAS-Roc1a^{R129}	*w*; *P{pUAST-Roc1a} #3/2*;	[132]
UAS-YFP-Nedd8$^{(II)}$	*w*; *UAS-YFP-Nedd8$^{(II)}$/SP-7*;	[86]

UAS-YFP-Nedd8$^{(III)}$	*w;; UAS-YFP-Nedd8$^{(III)}$/TM6B*	[86]
UAS-CSN5$^{(II)}$	*w; UAS-CSN5$^{(II)}$/CyO;*	[86]
UAS-CSN5$^{(III)}$	*w;; UAS-CSN5$^{(III)}$;*	[86]
UAS-CSN5^{D148N}	*w; UAS-CSN5^{D148N}/CyO;*	[86]
UAS-hHsp70	*w; P{UAS-Hsap\HSPA1L.W}53.1/CyO;*	[23]
tim-GAL4	*w; tim-GAL4/CyO;*	[133]

Table 2.15. RNAi fly lines used in this study

RNAi line	Genotype	Stock number	Stock centre
UAS-Cul1^{RNAi}	*w; UAS-Cul1^{RNAi}*	42445	VDRC
UAS-Cul1^{RNAi}	*w;; UAS-Cul1^{RNAi}*	1877R-2	NIG
UAS-Cul2^{RNAi}	*w;; UAS-Cul2^{RNAi}*	19298	VDRC
UAS-Cul3^{RNAi}	*w; UAS-Cul3^{RNAi};*	16332	VDRC
UAS-Cul4^{RNAi}	*w; UAS-Cul4^{RNAi};*	44829	VDRC
UAS-Cul4^{RNAi}	*w; UAS-Cul4^{RNAi};*	8711R-1	NIG
UAS-Cul5^{RNAi}	*w; UAS-Cul5^{RNAi};*	52175	VDRC
UAS-Roc1a^{RNAi}	*w; UAS-Roc1a^{RNAi};*	32399	VDRC
UAS-SkpA^{RNAi}	*w;; UAS-SkpA^{RNAi}*	46607	VDRC
UAS-Nedd8^{RNAi}	*w; UAS-Nedd8^{RNAi};*	28444	VDRC
UAS-Slmb^{RNAi}	*w;; UAS-Slmb^{RNAi}*	3412R-1	NIG
UAS-CG9144^{RNAi}	*w; UAS-CG9144^{RNAi};*	9144R-1	NIG
UAS-Ago^{RNAi}	*w; UAS-Ago^{RNAi};*	15010R-2	NIG

UAS-CG9772^{RNAi}	*w*; *UAS-CG9772^{RNAi}*;	15636	VDRC
UAS-CG9003^{RNAi}	*w*; *UAS-CG9003^{RNAi}*;	23482	VDRC
UAS-CG1839^{RNAi}	*w*; *UAS-CG1839^{RNAi}*;	15475	VDRC
UAS-CG4221^{RNAi}	*w UAS-CG4221^{RNAi}*; ;	34810	VDRC
UAS-CG11033^{RNAi}	*w*; *UAS-CG11033^{RNAi}*;	31402	VDRC
UAS-Ppa^{RNAi}	*w*; *UAS-Ppa^{RNAi}*;	29903	VDRC
UAS-CG8873^{RNAi}	*w UAS-CG8873^{RNAi}*; ;	45618	VDRC
UAS-CG32085^{RNAi}	*w*; *UAS-CG32085^{RNAi}*;	34053	VDRC
UAS-Rca1^{RNAi}	*w*;; *UAS-Rca1^{RNAi}*	10800R-1	NIG
UAS-CG5961^{RNAi}	*w*;; *UAS-CG5961^{RNAi}*	5961R-1	NIG
UAS-CG9461^{RNAi}	*w*; *UAS-CG9461^{RNAi}*;	24041	VDRC
UAS-CG11658^{RNAi}	*w*;; *UAS-CG11658^{RNAi}*	11658R-2	NIG
UAS-CG3428^{RNAi}	*w*;; *UAS-CG3428^{RNAi}*	3428R-1	NIG
UAS-CG4911^{RNAi}	*w*; *UAS-CG4911^{RNAi}*;	4911R-1	NIG
UAS-CG2010^{RNAi}	*w*; *UAS-CG2010^{RNAi}*;	2010R-2	NIG
UAS-CG2010^{RNAi}	*w*; *UAS-CG2010^{RNAi}*;	100736	VDRC
UAS-CG6758^{RNAi}	*w*; *UAS-CG6758^{RNAi}*;	43606	VDRC

Abbreviations: VDRC, Vienna *Drosophila* RNAi Center; NIG, National Institute of Genetics.

Cornmeal medium for *Drosophila* culture

Cornmeal medium was prepared by dissolving 12.5 g of agar (1.25% final, w/v; USB, USA), 105 g of dextrose (10.5% final, w/v), 105 g of cornmeal (10.5% final, w/v) and 21 g of yeast (2.1% final, w/v) in 900 mL of distilled water. The mixture was boiled for about 20 min. A volume of 80 mL of 1% nipagen (methyl p-hydroxybenzoate; dissolved in ethanol; Sigma, USA) was added to the mixture as a mold inhibitor. The mixture was made up to 1 L by distilled water. A volume of 15 mL of mixture was dispensed to a plastic fly vial and allowed to solidify at room temperature.

Sucrose medium for locomotor activity assay

Sucrose medium was prepared by dissolving 0.5 g of agar (5% final, w/v; USB, USA) and 1 g of sucrose (10% final, w/v; USB, USA) in 10 mL of distilled water. The mixture was boiled for about 5 min. It was then poured onto a petri dish and allowed to solidify at room temperature. The solidified medium was transferred to one end of a small, both-ends open-glass tube (Trikinetics Inc., USA) by stabbing the glass tube onto the medium vertically.

2.14.2 Semi-quantitative Reverse Transcription-Polymerase Chain Reaction

DEPC-treated water

DEPC water (0.1% final, v/v) was prepared by adding 500 μL of DEPC (USB, USA) into 500 mL of double distilled water. The DEPC water was stirred overnight and then autoclaved to inactivate DEPC. Autoclaved DEPC-treated water was stored as 1-mL aliquots at room temperature.

Primers

DNA oligonucleotide primers were synthesized by Tech Dragon Ltd., China and were of 100 μM. Working primer solution of 10 μM was prepared by diluting the stock solution by 10-fold with autoclaved double distilled water. Both stock and working solutions were kept at -20°C. The primers used were listed in Table 2.16.

Table 2.16. Primers used in this study

Primer	Sequence
actin forward primer	5' *ATG TGC AAG GCC GGT TTC GC* 3'
actin reverse primer	5' *CGA CAC GCA GCT CAT TGT AG* 3'
Cul1 forward primer	5' *ACG GAT TTG TGG CCG CTT TGG ACA A* 3'
Cul1 reverse primer	5' *TCC TTT GAG ACG CCA ATG TCC TGG A* 3'
Cul2 forward primer	5' *CGC TGA AGG GCG AAA ACA TCC ATA T* 3'
Cul2 reverse primer	5' *CAT TCC CTC CTC CGC ATC CAT GCT C* 3'
Cul3 forward primer	5' *TGC TGG GCA TGG TGA TGG AGG AAC G* 3'
Cul3 reverse primer	5' *GGC CAG ATC CTC GGT CTT TGA GTT C* 3'
Cul4 forward primer	5' *GCT GCA AAA TTC GAC CGT TCA CTC* 3'
Cul4 reverse primer	5' *GCT CGT TCT CCT CGG CCA AAC GCT T* 3'
Cul5 forward primer	5' *AGT TGC GTG AGG AGG AGG TTA GGG C* 3'
Cul5 reverse primer	5' *CAG TGA GGA AGC GGG GAT CGT* 3'
CG2010 forward primer	5' *TAC ATC GAG CTG CCC ATC GAG* 3'
CG2010 reverse primer	5' *AGG CAG GTG AGG CGC TTG GAA* 3'
CG9461 forward primer	5' *TAC AA TGC CCT GCA AAG ATG GA* 3'
CG9461 reverse primer	5' GAG GAC GAG GCG GAC GAA GA 3'
*Kpn*I-*myC-hCul1*^{N252} forward primer	5' GGT ACC ATG GAA CAA AAA CTT ATT TCT GAA GAA GAT CTG ATG TCG TCA ACC CGG AGC C 3'
*Xho*I-*hCul1*^{N252} reverse primer	5' *CCT CGA GTC ACA AGA ATT CAG TAC TCT CTC TG* 3'
BGH reverse primer	5' *CTT AGA AGG CAC AGT CGA GG* 3'

DNA loading dye

DNA loading dye (6X) was prepared by mixing 25 mg of bromophenol blue (0.25% final, w/v; USB, USA), 25 mg of xylene cyanol FF (0.25% final, w/v; ICN BioMedicals, USA), 4 g of sucrose (40% final, w/v; USB, USA) and 1.2 mL of 0.5 M EDTA (60 mM final; pH 8.0; USB, USA) in 10 mL of autoclaved double distilled water. Loading dye was stored as 1-mL aliquots at -20°C while the working dye solution was kept at 4°C.

TBE

The stock TBE buffer (5X) was prepared by mixing 54 g of Tris-base (0.45 M, final; USB, USA), 27.5 g of boric acid (0.45 M, final; USB, USA) and 20 mL of 0.5 M EDTA (10 mM, final; USB, USA) in 1 L of double distilled water. The pH value was calibrated to 8.0. The working TBE solution (1X) was prepared by diluting the stock buffer 5-fold with double distilled water. Both the stock and the working solutions were kept at room temperature.

Agarose gel for DNA electrophoresis

Agarose gel (1%, final; w/v) was prepared by melting 0.2 g of agarose (Bio-Rad Laboratories, USA) in 20 mL of 1X TBE by microwave at high power for about 1 min. The gel solution was cooled to hand-warm. One microlitre of ethidium bromide (10 mg/mL; Amresco, USA) was added to the gel solution. The gel was set using a gel caster (Bio-Rad Laboratories, USA) at room temperature.

DNA Ladder

The working solution of either 100 base-pair (bp) or 1 kilo bp DNA marker (Fermentas) was prepared by mixing 1 volume of the stock DNA marker, 1 volume of 6X DNA loading dye and 4 volumes of autoclaved double distilled water. Stock DNA marker was kept at -20°C while the working solution was stored at 4°C.

2.14.3 Bacterial Culture

Ampicillin

A stock solution (5 mg/mL) of ampicillin (GE Healthcare, UK) was prepared in autoclaved double distilled water. It was kept at -20 ℃.

LB medium

LB medium was prepared by adding 20 g of LB broth (USB, USA) in 1 L of double distilled water and autoclaved. The medium was stored at room temperature.

LBA plate

LBA solution was prepared by adding 20 g of LB broth (USB, USA) and 15 g of agar (USB, USA) in 1 L of double distilled water and autoclaved. The mixture was cooled to hand-warm and mixed with 10 mL of ampicillin (50 μg/mL final). It was then dispensed onto petri dishes (10 mL each) and allowed to solidify at room temperature. The LBA plates were then stored at 4℃.

2.14.4 Maintenance and transfection of Human Embryonic Kidney 293FT cells

Serum-free DMEM

The high glucose DMEM was prepared by dissolving one pack of powder

(Invitrogen, USA) in 1 L of double distilled water supplemented with 3.7 g of sodium bicarbonate (Sigma, USA). The medium was adjusted to pH 7.2 - 7.4 and sterilized by filtration through a 0.22 μm filter (Millipore, USA) in a cell culture hood. The medium was stored at 4℃.

Complete DMEM

The complete DMEM was prepared by adding Fetal Bovine Serum (10% final, v/v; JRH Biosciences, Australia) and Penicillin–Streptomycin (1% final, v/v; Invitrogen, USA) to 1 L of serum-free DMEM in a cell culture hood. The complete medium was stored at 4℃.

Phosphate Buffered Saline (PBS)

The stock PBS solution (10X) was prepared by dissolving 80 g of sodium chloride (NaCl; 1.37 M, final; USB, USA), 2 g of potassium chloride (KCl; 27 mM, final; USB, USA), 14.4 g of disodium hydrogen phosphate (Na_2HPO_4; 100 mM, final; USB, USA) and 2.4 g of dipotassium hydrogen phosphate (KH_2PO_4; 20 mM, final; USB, USA) in 1 L of double distilled water. The working PBS solution (1X) was prepared by 10-fold dilution of the stock solution and autoclaved. Both the stock and working solutions were kept at 4°C.

siRNA

The *control siRNA* (Catalog number: D-001210-01-05) and *Cul1 siRNA* (Catalog number: M-004086-01-0005) were purchased from Dharmacon (USA). They were diluted with 1X siRNA buffer to 20 μM and stored at -20°C in 5

μL-aliquots.

siRNA buffer

The siRNA buffer stock (5X) was prepared by adding 2.24 g of KCl (0.3 M final; USB, USA), 0.72 g of 4-(2-hydroxyethyl)-1-piperazineethanesulfonic acid-free acid (30 mM, final; USB, USA) and 0.02 g of magnesium chloride hexahydrate ($MgCl_2.6H_2O$; 0.9 mM final; USB, USA), 0.24 g of potassium hydroxide (KOH; 42.8 mM final; USB, USA) in 100 mL of DEPC-treated water. The buffer was adjusted to pH 7.3 – 7.6 and autoclaved. The working buffer (1X) was prepared by diluting the stock 5-fold with DEPC-treated water. Both the stock and the working buffers were stored at 4°C.

Hemacytometer

Cell number was determined by direct cell counting using a hemacytometer (Sigma, USA).

Microscope

Cell counting was performed under a light microscope (Olympus, USA) at 100X magnification.

2.14.5 Immunoblotting

SDS sample buffer

SDS sample buffer (6X) was prepared by mixing 10 mg of bromophenol blue (0.02% final, w/v; USB, USA), 5 mL of 1 M Tris-HCl (0.1 M final, pH6.8; USB,

USA), 10 mL of 10% SDS solution (2% final, v/v; USB, USA), 10 mL of glycerol (20% final, v/v; USB, USA) and 2.5 mL of β-mercaptoethanol (5% final, v/v; Sigma, USA) in 50 mL of double distilled water. The buffer was stored as 1.5-mL aliquots at -20°C.

Lysis buffer for lysing HEK 293FT cells

The lysis buffer stock was prepared by adding 6.06 g of Tris-HCl (50 mM final; pH 8.0; USB, USA), 7.01 g of NaCl (120 mM final; USB, USA), 5 mL of Nonidet P-40 (NP-4; 0.5% final, v/v; GE Healthcare, UK), 0.37 g of EDTA (1 mM final, USB, USA) in 1 L of double distilled water. It was stored at 4°C. The working buffer was freshly prepared by addition of protease inhibitor cocktail (Sigma, USA) in 100-fold dilution.

Running gel solution

For a 1.5 mm mini gel, running gel solution was freshly prepared by mixing 3.08 or 2.7 mL of 30% acrylamide (12% or 8% final, v/v; Bio-Rad Laboratories, USA), 2.86 mL of 1 M Tris-HCl (pH 8.8; 0.4M final; USB, USA)), 1.67 or 2.05 mL of double distilled water, 77 µL of 10% SDS solution (1% final, v/v; USB, USA), 35 µL of 10% ammonium persulfate (APS; 0.04% final, w/v; USB, USA) and 4 µL of N,N,N',N'-Di-(dimethylamino)ethane (TEMED; USB, USA).

Stacking gel solution

For a 1.5 mm mini gel, stacking gel solution was freshly prepared by mixing 0.54 mL of 30% acrylamide (4% final, v/v; Bio-Rad Laboratories, USA), 1.06 mL of

0.1 M Tris-HCl (pH 6.8; 0.03 M final; USB, USA), 2.16 mL of double distilled water, 35 µL of 10% SDS solution (1% final, v/v; USB, USA), 14 µL of 10% APS (0.04% final, w/v; USB, USA) and 4 µL of TEMED (USB, USA).

Electrophoresis buffer for SDS-PAGE

The stock electrophoresis buffer (10X) was prepared by dissolving 30.28 g of Tris-base (0.25 M final; USB, USA), 144.13 g of glycine (1.92 M final; USB, USA) and 10 g of SDS (1% final, w/v; USB, USA) in 1 L of double distilled water. The working electrophoresis buffer (1X) was prepared by diluting the stock buffer 10-fold with double distilled water. Both stock and working solutions were kept at room temperature.

Transfer buffer

The stock transfer buffer (10X) was prepared by dissolving 30.28 g of Tris-base (0.25 M final; USB, USA) and 144.13 g of glycine (1.92 M final; USB, USA) in 1 L of double distilled water. Stock solution was kept at room temperature. The working transfer buffer (1X) was freshly prepared by mixing 70 mL of stock transfer buffer, 70 mL of methanol and 560 mL double distilled water together.

TBS

The stock TBS buffer (10X) was prepared by dissolving 24.22 g of Tris-base (0.2 M final; USB, USA) and 80.06 g of NaCl (1.37 M final; USB, USA) in 1 L of double distilled water with pH adjusted to 7.6. The working TBS buffer (1X) was prepared by diluting the stock solution 10-fold with double distilled water. Both

stock and working solutions were kept at room temperature.

TBST

TBST solution was prepared by adding 1 mL of Tween-20 (0.1% final, v/v; USB, USA) to 1 L of 1X TBS. It was kept at room temperature.

Blocking solution

Blocking solution was freshly prepared by dissolving 2.5 g of skimmed milk powder (5% final, w/v) in 50 mL of 1X TBST.

ECL reagent A

ECL reagent A was prepared by adding 9 mL of double distilled water, 1 mL of 1M Tris-HCl (pH 8.5; USB, USA), 45 µL of coumaric acid (Sigma, USA) and 100 µL of luminal (Sigma, USA). The solution was kept at 4°C and was stable for a month.

ECL reagent B

ECL reagent B was prepared by adding 9 mL of double distilled water, 1 mL of 1M Tris-HCl (pH 8.5; USB, USA) and 6 µL of hydrogen peroxide (BDH, UK). The solution was kept at 4°C and was stable for a month.

2.14.6 Formic acid treatment

SDS sample buffer (2%)

SDS sample buffer (2%) was prepared by dissolving 0.46 g of dithiothreitol

(DTT; 50 mM final; USB, USA) in 60 mL of 2% SDS solution (v/v; USB, USA). The buffer was stored as 1.5-mL aliquots at -20°C.

2.14.7 Filter retardation assay

SDS solution

The stock SDS solution (10%, w/v) was prepared by dissolving 100 g of SDS (USB, USA) in 1 L of double distilled water. The working 2% (v/v) SDS solution was prepared by diluting the stock solution 5-fold with double distilled water. The working 0.01% (v/v) SDS solution was prepared by diluting the 2% (v/v; from 10% stock solution) SDS solution 200-fold with double distilled water. Both the stock and working solutions were kept at room temperature.

2.14.8 Co-immunoprecipitation

Co-IP buffer

The co-IP buffer stock was prepared by adding 6.06 g of Tris-base (50 mM final; USB, USA), 7.01 g of NaCl (120 mM final; USB, USA), 5 mL of NP-40 (0.5% final, v/v; GE Healthcare, UK), 0.37 g of EDTA (1 mM final, USB, USA), 0.42 g of sodium fluoride (NaF; 10 mM final; USB, USA) in 1 L of double distilled water. The pH value was calibrated to 8.0. It was stored at 4°C. The working buffer was freshly prepared by addition of protease inhibitor cocktail (Sigma, USA) in 100-fold dilution.

2.14.9 *In vivo* ubiquitination assay

Ubiquitination assay buffer

The ubiquitination assay buffer stock was prepared by adding 6.06 g of Tris-base (50 mM final; USB, USA), 7.01 g of NaCl (120 mM final; USB, USA), 5 mL of NP-40 (0.5% final, v/v; GE Healthcare, UK), 0.37 g of EDTA (1 mM final, USB, USA), 0.42 g of NaF (10 mM final; USB, USA) in 1 L of double distilled water. The pH value was calibrated to 8.0. It was stored at 4°C. The working buffer was freshly prepared by addition of protease inhibitor cocktail (Sigma, USA) in 100-fold dilution and n-ethylaleimide (10mM final; Sigma, USA).

Chapter 3 Involvement of Cul1-based CRL in polyglutamine pathogenesis

3.1 Introduction

As mentioned in Chapter 1 (section 1.5), the CRLs are a large family of E3 ubiquitin ligases. They can be categorized into five main groups depending on which cullin proteins (Cul1-5) are employed [81]. By associating with different substrate receptors, different cullin proteins form different CRL complexes that target specific substrate proteins for ubiquitination [81]. Several lines of evidence have suggested association of CRLs with polyQ pathogenesis (reviewed in Chapter 1 section 1.5). Due to the substrate specificity of different CRL complexes, it is likely that certain groups of CRLs are particularly involved in polyQ pathogenesis.

To test this hypothesis, endogenous expression of five *cullin* genes *(Cul1-5)* were individually knocked down by RNAi [134] in fly polyQ disease models [24, 25, 117, 129]. Knock-down efficiency of expression of individual *cullins* was confirmed to be higher than 50% by semi-quantitative RT-PCR (Figure 3.1). In polyQ diseases, expansion of polyQ domain in disease proteins causes accumulation of SDS-insoluble polyQ proteins in neurons and results in neurotoxcity [52, 53, 135]. Therefore, the corresponding modifications on neurotoxicity and SDS-solubility of expanded polyQ protein upon knock-down of expression of individual *cullins* were examined to define the roles of cullins in polyQ diseases.

Figure 3.1

A

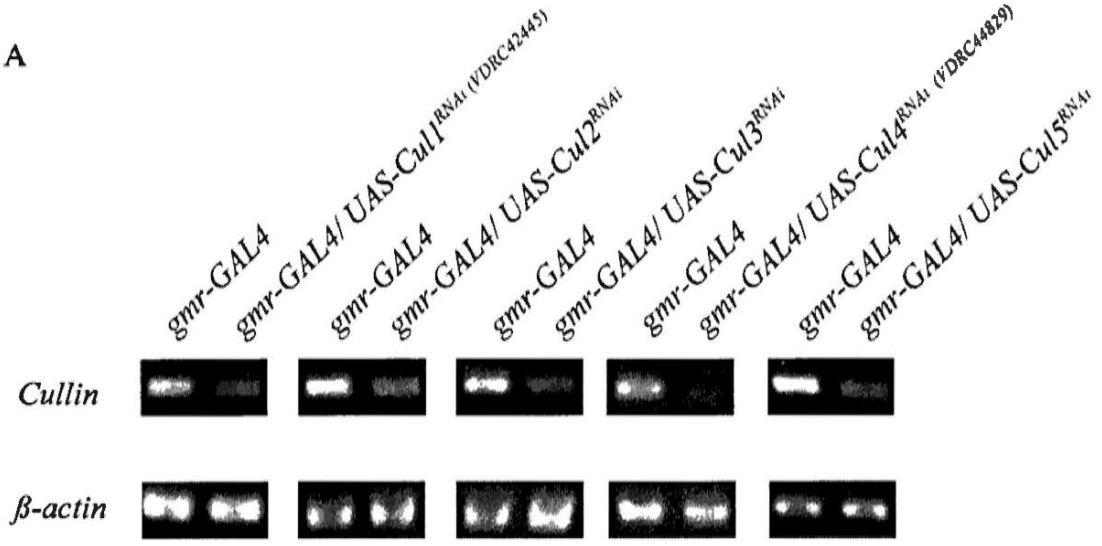
gmr-GAL4
gmr-GAL4/ UAS-Cul1RNAi (VDRC42445)
gmr-GAL4
gmr-GAL4/ UAS-Cul2RNAi
gmr-GAL4
gmr-GAL4/ UAS-Cul3RNAi
gmr-GAL4
gmr-GAL4/ UAS-Cul4RNAi (VDRC44829)
gmr-GAL4
gmr-GAL4/ UAS-Cul5RNAi
Cullin
ß-actin

B

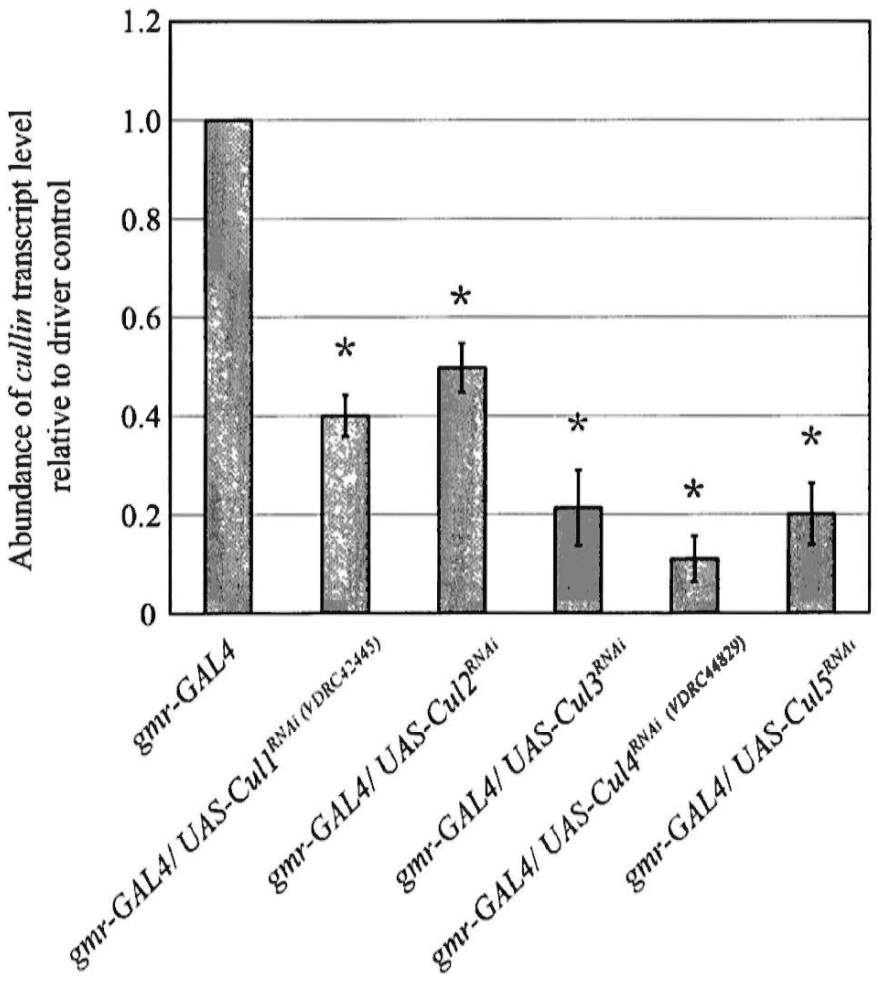
Abundance of cullin transcript level relative to driver control
1.2
1.0
0.8
0.6
0.4
0.2
0
*
*
*
*
*
gmr-GAL4
gmr-GAL4/ UAS-Cul1RNAi (VDRC42445)
gmr-GAL4/ UAS-Cul2RNAi
gmr-GAL4/ UAS-Cul3RNAi
gmr-GAL4/ UAS-Cul4RNAi (VDRC44829)
gmr-GAL4/ UAS-Cul5RNAi

Figure 3.1. Knock-down efficiency of expression of individual *cullins*.

(A) Transcript levels of individual *cullin* genes in different RNAi fly lines revealed by RT-PCR. *ß-actin* served as loading control. **(B)** Quantification of **(A)**. All RNAi fly lines achieved more than 50% reduction of corresponding *cullin* transcript level as compared to the *gmr-GAL4* driver-only control. N = 4, * $p < 0.01$ (Student's t-test); error bars represent mean ± SEM from four independent experiments. The flies were raised at 25°C and were assayed at 3 dpe. They were of genotypes:

w; *gmr-GAL4/+*; *+/+*,

w; *gmr-GAL4/+*; *UAS-Cul1*$^{RNAi\ (VDRC42445)}$*/+*,

w; *gmr-GAL4/+*; *UAS-Cul2*^{RNAi}*/+*,

w; *gmr-GAL4/UAS-Cul3*^{RNAi}; *+/+*,

w; *gmr-GAL4/UAS-Cul4*$^{RNAi\ (VDRC44829)}$; *+/+*,

w; *gmr-GAL4/UAS-Cul5*^{RNAi}; *+/+*.

In this study, it was found that *Cul1* modified polyQ toxicity and altered the abundance of SDS-insoluble expanded polyQ protein (sections 3.2 and 3.3). Toxicity assays were repeated in various polyQ disease models and a non-polyQ neurodegenerative disease model to test if the effect of *Cul1* was only specific to polyQ diseases (section 3.4). To investigate the detailed mechanisms behind the involvement of Cul1 protein in polyQ pathogenesis, the effect of *Cul1* on SDS-solubility of expanded polyQ protein was studied (section 3.5). Besides, physical interaction between Cul1 protein and expanded polyQ protein was examined to give insight into the functional relationship between them (section 3.6). Moreover, as the major function of Cul1-based CRL is on protein ubiquitination [81], the effect of *Cul1* on ubiquitination of expanded polyQ protein was studied as well (section 3.7). Furthermore, Hsp70 chaperone is a well-known suppressor of polyQ toxicity which works by promoting refolding of misfolded expanded polyQ protein [23, 135, 136]. By overexpression of *Hsp70*, the importance of protein refolding on the $Cul1^{RNAi}$-mediated enhancement on polyglutamine toxicity was examined (section 3.8). Lastly, to double confirm the effect of *Cul1* on polyglutamine toxicity, feasibility of overexpression study on effect of *Cul1* on polyglutamine toxicity was tested (section 3.9).

3.2 Involvement of cullins in polyglutamine toxicity

Examination of adult fly external eye depigmentation is a simple and reliable phenotypic assay for screening polyQ toxicity modifiers [137]. In the truncated SCA3 (SCA3tr) model [117], expression of a transgene encoding for the HA-tagged,

truncated form of the disease protein, ataxin-3, with unexpanded polyQ repeats of 27 glutamines (*HA-SCA3tr-Q27*) in the eye by *gmr-GAL4* did not cause degenerative phenotype (Figure 3.2A). However, weak expression of a transgene encoding for the HA-tagged, truncated ataxin-3 protein with expanded polyQ repeats of 78 glutamines (*HA-SCA3tr-Q78(w)*) induced late-onset progressive degeneration resulting in depigmentation at 32 days post-eclosion (dpe; Figure 3.2B). This *HA-SCA3tr-Q78(w)* line allows identification of any polyQ toxicity enhancers. Stronger expression of *HA-SCA3tr-Q78* transgene (*HA-SCA3tr-Q78(s)*) in another independent transgenic fly line induced more severe degeneration and earlier age of onset as shown by the extensive loss of pigmentation at 3 dpe (Figure 3.2C). This *HA-SCA3tr-Q78(s)* line allows identification of any polyQ toxicity suppressors. The difference in expression level of *HA-SCA3tr-Q78* transgene in two different transgenic fly lines was probably due to the difference in the chromosomal insertion site of the *HA-SCA3tr-Q78* transgene [117, 138].

Individual knock-down of *Cul2, 3* and *5* expression showed no effect on degeneration induced by *HA-SCA3tr-Q78* expression (Figure 3.3C, D and F). In contrast, knock-down of *Cul4* expression slightly enhanced degeneration as shown by the mild depigmentation in both *HA-SCA3tr-Q78(w)* and *HA-SCA3tr-Q78(s)*-expressing flies (Figure 3.3E). Knock-down of *Cul1* expression caused an even stronger enhancement as shown by the more extensive depigmentation and formation of necrotic scars on the eye surface in both *HA-SCA3tr-Q78(w)* and *HA-SCA3tr-Q78(s)*-expressing flies (Figure 3.3B). The stronger enhancing effect resulted from knock-down of *Cul1* expression when

Figure 3.2

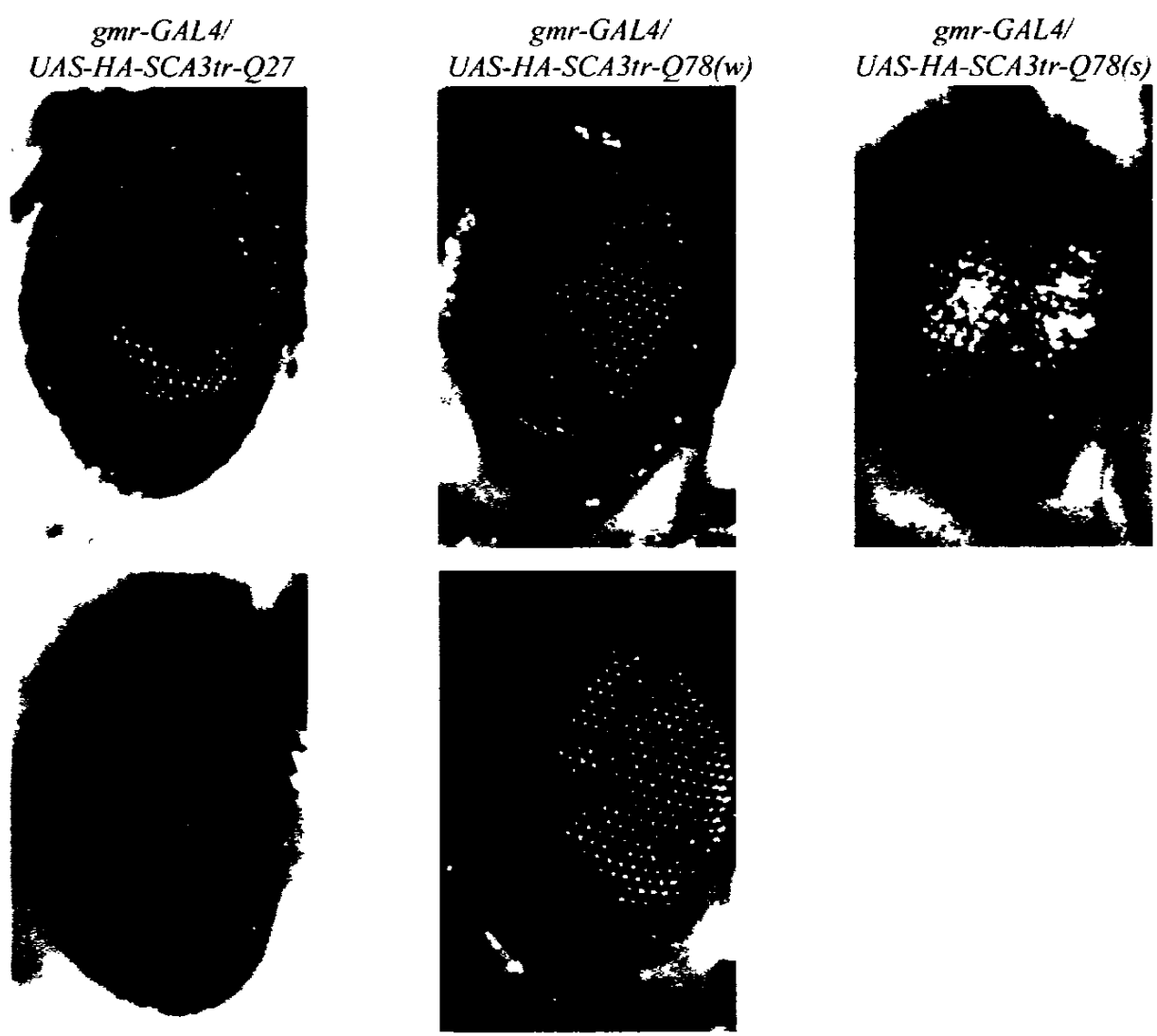
gmr-GAL4/
UAS-HA-SCA3tr-Q27
gmr-GAL4/
UAS-HA-SCA3tr-Q78(w)
gmr-GAL4/
UAS-HA-SCA3tr-Q78(s)
3dpe
32dpe

Figure 3.2. Expression of *HA-SCA3tr-Q78* transgene induced degenerative phenotype in adult fly eyes.

External eye depigmentation phenotypes of flies expressing truncated ataxin-3 transgenes (*HA-SCA3tr-Q27* or *HA-SCA3tr-Q78)* at 3 dpe and 32 dpe are shown. Transgenes were expressed using the *gmr-GAL4* driver. (**A**) Expression of *HA-SCA3tr-Q27* transgene did not cause any degenerative phenotype at both 3 dpe and 32 dpe. (**B**) Weak expression of *HA-SCA3tr-Q78* transgene (*HA-SCA3tr-Q78(w)*) induced mild depigmentation which could be observed at 32 dpe but not 3 dpe. (**C**) Strong expression of *HA-SCA3tr-Q78* transgene (*HA-SCA3tr-Q78(s)*) caused severe depigmentation at as early as 3 dpe. Most *HA-SCA3tr-Q78(s)*-expressing flies could not withstand the *HA-SCA3tr-Q78(s)*-induced toxicity and died before 32 dpe. Consistent results were obtained from three independent experiments. The flies were raised at 25°C. They were of genotypes:

(A) *w*; *gmr-GAL4 UAS-HA-SCA3tr-Q27/+*; *+/+*,

(B) *w*; *gmr-GAL4/+*; *UAS-HA-SCA3tr-Q78(w)/+*,

(C) *w*; *gmr-GAL4 UAS-HA-SCA3tr-Q78(s)/+*; *+/+*.

Figure 3.3

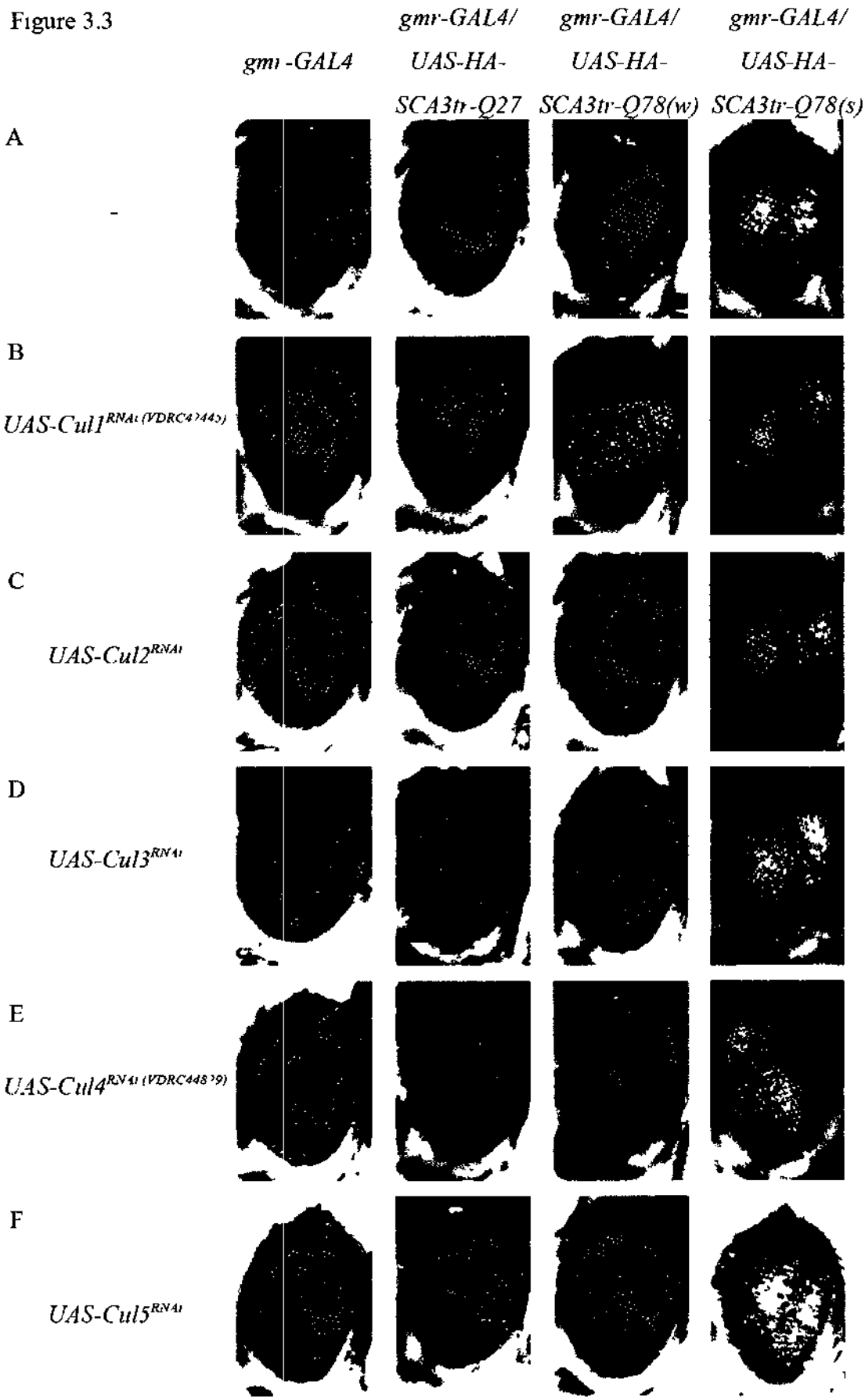
gmr-GAL4
gmr-GAL4/ UAS-HA-SCA3tr-Q27
gmr-GAL4/ UAS-HA-SCA3tr-Q78(w)
gmr-GAL4/ UAS-HA-SCA3tr-Q78(s)
A
-
B
UAS-Cul1RNAi (VDRC47445)
C
UAS-Cul2RNAi
D
UAS-Cul3RNAi
E
UAS-Cul4RNAi (VDRC44879)
F
UAS-Cul5RNAi

Figure 3.3. Knock-down of *Cul1* and *Cul4* expression enhanced degeneration induced by *HA-SCA3tr-Q78* expression in adult fly eyes.
External eye depigmentation phenotypes of *gmr-GAL4* driver-only control flies and flies expressing truncated ataxin-3 transgenes (*HA-SCA3tr-Q27* or *HA-SCA3tr-Q78)* with or without (as indicated by "-") individual knock-down of *cullins* expression are shown. Transgenes were expressed using the *gmr-GAL4* driver. (**A**) At 3 dpe, expression of *HA-SCA3tr-Q27* transgene did not cause any degenerative phenotype. Weak expression of *HA-SCA3tr-Q78* transgene (*HA-SCA3tr-Q78(w)*) did not cause any observable depigmentation while strong expression of *HA-SCA3tr-Q78* transgene (*HA-SCA3tr-Q78(s)*) caused extensive loss of pigmentation. (**B**) Knock-down of *Cul1* expression caused a Q-length specific enhancement of degenerative phenotype induced by both the weak and strong expressions of *HA-SCA3tr-Q78* transgene as indicated by the more extensive loss of pigmentation. (**C, D** and **F**) Knock-down of *Cul2* (**C**), *Cul3* (**D**) and *Cul5* (**F**) expression did not modify the *HA-SCA3tr-Q78*-induced degenerative phenotype. Knock-down of *Cul4* expression slightly enhanced depigmentation induced by *HA-SCA3tr-Q78* (**E**). (**G**) Depigmentation could be observed at 32 dpe but not at 3 dpe in *HA-SCA3tr-Q78(w)*-expressing flies. Consistent results were obtained from three independent experiments. The flies were raised at 25°C. They were of genotypes:
(**A**) *w; gmr-GAL4/+; +/+,*
w; gmr-GAL4 UAS-HA-SCA3tr-Q27/+; +/+,
w; gmr-GAL4/+; UAS-HA-SCA3tr-Q78(w)/+,
w; gmr-GAL4 UAS-HA-SCA3tr-Q78(s)/+; +/+
(**B**) *w; gmr-GAL4/+; UAS-Cul1$^{RNAi\ (VDRC42445)}$/+,*
w; gmr-GAL4 UAS-HA-SCA3tr-Q27/+; UAS-Cul1$^{RNAi\ (VDRC42445)}$/+,
w; gmr-GAL4/+; UAS-HA-SCA3tr-Q78(w)/UAS-Cul1$^{RNAi\ (VDRC42445)}$,
w; gmr-GAL4 UAS-HA-SCA3tr-Q78(s)/+; UAS-Cul1$^{RNAi\ (VDRC42445)}$/+
(**C**) *w; gmr-GAL4/+; UAS-Cul2^{RNAi}/+,*
w; gmr-GAL4 UAS-HA-SCA3tr-Q27/+; UAS-Cul2^{RNAi}/+,
w; gmr-GAL4/+; UAS-HA-SCA3tr-Q78(w)/UAS-Cul2^{RNAi},
w; gmr-GAL4 UAS-HA-SCA3tr-Q78(s)/+; UAS-Cul2^{RNAi}/+
(**D**) *w; gmr-GAL4/UAS-Cul3^{RNAi}; +/+,*
w; gmr-GAL4 UAS-HA-SCA3tr-Q27/UAS-Cul3^{RNAi}; +/+,
w; gmr-GAL4/UAS-Cul3^{RNAi}; UAS-HA-SCA3tr-Q78(w)/+,
w; gmr-GAL4 UAS-HA-SCA3tr-Q78(s)/UAS-Cul3^{RNAi}; +/+
(**E**) *w; gmr-GAL4/UAS-Cul4$^{RNAi\ (VDRC44829)}$; +/+,*
w; gmr-GAL4 UAS-HA-SCA3tr-Q27/UAS-Cul4$^{RNAi\ (VDRC44829)}$; +/+,
w; gmr-GAL4/UAS-Cul4$^{RNAi\ (VDRC44829)}$; UAS-HA-SCA3tr-Q78(w)/+,
w; gmr-GAL4 UAS-HA-SCA3tr-Q78(s)/UAS-Cul4$^{RNAi\ (VDRC44829)}$; +/+
(**F**) *w; gmr-GAL4/UAS-Cul5^{RNAi}; +/+,*
w; gmr-GAL4 UAS-HA-SCA3tr-Q27/UAS-Cul5^{RNAi}; +/+,
w; gmr-GAL4/UAS-Cul5^{RNAi}; UAS-HA-SCA3tr-Q78(w)/+,
w; gmr-GAL4 UAS-HA-SCA3tr-Q78(s)/UAS-Cul5^{RNAi}; +/+
(**G**) *w; gmr-GAL4/+; UAS-HA-SCA3tr-Q78(w)/+.*

compared to *Cul4* could not be due to the difference in the knock-down efficiency as the knock-down efficiency was higher in $Cul4^{RNAi}$ flies (Figure 3.1). Rather, the stronger enhancing effect by knock-down of *Cul1* expression was likely to be due to the intrinsic property of Cul1.

To exclude the possibility of off-target effect due to non-specific binding of double-stranded RNA (dsRNA) on mRNA of non-target gene(s), the above examination of adult fly external eye depigmentation was repeated using another independent $Cul1^{RNAi}$ fly line ($UAS\text{-}Cul1^{RNAi\ (NIG1877R\text{-}2)}$ of Figure 3.4) in which the *Cul1 dsRNA* sequence was distinct from the one in the $Cul1^{RNAi}$ fly line used in Figure 3.3B ($UAS\text{-}Cul1^{RNAi\ (VDRC42445)}$). It was found that the enhancing effect upon knock-down of *Cul1* expression was reproducible in this $UAS\text{-}Cul1^{RNAi\ (NIG1877R\text{-}2)}$ line (Figure 3.6B). Similarly, the examination of adult fly external eye depigmentation was repeated using another independent $Cul4^{RNAi}$ fly line ($UAS\text{-}Cul4^{RNAi\ (NIG8711R\text{-}2)}$ in Figure 3.5)) in which the *Cul4 dsRNA* sequence was distinct from the one in the $Cul4^{RNAi}$ fly line used in Figure 3.3E ($UAS\text{-}Cul4^{RNAi\ (VDRC44829)}$). The enhancing effect upon knock-down of *Cul4* expression was also reproducible in this $UAS\text{-}Cul4^{RNAi\ (NIG8711R\text{-}2)}$ line (Figure 3.6C). Hence, the enhancing effect observed was due to specific knock-down of *Cul1* and *Cul4* expression.

3.3 Distinct effects of knock-down of *Cul1* and *Cul4* expression on SDS-solubility of expanded polyglutamine protein

As it was found that both Cul1 protein and Cul4 protein were involved in polyQ toxicity, it is interesting to know if these two cullins played the same role in polyQ

Figure 3.4

A

```
Cul1 CDS                 GTTCTGACGGCGTTCAACAATGACAACGGATTTGTGGCCGCTTTGGACAAGGCGTGTGGA 1200
Cul1 dsRNA (VDRC42445)   ------------------------ACGGATTTGTGGCCGCTTTGGACAAGGCGTGTGGA 35
                                                  ************************************

Cul1 CDS                 AAGTTCATAAACTCGAACGTGGTCACGATCGCAAACAGTGCTAGCAAGTCGCCCGAATTG 1260
Cul1 dsRNA (VDRC42445)   AAGTTCATAAACTCGAACGTGGTCACGATCGCAAACAGTGCTAGCAAGTCGCCCGAATTG 95
                         ************************************************************

Cul1 CDS                 CTGGCCAAGTACTGCGATCTGTTATTAAAAAAATCCTCGAAAAATCCCGAGGACAAGGAG 1320
Cul1 dsRNA (VDRC42445)   CTGGCCAAGTACTGCGATCTGTTATTAAAAAAATCCTCGAAAAATCCCGAGGACAAGGAG 155
                         ************************************************************

Cul1 CDS                 CTCGAGGACAATCTTAACCAGGTGATGGTCGTGTTCAAGTATATCGAGGATAAGGACGTC 1380
Cul1 dsRNA (VDRC42445)   CTCGAGGACAATCTTAACCAGGTGATGGTCGTGTTCAAGTATATCGAGGATAAGGACGTC 215
                         ************************************************************

Cul1 CDS                 TTCCAAAAATATTACTCCAAGATGCTTGCTAAGCGCTTGGTTAACCACACATCGGCTTCG 1440
Cul1 dsRNA (VDRC42445)   TTCCAAAAATATTACTCCAAGATGCTTGCTAAGCGCTTGGTTAACCACACATCGGCTTCG 275
                         ************************************************************

Cul1 CDS                 GATGACGCCGAGGCTATGATGATCTCCAAACTGAAGCAGACATGTGGTTACGAATACACC 1500
Cul1 dsRNA (VDRC42445)   GATGACGCCGAGGCTATGATGATCTCCAAACTGAAGCAGACATGTGGTTACGAATACACC 335
                         ************************************************************

Cul1 CDS                 GTCAAGCTTCAGAGGATGTTCCAGGACATTGGCGTCTCAAAGGACTTGAACTCGTACTTT 1560
Cul1 dsRNA (VDRC42445)   GTCAAGCTTCAGAGGATGTTCCAGGACATTGGCGTCTCAAAGGA---------------- 379
                         *******************************************
```

B

```
Cul1 CDS                   ATGAACCGCTCCGGCAATTCCCAGACCACACAGAAACTCGTCAACCTGGACGATATCTGG 60
Cul1 dsRNA (NIG1877R-2)    ------------GGCAATTCCCAGACCACACAGAAACTCGTCAACCTGGACGATATCTGG 48
                                      ************************************************

Cul1 CDS                   AGCGAATTGGTCGAGGGCATTATGCAGGTGTTTGAGCACGAGAAGTCCCTCACCCGCAGC 120
Cul1 dsRNA (NIG1877R-2)    AGCGAATTGGTCGAGGGCATTATGCAGGTGTTTGAGCACGAGAAGTCCCTCACCCGCAGC 108
                           ************************************************************

Cul1 CDS                   CAGTACATGCGTTTCTACACTCACGTCTATGACTACTGCACCAGCGTGAGCGCGGCTCCA 180
Cul1 dsRNA (NIG1877R-2)    CAGTACATGCGTTTCTACACTCACGTCTATGACTACTGCACCAGCGTGAGCGCGGCTCCA 168
                           ************************************************************

Cul1 CDS                   AGCGGACGGAGCAGCGGAAAGACAGGCGGAGCGCAGCTGGTGGGCAAGAAGCTGTACGAC 240
Cul1 dsRNA (NIG1877R-2)    AGCGGACGGAGCAGCGGAAAGACAGGCGGAGCGCAGCTGGTGGGCAAGAAGCTGTACGAC 228
                           ************************************************************

Cul1 CDS                   CGGCTGGAACAATTTCTCAAGTCATACCTGAGCGAGCTGCTCACCAAGTTCAAGGCCATC 300
Cul1 dsRNA (NIG1877R-2)    CGGCTGGAACAATTTCTCAAGTCATACCTGAGCGAGCTGCTCACCAAGTTCAAGGCCATC 288
                           ************************************************************

Cul1 CDS                   AGCGGCGAGGAGGTACTCCTGTCGCGCTACACCAAACAGTGGAAGTCGTATCAGTTCTCC 360
Cul1 dsRNA (NIG1877R-2)    AGCGGCGAGGAGGTACTCCTGTCGCGCTACACCAAACAGTGGAAGTCGTATCAGTTCTCC 348
                           ************************************************************

Cul1 CDS                   AGTACCGTTCTGGACGGCATCTGCAACTACCTGAATCGGAACTGGGTGAAGCGCGAGTGC 420
Cul1 dsRNA (NIG1877R-2)    AGTACCGTTCTGGACGGCATCTGCAACTACCTGAATCGGAACTGGGTGAAGCGCGAGTGC 408
                           ************************************************************

Cul1 CDS                   GAGGAGGGGCAGAAGGGTATCTACAAGATCTACCGACTGGCCCTCGTCGCCTGGAAGGGA 480
Cul1 dsRNA (NIG1877R-2)    GAGGAGGGGCAGAAGGGTATCTACAAGATCTACCGACTGGCCCTCGTCGCCTGGAAGGGA 468
                            ***********************************************************

Cul1 CDS                   CATTTGTTCCAAGTGCTAAATGAGCCGGTCACCAAGGCAGTGCTCAAGTCCATTGAGGAG 540
Cul1 dsRNA (NIG1877R-2)    CATTTGTTCCAAGTGCTAAATGAGCCGGTCAC---------------------------- 500
                           *********************************
```

C

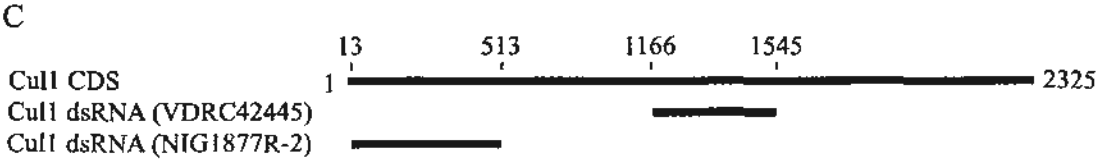

Figure 3.4. dsRNA sequences of two independent *Cul1*^{RNAi} fly lines.

There are 2,325 bp in the coding sequence (CDS) of fly *Cul1* (protein product: FBpp0087921 (FlyBase)). (**A**) The dsRNA sequence in *UAS-Cul1*$^{RNAi\ (VDRC42445)}$ fly line (Line No. 42445 from the Vienna *Drosophila* RNAi Center) targets at nt 1,166 to nt 1,545 of *Cul1* CDS. (**B**) The dsRNA sequence in *UAS-Cul1*$^{RNAi\ (NIG1877R-2)}$ fly line (Line No. 1877R-2 from the National Institute of Genetics) targets at nt 13 to nt 513 of *Cul1* CDS. "*" indicates perfect match between nt from two aligned sequences at the corresponding position while "-" indicates that there is no nt at the corresponding position. Nucleotide 1 is defined as the starting nt of the corresponding sequence. (**C**) Schematic diagram showing the overlapping region between *Cul1* CDS and the *Cul1 dsRNA* sequences of the two *Cul1*^{RNAi} lines used in this study.

Figure 3.5

A

```
Cul4 CDS                TATGTGCTGCAAAATTCGACCGTTCACTCGATTTGGGACATGGGGCTGGACCTTTTTCGC 720
Cul4 dsRNA (VDRC44829)  -----GCTGCAAAATTCGACCGTTCACTCGATTTGGGACATGGGGCTGGACCTTTTTCGC 55
                             ************************************************************

Cul4 CDS                ATCCATTTTGCTCAAAACAGCGTTGTCCAAAAGCGAACCGTCGACGGTTTACTAACGCTT 780
Cul4 dsRNA (VDRC44829)  ATCCATTTTGCTCAAAACAGCGTTGTCCAAAAGCGAACCGTCGACGGTTTACTAACGCTT 115
                        ************************************************************

Cul4 CDS                ATTGAAAAAGAACGACAAGGCTCCACCGTGGACCGTGGTTTGCTGAAGAGCTTGGTTCGC 840
Cul4 dsRNA (VDRC44829)  ATTGAAAAAGAACGACAAGGCTCCACCGTGGACCGTGGTTTGCTGAAGAGCTTGGTTCGC 175
                        ************************************************************

Cul4 CDS                ATGTTATGCGACCTGCAGATCTACACCAGCTCCTTTGAGGAGAAGTTCCTCGACGCAACC 900
Cul4 dsRNA (VDRC44829)  ATGTTATGCGACCTGCAGATCTACACCAGCTCCTTTGAGGAGAAGTTCCTCGACGCAACC 235
                        ************************************************************

Cul4 CDS                AATCAATTGTATAAGGCTGAGAGTCAACGCAAGATGCAAGAACTGGAAGTTCCCGAGTAC 960
Cul4 dsRNA (VDRC44829)  AATCAATTGTATAAGGCTGAGAGTCAACGCAAGATGCAAGAACTGGAAGTTCCCGAGTAC 295
                        ************************************************************

Cul4 CDS                TTACAACACGTCAACAAGCGTTTGGCCGAGGAGAACGAGCGTTTGCGTCACTATCTGGAC 1020
Cul4 dsRNA (VDRC44829)  TTACAACACGTCAACAAGCGTTTGGCCGAGGAGAACGAGC---------------------- 335
                        ****************************************
```

B

```
Cul4 CDS                AATATTGCCGCCTGCCTGAAGAAGGCCGAGAACGTCGCCCCCACCGCTGCTGCCGCCTCG 120
Cul4 dsRNA (NIG8711R-1) ----------CTGCCTGAAGAAGGCCGAGAACGTCGCCCCCACCGCTGCTGCCGCCTCG 49
                                   ************************************************

Cul4 CDS                AGCGTGGGCCGCAGTGCCTTCGCTGCCCAAAACATGAATTCTGCGTCCACCAACGGCGAG 180
Cul4 dsRNA (NIG8711R-1) AGCGTGGGCCGCAGTGCCTTCGCTGCCCAAAACATGAATTCTGCGTCCACCAACGGCGAG 109
                        ************************************************************

Cul4 CDS                CGCCTGCCAAACTTCTCCAAGCTAGGCGGCAGCCATGGCGAGATCCGCACGGCTTCAACT 240
Cul4 dsRNA (NIG8711R-1) CGCCTGCCAAACTTCTCCAAGCTAGGCGGCAGCCATGGCGAGATCCGCACGGCTTCAACT 169
                        ************************************************************

Cul4 CDS                ACCTCAAATCTCCTCAATCGCATGGGGGCTATTCACAACAGCAAGCCTGGCGATGTCAAG 300
Cul4 dsRNA (NIG8711R-1) ACCTCAAATCTCCTCAATCGCATGGGGGCTATTCACAACAGCAAGCCTGGCGATGTCAAG 229
                        ************************************************************

Cul4 CDS                AAGATAGTGATTAAGAACTTTAAGGATAAGCCTACACTGCCCGATAACTATTCCAAGGAC 360
Cul4 dsRNA (NIG8711R-1) AAGATAGTGATTAAGAACTTTAAGGATAAGCCTACACTGCCCGATAACTATTCCAAGGAC 289
                        ************************************************************

Cul4 CDS                ACGTACGTGAAGCTTGAAGAAGCCGTTATCGCCATCCAACTCTCCAAGCCCATTAAATAT 420
Cul4 dsRNA (NIG8711R-1) ACGTACGTGAAGCTTGAAGAAGCCGTTATCGCCATCCAACTCTCCAAGCCCATTAAATAT 349
                        ************************************************************

Cul4 CDS                TCGCTGGAGGAGCTCTACCAGGCGGTGGTGAACATGTGTAGCCACAAGATGGATGCACAA 480
Cul4 dsRNA (NIG8711R-1) TCGCTGGAGGAGCTCTACCAGGCGGTGGTGAACATGTGTAGCCACAAGATGGATGCACAA 409
                        ************************************************************

Cul4 CDS                TTATACGCGAAACTCAAGGAGCTAACAGAGCAACACGTAAAGCGCAATATTAAGCTCAAG 540
Cul4 dsRNA (NIG8711R-1) TTATACGCGAAACTCAAGGAGCTAACAGAGCAACACGTAAAGCGCAATATTAAGCTCAAG 469
                        ************************************************************

Cul4 CDS                GAGCTCACCGGCGGTAGCATGGACAAACTGATTTTGCTGGAAAAGATCAACCACTGGTGG 600
Cul4 dsRNA (NIG8711R-1) GAGCTCACCGGCGGTAGCATGGACAAACTGA---------------------------- 500
                        *********************************
```

C

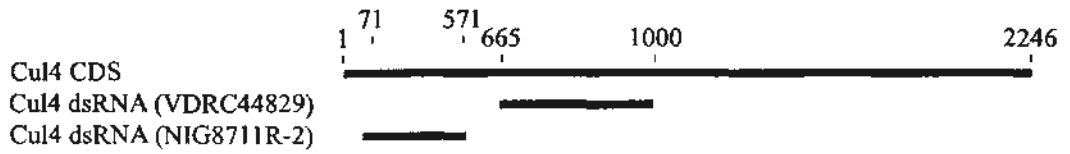

Figure 3.5. dsRNA sequences of two independent *Cul4*^{RNAi} fly lines.

There are 2,246 bp in the CDS of fly *Cul4* (protein product: FBpp0087897 (FlyBase)). (**A**) The dsRNA sequence in *UAS-Cul4*$^{RNAi\ (VDRC44829)}$ fly line (Line No. 44829 from the Vienna *Drosophila* RNAi Center) targets at nt 665 to nt 1,000 of *Cul4* CDS. (**B**) The dsRNA sequence in *UAS-Cul4*$^{RNAi\ (NIG8711R-1)}$ fly line (Line No. 8711R-1 from the National Institute of Genetics) targets at nt 71 to nt 571 of *Cul4* CDS. "*" indicates perfect match between nt from two aligned sequences at the corresponding position while "-" indicates that there is no nt at the corresponding position. Nucleotide 1 is defined as the starting nt of the corresponding sequence. (**C**) Schematic diagram showing the overlapping region between *Cul4* CDS and the *Cul4 dsRNA* sequences of the two *Cul4*^{RNAi} lines used in this study.

Figure 3 6

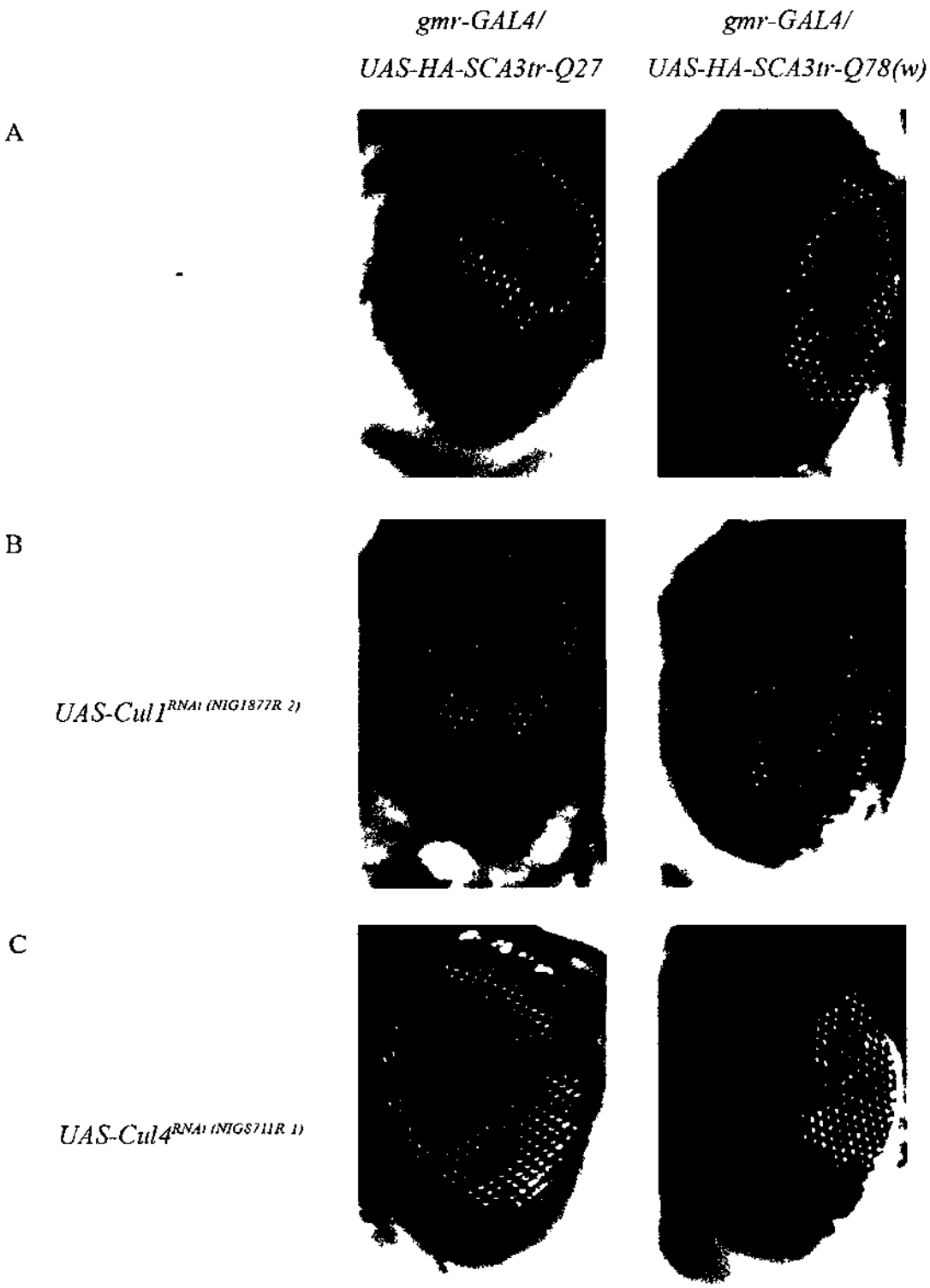
gmr-GAL4/
UAS-HA-SCA3tr-Q27
gmr-GAL4/
UAS-HA-SCA3tr-Q78(w)
A
B
UAS-Cul1RNAi (NIG1877R 2)
C
UAS-Cul4RNAi (NIG5711R 1)

Figure 3.6 Effect by knock-down of *Cul1* and *Cul4* expression was reproducible in another independent $Cul1^{RNAi}$ and $Cul4^{RNAi}$ lines.

External eye depigmentation phenotypes of flies expressing truncated ataxin-3 transgenes (*HA-SCA3tr-Q27* or *HA-SCA3tr-Q78)* with or without (as indicated by "-") knock-down of *Cul1* or *Cul4* expression are shown. Transgenes were expressed using the *gmr-GAL4* driver. (**A**) At 3 dpe, expression of *HA-SCA3tr-Q27* transgene did not cause any degenerative phenotype. Weak expression of *HA-SCA3tr-Q78* transgene (*HA-SCA3tr-Q78(w)*) did not cause any observable depigmentation. (**B** and **C**) Knock-down of either *Cul1* (**B**) or *Cul4* (**C**) expression caused a Q-length specific enhancement on degenerative phenotype induced by expression of *HA-SCA3tr-Q78* transgene as indicated by the more extensive loss of pigmentation. The flies were raised at 25°C. They were of genotypes:

(**A**) *w*; *gmr-GAL4 UAS-HA-SCA3tr-Q27/+*; *+/+*,

w; *gmr-GAL4/+*; *UAS-HA-SCA3tr-Q78(w)/+*

(**B**) *w*; *gmr-GAL4 UAS-HA-SCA3tr-Q27/+*; $UAS\text{-}Cul1^{RNAi\ (NIG1877R-2)}/+$,

w; *gmr-GAL4/+*; $UAS\text{-}HA\text{-}SCA3tr\text{-}Q78(w)/UAS\text{-}Cul1^{RNAi\ (NIG1877R-2)}$,

(**C**) *w*; *gmr-GAL4 UAS-HA-SCA3tr-Q27/*$UAS\text{-}Cul4^{RNAi\ (NIG8711R-1)}$; *+/+*,

w; *gmr-GAL4/*$UAS\text{-}Cul4^{RNAi\ (NIG8711R-1)}$; *UAS-HA-SCA3tr-Q78(w)/+*.

pathogenesis.

In the full-length SCA3 (SCA3fl) model [129], a myc-tagged, full-length ataxin-3 protein with either unexpanded polyQ repeats of 27 glutamines (myc-SCA3fl-Q27) or expanded polyQ repeats of 84 glutamines (myc-SCA3fl-Q84) was expressed [129]. The study on the effect of *Cul1* and *Cul4* on polyQ toxicity was repeated in this model because of the following reasons. First, this model tested if the protein context of ataxin-3 affected the modification by *Cul1* and *Cul4*. Second, it is reported that truncated polyQ disease proteins are more prone to aggregation [139]. Due to the full-length nature of myc-SCA3fl-Q84 protein, myc-SCA3fl-Q84 protein is more SDS-soluble [129, 140] than HA-SCA3tr-Q78 protein which was largely SDS-insoluble [117]. Thus, in comparison with the SCAtr model, the SCA3fl model allowed study on both the SDS-soluble and the SDS-insoluble fractions of expanded polyQ protein [140]. As a result, the SCA3fl model allowed exploration on the link between the effect on polyQ toxicity and any alteration on SDS-solubility of expanded polyQ protein by *Cul1* and *Cul4*.

Besides higher SDS-solubility, myc-SCA3fl-Q84 protein is less toxic than HA-SCA3tr-Q78 protein [129, 140]. Therefore, a more sensitive toxicity assay named the deep pseudopupil assay was used to measure the effect of *Cul1* and *Cul4* on the relatively mild degeneration induced by *myc-SCA3fl-Q84* expression [141-144]. In *Drosophila*, each compound eye contains many repeating units named ommatidia. In each ommatidium, there is a cluster of photoreceptor neurons (Figure 3.7). Rhabdomeres refer to the light-capturing organelles in the photoreceptor

Figure 3.7

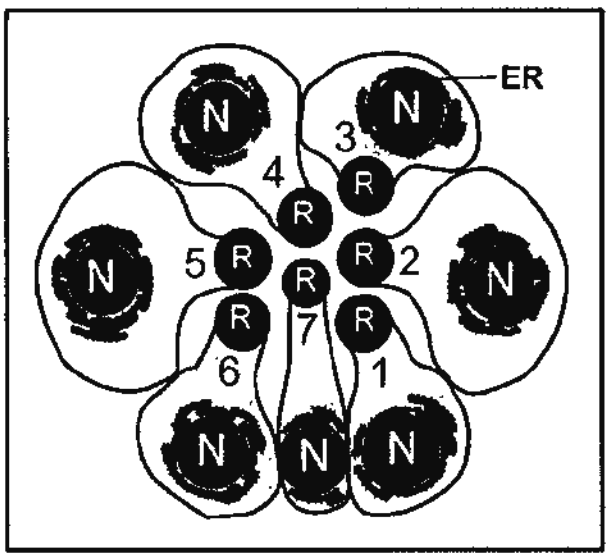

Figure 3.7. Schematic diagram showing the transverse cross-section of R1-7 photoreceptor neurons.

Rhabdomere (R; black structure) is a photosensitive organelle inside a photoreceptor neuron (in grey). It is composed of microvili which carry the rhodopsin photopigments and other components of the phototransduction cascade. Red structures: endoplasmic reticular (ER) membrane system; Blue structures: nuclei (N; adapted from [145]).

neurons [145]. In the deep pcusdopupil assay, each intact rhabdomere can be observed as a light spot under microscopic observation. Polyglutamine-induced degeneration in the eyes disrupts the rhabdomeres structure and causes a reduction of light spots being observed [25]. This inverse correlation between the degree of degeneration and the number of rhabdomeres per ommatidium is widely used to assay the modification on polyQ degeneration quantitatively [141-144]. Here, in fly eyes expressing myc-SCA3fl-Q27 protein, nearly 6 rhabdomeres (an average of 5.81) could be observed, while expression of the expanded polyQ domain-containing protein myc-SCA3fl-Q84 caused a reduction in rhabdomere score to close to 5 (an average of 4.88; Figure 3.8A). This shows that expansion of the polyQ domain induced degeneration which disrupted the rhabdomeres structure. Knock-down of *Cul1* or *Cul4* expression caused a Q-length specific reduction in the rhabdomere score to around 4 (Figure 3.8B). These data are consistent with the finding in SCA3tr model (Figure 3.3B and E) and confirm that *Cul1* and *Cul4* modify polyQ toxicity regardless of the protein context of the disease protein in polyQ diseases.

To test if the above modification was linked to any alteration on the SDS-solubility of expanded polyQ protein, the fly head lysate was subjected to filter retardation assay [146]. In this assay, the protein sample was pumped through a cellulose membrane with 0.22 μm pore size. Any SDS-insoluble protein aggregates with diameter larger than 0.22 μm would be captured by the membrane for subsequent immunodetection. This assay was therefore used to capture any SDS-insoluble myc-SCA3fl-Q84 protein aggregates with diameter larger than 0.22 μm for immunodetection [146] (Figure 3.9). Knock-down of *Cul1*, but not *Cul4*

Figure 3.8

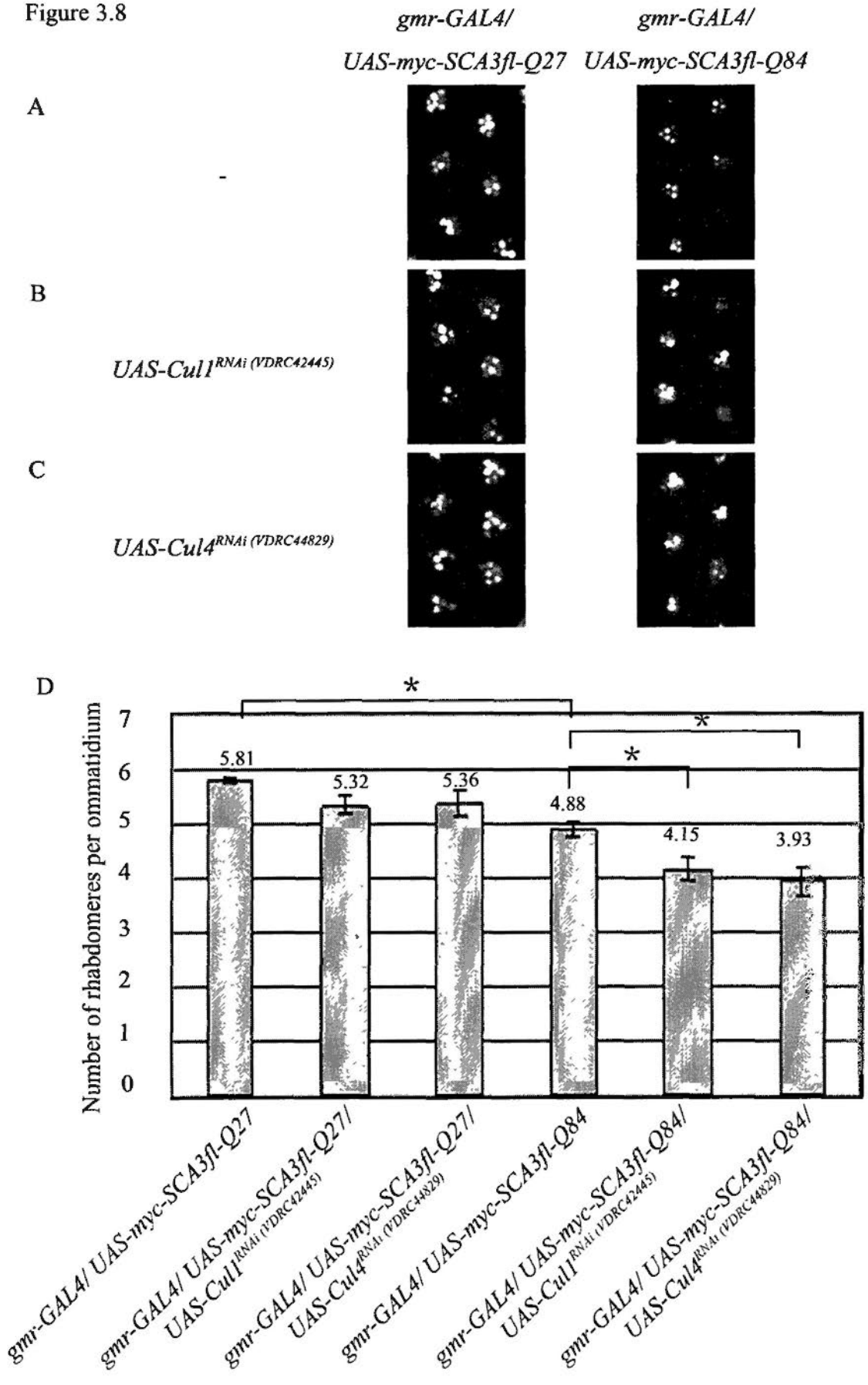
gmr-GAL4/
UAS-myc-SCA3fl-Q27
gmr-GAL4/
UAS-myc-SCA3fl-Q84
A
B
UAS-Cul1RNAi (VDRC42445)
C
UAS-Cul4RNAi (VDRC44829)
D
Number of rhabdomeres per ommatidium
0
1
2
3
4
5
6
7
5.81
5.32
5.36
4.88
4.15
3.93
*
*
*
gmr-GAL4/ UAS-myc-SCA3fl-Q27
gmr-GAL4/ UAS-myc-SCA3fl-Q27/ UAS-Cul1RNAi (VDRC42445)
gmr-GAL4/ UAS-myc-SCA3fl-Q27/ UAS-Cul4RNAi (VDRC44829)
gmr-GAL4/ UAS-myc-SCA3fl-Q84
gmr-GAL4/ UAS-myc-SCA3fl-Q84/ UAS-Cul1RNAi (VDRC42445)
gmr-GAL4/ UAS-myc-SCA3fl-Q84/ UAS-Cul4RNAi (VDRC44829)

Figure 3.8. Enhancement by knock-down of *Cul1* and *Cul4* expression was reproducible in the SCA3fl model.

(**A** - **C**) Deep pseudopupil images of flies expressing full-length ataxin-3 transgenes (*myc-SCAfl-Q27* or *myc-SCA3fl-Q78)* with or without (as indicated by "-") knock-down of *Cul1* and *Cul4* expression are shown. Transgenes were expressed using the *gmr-GAL4* driver. On average, 5.81 rhabdomeres per ommatidium could be observed under microscope in flies expressing *myc-SCA3fl-Q27* transgene (**A**). Expansion of the polyQ tract to Q84 caused a reduction in the rhabdomere score to an average of 4.88. Knock-down of either *Cul1* (**B**) or *Cul4* (**C**) expression caused a Q-length specific enhancement on degeneration induced by *myc-SCA3fl-Q84* expression and reduced the rhabdomere score to an average of 4.1 and 3.93 respectively. (**D**) Quantification of (**A** - **C**). N = 16, * $p < 0.01$ (Mann-Whitney Rank Sum Test); error bars represent mean ± SEM from at least 16 flies from three independent experiments. At least 320 ommatidia were scored per group. The flies were raised at 21°C and were assayed at 2 dpe. They were of genotypes:

(**A**) *w*; *gmr-GAL4 UAS-myc-SCA3fl-Q27/+*; *+/+*,

w; *gmr-GAL4/+*; *UAS-myc-SCA3fl-Q84/+*

(**B**) *w*; *gmr-GAL4 UAS-myc-SCA3fl-Q27/+*; *UAS-Cul1*$^{RNAi\ (VDRC42445)}$*/+*,

w; *gmr-GAL4/+*; *UAS-myc-SCA3fl-Q84/UAS-Cul1*$^{RNAi\ (VDRC42445)}$

(**C**) *w*; *gmr-GAL4 UAS-myc-SCA3fl-Q27/UAS-Cul4*$^{RNAi\ (VDRC44829)}$; *+/+*,

w; *gmr-GAL4/UAS-Cul4*$^{RNAi\ (VDRC44829)}$; *UAS-myc-SCA3fl-Q84/+*.

Figure 3.9

gmr-GAL4	+	+	+	+	+
UAS-myc-SCA3fl-Q84	-	+	+	+	+
UAS-Cul1$^{RNAi\ (VDRC42445)}$	-	-	+	-	-
UAS-Cul2^{RNAi}	-	-	-	+	-
UAS-Cul4$^{RNAi\ (VDRC44829)}$	-	-	-	-	+

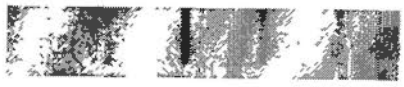

Figure 3.9. Knock-down of *Cul1* expression increased the level of SDS-insoluble myc-SCA3fl-Q84 protein.

Adult head lysate of *gmr-GAL4* control flies and *myc-SCA3fl-Q84*-expressing flies with or without knock-down of individual *cullin* genes was subjected to filter retardation assay. The immunoblot was probed with anti-myc antibody to detect presence of any SDS-insoluble myc-SCA3fl-Q84 protein aggregates with size larger than 0.22 μm. Knock-down of *Cul1* expression intensified the signal for insoluble myc-SCA3fl-Q84 protein. The experiment was performed once. The flies were raised at 21°C and were assayed at 2 dpe. They were of genotypes:

w; *gmr-GAL4/+*; *+/+*,

w; *gmr-GAL4/+*; *UAS-myc-SCA3fl-Q84/+*,

w; *gmr-GAL4/+*; *UAS-myc-SCA3fl-Q84/UAS-Cul1*$^{RNAi\ (VDRC42445)}$,

w; *gmr-GAL4/+*; *UAS-myc-SCA3fl-Q84/UAS-Cul2*^{RNAi},

w; *gmr-GAL4/UAS-Cul4*$^{RNAi\ (VDRC44829)}$; *UAS-myc-SCA3fl-Q84/+*.

expression, caused an increase in the level of SDS-insoluble myc-SCA3fl-Q84 protein (Figure 3.9). This suggests that *Cul1*, but not *Cul4*, modifies the SDS-solubility of expanded polyQ protein.

3.4 Specificity of the enhancement on polyglutamine toxicity by knock-down of *Cul1* expression

To test if the effect of *Cul1* on toxicity is specific to the polyQ domain, examination of adult fly external eye depigmentation was performed in two additional polyQ disease models. The first one is the truncated AR (ARtr) model [24]. PolyQ tract-expanded AR protein is the disease protein for the polyQ disease named SBMA [24, 147]. Flies expressing a transgene encoding for a truncated form of AR with normal Q-length (*ARtr-Q16*) in the eyes by *gmr-GAL4* driver did not induce any degenerative phenotype (Figure 3.10A). Conversely, weak expression of a transgene encoding for an expanded form of ARtr (*ARtr-Q112(w)*) induced degeneration resulting in mild depigmentation (Figure 3.10A). Knock-down of *Cul1* expression in the eyes of the *ARtr-Q112(w)*-expressing flies caused extensive loss of pigmentation and formation of necrotic scars (Figure 3.10B).

In another polyQ disease model, the eGFP-polyQ model, an eGFP is fused to a polyQ tract with an expanded polyQ repeat of 76 glutamines [52]. Expression of *eGFP-Q76* in the eyes by *gmr-GAL4* driver induced degeneration resulting in depigmentation (Figure 3.11A). Knock-down of *Cul1* expression in the eyes enhanced the *eGFP-Q76*-induced toxicity and led to more extensive loss of pigmentation and formation of necrotic scars (Figure 3.11B). These data are

Figure 3.10

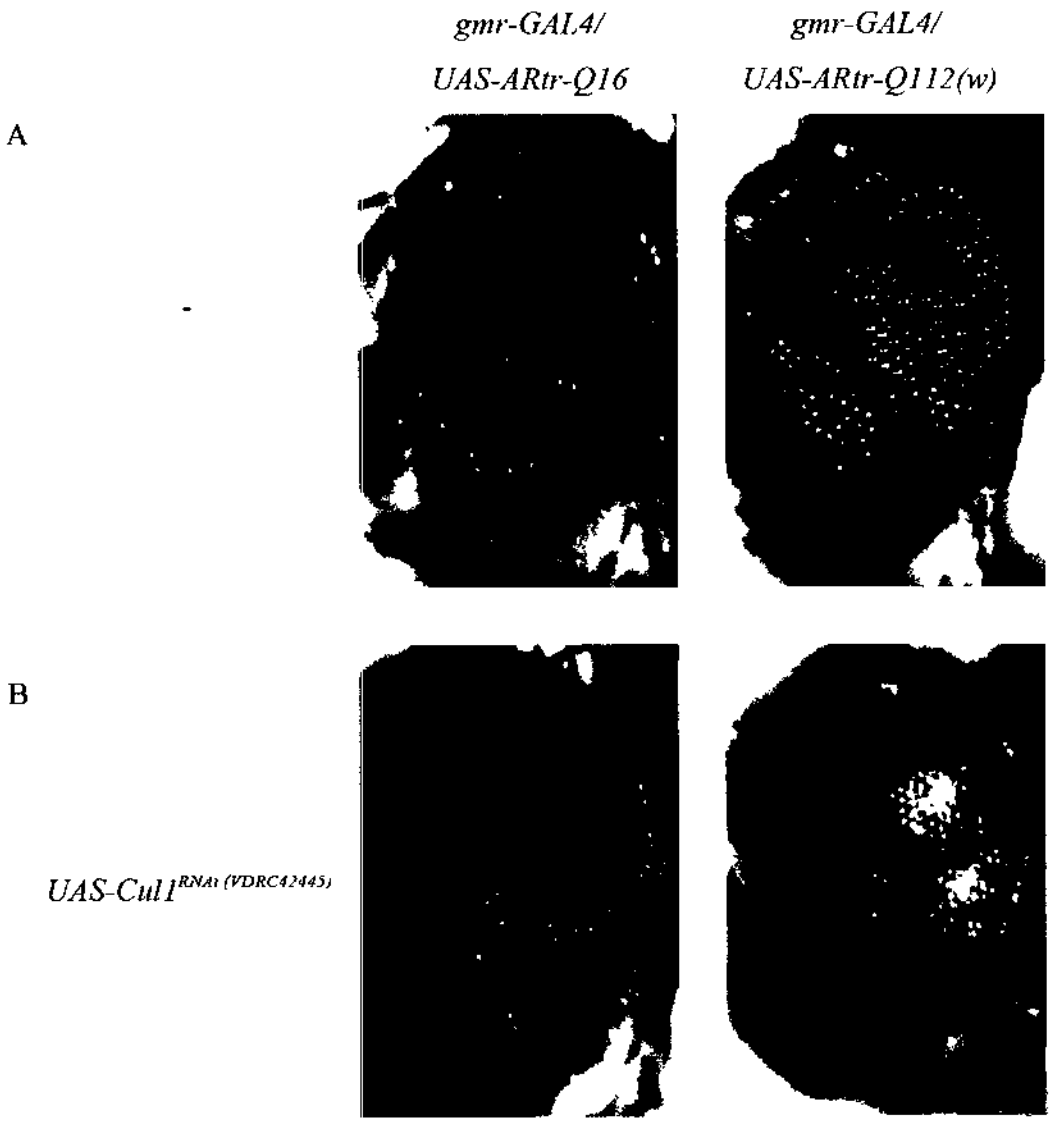
gmr-GAL4/
UAS-ARtr-Q16
gmr-GAL4/
UAS-ARtr-Q112(w)
A
B
UAS-Cul1RNAi (VDRC42445)

Figure 3.10. Knock-down of *Cul1* expression enhanced degeneration induced by *ARtr-Q112* expression in adult fly eyes.

External eye depigmentation phenotypes of flies expressing *ARtr* transgenes (*ARtr-Q16* or *ARtr-Q112)* with or without (as indicated by "-") knock-down of *Cul1* expression are shown. Transgenes were expressed using the *gmr-GAL4* driver. **(A)** At 3 dpe, expression of *ARtr-Q16* transgene did not cause any degenerative phenotype while weak expression of *ARtr-Q112* transgene (*ARtr-Q112(w)*) caused slight loss of pigmentation. **(B)** Knock-down of *Cul1* expression caused a Q-length specific enhancement on degeneration as shown by the extensive loss of pigmentation and formation of necrotic scars. Consistent results were obtained from three independent experiments. The flies were raised at 25°C. They were of genotypes:

(A) *w*; *gmr-GAL4/+*; *UAS-ARtr-Q16/+*,

w; *gmr-GAL4/+*; *UAS-ARtr-Q112(w)/+*

(B) *w*; *gmr-GAL4/+*; *UAS-ARtr-Q16/UAS-Cul1*^{RNAi},

w; *gmr-GAL4/+*; *UAS-ARtr-Q112(w)/UAS-Cul1*^{RNAi}.

Figure 3.11

gmr-GAL4/ UAS-eGFP-Q76

A

B

UAS-Cul1$^{RNAi\ (VDRC42445)}$

Figure 3.11. Knock-down of *Cul1* expression enhanced degeneration induced by *eGFP-Q76* expression in adult fly eyes.

External eye depigmentation phenotypes of flies expressing *eGFP-Q76* transgene with or without (as indicated by "-") knock-down of *Cul1* expression are shown. Transgenes were expressed using the *gmr-GAL4* driver. (**A**) At 3 dpe, expression of *eGFP-Q76* transgene caused mild loss of pigmentation. (**B**) Knock-down of *Cul1* expression caused a Q-length specific enhancement on degeneration as shown by the extensive loss of pigmentation and formation of necrotic scars. Consistent results were obtained from three independent experiments. The flies were raised at 25°C. They were of genotypes:

(**A**) *w; gmr-GAL4/+; UAS-eGFP-Q76/+*

(**B**) *w; gmr-GAL4/+; UAS-eGFP-Q76/UAS-Cul1*$^{RNAi\ (VDRC42445)}$.

consistent with the finding in the SCA3tr model in the sense that knock-down of *Cul1* expression enhanced polyQ toxicity (Figure 3.3B). As the SCA3tr, ARtr and eGFP models are in common only in the presence of polyQ domain, the effect of *Cul1* on polyQ toxicity is specific to the polyQ domain.

To test if the effect of *Cul1* on neurotoxicity is only specific to polyQ diseases, the effect of *Cul1* on another protein-misfolding neurodegenerative disease PD was examined. *Alpha-synuclein* is a familial PD gene [148] and its protein product is a major component of the protein aggregates found in neuronal tissues of PD patients [149]. Expression of wild-type *α-synuclein (α-synuclein^{WT})* in fly eyes by *gmr-GAL4* driver did not cause observable degenerative phenotype on the external eye surface (data not shown). However, it induced mild retinal degeneration which could be observed by deep pseudopupil assay [150]. Only around 5 (an average of 5.09) rhabdomeres per ommatidium were observed under microscope as tested by deep pseudopupil assay (Figure 3.12A). Knock-down of *Cul1* expression neither reduced nor rescued the rhabdomere score (Figure 3.12B). This shows that the effect of *Cul1* is only specific to polyQ diseases. Taken together, *Cul1* specifically affects toxicity induced by expanded polyQ domain.

3.5 Effects of knock-down of *Cul1* expression on SDS-solubility of expanded polyglutamine protein

To investigate the mechanism behind the effect of *Cul1* on polyQ toxicity in relation to the SDS-solubility and abundance of total expanded polyQ protein, the SCA3fl model [129] was employed. As mentioned in section 3.3, this model

Figure 3.12

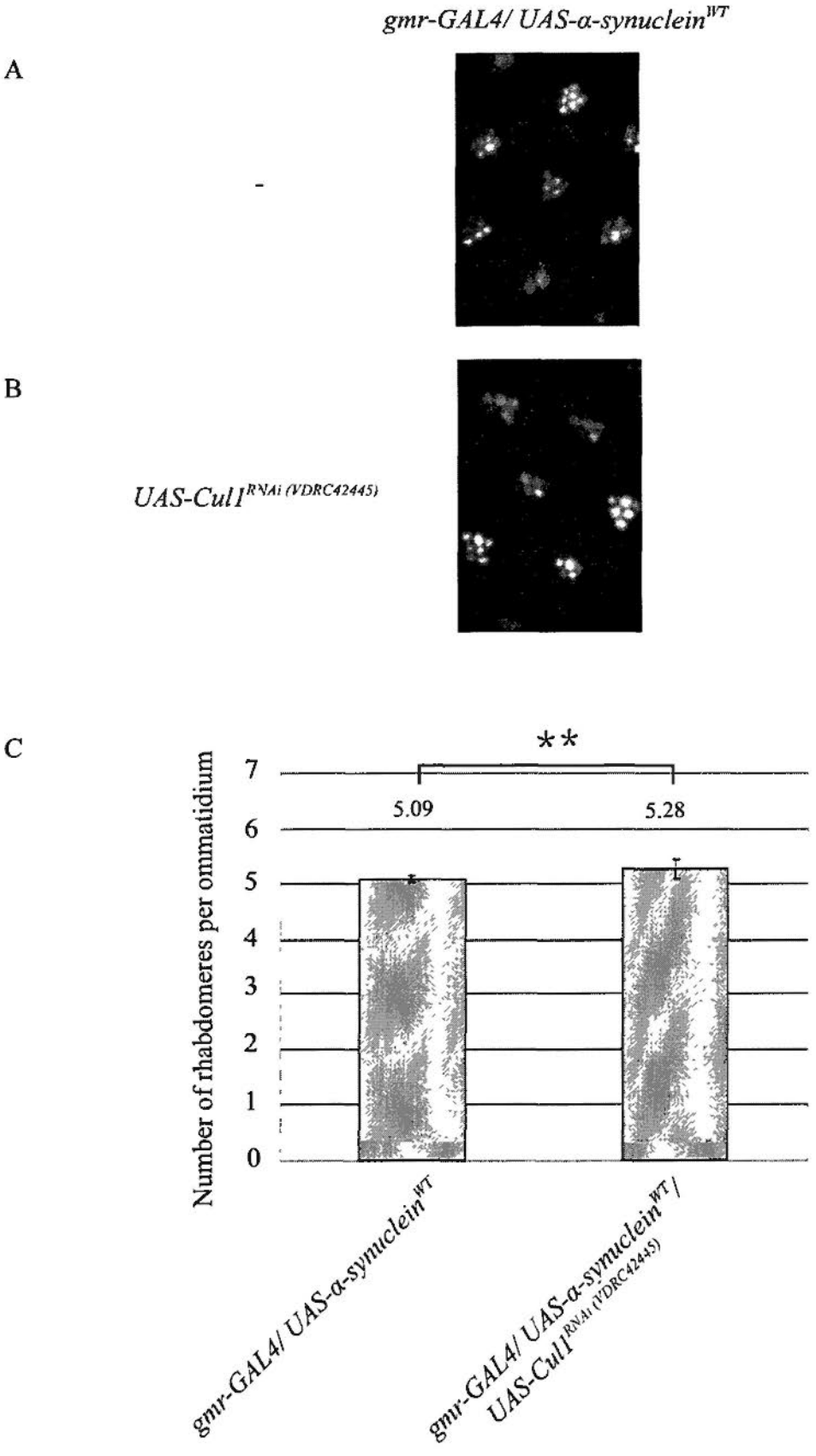
gmr-GAL4/ UAS-α-synuclein^WT
A
-
B
UAS-Cul1^RNAi (VDRC42445)
C
**
5.09
5.28
Number of rhabdomeres per ommatidium
0
1
2
3
4
5
6
7
gmr-GAL4/ UAS-α-synuclein^WT
gmr-GAL4/ UAS-α-synuclein^WT / UAS-Cul1^RNAi (VDRC42445)

Figure 3.12. Knock-down of *Cul1* expression did not modify α-synuclein toxicity. **(A - B)** Deep pseudopupil images of flies expressing *α-synuclein*^{WT} with or without knock-down of *Cul1* expression are shown. Transgenes were expressed using the *gmr-GAL4* driver. **(A)** On average, 5.09 rhabdomeres per ommatidium could be observed in flies expressing *α-synuclein*^{WT}. **(B)** Knock-down of *Cul1* expression did not cause statistical significant modification on the rhabdomere score when compared to *α-synuclein*^{WT}-expressing flies without knock-down of *Cul1* expression. **(C)** Quantification of **(A - B)**. N = 22, ** $p = 0.30$ (Mann-Whitney Rank Sum Test); error bars represent mean ± SEM from three independent experiment. At least 250 ommatidia from 30 flies were scored per group. The flies were raised at 21°C and were assayed at 2 dpe. They were of genotypes:

(A) *w*; *gmr-GAL4/+*; *UAS-α-synuclein*^{WT}*/+*

(B) *w*; *gmr-GAL4/+*; *UAS-α-synuclein*^{WT}*/UAS-Cul1*$^{RNAi\ (VDRC42445)}$.

expresses the myc-SCA3fl-Q84 protein which is only partly SDS-insoluble [140]. Therefore, SCA3fl model allows studies on both the soluble and insoluble fractions of myc-SCA3fl-Q84 protein.

To study the effect of *Cul1* on SDS-solubility of myc-SCA3fl-Q84 protein, fly head lysate was subjected to immunoblotting. The SDS-soluble fraction of myc-SCA3fl-Q84 protein was resolved in the running gel (Figure 3.13). Knock-down of *Cul1* expression reduced the level of SDS-soluble fraction of myc-SCA3fl-Q84 protein in the running gel (Figure 3.13).

To quantify the SDS-insoluble fraction of myc-SCA3fl-Q84 protein, the fly head lysate was subjected to ultracentrifugation to isolate the SDS-insoluble fraction of myc-SCA3fl-Q84 protein [25]. Formic acid (100%) was then used to disrupt the ionic interactions among the SDS-insoluble aggregated myc-SCA3fl-Q84 proteins and dissociate the aggregated proteins into monomers [25, 151]. The formic acid treated sample was then subjected to immunoblotting (Figure 3.14). It was found that knock-down of *Cul1* expression enhanced the level of SDS-insoluble myc-SCA3fl-Q84 protein (Figure 3.14). To double confirm the enrichment of SDS-insoluble fraction of myc-SCA3fl-Q84 protein, filter retardation assay was performed [146] to capture the SDS-insoluble myc-SCA3fl-Q84 protein aggregates with size larger than 0.22 μm for subsequent immunodetection (Figure 3.15). Consistently, knock-down of *Cul1* expression enhanced the level of SDS-insoluble myc-SCA3fl-Q84 protein (Figure 3.15). Combining all the data together, *Cul1* modulates the SDS-solubility of myc-SCA3fl-Q84 protein.

Figure 3.13

A

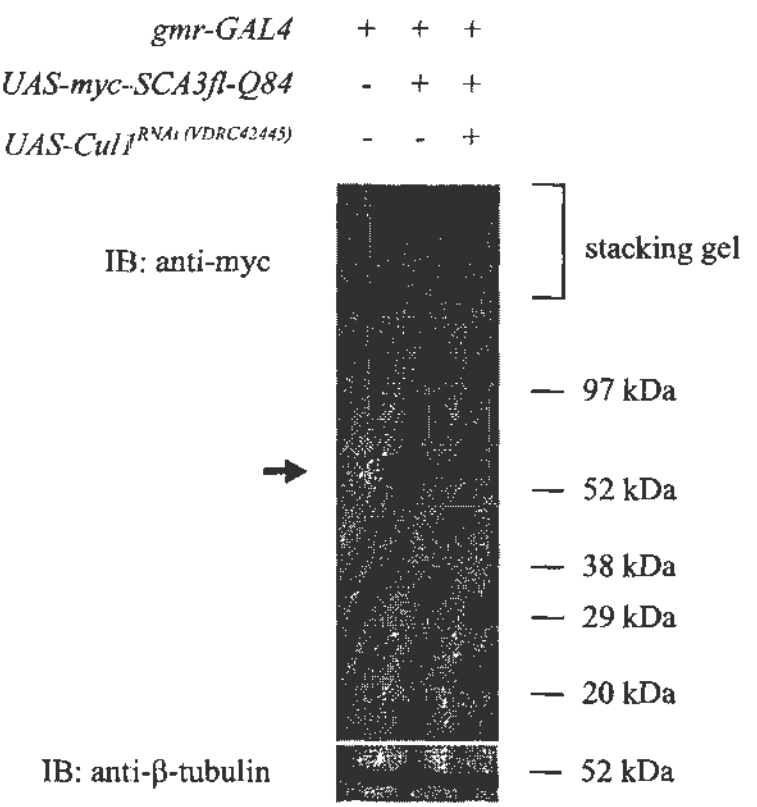

B

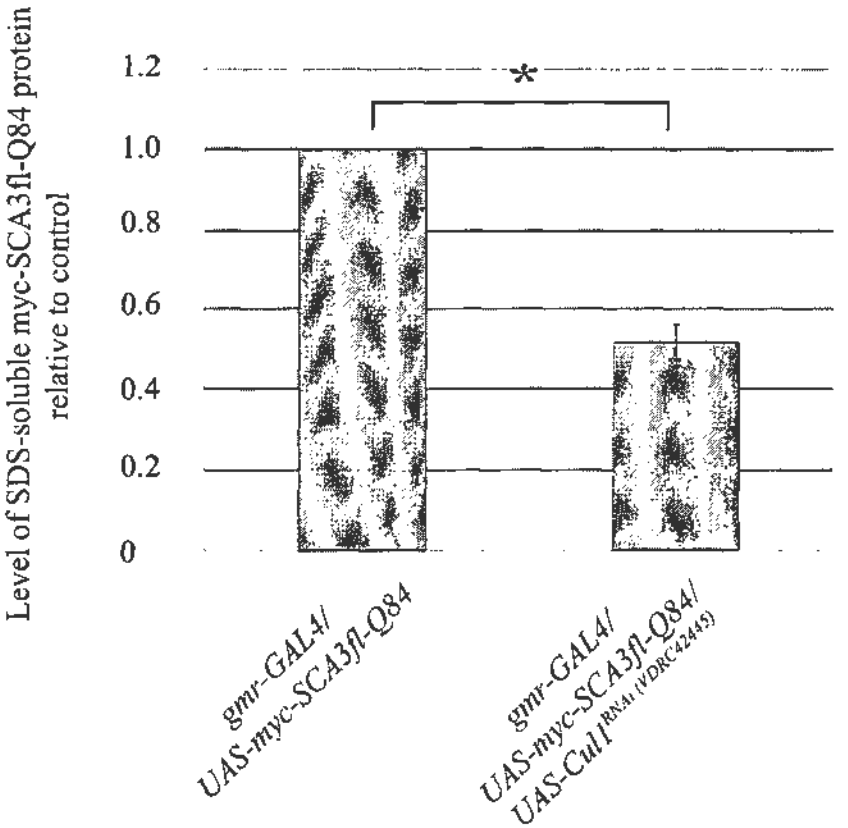

Figure 3.13. Knock-down of *Cul1* expression reduced the level of SDS-soluble myc-SCA3fl-Q84 protein.

(**A**) Adult head lysate of control flies and *myc-SCA3fl-Q84*-expressing flies with or without knock-down of *Cul1* was subjected to immunoblotting. The immunoblot was probed with anti-myc antibody to detect the presence of myc-SCA3fl-Q84 protein. The arrow (→) indicates the monomeric, SDS-soluble myc-SCA3fl-Q84 protein while the signal in stacking gel represents the SDS-insoluble myc-SCA3fl-Q84 protein. Knock-down of *Cul1* expression reduced the level of SDS-soluble myc-SCA3fl-Q84 protein. The immunoblot was stripped and reprobed with anti-β-tubulin antibody to confirm equal amount of protein loaded n every lane. (**B**) Quantification on the monomeric band of (**A**). Band intensity was relative to *myc-SCA3fl-Q84*-expressing flies without knock-down of *Cul1* expression. N = 4, * $p < 0.05$ (Student's t-test); error bar represents mean ± SEM from four independent experiments. The flies were raised at 21°C and were assayed at 3 dpe. They were of genotypes:

w; *gmr-GAL4/+*; *+/+*,

w; *gmr-GAL4/+*; *UAS-myc-SCA3fl-Q84/+*,

w; *gmr-GAL4/+*; *UAS-myc-SCA3fl-Q84/UAS-Cul1*$^{RNAi\ (VDRC42445)}$.

Figure 3.14

A

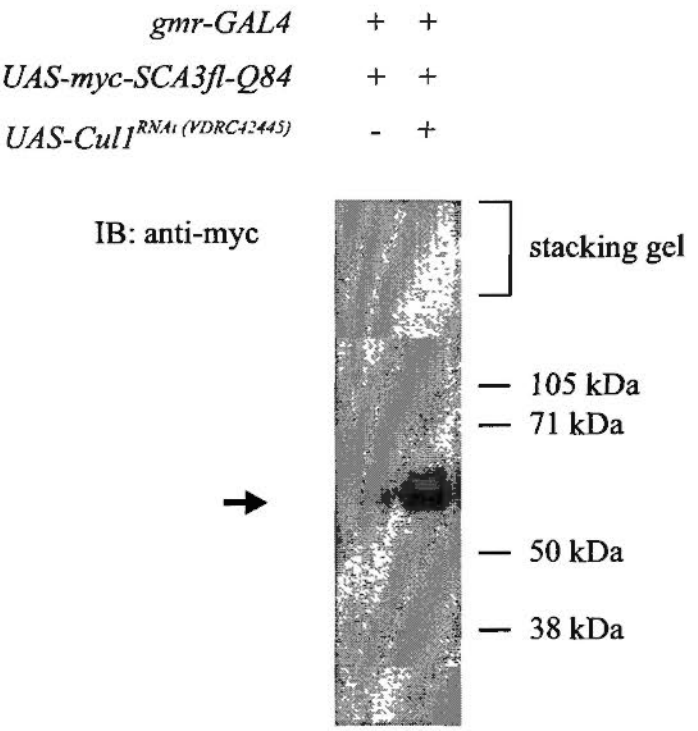

B

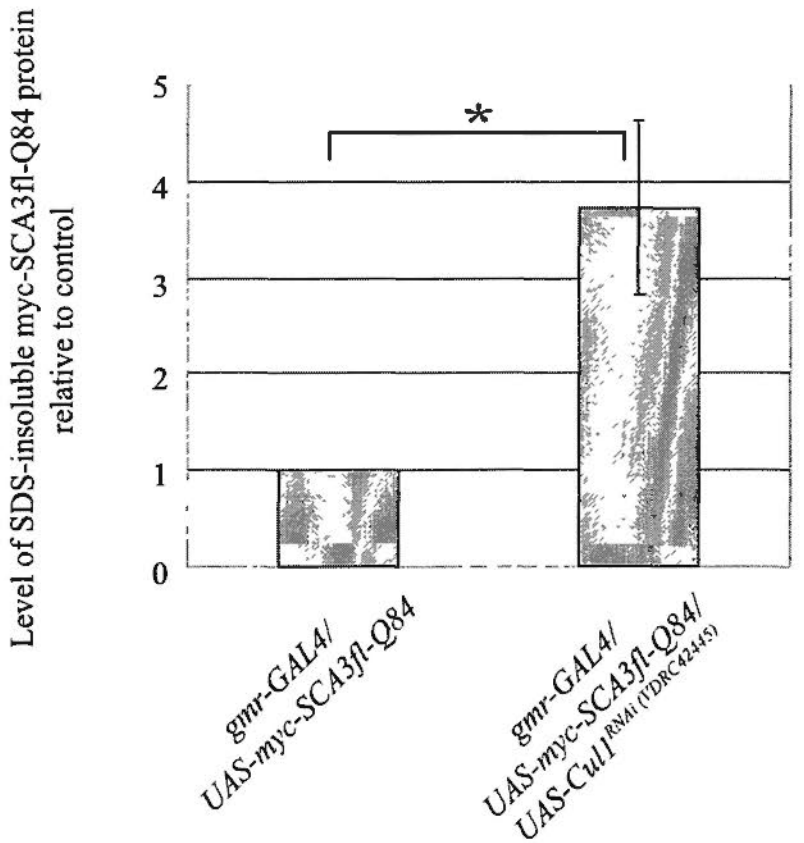

Figure 3.14. Knock-down of *Cul1* expression increased the level of SDS-insoluble myc-SCA3fl-Q84 protein.

(A) Adult head lysate of *myc-SCA3fl-Q84*-expressing flies with or without knock-down of *Cul1* expression was subjected to ultracentrifugation to isolate any SDS-insoluble protein aggregates and also to remove the SDS-soluble protein. The resulting pellet was treated with 100% formic acid to dissociate the aggregates into monomers and then subjected to immunoblotting. The immunoblot was probed with anti-myc antibody to detect the presence of any SDS-insoluble myc-SCA3fl-Q84 protein. The arrow (→) indicates the solubilized insoluble myc-SCA3fl-Q84 protein and the signal intensity represents its level. Knock-down of *Cul1* expression intensified this band. **(B)** Quantification of the SDS-insoluble myc-SCA3fl-Q84 protein in **(A)**. Band intensity was relative to *myc-SCA3fl-Q84*-expressing flies without knock-down of *Cul1* expression. N = 4, * $p < 0.05$ (Student's t-test); error bar represents mean ± SEM from four independent experiments. The flies were raised at 21°C and were assayed at 3 dpe. They were of genotypes:

w; *gmr-GAL4/+*; *UAS-myc-SCA3fl-Q84/+*,

w; *gmr-GAL4/+*; *UAS-myc-SCA3fl-Q84/UAS-Cul1*$^{RNAi\ (VDRC42445)}$.

Figure 3.15

A

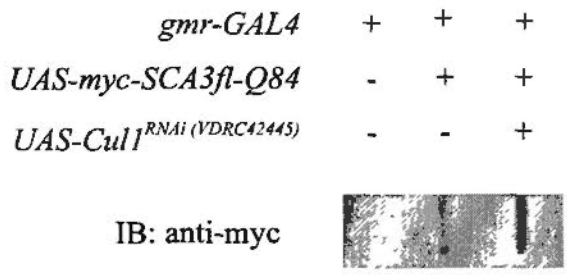

B

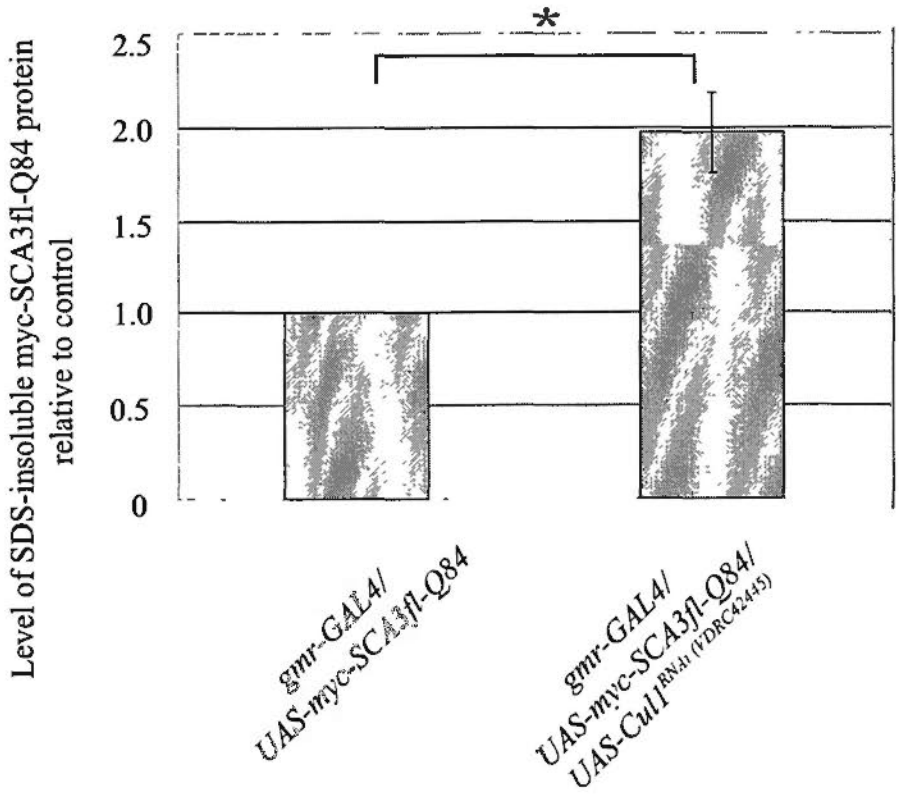

Figure 3.15. Knock-down of *Cul1* expression increased the level of SDS-insoluble myc-SCA3fl-Q84 protein with size larger than 0.22 µm.

(A) Adult head lysate of control flies and *myc-SCA3fl-Q84*-expressing flies with or without knock-down of *Cul1* was subjected to filter retardation assay to capture any SDS-insoluble proteins with size larger than 0.22 µm. The immunoblot was probed with anti-myc antibody to detect presence of any SDS-insoluble myc-SCA3fl-Q84 protein with size larger than 0.22 µm. Knock-down of *Cul1* expression intensified the signal for insoluble myc-SCA3fl-Q84 protein. **(B)** Quantification of **(A)**. Band intensity was relative to *myc-SCA3fl-Q84*-expressing flies without knock-down of *Cul1* expression. N = 4, * $p < 0.05$ (Student's t-test); error bar represents mean ± SEM from four independent experiments. The flies were raised at 21°C and were assayed at 3 dpe. They were of genotypes:

w; *gmr-GAL4/+*; *+/+*,

w; *gmr-GAL4/+*; *UAS-myc-SCA3fl-Q84/+*,

w; *gmr-GAL4/+*; *UAS-myc-SCA3fl-Q84/UAS-Cul1*$^{RNAi\ (VDRC42445)}$.

To test the effect of *Cul1* on the abundance of total myc-SCA3fl-Q84 protein, 100% formic acid was used to solubilize the SDS-insoluble fraction of myc-SCA3fl-Q84 protein to obtain the total myc-SCA3fl-Q84 protein for immunoblotting [151] (Figure 3.16). Knock-down of *Cul1* expression did not change the total level of myc-SCA3fl-Q84 protein (Figure 3.16). This suggests that *Cul1* does not affect the abundance of total myc-SCA3fl-Q84 protein. Taken together, *Cul1* acts on the SDS-solubility of myc-SCA3fl-Q84 protein without affecting the abundance of total myc-SCA3fl-Q84 protein.

3.6 Physical interaction between Cul1 protein and expanded polyglutamine protein

Physical interaction between two proteins suggests a functional relationship between them. To test for physical interaction between Cul1 protein and myc-SCA3fl-Q84 protein, co-immunoprecipitation was performed in flies. Myc-SCA3fl-Q84 protein was immunoprecipitated by anti-myc antibody. The eluate was subjected to immunoblotting and the immunoblot was probed against anti-Cul1 antibody. It was found that a substantial amount of Cul1 protein was detected in the eluate but not the 'minus antibody' control (Figure 3.17). The immunoblot was stripped and reprobed with anti-myc antibody. Myc-SCA3fl-Q84 protein was detected in the eluate but not the 'minus antibody' control (Figure 3.17). This indicates successful and specific immunoprecipitation of myc-SCA3fl-Q84 protein. The data here demonstrate that myc-SCA3fl-Q84 protein physically interacts with endogenous Cul1 protein.

Figure 3.16

A

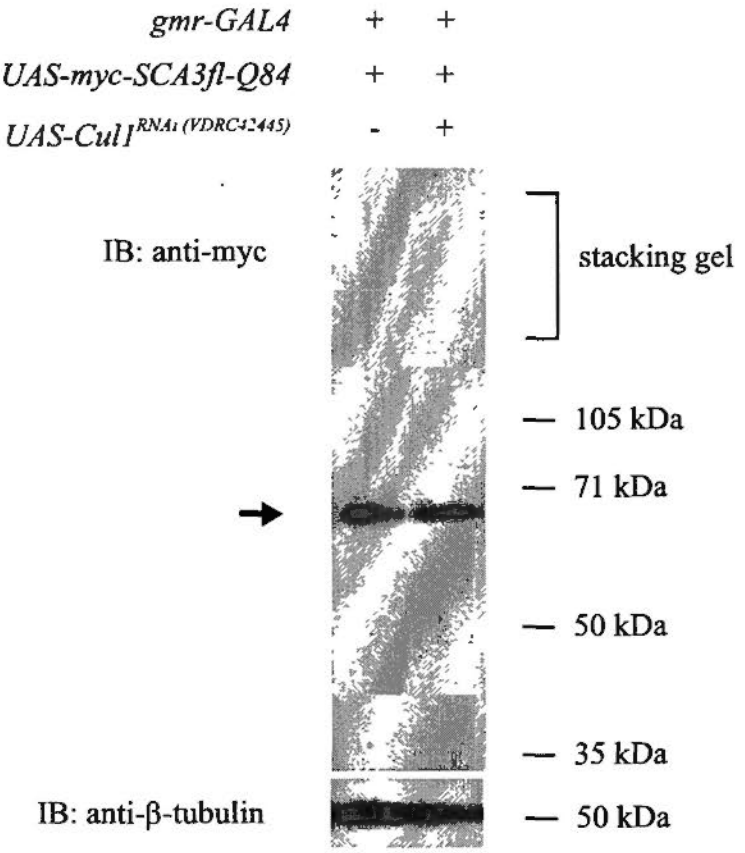

B

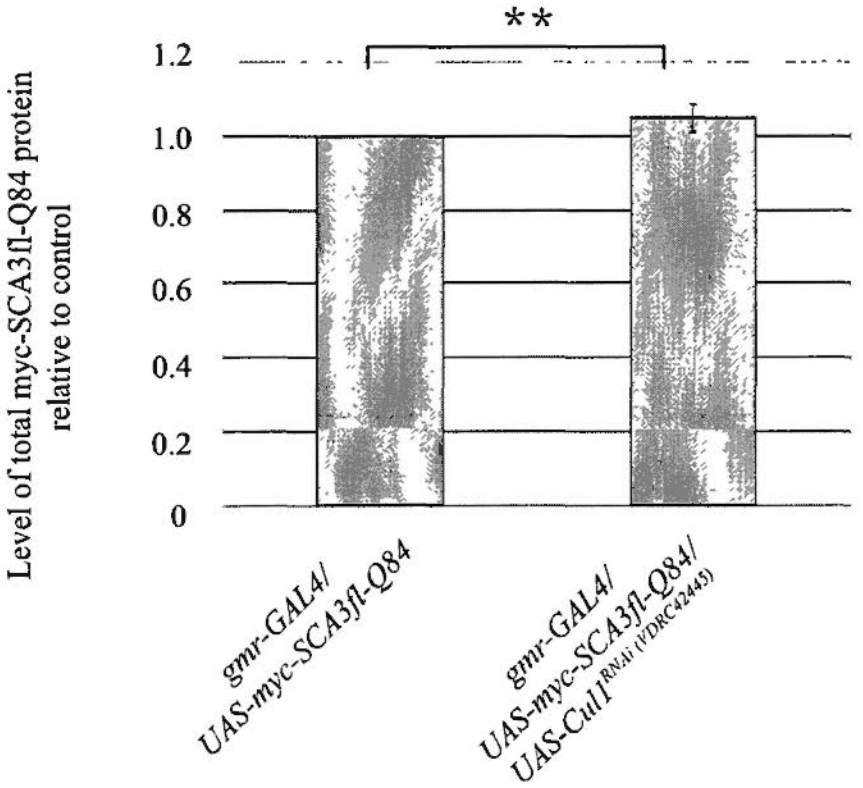

Figure 3.16. Knock-down of *Cul1* expression did not modify the abundance of total myc-SCA3fl-Q84 protein.

(A) Adult head lysate of *myc-SCA3fl-Q84*-expressing flies with or without knock-down of *Cul1* expression was treated with 100% formic acid to dissociate the aggregates into monomers and then subjected to immunoblotting. The immunoblot was probed with anti-myc antibody to detect the myc-SCA3fl-Q84 protein. The arrow (→) indicates the total myc-SCA3fl-Q84 protein and the signal intensity represents its level. Knock-down of *Cul1* expression did not modify this band. The immunoblot was stripped and reprobed with anti-β-tubulin antibody to confirm that equal amount of protein was loaded in every lane. **(B)** Quantification of the total myc-SCA3fl-Q84 protein in **(A)**. Band intensity was relative to *myc-SCA3fl-Q84*-expressing flies without knock-down of *Cul1* expression. N = 3, ** $p = 0.39$ (Student's t-test); error bar represents mean ± SEM from three independent experiments. The flies were raised at 21°C and were assayed at 3 dpe. They were of genotypes:

w; *gmr-GAL4/+*; *UAS-myc-SCA3fl-Q84/+*,

w; *gmr-GAL4/+*; *UAS-myc-SCA3fl-Q84/UAS-Cul1*$^{RNAi\ (VDRC42445)}$.

Figure 3.17

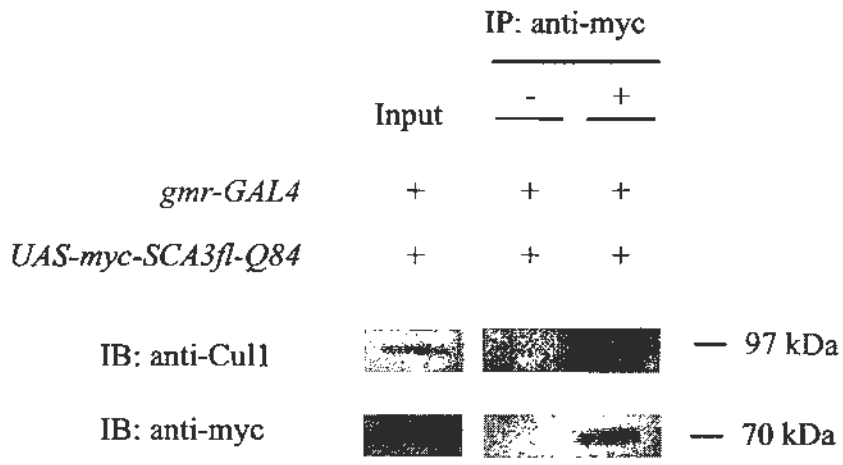
IP: anti-myc
Input
-
+
gmr-GAL4
+
+
+
UAS-myc-SCA3fl-Q84
+
+
+
IB: anti-Cul1
— 97 kDa
IB: anti-myc
— 70 kDa

Figure 3.17. Endogenous Cul1 protein physically interacted with myc-SCA3fl-Q84 protein.

Adult head lysate of flies expressing *myc-SCA3fl-Q84* transgene was subjected to co-immunoprecipitation using anti-myc antibody to immunoprecipitate myc-SCA3fl-Q84 protein. Upper row: the immunoblots were probed against anti-Cul1 antibody to detect the presence of Cul1 protein. A substantial amount of Cul1 protein was co-immunoprecipitated by myc-SCA3fl-Q84 protein using anti-myc antibody in the eluate. The input shows the expression of endogenous Cul1 protein. Lower row: the immunoblots were stripped and reprobed with anti-myc antibody to detect the myc-SCA3fl-Q84 protein. Positive signal in the eluate confirms successful immunoprecipitation of myc-SCA3fl-Q84 protein. The input shows the expression of myc-SCA3fl-Q84 protein. The experiment was performed once. The flies were raised at 21°C and were assayed at 3 dpe. They were of genotype:

w; *gmr-GAL4/+*; *UAS-myc-SCA3fl-Q84/+*.

To test for the important domain required for the interaction between Cul1 protein and myc-SCA3fl-Q84 protein, HEK 293FT cells were employed. HEK 293FT cells were widely used not only in investigations of function of Cul1 protein but also in studies of polyQ diseases [152-156]. In this study, an eGFP-polyQ model was employed [25] (Figure 3.18A). This model recapitulates the aggregating property of expanded polyQ protein. Cells transiently transfected with a construct carrying an *eGFP* transgene fused to an expanded *CAG*-repeats of 75 *CAG*s (*eGFP-Q75)* but not that with a normal length of *CAG*-repeats of 27 *CAGs* (*eGFP-Q27),* formed SDS-insoluble aggregates at 48 hours post-transfection (hpt) (Figure 3.18B). The effect of *Cul1* on the solubility of polyQ protein in the fly polyQ model could be reproduced in this model. Knock-down of *Cul1* expression by siRNA reduced the level of SDS-soluble eGFP-Q75 protein (Figure 3.19A) and increased the level of SDS-insoluble eGFP-Q75 protein (Figure 3.19B). As the effect of knock-down of *Cul1* expression on SDS-solubility of expanded polyQ protein was reproducible in this eGFP-polyQ model, this model could be used to study the interaction between Cul1 protein and expanded polyQ protein in mammalian cultured cells.

Co-immunoprecipitation experiment between Cul1 protein and expanded polyQ protein was repeated in this model. Upon transient co-transfection of a construct bearing a *myc*-tagged wild-type human *Cul1* (*myc-hCul1)* transgene (F. T. Liang and H. Y. E. Chan, unpublished observations) and the *eGFP or eGFP-Q27* construct, no eGFP or eGFP-Q27 protein was co-immunoprecipitated out together with myc-hCul1

Figure 3.18

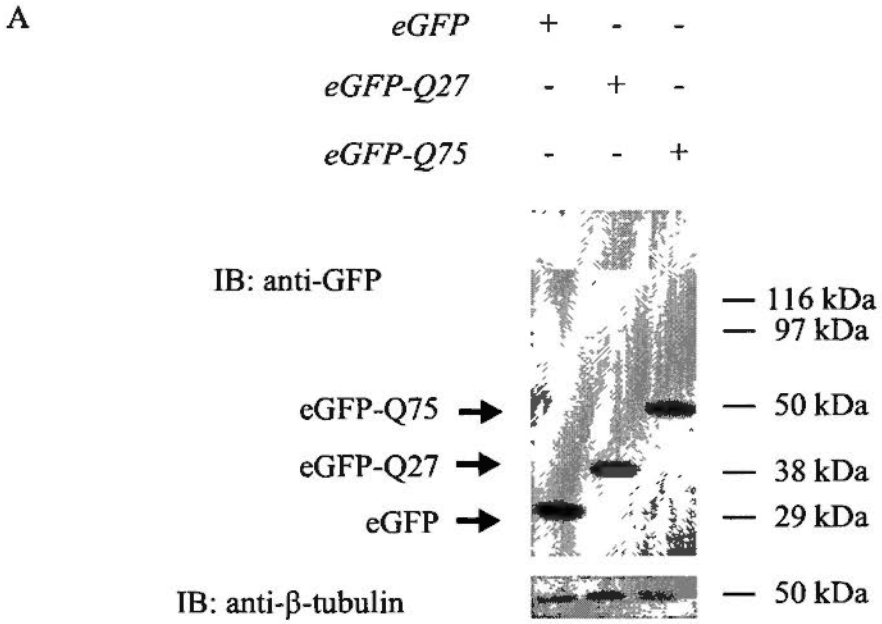
A
eGFP + - -
eGFP-Q27 - + -
eGFP-Q75 - - +
IB: anti-GFP
116 kDa
97 kDa
eGFP-Q75
50 kDa
eGFP-Q27
38 kDa
eGFP
29 kDa
IB: anti-β-tubulin
50 kDa

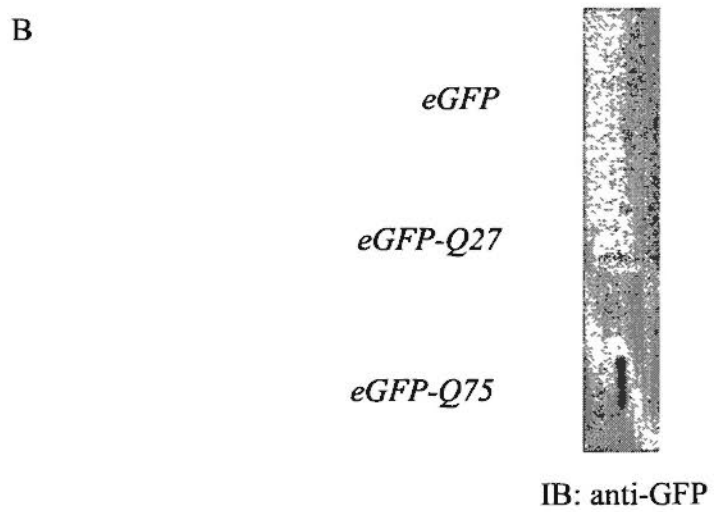
B
eGFP
eGFP-Q27
eGFP-Q75
IB: anti-GFP

Figure 3.18. Characterization of the eGFP-polyQ model in HEK 293FT cells.

(A) Cells were transiently transfected with construct carrying *eGFP-Q0*, *eGFP-Q27* or *eGFP-Q75* transgene and harvested at 48 hours post-transfection (hpt). Cell lysate was subjected to immunoblotting. The immunoblot was probed against anti-GFP antibody to detect the eGFP, eGFP-Q27 and eGFP-Q75 proteins. The immunoblot showed comparable expression levels between the three transgenes. The immunoblot was stripped and reprobed with anti-β-tubulin antibody to confirm that equal amount of protein was loaded in every lane. **(B)** Cells were transiently transfected with construct carrying *eGFP*, *eGFP-Q27* or *eGFP-Q75* transgene and harvested at 48 hpt. Cell lysate was subjected to filter retardation assay to capture any SDS-insoluble protein aggregates with size larger than 0.22 μm. The immunoblot was probed against anti-GFP antibody to detect presence of any SDS-insoluble eGFP-polyQ protein aggregates with size larger than 0.22 μm. There was a signal which indicated the presence of SDS-insoluble protein upon expression of *eGFP-Q75*, but not *eGFP-Q27* or *eGFP*. The experiments were performed twice.

Figure 3.19

A

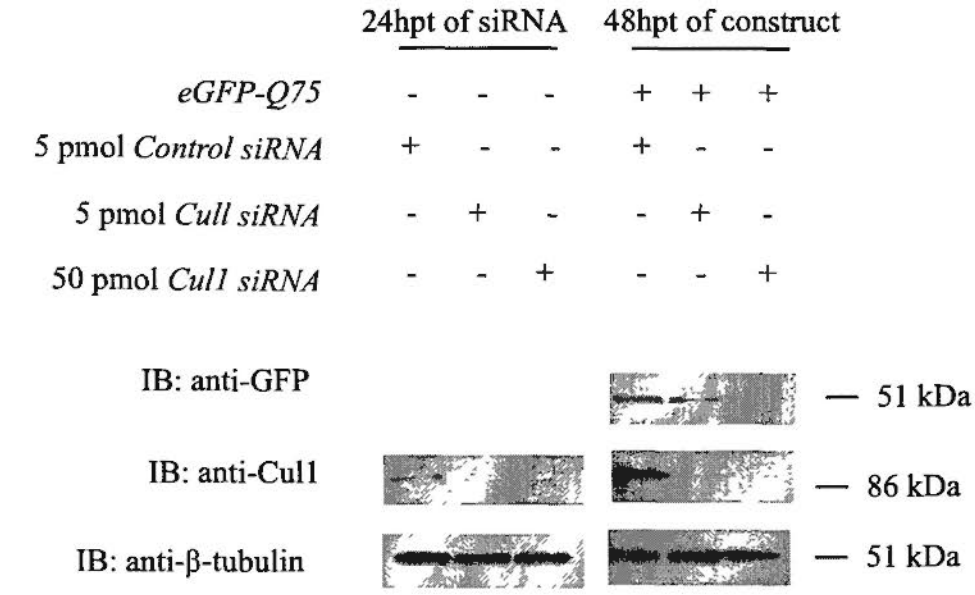

B

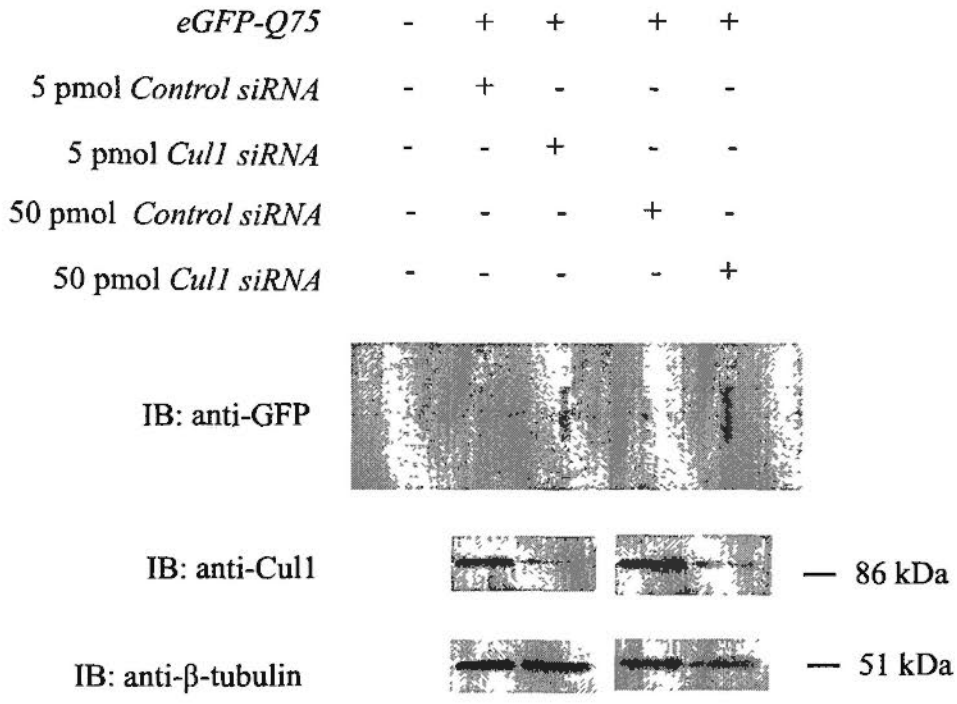

Figure 3.19. Knock-down of *Cul1* expression reduced the solubility of eGFP-Q75 protein in HEK 293FT cells.

(A) Left panel: Cells were transiently transfected with different amounts of *control siRNA* or *Cul1 siRNA*. At 24 hpt of *siRNA*, cell lysate was subjected to immunoblotting. The immunoblot was probed against anti-Cul1 antibody to detect the endogenous Cul1 protein. Transfection of *Cul1 siRNA* at 5 pmol already caused a reduction in the level of endogenous Cul1 protein. The immunoblot was stripped and reprobed with anti-β-tubulin antibody to confirm that equal amount of protein was loaded in every lane. (Right panel) At 24 hpt of *siRNA*, cells were then transiently transfected with construct carrying the *eGFP-Q75* transgene. At 48 hpt of *eGFP-Q75* construct, cell lysate was subjected to immunoblotting. The immunoblot was probed against anti-GFP antibody to detect the SDS-soluble eGFP-Q75 protein. Previous transfection of *Cul1 siRNA* at 5 pmol caused a mild reduction in the level of SDS-soluble eGFP-Q75 protein. Such reduction was stronger with the use of 50 pmol of *Cul1 siRNA*. The immunoblot was stripped and reprobed with anti-Cul1 antibody to confirm the reduction of Cul1 protein level. The immunoblot was then stripped and reprobed with anti-β-tubulin antibody to confirm that equal amount of protein was loaded in every lane. The experiment was performed twice **(B)** Cells were transiently transfected with different amounts of *control siRNA* or *Cul1 siRNA*. At 24 hpt of *siRNA*, cells were transiently transfected with construct carrying the *eGFP-Q75* transgene. At 48 hpt of *eGFP-Q75* construct, cell lysate was subjected to filter retardation assay to capture any SDS-insoluble protein aggregates with size larger than 0.22 μm. The immunoblot was probed against anti-GFP antibody to detect the presence of any SDS-insoluble eGFP-Q75 protein with size larger than 0.22 μm. Previous transfection of *Cul1 siRNA* at 5 pmol caused a mild increase in the level of SDS-insoluble eGFP-Q75 protein. Such enhancement was stronger with the use of 50 pmol of *Cul1 siRNA*. Lysate from same batch of cells was subjected to immunoblotting. The immunoblot was probed with anti-Cul1 antibody to confirm the reduction of Cul1 protein level. It was then stripped and reprobed with anti-β-tubulin antibody to confirm that equal amount of protein was loaded in every lane. The experiment was performed once.

protein by anti-myc antibody at 48hpt (Figure 3.20A). In contrast, upon transient co-transfection of *myc-hCul1* construct and the *eGFP-Q75* construct, eGFP-Q75 protein was co-immunoprecipitated out together with myc-hCul1 protein by anti-myc antibody (Figure 3.20A). Consistent with the fly data, this result indicates positive physical interaction between Cul1 protein and expanded polyQ protein.

In Cul1 protein, there are two important domains namely the Skp1-binding domain and the Roc1-binding domain [157]. At the N-terminus, Cul1 protein binds to Skp1 protein through the Skp1-binding domain and Skp1 protein in turn binds to the substrate receptor protein [157, 158]. At the C-terminus, Cul1 protein binds to Roc1 protein through the Roc1-binding domain and Roc1 protein in turn recruits the ubiquitin-loaded E2 ubiquitin conjugation enzyme to the CRL complex [157, 158]. To test which domain is important for the interaction between Cul1 protein and expanded polyQ protein, the above co-immunoprecipitation was repeated in HEK 293FT cells using a *myc*-tagged human *Cul1* deletion mutant construct (*myc-hCul1*^{N252}) instead of the wild-type full-length *myc-hCul1*. In the protein product of this *myc-hCul1*^{N252} construct, the amino acids C-terminal to the 252nd residues including the Roc1-binding domain were deleted [159]. Only the Skp1-binding domain is left. As a result, this mutant Cul1 protein could only bind to Skp1 protein and in turn the substrate receptor protein but not Roc1 protein [159]. It was found that deleting the Roc1-binding domain did not abolish the interaction between Cul1 protein and eGFP-Q75 protein (Figure 3.20B). This shows that the presence of Skp1-binding domain was already sufficient for the interaction between Cu1 protein and eGFP-Q75 protein. Hence, Cul1 protein interacts with expanded

Figure 3.20

A

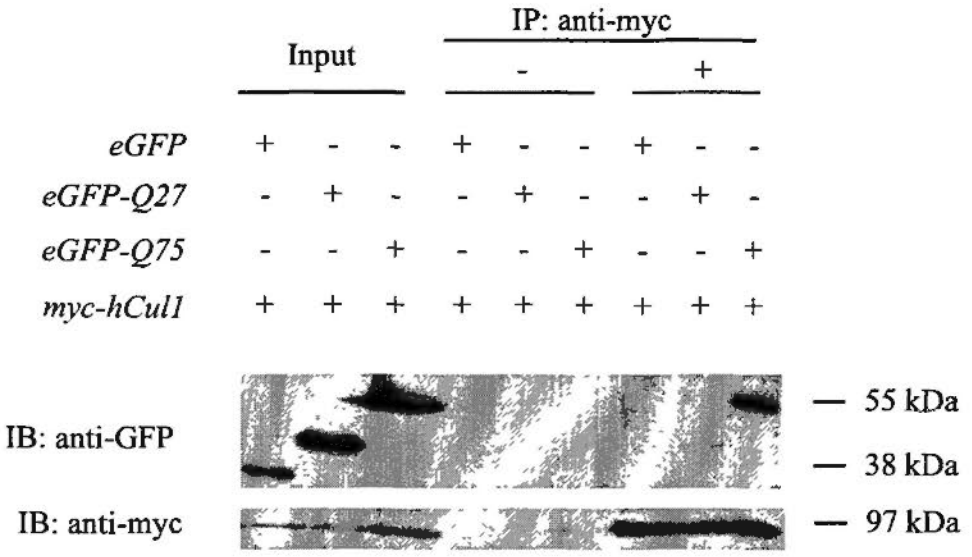

B

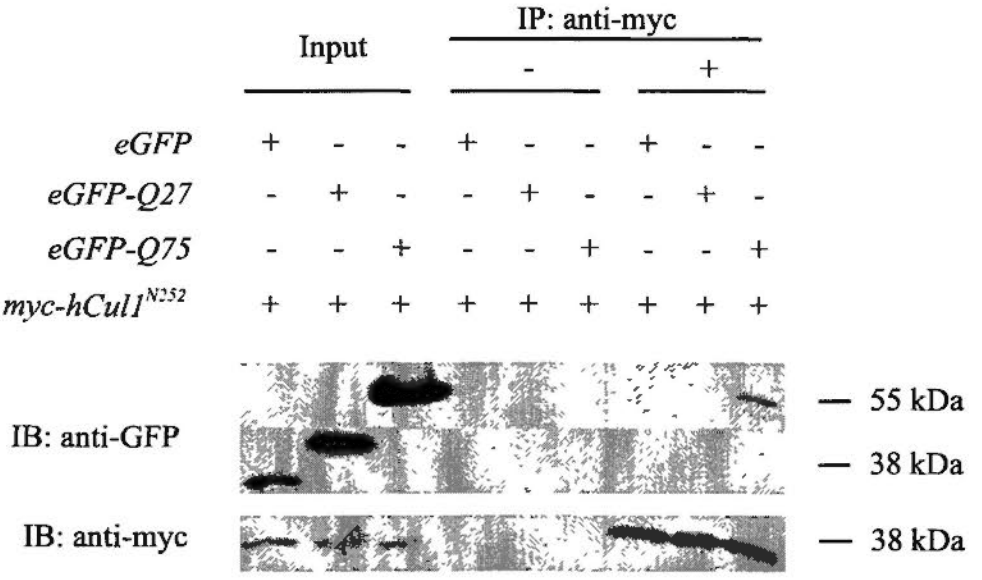

Figure 3.20. Cul1 protein physically interacted with eGFP-Q75 protein through at least the Skp1-binding domain in HEK 293FT cells.

(A) Cells were transiently co-transfected with construct carrying the *myc-hCul1* transgene and construct carrying the *eGFP*, *eGFP-Q27* or *eGFP-Q75* transgene. At 48 hpt, cell lysate was subjected to co-immunoprecipitation using anti-myc antibody to immunoprecipitate the myc-hCul1 protein. Upper row: the immunoblot was probed against anti-GFP antibody to detect the eGFP-polyQ proteins. EGFP-Q75 protein, but not eGFP-Q27 protein or eGFP protein, was co-immunoprecipitated by myc-hCul1 protein using anti-myc antibody in the eluate. The input shows the expression of eGFP, eGFP-Q27 and eGFP-Q75 proteins. Lower row: the immunoblot was stripped and reprobed with anti-myc antibody to detect the myc-hCul1 protein. Positive signal confirms successful immunoprecipitation of myc-hCul1 protein in the eluate. The input shows the expression of myc-hCul1 protein. **(B)** Cells were transiently co-transfected with construct carrying *myc-hCul1*^{N252} transgene and construct carrying *eGFP*, *eGFP-Q27* or *eGFP-Q75* transgene. At 48 hpt, cell lysate was subjected to co-immunoprecipitation using anti-myc antibody to immunoprecipitate the myc-hCul1^{N252} protein. Upper row: the immunoblot was probed against anti-GFP antibody to detect the eGFP-polyQ proteins. EGFP-Q75 protein, but not eGFP-Q27 protein or eGFP protein, was co-immunoprecipitated by myc-hCul1^{N252} protein using anti-myc antibody in the eluate. The input shows the expression of eGFP, eGFP-Q27 and eGFP-Q75 proteins. Lower row: the immunoblot was stripped and reprobed with anti-myc antibody to detect the myc-hCul1^{N252} protein. Positive signal in the eluate confirms successful immunoprecipitation of myc-hCul1^{N252} protein. The input shows the expression of myc-hCul1^{N252} protein. The above experiments were performed twice.

polyQ protein through at least the Skp1-binding domain.

3.7 Knock-down of *Cul1* expression reduced ubiquitination of SDS-insoluble expanded polyglutamine protein

The N-terminus of Cul1 protein binds to Skp1 protein which in turn binds to the substrate receptor protein that recruits substrate proteins to the CRL complex for ubiquitination [157, 158]. Ubiquitination of substrate protein promotes its degradation [160], while inhibiting substrate ubiquitination could result in its accumulation in cells [161]. As it was found that Cul1 protein interacted with expanded polyQ protein through at least the Skp1-binding domain (Figure 3.20B) and knock-down of *Cul1* expression enhanced the accumulation of SDS-insoluble expanded polyQ protein (Figure 3.19B), it is likely that Cul1 protein nucleates a CRL complex and ubiquitinates SDS-insoluble expanded polyQ protein.

To test this hypothesis, an *in vivo* ubiquitination assay was used to examined the effect of knock-down of *Cul1* expression on the ubiquitination of myc-SCA3fl-Q84 protein in flies [162, 163]. First of all, immunoprecipitation was used to capture total myc-SCA3fl-Q84 protein by anti-myc antibody (Figure 3.21). The eluate was subjected to immunoblotting (Figure 3.21). The immunoblot was first probed against anti-ubiquitin antibody to detect the presence of ubiquitinated SDS-soluble myc-SCA3fl-Q84 protein in the running gel and subsequently reprobed with anti-myc antibody to confirm successful immunoprecipitation of myc-SCA3fl-Q84 protein (Figure 3.21). It was found that knock-down of *Cul1* expression did not significantly alter the level of ubiquitinated SDS-soluble myc-SCA3fl-Q84 protein

Figure 3.21

A

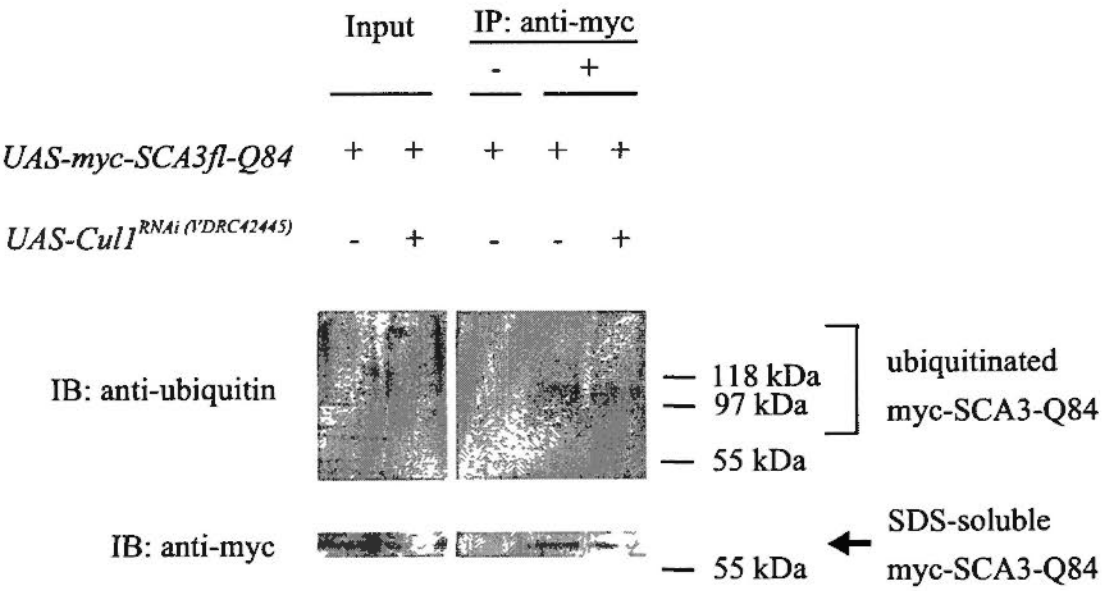

B

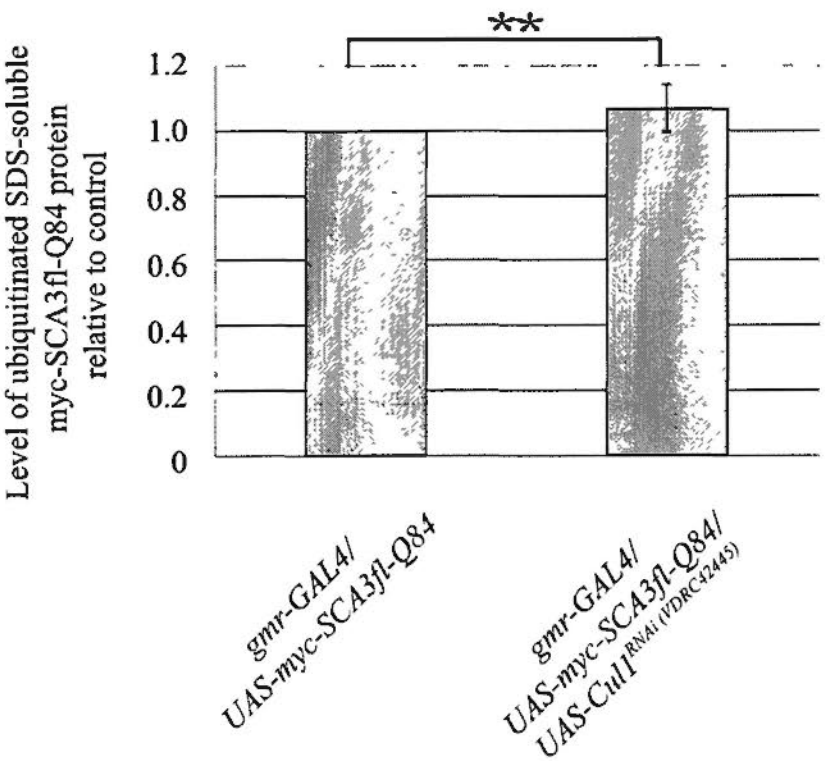

Figure 3.21. Knock-down of *Cul1* expression did not alter the level of ubiquitinated SDS-soluble myc-SCA3fl-Q84 protein.

(**A**) Adult head lysate of flies expressing myc-SCA3fl-Q84 protein with or without knock-down of *Cul1* expression was subjected to immunoprecipitation using anti-myc antibody to immunoprecipitate myc-SCA3fl-Q84 protein. The input and the eluate were subjected to immunoblotting. Upper row: the immunoblots were probed against anti-ubiquitin antibody to detect the ubiquitinated SDS-soluble protein in the running gel. Lower row: the immunoblots were stripped and reprobed with anti-myc antibody to detect the SDS-soluble myc-SCA3fl-Q84 protein. The input shows the presence of SDS-soluble myc-SCA3fl-Q84 protein in the lysate while positive signal in the eluate confirmed positive immunoprecipitation of SDS-soluble myc-SCA3fl-Q84 protein. Knock-down of *Cul1* expression did not alter the level of ubiquitinated SDS-soluble myc-SCA3fl-Q84 protein. (**B**) Quantification of the ubiquitinated SDS-soluble myc-SCA3fl-Q84 protein in (**A**). Band intensity was relative to *myc-SCA3fl-Q84*-expressing flies without knock-down of *Cul1* expression. N = 3, ** $p = 0.57$ (Student's t-test); error bar represents mean ± SEM from three independent experiments. The flies were raised at 21°C and were assayed at 3 dpe. They were of genotypes:

w; *gmr-GAL4/+*; *UAS-myc-SCA3fl-Q84/+*,

w; *gmr-GAL4/+*; *UAS-myc-SCA3fl-Q84/UAS-Cul1*$^{RNAi\ (VDRC42445)}$.

(Figure 3.21). This shows that *Cul1* does not affect the ubiquitination of the SDS-soluble fraction of expanded polyQ protein.

On the other hand, to test the effect of knock-down of *Cul1* expression on the ubiquitination of SDS-insoluble myc-SCA3fl-Q84 protein, the above immunoprecipitation was repeated to capture total myc-SCA3fl-Q84 protein by anti-myc antibody. Instead of immunoblotting, the eluate was subjected to filter retardation assay to capture the SDS-insoluble myc-SCA3fl-Q84 protein with size larger than 0.22 μm [146] (Figure 3.22). The signal on the immunoblot obtained upon immunodetection with anti-myc antibody indicates successful immunoprecipitation of the SDS-insoluble myc-SCA3fl-Q84 protein (Figure 3.22A, upper row). The signal on the immunoblot obtained upon immunodetection with anti-ubiquitin antibody indicates the ubiquitinated SDS-insoluble myc-SCA3fl-Q84 protein (Figure 3.22A, lower row). It was found that knock-down of *Cul1* expression reduced the level of ubiquitinated SDS-insoluble myc-SCA3fl-Q84 (Figure 3.22). Taken together, the data suggest that *Cul1* specifically modifies the ubiquitination of SDS-insoluble myc-SCA3fl-Q84 protein.

3.8 Suppression by expression of human *Hsp70* transgene on the *Cul1*^{RNAi}-mediated enhancement on polyglutamine toxicity

As mentioned in Chapter 1 (section 1.3), it is common that polyQ proteins become misfolded and insoluble upon expansion of polyQ domain in various polyQ diseases [53]. It is widely reported that promoting protein refolding activity of cellular chaperones enhances solubility of expanded polyQ proteins and suppresses

Figure 3.22

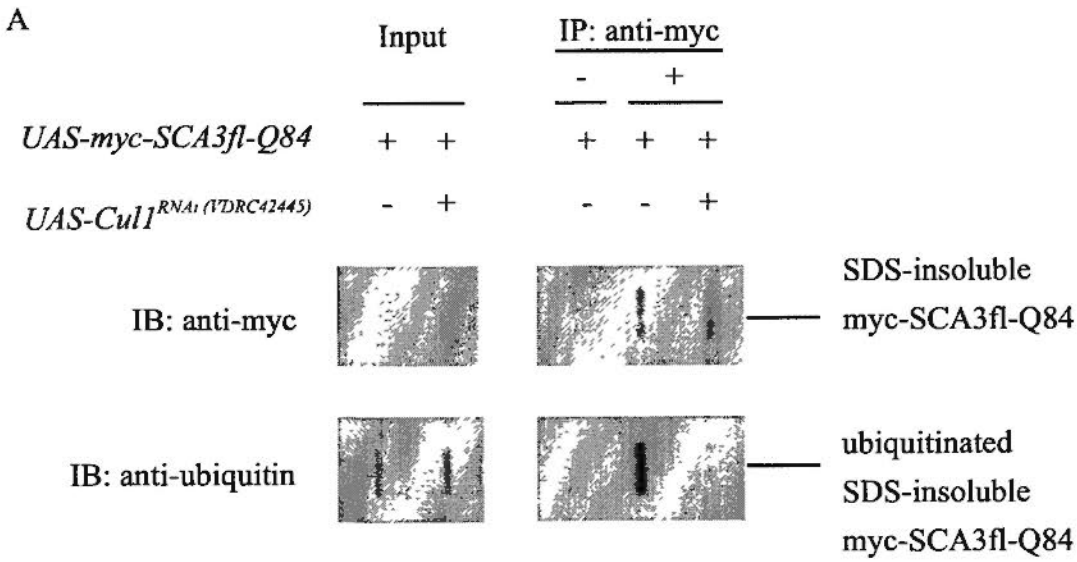
A
Input
IP: anti-myc
-
+
UAS-myc-SCA3fl-Q84
+ +
+ + +
UAS-Cul1RNAi (VDRC42445)
- +
- - +
IB: anti-myc
SDS-insoluble
myc-SCA3fl-Q84
IB: anti-ubiquitin
ubiquitinated
SDS-insoluble
myc-SCA3fl-Q84

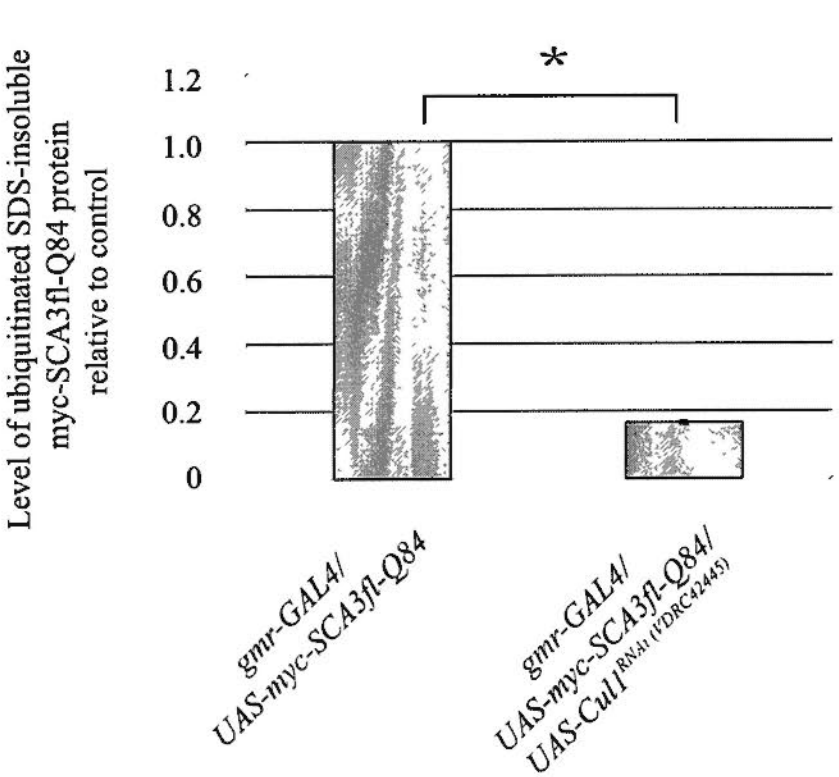
B
Level of ubiquitinated SDS-insoluble myc-SCA3fl-Q84 protein relative to control
1.2
1.0
0.8
0.6
0.4
0.2
0
*
gmr-GAL4/ UAS-myc-SCA3fl-Q84
gmr-GAL4/ UAS-myc-SCA3fl-Q84/ UAS-Cul1RNAi (VDRC42445)

Figure 3.22. Knock-down of *Cul1* expression reduced level of ubiquitinated SDS-insoluble myc-SCA3fl-Q84 protein captured by filter retardation assay.

(**A**) Adult head lysate of flies expressing myc-SCA3fl-Q84 protein with or without knock-down of *Cul1* expression was subjected to immunoprecipitation using anti-myc antibody to immunoprecipitate myc-SCA3fl-Q84 protein. The input and the eluate were then subjected to filter retardation assay to capture any SDS-insoluble protein aggregates with size larger than 0.22 μm. As both of the antibodies to be used for immunodetection were purified from mice, the samples were divided into two equal halves and loaded into two separate wells. The immunoblot was then cut into two halves for separate immunodetection. Upper row: the half-blot carrying a complete set of samples was probed with anti-myc antibody to detect the SDS-insoluble myc-SCA3fl-Q84 protein aggregates. Positive signal in the input shows the presence of SDS-insoluble myc-SCA3fl-Q84 protein in the lysate. The signal in the eluate confirmed positive immunoprecipitation of the SDS-insoluble myc-SCA3fl-Q84 protein and presence of equal amount of immunoprecipitated SDS-insoluble myc-SCA3fl-Q84 protein in each well. Lower row: the other half-blot carrying a complete set of samples was probed against anti-ubiquitin antibody to detect any ubiquitinated SDS-insoluble protein aggregates. The input indicates the presence of ubiquitinated SDS-insoluble protein aggregates in the lysate. Positive signal in the eluate indicates the ubiquitinated SDS-insoluble myc-SCA3fl-Q84 protein. Knock-down of *Cul1* expression reduced the level of ubiquitinated SDS-insoluble myc-SCA3fl-Q84 protein. (**B**) Quantification of the ubiquitinated SDS-insoluble myc-SCA3fl-Q84 protein in (**A**). Band intensity was relative to *myc-SCA3fl-Q84*-expressing flies without knock-down of *Cul1* expression. N = 3, * $p < 0.05$ (Student's t-test); error bar represents mean ± SEM from three independent experiments. The flies were raised at 21°C and were assayed at 3 dpe. They were of genotypes:

w; *gmr-GAL4/+*; *UAS-myc-SCA3fl-Q84/+*,

w; *gmr-GAL4/+*; *UAS-myc-SCA3fl-Q84/UAS-Cul1*$^{RNAi\ (VDRC42445)}$.

polyQ toxicity [23, 135, 136]. The suppressive effect on polyQ toxicity by chaperones demonstrates that reduced solubility of expanded polyQ protein is one of the major pathological mechanisms of polyQ diseases [23, 135, 136].

As mentioned in section 3.2, it was found that knock-down of *Cul1* expression enhanced polyQ toxicity. In sections 3.4 and 3.5, it was demonstrated that such enhancement on polyQ toxicity upon knock-down of *Cul1* expression was associated with reduced SDS-solubility of expanded polyQ protein. To test if the enhancing effect on polyQ toxicity upon knock-down of *Cul1* expression was due to the reduction in SDS-solubility of expanded polyQ protein, a transgenic line bearing human *Hsp70 (hHsp70)* [23] was employed. Hsp70 is a well-known chaperone that suppresses polyQ toxicity by increasing solubility of expanded polyQ proteins [23, 135, 164]. Human Hsp70 protein is homologous to *Drosophila melanogaster* Hsp70 protein (74% identical in amino acid sequence, 85% similar at protein level) [23]. In an external eye depigmentation assay [129], expression of *myc-SCA3fl-Q84* transgene in the fly eyes by *gmr-GAL4* driver did not have any observable depigmentation (Figure 3.23A). However, knock-down of *Cul1* expression in *myc-SCA3fl-Q84*-expressing flies enhanced degeneration and resulted in depigmentation and formation of necrotic scars on the eye surface (Figure 3.23B). Expression of *hHsp70* transgene in these *myc-SCA3fl-Q84*-expressing flies with knock-down of *Cul1* expression totally suppressed the above degenerative phenotype (Figure 3.23C). Combining the data here and the results shown in sections 3.2, 3.4 and 3.5, it is suggested that the enhancement on polyQ toxicity by knock-down of *Cul1* expression was due to reduced SDS-solubility of expanded polyQ protein.

Figure 3.23

A

gmr-GAL4/ UAS-myc-SCA3fl-Q84

B

gmr-GAL4/ UAS-myc-SCA3fl-Q84/
UAS-Cul1$^{RNAi\ (VDRC42445)}$

C

gmr-GAL4/ UAS-myc-SCA3fl-Q84/
UAS-Cul1$^{RNAi\ (VDRC42445)}$*/*
UAS-hHsp70

Figure 3.23 Expression of human *Hsp70* suppressed the *Cul1*^{RNAi}-mediated enhancement on polyglutamine toxicity.

External eye depigmentation phenotypes of flies with different genotypes are shown. Transgenes were expressed using the *gmr-GAL4* driver. **(A)** At 5 dpe, expression of *myc-SCA3fl-Q84* transgene did not show any observable degenerative phenotype. **(B)** Knock-down of *Cul1* expression enhanced polyQ toxicity and led to depigmentation and formation of necrotic scars. **(C)** Expression of human *Hsp70* transgene completely rescued the degenerative phenotype enhanced by knock-down of *Cul1* expression. Consistent results were obtained from two independent experiments. The flies were raised at 25°C. They were of genotypes:

(A) *w*; *gmr-GAL4/+*; *UAS-myc-SCA3fl-Q84/+*

(B) *w*; *gmr-GAL4/+*; *UAS-myc-SCA3fl-Q84, UAS-Cul1*$^{RNAi\ (VDRC42445)}$*/+*

(C) *w*; *gmr-GAL4/UAS-hHsp70*; *UAS-myc-SCA3fl-Q84, UAS-Cul1*$^{RNAi\ (VDRC42445)}$*/+*.

3.9 Feasibility of studying the effect of *Cul1* on polyglutamine toxicity by overexpression

All the data presented in previous sections described the effect of *Cul1* on polyQ pathogenesis through knock-down of *Cul1* expression. In order to double confirm the effect of *Cul1* on polyQ toxicity, the feasibility of studying the effect of *Cul1* on polyQ pathogenesis by overexpression was examined.

Firstly, the feasibility of studying the effect of overexpressing *Cul1* on polyQ toxicity was examined using the external eye depigmentation assay in the SCA3tr model [117]. In this model, expression of *HA-SCA3tr-Q78* transgene in the eyes by *gmr-GAL4* driver induced depigmentation (Figure 3.24A). This degenerative phenotype was absence in the *gmr-GAL4* driver control flies and the *HA-SCA3tr-Q27*-expressing flies (Figure 3.24A). Thus the *gmr-GAL4* driver control flies and the *HA-SCA3tr-Q27*-expressing flies served as controls to show the Q-length specificity of polyQ toxicity. When Cul1 protein was overexpressed using a *UAS-Cul1* transgenic line [131] in either the *gmr-GAL4* driver fly line or the *HA-SCA3tr-Q27*-expressing fly line, the external eye surface became rough (Figure 3.24B). This rough eye phenotype was reproducible using another independent *UAS-Cul1* transgenic fly line [131] (Figure 3.24C). This indicates that overexpressing *Cul1* in the eyes causes dominant phenotype that is not specific to polyQ toxicity. To double confirm the dominant phenotype by overexpressing *Cul1*, the above experiment was repeated using transgenic fly lines expressing

Figure 3.24

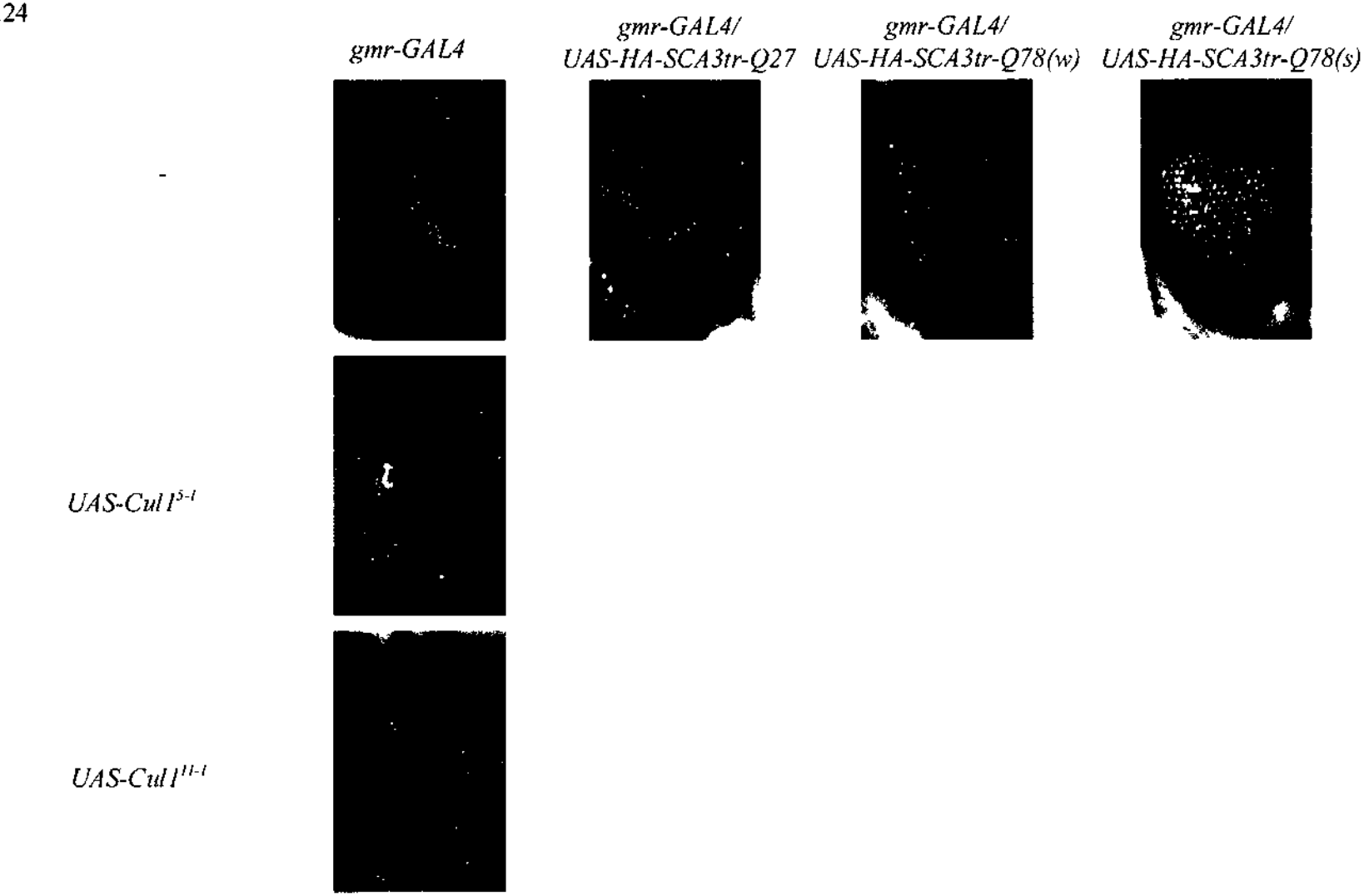
gmr-GAL4
gmr-GAL4/ UAS-HA-SCA3tr-Q27
gmr-GAL4/ UAS-HA-SCA3tr-Q78(w)
gmr-GAL4/ UAS-HA-SCA3tr-Q78(s)
A
B
UAS-Cul1^5-1
C
UAS-Cul1^11-1

Figure 3.24. Overexpressing *Cul1* showed dominant phenotype in adult fly eye depigmentation assay.

(A) At 3 dpe, expression of *HA-SCA3tr-Q27* transgene by *gmr-GAL4* driver did not cause any degenerative phenotype. Weak expression of *HA-SCA3tr-Q78* transgene (*HA-SCA3tr-Q78(w)*) caused mild depigmentation while strong expression of *HA-SCA3tr-Q78* transgene (*HA-SCA3tr-Q78(s)*) caused severe depigmentation. **(B** and **C)** Overexpressing *Cul1* by expression of *UAS-Cul1* transgene in two independent transgenic lines led to rough external eye surface. The experiment was performed once. The flies were raised at 25°C. They were of genotypes:

(A) *w*; *gmr-GAL4/+*; *+/+*,

w; *gmr-GAL4 UAS-HA-SCA3tr-Q27/+*; *+/+*,

w; *gmr-GAL4/+*; *UAS-HA-SCA3tr-Q78(w)/+*,

w; *gmr-GAL4 UAS-HA-SCA3tr-Q78(s)/+*; *+/+*

(B) *w*; *gmr-GAL4/UAS-Cul1*$^{5\text{-}1}$; *+/+*

(C) *w*; *gmr-GAL4/UAS-Cul1*$^{11\text{-}1}$; *+/+*.

FLAG-tagged Cul1 protein (FLAG-Cul1) [86] and FLAG-tagged Cul1^{KR} mutant protein (FLAG-Cul1^{KR}) [86] in which the lysine residue for neddylation on Cul1 protein was mutated (Figure 3.25). It was found that expression of *FLAG-Cul1* transgene in either the *gmr-GAL4* driver fly line or the *HA-SCA3tr-Q27*-expressing fly line gave rise to rough external eye surface (Figure 3.25B). This dominant phenotype was absent in *FLAG-Cul1^{KR}*-expressing flies (Figure 3.25C). This suggests that the dominant phenotype resulted by overexpressing *Cul1* was dependent on neddylation of Cul1 protein. Taken together, the effect of overexpressing *Cul1* on polyQ toxicity could not be studied using the external eye depigmentation assay and possibly other assays involving examination of eye phenotype.

Secondly, the feasibility of studying the effect of overexpressing *Cul1* on polyQ toxicity was examined using circadian locomotor behavior assay [126, 165]. It was reported that expanded polyQ proteins affect expression of clock genes and disrupt the circadian locomotor behavior in mouse and fly polyQ models [165, 166]. In this project, the circadian locomotor behavior of flies expressing *HA-SCA3tr-Q27* transgene and *HA-SCA3tr-Q78* transgene in the adult clock neurons by *tim-GAL4* driver was examined. It was found that flies expressing *HA-SCA3tr-Q27* transgene showed rhythmic circadian locomotor activity as compared to the *tim-GAL4* driver control flies (Figure 3.26B) and normal accumulative locomotor activity (Figure 3.27). However, the expression of *HA-SCA3tr-Q78* transgene resulted in arrhythmic locomotor activity (Figure 3.26C) and a slight reduction in the accumulative locomotor activity both in light phase and in night phase (Figure 3.27) as compared

Figure 3.25

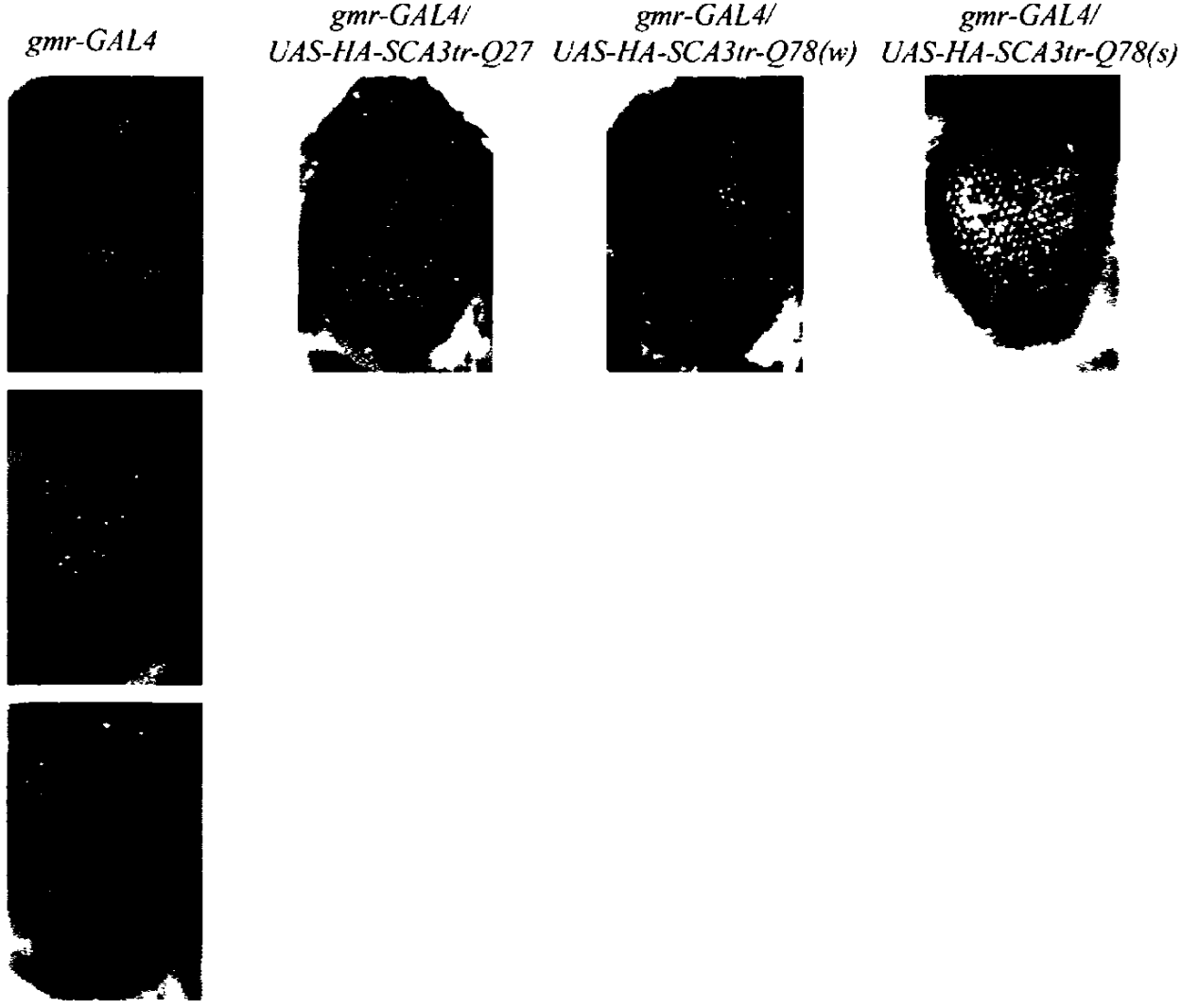
gmr-GAL4
gmr-GAL4/
UAS-HA-SCA3tr-Q27
gmr-GAL4/
UAS-HA-SCA3tr-Q78(w)
gmr-GAL4/
UAS-HA-SCA3tr-Q78(s)
A
-
B
UAS-FLAG-Cul1
C
UAS-FLAG-Cul1KR

Figure 3.25. The dominant phenotype upon overexpressing *Cul1* in adult fly eye depigmentation assay was dependent on neddylation of Cul1 protein.

(**A**) At 3 dpe, expression of *HA-SCA3tr-Q27* transgene by *gmr-GAL4* driver did not cause any degenerative phenotype. Weak expression of *HA-SCA3tr-Q78* transgene (*HA-SCA3tr-Q78(w)*) caused mild depigmentation while strong expression of *HA-SCA3tr-Q78* transgene (*HA-SCA3tr-Q78(s)*) caused severe depigmentation. (**B**) Overexpressing *FLAG*-tagged *Cul1* led to rough external eye surface. (**C**) This rough eye phenotype was absent if the neddylation site on Cul1 protein was mutated. The experiment was performed once. The flies were raised at 25°C. They were of genotypes:

(**A**) *w*; *gmr-GAL4*/+; +/+,

w; *gmr-GAL4 UAS-HA-SCA3tr-Q27*/+; +/+,

w; *gmr-GAL4*/+; *UAS-HA-SCA3tr-Q78(w)*/+,

w; *gmr-GAL4 UAS-HA-SCA3tr-Q78(s)*/+; +/+

(**B**) *w*; *gmr-GAL4/UAS-FLAG-Cul1*; +/+

(**C**) *w*; *gmr-GAL4*/+; *UAS-FLAG-Cul1*^{KR}/+.

Figure 3.26

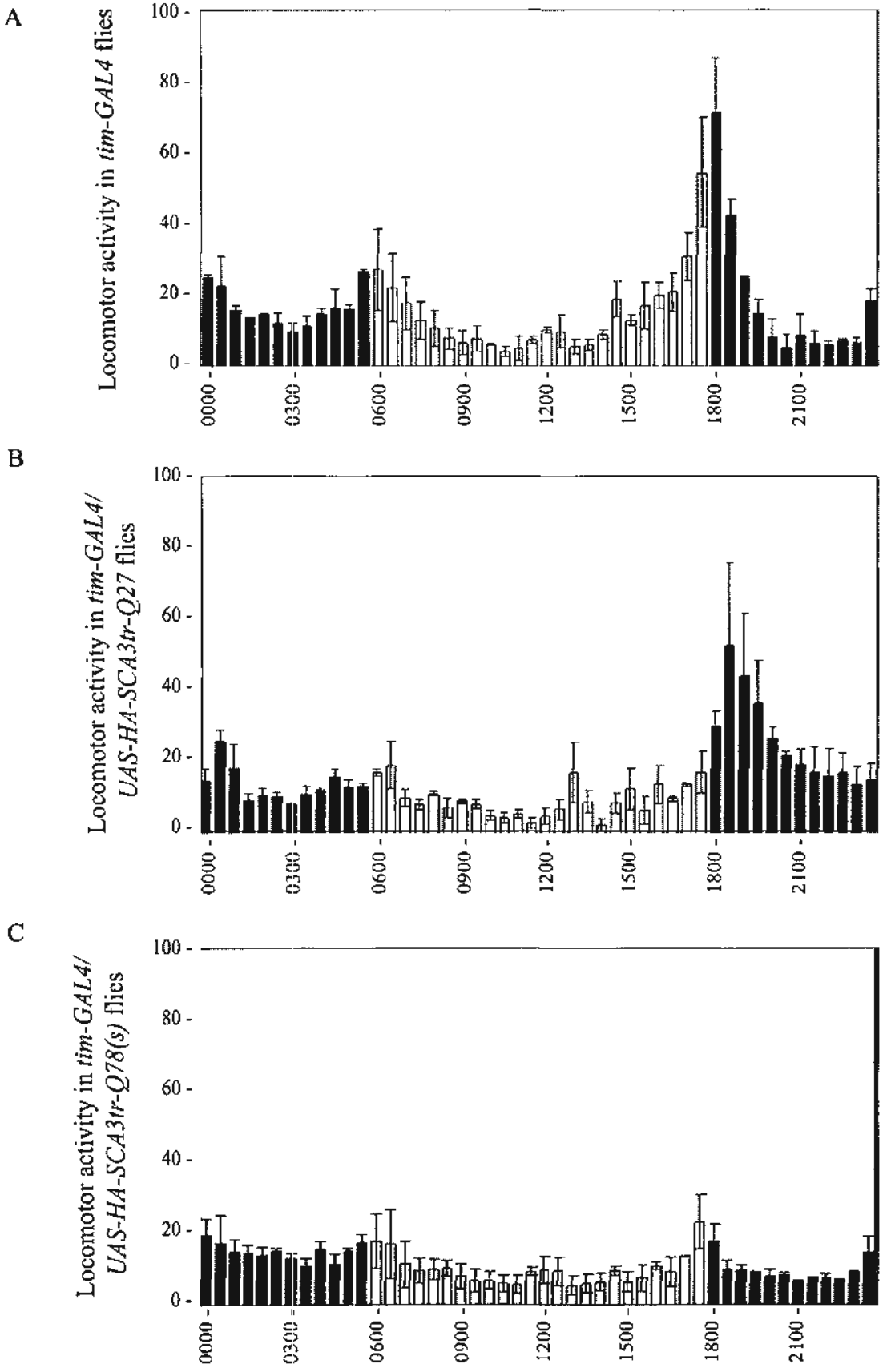
A
Locomotor activity in tim-GAL4 flies
B
Locomotor activity in tim-GAL4/ UAS-HA-SCA3tr-Q27 flies
C
Locomotor activity in tim-GAL4/ UAS-HA-SCA3tr-Q78(s) flies
100
80
60
40
20
0
0000
0300
0600
0900
1200
1500
1800
2100

Figure 3.26. The circadian locomotor activity rhythm of polyQ flies.

Histograms on the average locomotor activity of adult flies through 24 hr are shown. **(A)** *tim-GAL4* driver control flies displayed normal circadian locomotor activity rhythm which was characterized by a minor peak at time point 0600 and a major peak at time point 1800. **(B)** Expression of *HA-SCA3tr-Q27* transgene did not cause any modification on the circadian locomotor activity rhythm as compared to that in **(A)**. **(C)** In flies with strong expression of *HA-SCA3tr-Q78* transgene (*HA-SCA3tr-Q78(s)*), the major peak at time point 1800 was disappeared. The flies were kept in LD cycle during experiment. Open and filled bars indicate day and night periods respectively. Total activity in 0.5 hr was averaged from 16 male flies. Each bar represents the activity in 0.5 hr averaged from three consecutive days. The experiment was repeated and the error bars represent the S.E.M. from two sets of experiment. The flies were raised at 25°C and were of genotypes:

(A) *w*; *tim-GAL4/+*; *+/+*

(B) *w*; *tim-GAL4 UAS-HA-SCA3tr-Q27/+*; *+/+*

(C) *w*; *tim-GAL4 UAS-HA-SCA3tr-Q78(s)/+*; *+/+*.

Figure 3.27

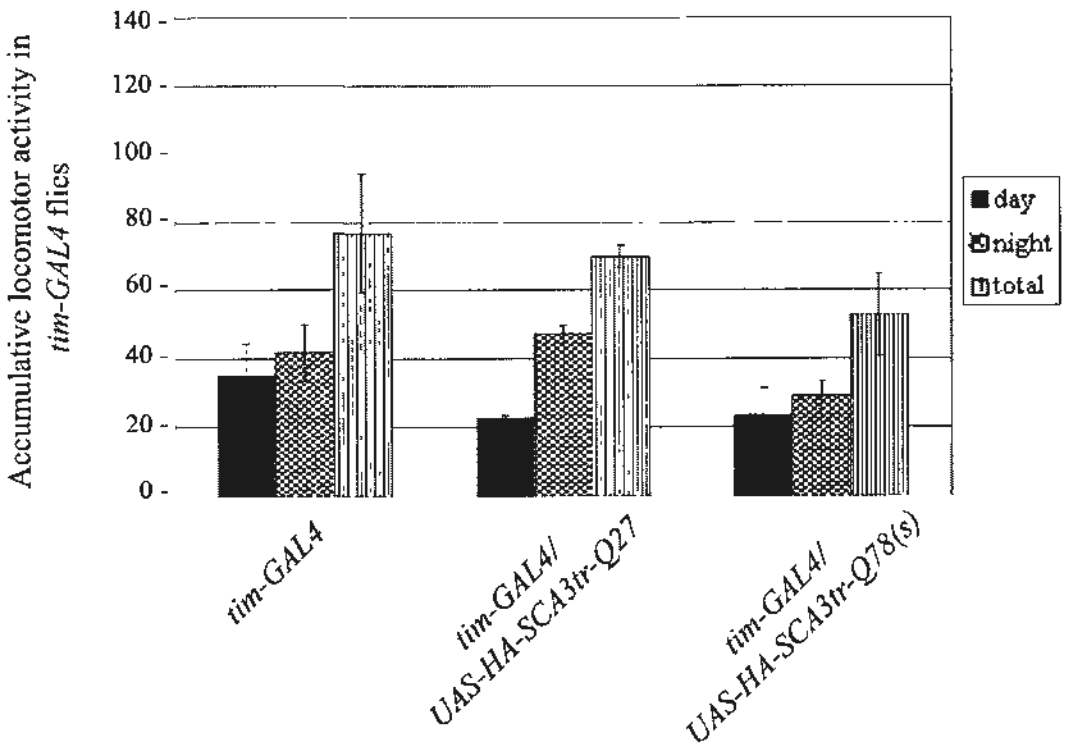
Accumulative locomotor activity in tim-GAL4 flies
140
120
100
80
60
40
20
0
day
night
total
tim-GAL4
tim-GAL4/ UAS-HA-SCA3tr-Q27
tim-GAL4/ UAS-HA-SCA3tr-Q78(s)

Figure 3.27. The accumulative locomotor activity of polyQ flies.

The flies were kept in LD cycle during experiment. The accumulative activity in light phase, in night phase and throughout 24 hr was recorded respectively. Expression of *HA-SCA3tr-Q27* transgene did not cause any large modification on the accumulative activity compared to that of *tim-GAL4* driver control flies. Strong expression of *HA-SCA3tr-Q78(w)* transgene led to reduced accumulative activity in night phase as compared to that of *tim-GAL4* driver control flies. The accumulative activity was averaged from 16 male flies and further averaged from three consecutive days. The experiment was repeated and the error bars represent the S.E.M. from two sets of experiment. The flies were raised at 25°C and were of genotypes:

w; *tim-GAL4/+*; *+/+*,

w; *tim-GAL4 UAS-HA-SCA3tr-Q27/+*; *+/+*,

w; *tim-GAL4 UAS-HA-SCA3tr-Q78(s)/+*; *+/+*.

to the *gmr-GAL4* driver control. This shows the Q-length specificity of polyQ toxicity. As compared to the *tim-GAL4* driver control, expression of either *FLAG-Cul1* transgene [86] or *FLAG-Cul1*^{KR} transgene [86] alone particularly disrupted the circadian locomotor activity rhythm at night (Figure 3.28B and C) and caused an increase in the accumulative locomotor activity at night (Figure 3.29). This indicates that overexpressing *Cul1* has dominant phenotype which is independent of neddylation of Cul1 protein. Therefore, the effect of overexpressing *Cul1* on polyQ toxicity cannot be studied using the circadian locomotor behavior assay.

3.10 Discussion

As mentioned before, CRLs are a large family of E3 ubiquitin ligases which can be classified into five main groups based on the cullin proteins employed [81]. To test if certain groups of CRLs are involved in polyQ pathogenesis, endogenous expression of five *cullin* genes *(Cul1-5)* were individually knocked down by RNAi [134] in two polyQ transgenic fly models, the SCA3tr [117] and SCA3fl [129] models. The corresponding modification on neurotoxicity and SDS solubility of expanded polyQ protein were examined.

It was found that among the five cullins studied, only *Cul1* and *Cul4* modified polyQ toxicity (Figure 3.3). This suggests that Cul1- and Cul4-based CRLs are involved in polyQ pathogenesis. The specificity may be due to the specific adaptor(s) and substrate receptor(s) employed to form CRLs by different cullins [81]. As reviewed by Petroski *et al.* (2005) [81], Cul1-based CRL employs Skp1 protein as adaptor and F-box protein as substrate receptor. Cul2- and Cul5-based CRLs recruit

Figure 3.28

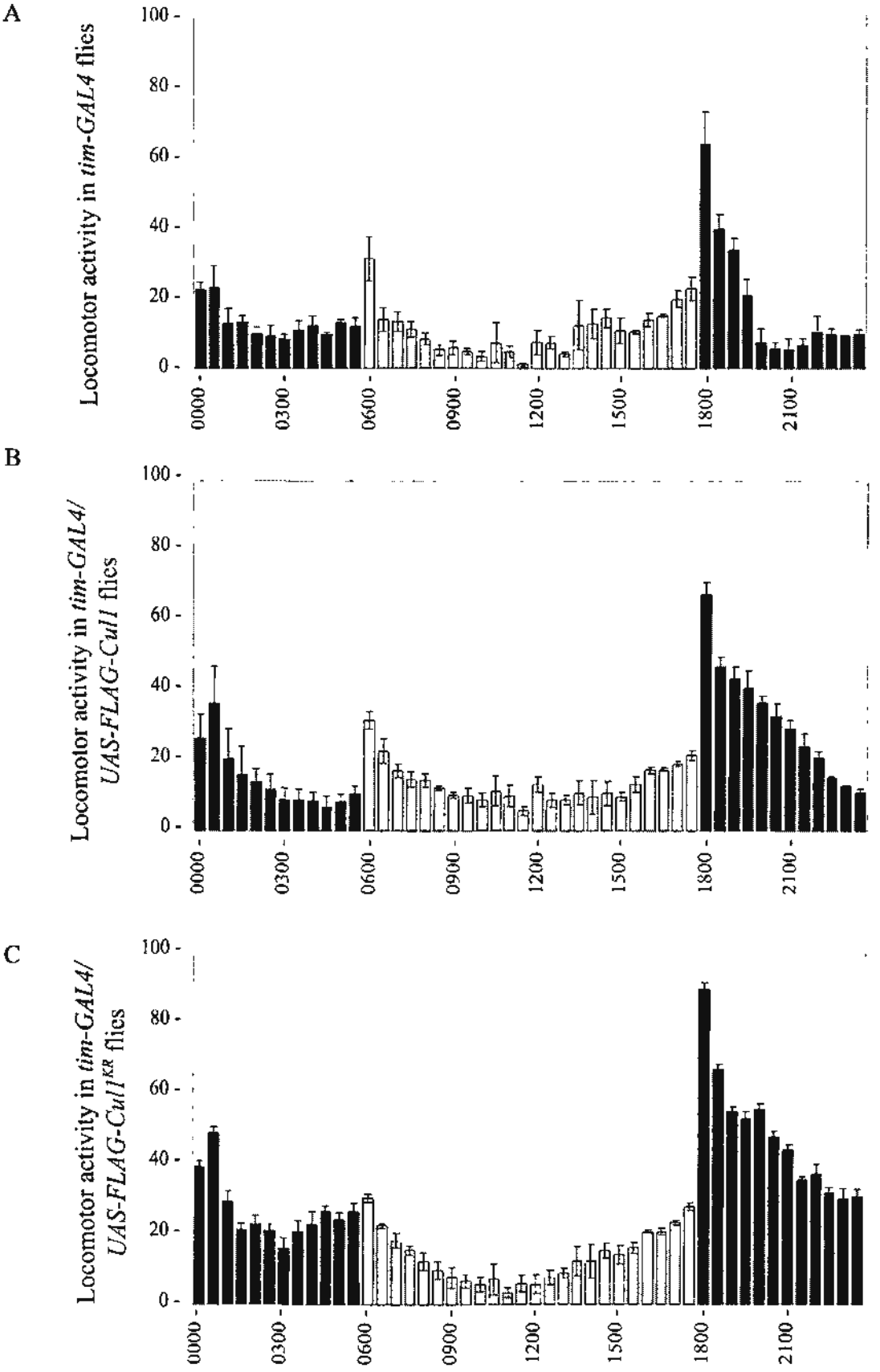
A
Locomotor activity in tim-GAL4 flies
B
Locomotor activity in tim-GAL4/ UAS-FLAG-Cul1 flies
C
Locomotor activity in tim-GAL4/ UAS-FLAG-Cul1KR flies
100
80
60
40
20
0
0000
0300
0600
0900
1200
1500
1800
2100

Figure 3.28. The circadian locomotor activity rhythm of *Cul1*-overexpressing flies.

Histograms on the average locomotor activity of adult flies through 24 hr are shown. (**A**) *tim-GAL4* driver control flies displayed normal circadian locomotor activity rhythm which was characterized by a minor peak at time point 0600 and a major peak at time point 1800. (**B** and **C**) Expression of either *FLAG-Cul1* (**B**) or *FLAG-Cul1*^{KR} (**C**) led to a slower drop in activity after the major peak at time point 1800. The flies were kept in LD cycle during experiment. Open and filled bars indicate day and night periods respectively. Total activity in 0.5 hr is averaged from 16 male flies. Each bar represents the activity in 0.5 hr averaged from three consecutive days. The experiment was repeated and the error bars represent the S.E.M. from two sets of experiment. The flies were raised at 25°C and were of genotypes:

(**A**) *w*; *tim-GAL4/+*; *+/+*

(**B**) *w*; *tim-GAL4 UAS-FLAG-Cul1/+*; *+/+*

(**C**) *w*; *tim-GAL4/+*; *UAS-FLAG-Cul1*^{KR}*/+*.

Figure 3.29

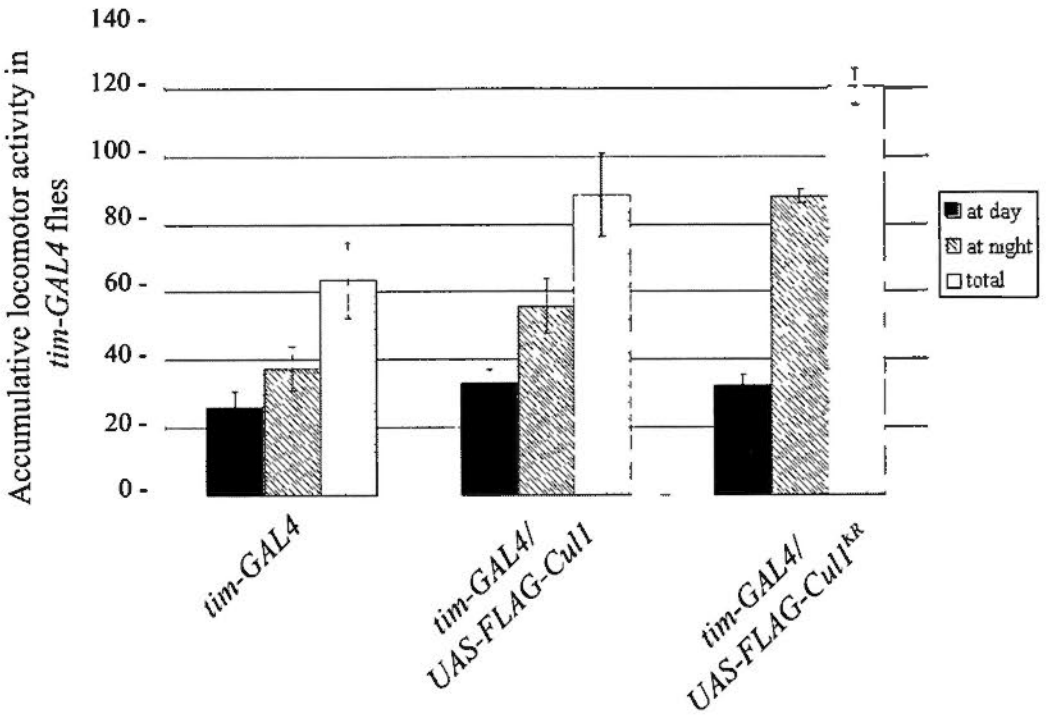
Accumulative locomotor activity in tim-GAL4 flies
140 -
120 -
100 -
80 -
60 -
40 -
20 -
0 -
at day
at night
total
tim-GAL4
tim-GAL4/ UAS-FLAG-Cul1
tim-GAL4/ UAS-FLAG-Cul1KR

Figure 3.29. The accumulative locomotor activity of *Cul1*-overexpressing flies.

The flies were kept in LD cycle during experiment. The accumulative activity in light phase, in night phase and throughout 24 hr was recorded respectively. Expression of either *FLAG-Cul1* or *FLAG-Cul1*^{KR} led to higher accumulative activity in night phase as compared to that of *tim-GAL4* driver control flies. The accumulative activity was averaged from 16 male flies and further averaged from three consecutive days. The experiment was repeated and the error bars represent the S.E.M. from two sets of experiment. The flies were raised at 25°C and were of genotypes:

w; *tim-GAL4*/+; +/+,

w; *tim-GAL4 UAS-FLAG-Cul1*/+; +/+,

w; *tim-GAL4*/+; *UAS-FLAG-Cul1*^{KR}/+.

substrates through an elongin-BC adaptor and a suppressor of cytokine signaling/elongin BC-box-protein substrate receptor. In Cul3-based CRL, BTB-domain-containing protein serves as both adaptor and substrate receptor. Less is known for Cul4-based CRL. Cul4-CRL might recruit substrate through adaptor DNA-damage-binding protein-1 and a putative substrate receptor [81].

The finding that knock-down of *Cul1* expression enhanced polyQ toxicity (Figure 3.3B) is consistent with the result from an RNAi screen performed by Mehta *et al.* (2009) [95]. The authors reported that *cul-1*, the worm homolog of *Cul1*, enhanced polyQ toxicity in *C. elegans* [95]. The effect of *Cul1* on neurotoxicity was not a general effect on general protein-misfolding neurodegenerative diseases such as PD (Figure 3.12). It was specific to polyQ diseases (Figures 3.10 and 3.11). This highlights the specific role of Cul1 protein in polyQ diseases. The enhancing effect of *Cul1* on polyQ toxicity (Figure 3.8B) was accompanied with a reduction on the SDS-solubility of expanded polyQ protein (Figure 3.9). The effect of *Cul1* on SDS-solubility of expanded polyQ protein was consistent with a previous report by Manfiolli *et al.* (2008). The authors showed that deleting the N-terminal domain of Cul1 protein enhanced polyQ protein aggregation [94]. Therefore, the specific role of Cul1 protein in polyQ diseases could be explained by the functional relationship between Cul1 protein and expanded polyQ protein.

In contrast, *Cul4* modulated polyQ toxicity without changing the SDS-solubility of expanded polyQ protein (Figures 3.3E, 3.6C, 3.8C and 3.9). It is likely that *Cul4* affects polyQ toxicity through mechanisms other than protein quality control.

Cul4-based CRL has been demonstrated to be critical regulators of diverse cellular pathways including DNA damage and repair, DNA replication, epigenetic control of gene expression, histone lysine methylation, genome stability, cell cycle and developmental patterning [167]. It is likely that Cul4 protein acts on polyQ toxicity through one or several of these pathways.

In addition to *cul-1*, the RNAi screen by Mehta *et al.* (2009) also reported the involvement of *cul-2*, the worm homologs of *Cul-2,* in polyQ toxicity [95]. However, in the present study, knock-down of *Cul2* expression did not modify polyQ toxicity (Figure 3.3C). The difference in findings compared with the present study may be due to the difference in polyQ model and the phenotype assays used. Mehta *et al.* (2009) employed a *C. elegans* model expressing an YFP fused with 35 residues of glutamine [95]. Among the nine currently found polyQ diseases, 35 residues of glutamine are just around the threshold for disease development [168]. The low number of glutamine repeats and the lack of an unexpanded control lead to query about whether the effect by *cul-2* is specific to expanded polyQ protein [95]. Besides, the stringency and detection sensitivity between two studies may also be different and therefore difficult to compare directly [95].

Further studies were performed to investigate the role of Cul1 protein in polyQ diseases. In Cul1-based CRL, Cul1 protein binds Skp1 adaptor protein through the Skp1-binding domain [157, 158]. The Skp1 adaptor protein in turn binds to the substrate receptor which recruits specific substrate protein for ubiquitination [157, 158]. It has been demonstrated that ubiquitination of substrate protein regulates the

abundance of substrate protein in cells [161]. In this study, it was found that Cul1 protein physically interacted with expanded polyQ protein at least through the Skp1-binding domain (Figure 3.20). Moreover, the reduction of SDS-solubility of expanded polyQ protein upon knock-down of *Cul1* expression (Figure 3.15) was accompanied with a reduction in the ubiquitination of the SDS-insoluble fraction of myc-SCA3fl-Q84 protein specifically (Figure 3.22) but not the SDS-soluble fraction (Figure 3.21). These data suggest that Cul1-based CRL specifically recognizes the SDS-insoluble form of expanded polyQ protein, ubiquitinates it and targets it to degradation. As reviewed in Chapter 1 (section 1.3), expanded polyQ tract makes polyQ protein prone to aggregate. Aggregation is a progressive process in which the SDS-solubility of expanded polyQ protein reduces gradually. Structurally, expanded polyQ protein undergoes conformational transition from monomer, oligomer and fibril to aggregate. It is likely that certain Cul1-based CRL substrate receptor(s) specifically recognize(s) particular SDS-insoluble conformation(s) of expanded polyQ protein.

SDS-insoluble species expanded polyQ protein has been reported to be neurotoxic [52, 53, 135]. Its accumulation in cells could lead to degeneration [52, 53, 135]. Many studies have shown that promoting the protein refolding activity of chaperones such as Hsp70 enhances solubility of expanded polyQ protein and suppresses polyQ toxicity [135]. It was found that overexpressing human Hsp70 protein totally suppressed the degenerative phenotype which was enhanced upon knock-down of *Cul1* expression (Figure 3.23). These data support the above idea that the enhancement on polyQ toxicity by knock-down of *Cul1* expression (Figure 3.8B)

was due to an increase in the level of toxic SDS-insoluble expanded polyQ protein (Figure 3.15). To strengthen this hypothesis, it is desirable to check if the level of SDS-insoluble expanded polyQ protein in flies with knock-down of *Cul1* expression was reduced by overexpression *Hsp70*.

Various studies have shown that lowering the level of insoluble expanded polyQ protein aggregates reduced polyQ toxicity [77, 80, 169-171]. In particular, Tsai *et al.* (2008) demonstrated that elimination of expanded polyQ protein aggregates by overexpression Parkin relieved the proteasomal impairment and the caspase activation induced by expanded polyQ protein [80]. It is likely that through ubiquitinating and targeting the toxic SDS-insoluble expanded polyQ protein for degradation, Cul1-based CRL helps relieving the cellular stresses such as proteasomal impairment, transcriptional dysregulation and mitochondrial dysfunction induced by the toxic SDS-insoluble expanded polyQ protein [28].

In order to make the above hypothesis more convincing, feasibility of studying the effect of *Cul1* on polyQ toxicity by overexpression was examined using adult external eye depigmentation assay [117]. As mentioned before, adult external eye depigmentation assay is a simple and reliable assay for screening toxicity modifiers [137]. Unfortunately, overexpressing *Cul1* resulted in dominant phenotype that was not specific to polyQ toxicity in adult external eye depigmentation assay (Figures 3.24 and 3.25). This dominant phenotype is probably due to the involvement of Cul1-based CRL in fly eye development. During development of fly eyes, Cubitus interruptus (Ci) from the Hh signaling pathway controls cell differentiation, while the

cell cycle regulator, cyclin E (CycE), controls cell proliferation [172]. Cul1-based CRLs regulate the proteolysis of Ci and CycE through substrate receptors Slimb (Slmb) and Archipelago (Ago) respectively [172]. Overexpressing *Cul1* could disturb the above pathways and affect eye development, resulting in rough eye surface. The above dominant phenotype was not observed upon knock-down of *Cul1* expression. This may be due to the following reasons. First, knock-down efficiency of *Cul1* expression is just around 40% (Figure 3.1). Second, the proteolysis of Ci and CycE is also regulated by other E3 ubiquitin ligases such as Cul3-based CRL [81, 173].

The feasibility of studying the effect of *Cul1* on polyQ toxicity by overexpression was also explored using locomotor behavior assay. Polyglutamine patients have disturbed night-day activity patterns [166]. Locomotor behavior assay has been used to studied the effect of expanded poly polyQ protein expression on circadian clock [165]. In the present study, it was found that overexpressing *Cul1* modified the normal circadian locomotor behavior as compared to the *tim-GAL4* driver control (Figures 3.28 and 3.29). The dominant phenotype here might be due to the regulation of Cul1-based CRL on expression of some of the clock proteins. Daily fluctuation of levels of clock proteins Period (Per) and Timeless (Tim) drive the circadian clock in flies. It is reported that Cul1-based CRL regulates the degradation of Per and Tim through Slmb substrate receptor [174]. Overexpressing *Cul1* could disturb the above pathways and modify the normal circadian locomotor behavior.

To sum up, it was found that among five major cullin proteins, *Cul1* modified polyQ toxicity possible through modulating the ubiquitination of SDS-insoluble

expanded polyQ protein.

Chapter 4 F-box proteins are involved in the Cul1^{RNAi}-mediated modification on polyglutamine toxicity

4.1 Introduction

According to Chapter 3, it was suggested that SDS-insoluble expanded polyQ protein is a substrate of Cul1-based CRL. To consolidate this hypothesis, it is essential to identify the specific substrate receptor employed to target the SDS-insoluble expanded polyQ protein for ubiquitination. Cul1-based CRL recruits substrate protein using F-box proteins as substrate receptors [81]. F-box proteins belong to a large protein family [175, 176]. So far, 69 F-box proteins have been identified in humans and 27 in *Drosophila* [177, 178]. In a F-box protein, the conserved Skp1-binding domain at the N-terminus binds to the adaptor protein Skp1 while the variable substrate-binding domain at the C-terminus binds to the substrate proteins [175, 176]. Cul1-based CRL recognizes specific substrate protein by assembling with specific F-box proteins [179].

To look for the F-box protein involved in the Cul1^{RNAi}-mediated modification on polyQ pathogenesis, a RNAi screening was performed in the truncated Spinal Cerebullar Ataxia 3 (SCA3tr) model [117]. Expression of 19 F-box proteins which are conserved from *Drosophila* to humans were individually knocked down by RNAi [134] in the adult fly eyes. Adult external eye depigmentation assay was used as a direct and reliable method to study the effect by knock-down of expression of individual F-box proteins on toxicity induced by weak expression of *HA-SCA3tr-Q78 (HA-SCA3tr-Q78(w))* [137] (section 4.2). Any F-box protein that

enhanced polyQ toxicity upon knock-down of expression would likely act in the same pathway in polyQ pathogenesis as Cul1 protein. It was found that knock-down of expression of an F-box protein, CG2010, enhanced polyQ toxicity (section 4.2). Further investigations into the effect of CG2010 on expanded polyQ protein were performed in order to test if CG2010 protein is involved in polyQ pathogenesis through Cul1-based CRL. These investigations include specificity of enhancement on polyQ toxicity (section 4.3), modification on SDS-solubility (section 4.4) and ubiquitination of expanded polyQ protein (section 4.5) upon knock-down of *CG2010* expression. Besides, genetic interaction between *CG2010* and *Cul1* was also performed to test if CG2010 and Cul1 proteins acted in same pathway in polyQ toxicity (section 4.6).

4.2 Screening for F-box proteins which modified polyglutamine toxicity similarly as Cul1

Although 69 F-box proteins have been identified in humans, only 19 of them have homologs in *Drosophila* [175, 177, 178]. Since knock-down of endogenous *Cul1* expression enhanced polyQ toxicity in flies, these 19 fly F-box proteins are therefore possible substrate receptors employed by Cul1-based CRL in modification of polyQ toxicity in fly. To test which F-box protein was involved in polyQ toxicity, expression of these F-box proteins was individually knocked down by RNAi [134] in the well-characterized SCAtr model [117].

As described in Chapter 3 (section 3.2), the SCA3tr model expresses a HA-tagged, truncated form of ataxin-3 protein. Expression of the transgene encoding

for the truncated ataxin-3 protein with unexpanded polyQ repeats of 27 glutamines (*HA-SCA3tr-Q27*) in the eyes by *gmr-GAL4* did not cause any degenerative phenotype even after aging for 32 days (Figures 3.2A and 4.1A). Weak expression of the transgene encoding for the truncated ataxin-3 protein with expanded polyQ repeats of 78 glutamines (*HA-SCA3tr-Q78(w)*) induced late-onset progressive degeneration resulting in depigmentation phenotype which could be observed at 32 dpe but not at 3 dpe (Figures 3.2B and 4.1A). This *HA-SCA3tr-Q78(w)* transgenic fly line allows identification of any polyQ toxicity enhancers. Knock-down of expression of most F-box protein genes showed no enhancing effect on *HA-SCA3tr-Q78(w)*-induced toxicity (Figure 4.1E - T). Knock-down of *Slimb (Slmb)* expression resulted in a non-expanded polyQ-specific dominant phenotype as shown by the rough external eye surface in the unexpanded control flies expressing *HA-SCA3tr-Q27* (Figure 4.1B). This indicates that *Slmb* has non-polyQ related functions in cells. Knock-down of *Regulator of cyclin A* (*Rca1*) expression caused mild degeneration as shown by the slight depigmentation phenotype resulted in the *HA-SCA3tr-Q78(w)*-expressing flies (Figure 4.1C). Knock-down of *CG2010* expression strongly enhanced degeneration as shown by the extensive loss of pigmentation and formation of necrotic scars in the *HA-SCA3tr-Q78(w)*-expressing flies (Figure 4.1D). Semi-quantitative RT-PCR confirmed that the knock-down efficiency of *CG2010* expression was higher than 90% (92%; Figure 4.2). This indicates that the modification observed was caused by *CG2010*.

To exclude the possibility of off-target effect due to non-specific binding of dsRNA on mRNA of non-target gene(s), the above examination of adult fly external

Figure 4.1

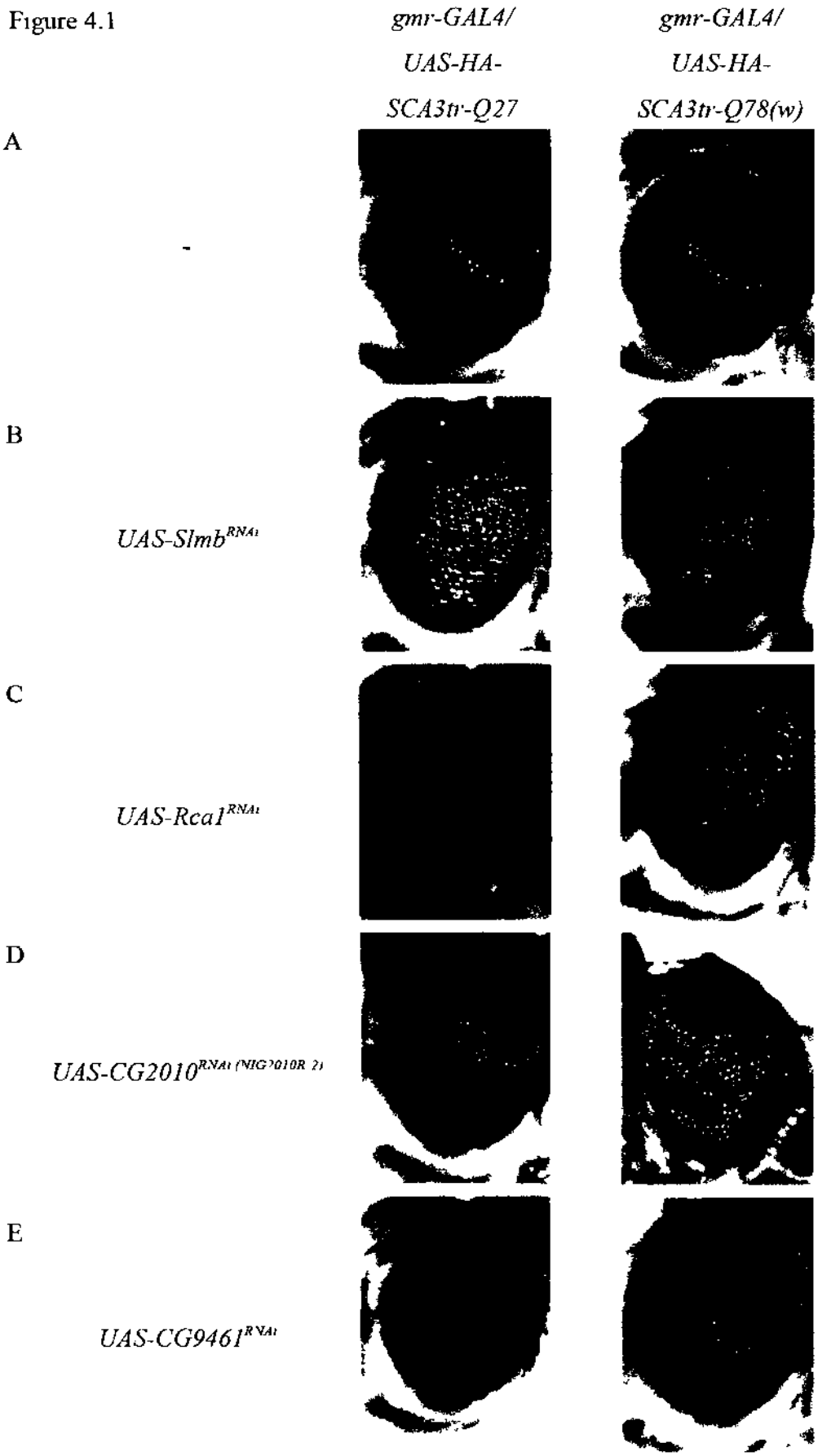
gmr-GAL4/ UAS-HA-SCA3tr-Q27
gmr-GAL4/ UAS-HA-SCA3tr-Q78(w)
A
-
B
UAS-Slmb^RNAi
C
UAS-Rca1^RNAi
D
UAS-CG2010^RNAi (NIG?010R 2)
E
UAS-CG9461^RNAi

Figure 4.1

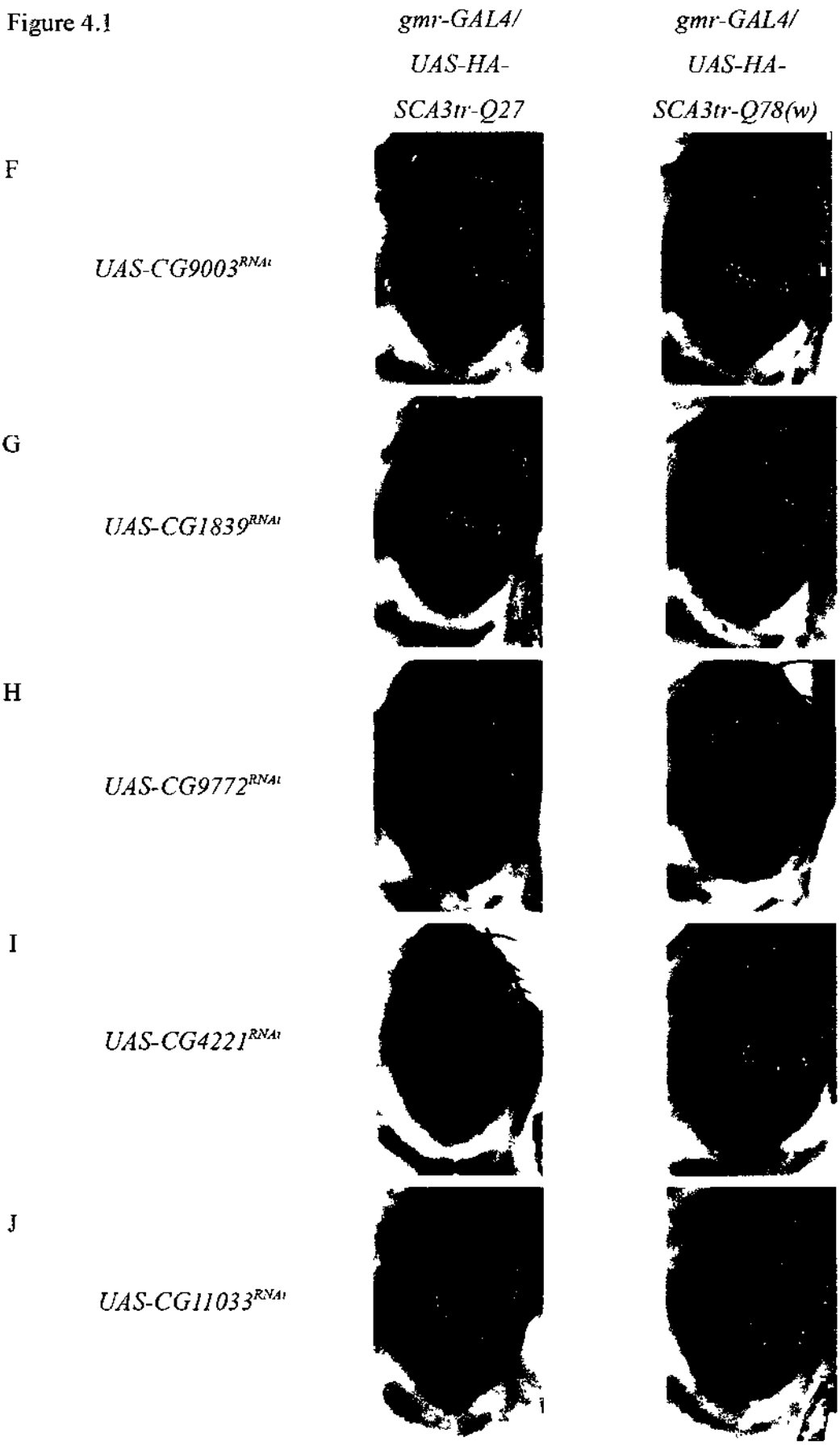
gmr-GAL4/ UAS-HA-SCA3tr-Q27
gmr-GAL4/ UAS-HA-SCA3tr-Q78(w)
F
UAS-CG9003RNAi
G
UAS-CG1839RNAi
H
UAS-CG9772RNAi
I
UAS-CG4221RNAi
J
UAS-CG11033RNAi

Figure 4.1

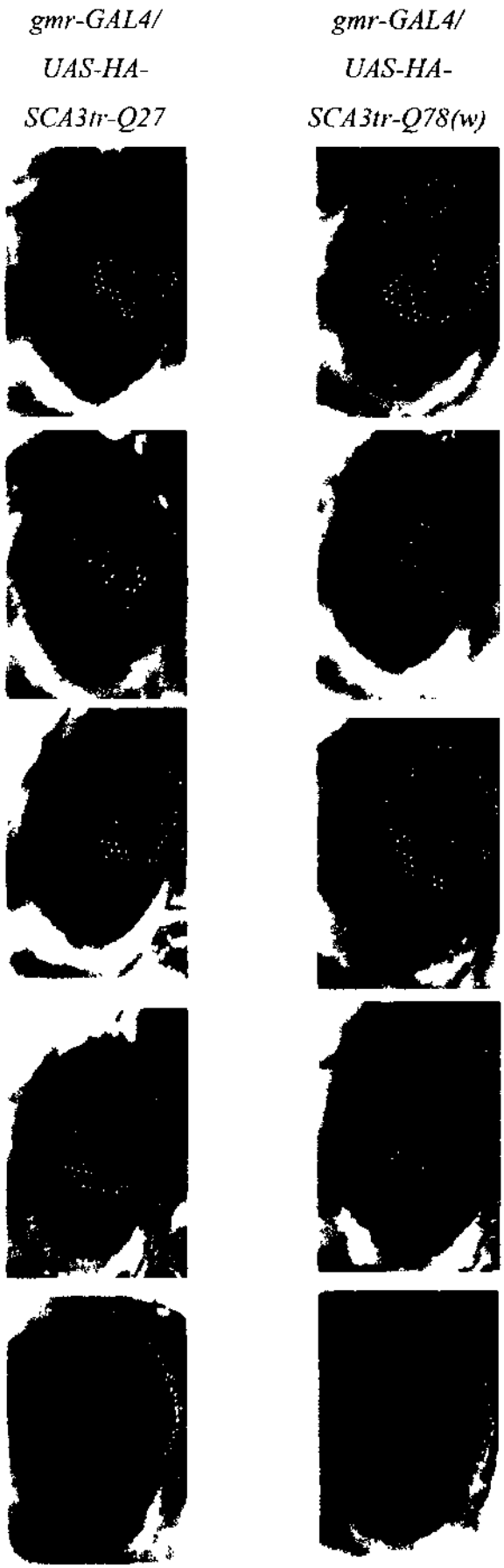
gmr-GAL4/ UAS-HA- SCA3tr-Q27
gmr-GAL4/ UAS-HA- SCA3tr-Q78(w)
K
UAS-Ppα^RNAi
L
UAS-CG8873^RNAi
M
UAS-CG32085^RNAi
N
UAS-CG9144^RNAi
0
UAS-CG5961^RNAi

Figure 4.1

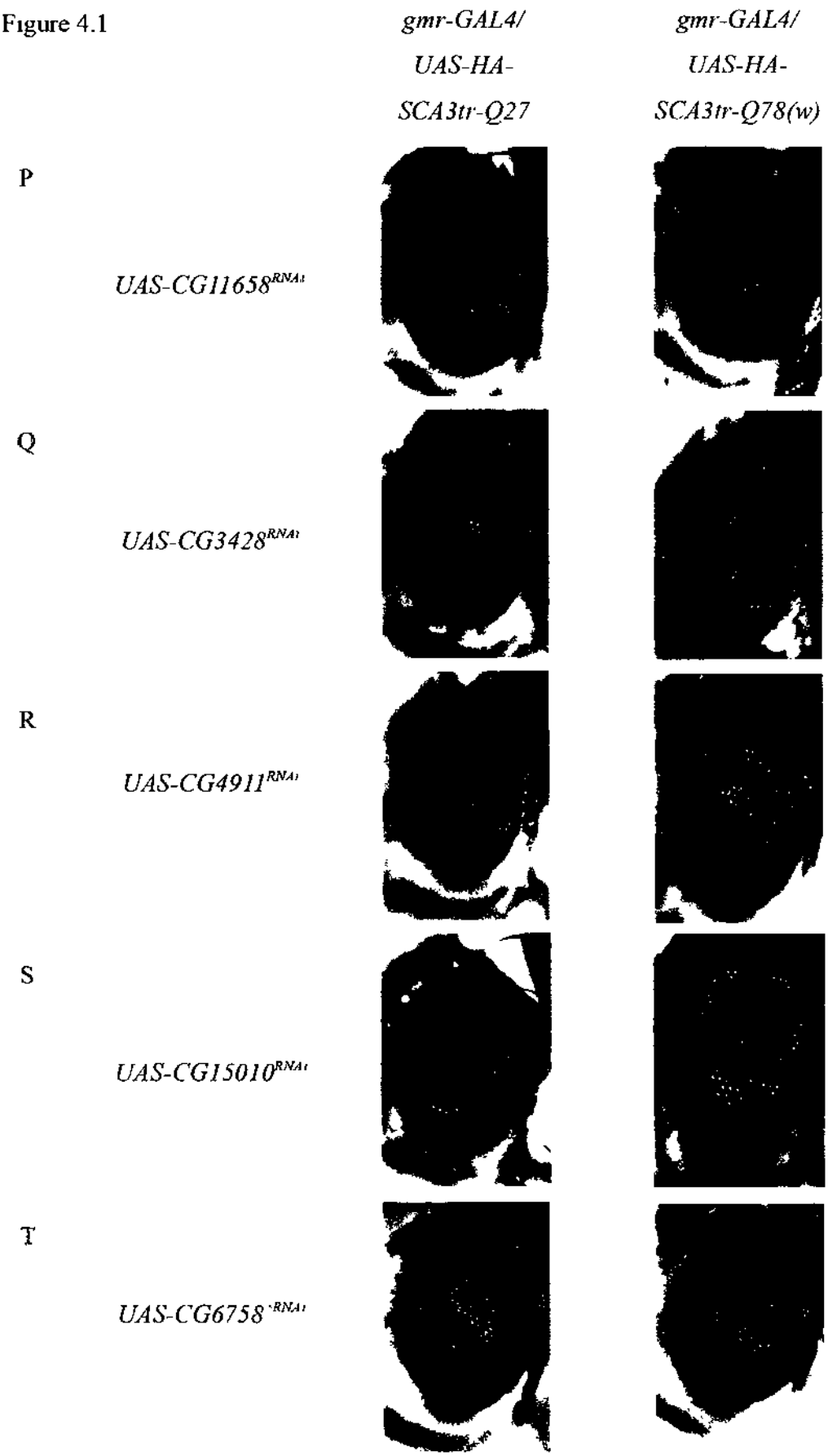
gmr-GAL4/ UAS-HA-SCA3tr-Q27
gmr-GAL4/ UAS-HA-SCA3tr-Q78(w)
P
UAS-CG11658RNAi
Q
UAS-CG3428RNAi
R
UAS-CG4911RNAi
S
UAS-CG15010RNAi
T
UAS-CG6758RNAi

Figure 4.1. Knock-down of *CG2010* expression enhanced degeneration induced by *HA-SCA3tr-Q78* expression in adult fly eyes.

Adult external eye depigmentation phenotypes of flies expressing *truncated ataxin-3* transgenes (*HA-SCA3tr-Q27* or *HA-SCA3tr-Q78)* with or without (indicated by "-") knock-down of expression of individual F-box protein genes are shown. Transgenes were expressed using the *gmr-GAL4* driver. (**A**) At 3 dpe, expression of *HA-SCA3tr-Q27* did not cause any degenerative phenotype. Weak expression of *HA-SCA3tr-Q78* (*HA-SCA3tr-Q78(w)*) did not cause any observable depigmentation. (**B**) Knock-down of *Slmb* expression resulted in rough external eye surface in *HA-SCA3tr-Q27*-expressing flies. (**C**) Knock-down of *Rca1* expression slightly enhanced depigmentation induced by *HA-SCA3tr-Q78(w)* as indicated by mild depigmentation. (**D**) Knock-down of *CG2010* expression caused a more severe enhancement of depigmentation induced by *HA-SCA3tr-Q78(w)* as indicated by extensive loss of pigmentation and formation of necrotic scars. (**E** - **T**) Individual knock-down of expression of other F-box proteins did not modify the *HA-SCA3tr-Q78*-induced degenerative phenotype. The experiment on *CG2010* (**D**) was repeated for two times and consistent results were obtained from three independent experiments. The flies were raised at 25°C. They were of genotypes:

(**A**) *w; gmr-GAL4 UAS-HA-SCA3tr-Q27/+; +/+,*
w; gmr-GAL4/+; UAS-HA-SCA3tr-Q78(w)/+
(**B**) *w; gmr-GAL4 UAS-HA-SCA3tr-Q27/+; UAS-Slmb^{RNAi}/+,*
w; gmr-GAL4/+; UAS-HA-SCA3tr-Q78(w)/UAS-Slmb^{RNAi}
(**C**) *w; gmr-GAL4 UAS-HA-SCA3tr-Q27/+; UAS-Rca1^{RNAi}/+,*
w; gmr-GAL4/+; UAS-HA-SCA3tr-Q78(w)/UAS-Rca1^{RNAi}
(**D**) *w; gmr-GAL4 UAS-HA-SCA3tr-Q27/UAS-CG2010$^{RNAi\ (NIG2010R-2)}$; +/+,*
w; gmr-GAL4/UAS-CG2010$^{RNAi\ (NIG2010R-2)}$; UAS-HA-SCA3tr-Q78(w)/+
(**E**) *w; gmr-GAL4 UAS-HA-SCA3tr-Q27/UAS-CG9461^{RNAi}; +/+,*
w; gmr-GAL4/UAS-CG9461^{RNAi}; UAS-HA-SCA3tr-Q78(w)/+
(**F**) *w; gmr-GAL4 UAS-HA-SCA3tr-Q27/UAS-CG9003^{RNAi}; +/+,*
w; gmr-GAL4/UAS-CG9003^{RNAi}; UAS-HA-SCA3tr-Q78(w)/+
(**G**) *w; gmr-GAL4 UAS-HA-SCA3tr-Q27/UAS-CG1839^{RNAi}; +/+,*
w; gmr-GAL4/UAS-CG1839^{RNAi}; UAS-HA-SCA3tr-Q78(w)/+
(**H**) *w; gmr-GAL4 UAS-HA-SCA3tr-Q27/UAS-CG9772^{RNAi}; +/+,*
w; gmr-GAL4/UAS-CG9772^{RNAi}; UAS-HA-SCA3tr-Q78(w)/+
(**I**) *w UAS-CG4221^{RNAi}; gmr-GAL4 UAS-HA-SCA3tr-Q27/+; +/+*
w UAS-CG4221^{RNAi}; gmr-GAL4/+; UAS-HA-SCA3tr-Q78(w)/+
(**J**) *w; gmr-GAL4 UAS-HA-SCA3tr-Q27/UAS-CG11033^{RNAi}; +/+,*
w; gmr-GAL4/UAS-CG11033^{RNAi}; UAS-HA-SCA3tr-Q78(w)/+
(**K**) *w; gmr-GAL4 UAS-HA-SCA3tr-Q27/UAS-Ppa^{RNAi}; +/+,*
w; gmr-GAL4/UAS-Ppa^{RNAi}; UAS-HA-SCA3tr-Q78(w)/+
(**L**) *w UAS-CG8873^{RNAi}; gmr-GAL4 UAS-HA-SCA3tr-Q27/+; +/+,*
w UAS-CG8873^{RNAi}; gmr-GAL4/+; UAS-HA-SCA3tr-Q78(w)/+
(**M**) *w; gmr-GAL4 UAS-HA-SCA3tr-Q27/UAS-CG32085^{RNAi}; +/+,*
w; gmr-GAL4/UAS-CG32085^{RNAi}; UAS-HA-SCA3tr-Q78(w)/+
(**N**) *w; gmr-GAL4 UAS-HA-SCA3tr-Q27/UAS-CG9144^{RNAi}; +/+,*
w; gmr-GAL4/UAS-CG9144^{RNAi}; UAS-HA-SCA3tr-Q78(w)/+
(**O**) *w; gmr-GAL4 UAS-HA-SCA3tr-Q27/+; UAS-CG5961^{RNAi}/+,*
w; gmr-GAL4/+; UAS-HA-SCA3tr-Q78(w)/UAS-CG5961^{RNAi}
(**P**) *w; gmr-GAL4 UAS-HA-SCA3tr-Q27/+; UAS-CG11658^{RNAi}/+,*
w; gmr-GAL4/+; UAS-HA-SCA3tr-Q78(w)/UAS-CG11658^{RNAi}
(**Q**) *w; gmr-GAL4 UAS-HA-SCA3tr-Q27/+; UAS-CG3428^{RNAi}/+,*
w; gmr-GAL4/+; UAS-HA-SCA3tr-Q78(w)/UAS-CG3428^{RNAi}
(**R**) *w; gmr-GAL4 UAS-HA-SCA3tr-Q27/UAS-CG4911^{RNAi}; +/+,*
w; gmr-GAL4/UAS-CG4911^{RNAi}; UAS-HA-SCA3tr-Q78(w)/+
(**S**) *w; gmr-GAL4 UAS-HA-SCA3tr-Q27/UAS-Ago^{RNAi}; +/+,*
w; gmr-GAL4/UAS-Ago^{RNAi}; UAS-HA-SCA3tr-Q78(w)/+
(**T**) *w; gmr-GAL4 UAS-HA-SCA3tr-Q27/UAS-CG6758^{RNAi}; +/+,*
w; gmr-GAL4/UAS-CG6758^{RNAi}; UAS-HA-SCA3tr-Q78(w)/+.

Figure 4.2

A

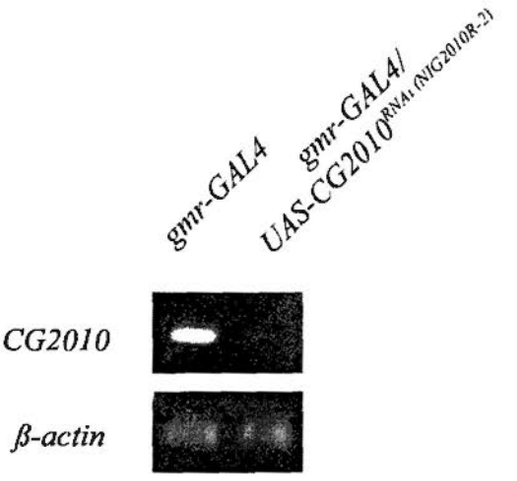
gmr-GAL4
gmr-GAL4/
UAS-CG2010RNAi (NIG2010R-2)
CG2010
ß-actin

B

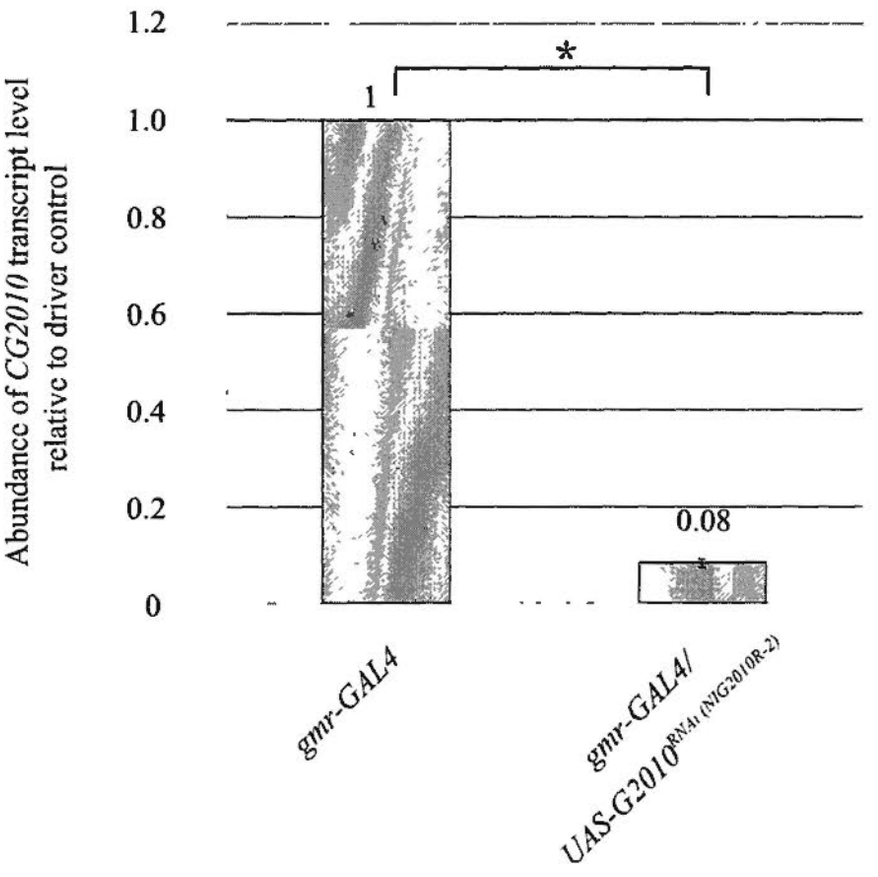
Abundance of CG2010 transcript level relative to driver control
1.2
1.0
0.8
0.6
0.4
0.2
0
*
1
0.08
gmr-GAL4
gmr-GAL4/
UAS-G2010RNAi (NIG2010R-2)

Figure 4.2. Knock-down efficiency of *CG2010* expression.

(**A**) Transcript level of *CG2010* in *gmr-GAL4* driver control flies and *UAS-CG2010*$^{RNAi\ (NIG2010R-2)}$ flies revealed by RT-PCR. *ß-actin* served as loading control. (**B**) Quantification of (**A**). *UAS-CG2010*$^{RNAi\ (NIG2010R-2)}$ flies achieved 92% reduction of *CG2010* transcript level. N = 4, * $p < 0.01$ (Student's t-test); error bars represent mean ± SEM from four independent experiments. The flies were raised at 25°C and were assayed at 3 dpe. They were of genotypes:

w; *gmr-GAL4*/+;+/+,

w; *gmr-GAL4/UAS-CG2010*$^{RNAi\ (NIG2010R-2)}$;+/+.

eye depigmentation was repeated using an independent *CG2010*^{RNAi} fly line (*UAS-CG2010*$^{RNAi\ (VDRC100736)}$; Figure 4.5). Although 43% of the *CG2010 dsRNA* sequence of *UAS-CG2010*$^{RNAi\ (VDRC100736)}$ fly line overlaps with that of *UAS-CG2010*$^{RNAi\ (NIG2010R-2)}$ fly line used in Figure 4.1D (Figure 4.3), both of the two *CG2010 dsRNA* sequences did not align well with mRNA of any genes other than CG2010 according to a BLASTN search against the fly annotated genes database [180] (Figure 4.4). It was found that the enhancing effect upon knock-down of *CG2010* expression was reproducible in this *UAS-CG2010*$^{RNAi\ (VDRC100736)}$ fly line (Figure 4.5). Thus, the enhancing effect observed was due to specific knock-down of *CG2010* expression.

4.3 Knock-down of *CG2010* expression caused a specific enhancement of polyglutamine toxicity

To test if the effect of *CG2010* on toxicity is specific to the polyQ domain, examination of adult fly external eye depigmentation was performed in two additional polyQ disease models. The first one is the ARtr model [24]. As mentioned in Chapter 3 (section 3.4), polyQ tract-expanded AR protein is the disease protein for the polyQ disease named SBMA [24, 147]. Flies expressing the transgene encoding for the truncated form of AR with normal Q-length (*ARtr-Q16*) in the eyes by *gmr-GAL4* driver did not induce any degenerative phenotype (Figure 4.6A). Conversely, weak expression of the transgene encoding for the expanded form of ARtr (*ARtr-Q112(w)*) induced degeneration resulting in mild depigmentation (Figure 4.6A). Knock-down of *CG2010* expression in the eyes of the *ARtr-Q112*-expressing flies, but not *ARtr-Q16*-expressing flies, caused more extensive loss of pigmentation

Figure 4.3

A

```
CG2010 CDS                ACTCTGCGCTACATCGAGCTGCCCATCGAGCTGATCACGCACACGGTGCTCCACGAACTG 360
CG2010 dsRNA (NIG2010R-2) ---------TACATCGAGCTGCCCATCGAGCTGATCACGCACACGGTGCTCCACGAACTG 51
                          **************************************************

CG2010 CDS                TCCGCCAAGTGCCCCAATTTGACCCACATGCTGCTGGACTTCTCCACAGCCATGCAGCTG 420
CG2010 dsRNA (NIG2010R-2) TCCGCCAAGTGCCCCAATTTGACCCACATGCTGCTGGACTTCTCCACAGCCATGCAGCTG 111
                          ************************************************************

CG2010 CDS                CACGACTTCAGCGAGATGCAGGCCTTTCCCACCAAGCTGCGCTACATGTGCGTCTGCCTC 480
CG2010 dsRNA (NIG2010R-2) CACGACTTCAGCGAGATGCAGGCCTTTCCCACCAAGCTGCGCTACATGTGCGTCTGCCTC 171
                          ************************************************************

CG2010 CDS                TCGGAGGTGATCTTCATGGAGGGCTTCATGCGCAAAATCTACAACTTCATCAACGGCCTG 540
CG2010 dsRNA (NIG2010R-2) TCGGAGGTGATCTTCATGGAGGGCTTCATGCGCAAAATCTACAACTTCATCAACGGCCTG 231
                          ************************************************************

CG2010 CDS                GAGGTGCTGCATCTAATTGGCACGTACGAGAAGTGCGAGGAGGAGGAGGAGGAGATCTAC 600
CG2010 dsRNA (NIG2010R-2) GAGGTGCTGCATCTAATTGGCACGTACGAGAAGTGCGAGGAGGAGGAGGAGGAGATCTAC 291
                          ************************************************************

CG2010 CDS                GAGGTGATCAACGTGCACAAGCTCAAGTCGGCCACGCCCAATTTGCGTGTGATCAACCTG 660
CG2010 dsRNA (NIG2010R-2) GAGGTGATCAACGTGCACAAGCTCAAGTCGGCCACGCCCAATTTGCGTGTGATCAACCTG 351
                          ************************************************************

CG2010 CDS                TACGGCATCAACTTCATCGATGACTCGCACATCGACGCCTTCAGCTCGAACTGCATCCAG 720
CG2010 dsRNA (NIG2010R-2) TACGGCATCAACTTCATCGATGACTCGCACATCGACGCCTTCAGCTCGAACTGCATCCAG 411
                          ************************************************************

CG2010 CDS                CTGGAGTGCCTGGCCGTCAACTTCTGCAACAAAGTGACCGGCTCCACCCTGAAGACCCTG 780
CG2010 dsRNA (NIG2010R-2) CTGGAGTGCCTGGCCGTCAACTTCTGCAACAAAGTGACCGGCTCCACCCTGAAGACCCTG 471
                          ************************************************************

CG2010 CDS                ATCCAGCGTTCCAAGCGCCTCACCTGCCTGCTCATGAACGGCACCAGCCTGAAGTCGGAG 840
CG2010 dsRNA (NIG2010R-2) ATCCAGCGTTCCAAGCGCCTCACCTGCCT---------------------------------- 500
                          *******************************
```

B

```
CG2010 CDS                GAGGTGATCAACGTGCACAAGCTCAAGTCGGCCACGCCCAATTTGCGTGTGATCAACCTG 660
CG2010 dsRNA (VDRC100736) --------CAACGTGCACAAGCTCAAGTCGGCCACGCCCAATTTGCGTGTGATCAACCTG 52
                          ************************************************

CG2010 CDS                TACGGCATCAACTTCATCGATGACTCGCACATCGACGCCTTCAGCTCGAACTGCATCCAG 720
CG2010 dsRNA (VDRC100736) TACGGCATCAACTTCATCGATGACTCGCACATCGACGCCTTCAGCTCGAACTGCATCCAG 112
                          ************************************************************

CG2010 CDS                CTGGAGTGCCTGGCCGTCAACTTCTGCAACAAAGTGACCGGCTCCACCCTGAAGACCCTG 780
CG2010 dsRNA (VDRC100736) CTGGAGTGCCTGGCCGTCAACTTCTGCAACAAAGTGACCGGCTCCACCCTGAAGACCCTG 172
                          ************************************************************

CG2010 CDS                ATCCAGCGTTCCAAGCGCCTCACCTGCCTGCTCATGAACGGCACCAGCCTGAAGTCGGAG 840
CG2010 dsRNA (VDRC100736) ATCCAGCGTTCCAAGCGCCTCACCTGCCTGCTCATGAACGGCACCAGCCTGAAGTCGGAG 232
                          ************************************************************

CG2010 CDS                TTCGTCATGCAGGCCGAGTGGGACAAGTGCGCCCTGCAGGAGCTGGACATCACGGCCACC 900
CG2010 dsRNA (VDRC100736) TTCGTCATGCAGGCCGAGTGGGACAAGTGCGCCCTGCAGGAGCTGGACATCACGGCCACC 292
                          ************************************************************

CG2010 CDS                GATCTTTCGACCGAATGCCTCGTGGACATGCTGAGCAGGATCCCCAGCCTCAAGTTCCTC 960
CG2010 dsRNA (VDRC100736) GATCTTTCGACCGAATGCCTCGTGGACATGCTGAGCAGGATCCCCAGCCTCAAGTTCCTC 352
                          ************************************************************

CG2010 CDS                TCAGCCGGCCAGATCAATGGCTTCAACGACAGCGTTCTCAAGCAGTGGATGGAATCGGGC 1020
CG2010 dsRNA (VDRC100736) TCAGCCGGCCAGATCAATGGCTTCAACGACAGCGTTCTCAAGCAGTGGAT---------- 402
                          **************************************************
```

C

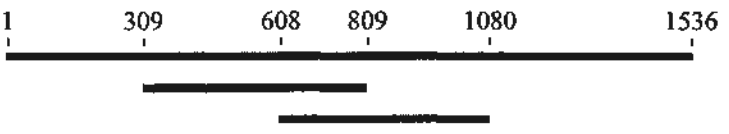

Figure 4.3. dsRNA sequences of two independent *CG2010*^{RNAi} fly lines.

There are 1,536 base pairs in the CDS of fly *CG2010* (protein product: FBpp0084795 (FlyBase)). (**A**) The dsRNA sequence in *UAS-CG2010*$^{RNAi\ (NIG2010R-2)}$ fly line (Line No. 2010R-2 from the National Institute of Genetics) targets at nt 309 to nt 809 of *CG2010* CDS. (**B**) The dsRNA sequence in *UAS-CG2010*$^{RNAi\ (VDRC100736)}$ fly line (Line No. 100736 from the Vienna *Drosophila* RNAi Center) targets at nt 608 to nt 1,080 of *CG2010* CDS. "*" indicates perfect match between nt from two aligned sequences at the corresponding position and "-" indicates that there is no nt at the corresponding position. Nucleotide 1 is defined as the starting nt of the corresponding sequence. (**C**) Schematic diagram showing the overlapping region between *CG2010* CDS and the C*G2010 dsRNA* sequences of the two *CG2010*^{RNAi} lines used in this study.

Figure 4.4

A

Query	
Description	**Length**
CG2010_dsRNA(NIGCG2010R-2)	500

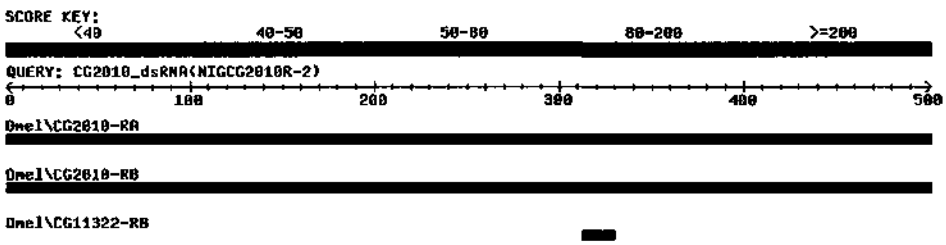

Send BLAST Hits to HitList

BLAST Hit Summary				
☑	**Description**	**Species**	**Score**	**E value**
☑	CG2010-RA	Dmel	884 623	0
☑	CG2010-RB	Dmel	884.623	0
☑	CG11322-RB	Dmel	36 1753	0 343712

B

Query	
Description	**Length**
CG2010_dsRNA(VDRC100736)	402

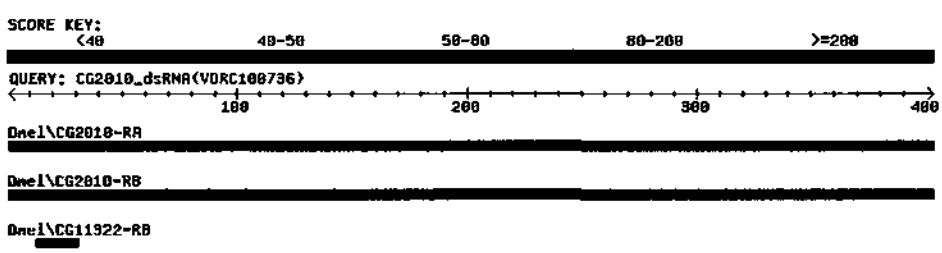

Send BLAST Hits to HitList

BLAST Hit Summary				
☑	**Description**	**Species**	**Score**	**E value**
☑	CG2010-RA	Dmel	797 399	0
☑	CG2010-RB	Dmel	797 399	0
☑	CG11322-RB	Dmel	36 1753	0 274657

Figure 4.4. Results on the BLASTN search of the two *CG2010* dsRNA sequences against the fly annotated genes database.

The dsRNA sequence of *UAS-CG2010*$^{RNAi\ (NIG2010R-2)}$ line (**A**) and that of *UAS-CG2010*$^{RNAi\ (VDRC100736)}$ line (**B**) align perfectly with the two transcript variants of *CG2010* mRNA (*CG2010-RA* and *CG2010-RB*, in red) as indicated by the E value of 0. (**A**) Apart from *CG2010*, these two *CG2010 dsRNA* sequences only poorly align with a transcript variant of *CG11322* (*CG11322-RB*, in black) among all the fly annotated genes with an E value > 0.27.

Figure 4.5

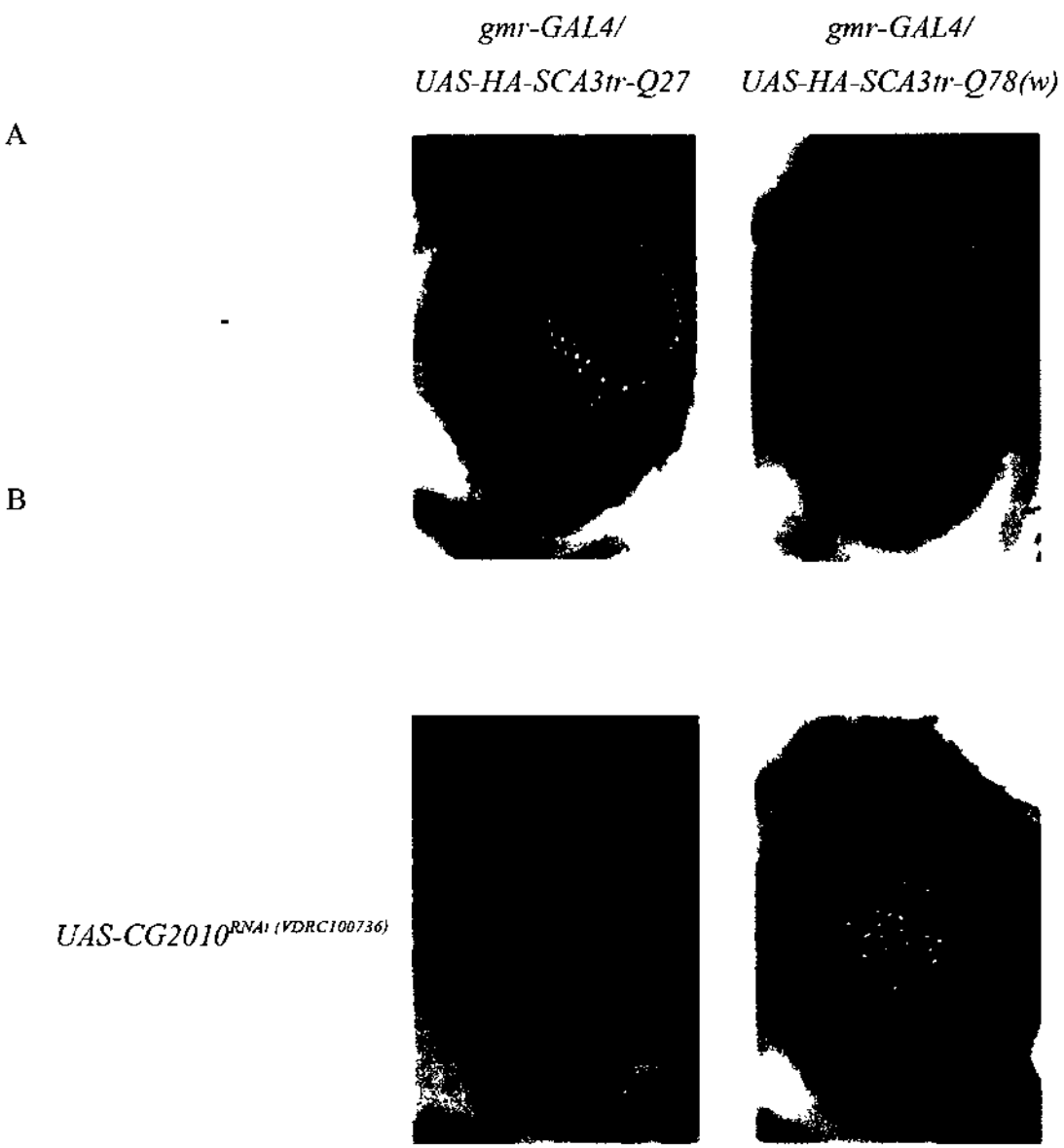
gmr-GAL4/
UAS-HA-SCA3tr-Q27
gmr-GAL4/
UAS-HA-SCA3tr-Q78(w)
A
B
UAS-CG2010RNAi (VDRC100736)

Figure 4.5. Effect by knock-down of *CG2010* expression on *HA-SCA3tr-Q78*-induced toxicity was reproducible in another independent *CG2010*^{RNAi} line.

Adult external eye depigmentation phenotypes of flies expressing truncated ataxin-3 transgenes (*HA-SCA3tr-Q27* or *HA-SCA3tr-Q78)* with or without (indicated by "-") knock-down of *CG2010* expression are shown. Transgenes were expressed using the *gmr-GAL4* driver. (**A**) At 3 dpe, expression of *HA-SCA3tr-Q27* transgene did not cause any degenerative phenotype. Weak expression of *HA-SCA3tr-Q78* (*HA-SCA3tr-Q78(w)*) did not cause any observable depigmentation. (**B**) Knock-down of *CG2010* expression caused a Q-length specific enhancement on depigmentation induced by *HA-SCA3tr-Q78(w)* as indicated by extensive loss of pigmentation. The flies were raised at 25°C. They were of genotypes:

(**A**) *w*; *gmr-GAL4 UAS-HA-SCA3tr-Q27/+*; *+/+*,

w; *gmr-GAL4/+*; *UAS-HA-SCA3tr-Q78(w)/+*

(**B**) *w*; *gmr-GAL4 UAS-HA-SCA3tr-Q27/UAS-CG2010*$^{RNAi\ (VDRC100736)}$; *+/+*,

w; *gmr-GAL4/UAS-CG2010*$^{RNAi\ (VDRC100736)}$; *UAS-HA-SCA3tr-Q78(w)/+*.

Figure 4.6

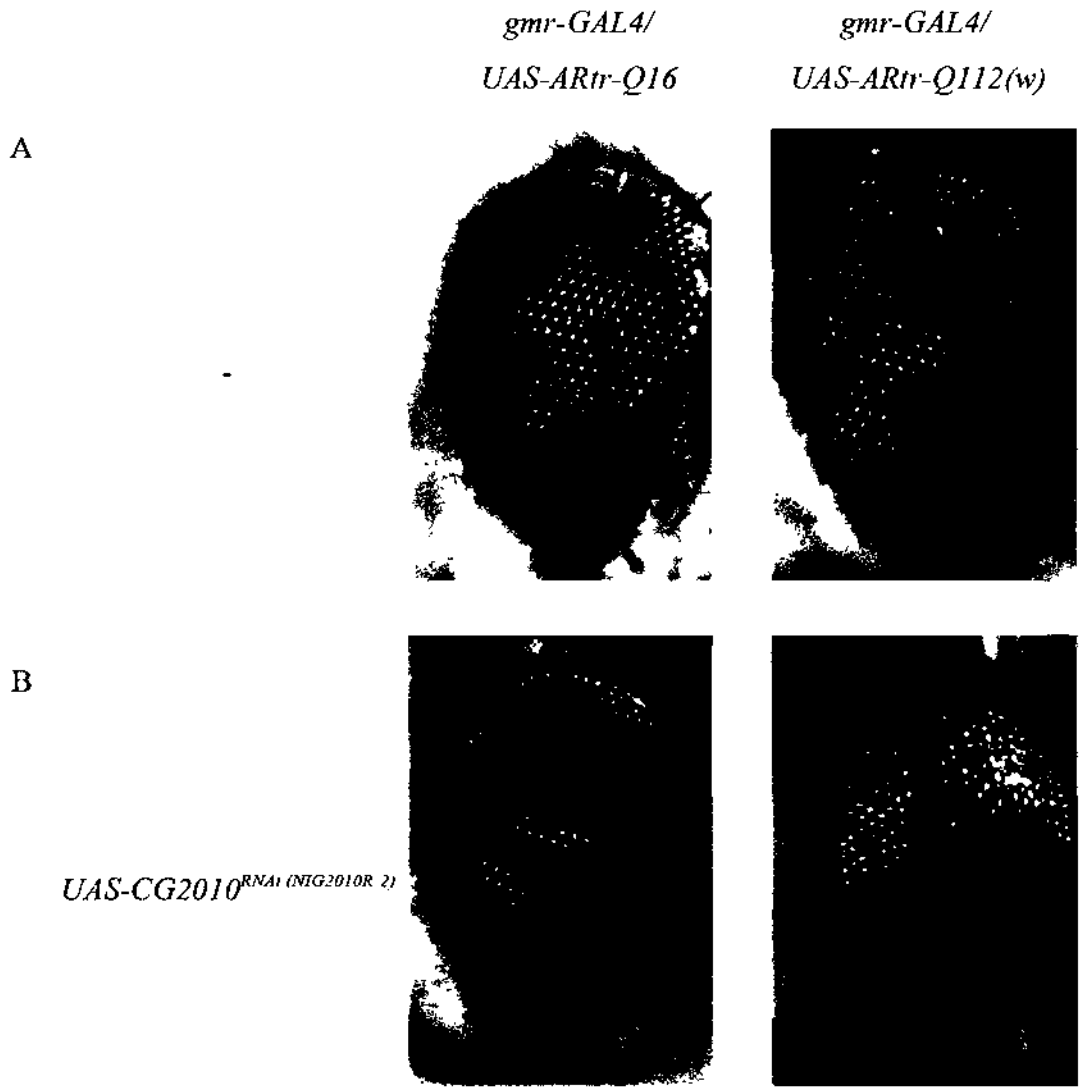
gmr-GAL4/
UAS-ARtr-Q16
gmr-GAL4/
UAS-ARtr-Q112(w)
A
B
UAS-CG2010RNAi (NIG2010R 2)

Figure 4.6. Knock-down of *CG2010* expression enhanced degeneration induced by *ARtr-Q112* expression in adult fly eyes.

Adult external eye depigmentation phenotypes of flies expressing *ARtr* transgenes (*ARtr-Q16* or *ARtr-Q112)* with or without (indicated by "-") knock-down of *CG2010* expression are shown. Transgenes were expressed using the *gmr-GAL4* driver. **(A)** At 3 dpe, expression of *ARtr-Q16* transgene did not cause any degenerative phenotype while weak expression of *ARtr-Q112* (*ARtr-Q112(w)*) caused mild degeneration as indicated by slight loss of pigmentation. **(B)** Knock-down of *CG2010* expression caused a Q-length specific enhancement on degeneration as shown by the more extensive loss of pigmentation. Consistent results were obtained from three independent experiments. The flies were raised at 25°C. They were of genotypes:

(A) *w*; *gmr-GAL4/+*; *UAS-ARtr-Q16/+*,

w; *gmr-GAL4/+*; *UAS-ARtr-Q112(w)/+*

(B) *w*; *gmr-GAL4/UAS-CG2010*$^{RNAi\ (NIG2010R-2)}$; *UAS-ARtr-Q16/+*,

w; *gmr-GAL4/UAS-CG2010*$^{RNAi\ (NIG2010R-2)}$; *UAS-ARtr-Q112(w)/+*.

(Figure 4.6B).

In another polyQ disease model, the eGFP-polyQ model, an eGFP is fused to a polyQ tract with an expanded polyQ repeat length of 76 glutamines [52]. As described in Chapter 3 (section 3.4), expression of *eGFP-Q76* in the eyes by *gmr-GAL4* driver induced degeneration resulting in depigmentation (Figure 4.7A). Knock-down of *CG2010* expression in the eyes enhanced the *eGFP-Q76*-induced degeneration and led to more extensive loss of pigmentation and formation of necrotic scars (Figure 4.7B).

The above data are consistent with the finding in the SCA3tr model in the sense that knock-down of *CG2010* expression enhanced polyQ toxicity (Figure 4.1D). As the SCAtr, ARtr and eGFP-polyQ models are in common only in the presence of polyQ domain, the effect of *CG2010* on polyQ toxicity is specific to the polyQ domain.

To test the importance of protein context of polyQ disease protein on the effect of *CG2010* on polyQ toxicity, a SCA3fl model was employed [129]. This model expresses a myc-tagged, full-length ataxin-3 protein with either unexpanded polyQ repeats of 27 glutamines (myc-SCA3fl-Q27) or expanded polyQ repeats of 84 glutamines (myc-SCA3fl-Q84) [129]. As mentioned in Chapter 3 (section 3.3), myc-SCA3fl-Q84 protein is less toxic than HA-SCA3tr-Q78 protein of the SCA3tr model [129, 140]. Thus, a more sensitive assay, the deep pseudopupil assay [181], was used to study the effect of *CG2010* on polyQ toxicity. Here, in fly eyes

Figure 4.7

gmr-GAL4/ UAS-eGFP-Q76

A

B

UAS-CG2010$^{RNAi\ (NIG2010R\ 2)}$

Figure 4.7. Knock-down of *CG2010* expression enhanced degeneration induced by *eGFP-Q76* expression in adult fly eyes.

Adult external eye depigmentation phenotype of flies expressing *eGFP-Q76* transgene with or without (indicated by "-") knock-down of *CG2010* expression are shown. Transgenes were expressed using the *gmr-GAL4* driver. **(A)** At 3 dpe, expression of *eGFP-Q76* transgene caused degeneration as indicated by depigmentation. **(B)** Knock-down of *CG2010* expression enhanced degeneration as shown by the extensive loss of pigmentation and formation of necrotic scars. Consistent results were obtained from three independent experiments. The flies were raised at 25°C. They were of genotypes:

(A) *w*; *gmr-GAL4/*; *UAS-eGFP-Q76/+*,

(B) *w*; *gmr-GAL4/UAS-CG2010*$^{RNAi\ (NIG2010R-2)}$; *UAS-eGFP-Q76/+*.

expressing myc-SCA3fl-Q27 protein, more than 5 rhabdomeres (an average of 5.2) could be observed, while expression of the expanded polyQ domain-containing protein myc-SCA3fl-Q84 caused a reduction in rhabdomere score to around 4 (an average of 4.1; Figure 4.8A). This shows that expansion of the polyQ domain induced degeneration which disrupted the rhabdomeres structure. Knock-down of *CG2010* expression caused a Q-length specific reduction in the rhabdomere score to around 3 (an average of 3.1; Figure 4.8B). These data are consistent with the finding in the SCA3tr model (Figure 4.1D) and confirm that *CG2010* modifies polyQ toxicity regardless of the protein context of the disease protein in polyQ diseases.

4.4 Effects of knock-down of *CG2010* expression on SDS-solubility of expanded polyglutamine protein

According to section 4.2, similar to knock-down of *Cul1* expression (Figure 3.3B), knock-down of *CG2010* expression enhanced polyQ toxicity (Figure 4.1D). It is likely that *CG2010* modifies polyQ toxicity by modulating solubility of expanded polyQ protein as in the case of *Cul1* (Figure 3.14). To test this hypothesis, the effect of *CG2010* on SDS-solubility of expanded polyQ protein was examined using the SCA3fl model [129]. As mentioned in Chapter 3 (section 3.3), this model expresses the myc-SCA3fl-Q84 protein which is only partly SDS-insoluble [140]. Therefore, SCA3fl model allows studies on both the soluble and insoluble fractions of myc-SCA3fl-Q84 protein.

To study the effect of *CG2010* on SDS-solubility of myc-SCA3fl-Q84 protein, fly adult head lysate was subjected to immunoblotting. The SDS-soluble fraction of

Figure 4.8

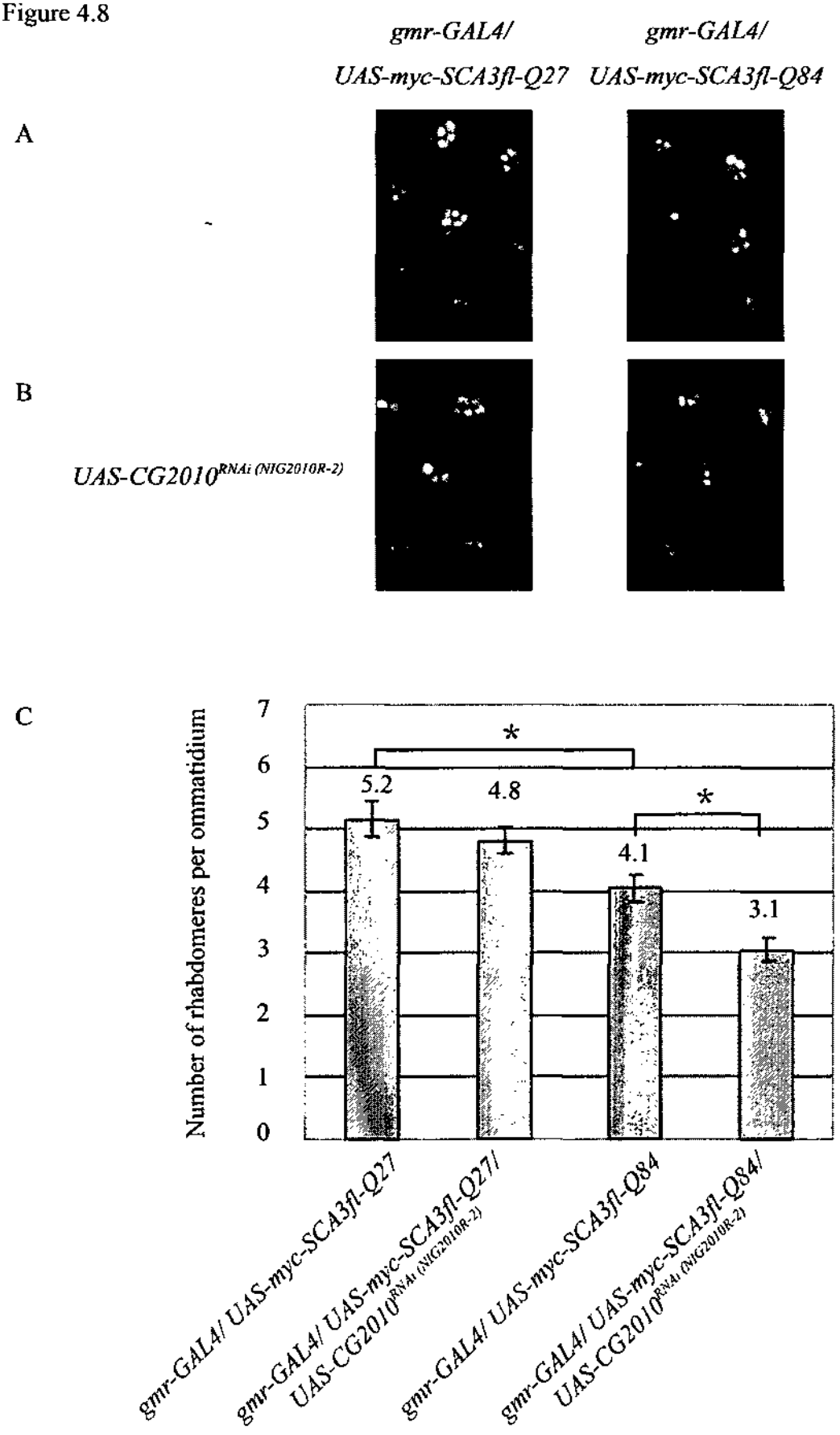
gmr-GAL4/
UAS-myc-SCA3fl-Q27
gmr-GAL4/
UAS-myc-SCA3fl-Q84
A
B
UAS-CG2010RNAi (NIG2010R-2)
C
Number of rhabdomeres per ommatidium
0
1
2
3
4
5
6
7
*
*
5.2
4.8
4.1
3.1
gmr-GAL4/ UAS-myc-SCA3fl-Q27
gmr-GAL4/ UAS-myc-SCA3fl-Q27/
UAS-CG2010RNAi (NIG2010R-2)
gmr-GAL4/ UAS-myc-SCA3fl-Q84
gmr-GAL4/ UAS-myc-SCA3fl-Q84/
UAS-CG2010RNAi (NIG2010R-2)

Figure 4.8. Enhancement by knock-down of *CG2010* expression was reproducible in the SCA3fl model.

(A - B) Deep pseudopupil images of flies expressing full-length ataxin-3 transgenes (*myc-SCAfl-Q27* or *myc-SCA3fl-Q84)* with or without (indicated by "-") knock-down of *CG2010* expression are shown. Transgenes were expressed using the *gmr-GAL4* driver. On average, 5.2 rhabdomeres per ommatidium was observed under microscope in flies expressing *myc-SCA3fl-Q27* (**A**). Expansion of the polyQ tract to Q84 caused a reduction in the rhabdomere score to 4.1. (**A**) Knock-down of *CG2010* expression caused a Q-length specific enhancement on degeneration induced by *myc-SCA3fl-Q84* and reduced the rhabdomere score to 3.1 (**B**). (**C**) Quantification of (**A** and **B**). N = 29, * $p < 0.01$ (Mann-Whitney Rank Sum Test); error bars represent mean ± SEM from at least 29 flies from three independent experiments. At least 570 ommatidia were scored per group. The flies were raised at 21°C and were assayed at 2 dpe. They were of genotypes:

(**A**) *w*; *gmr-GAL4 UAS-myc-SCA3fl-Q27/+*; +/+,

w; *gmr-GAL4/+*; *UAS-myc-SCA3fl-Q84/+*

(**B**) *w*; *gmr-GAL4 UAS-myc-SCA3fl-Q27/UAS-CG2010*$^{RNAi\ (NIG2010R-2)}$; +/+,

w; *gmr-GAL4/UAS-CG2010*$^{RNAi\ (NIG2010R-2)}$; *UAS-myc-SCA3fl-Q84/+*.

myc-SCA3fl-Q84 protein was resolved in the running gel (Figure 4.9). Knock-down of *CG2010* expression reduced the level of SDS-soluble fraction of myc-SCA3fl-Q84 protein in the running gel (Figure 4.9).

To quantify the SDS-insoluble fraction of myc-SCA3fl-Q84 protein, the adult fly head lysate was subjected to ultracentrifugation to isolate the SDS-insoluble protein and remove the SDS-soluble protein [25]. Formic acid (100%) was then used to disrupt the ionic interactions among the SDS-insoluble aggregated proteins and dissociate the aggregated proteins into monomers [25, 151]. The formic acid treated sample was then subjected to immunoblotting (Figure 4.10). It was found that knock-down of *CG2010* expression caused an increase in the level of SDS-insoluble myc-SCA3fl-Q84 protein (Figure 4.10). Taken together, *CG2010* modulates the SDS-solubility of myc-SCA3fl-Q84 protein.

Next, total polyQ protein was recovered from the sample to test the effect of *CG2010* on the abundance of total myc-SCA3fl-Q84 protein. Formic acid (100%) was used to solubilize the SDS-insoluble fraction of myc-SCA3fl-Q84 protein to obtain the total myc-SCA3fl-Q84 protein for immunoblotting [151] (Figure 4.11). Knock-down of *CG2010* expression did not change the total level of myc-SCA3fl-Q84 protein (Figure 4.11). This suggests that *CG2010* does not affect the abundance of total myc-SCA3fl-Q84 protein. Combining all the data together, *CG2010* acts on the SDS-solubility of myc-SCA3fl-Q84 protein without affecting the abundance of total myc-SCA3fl-Q84 protein.

Figure 4.9

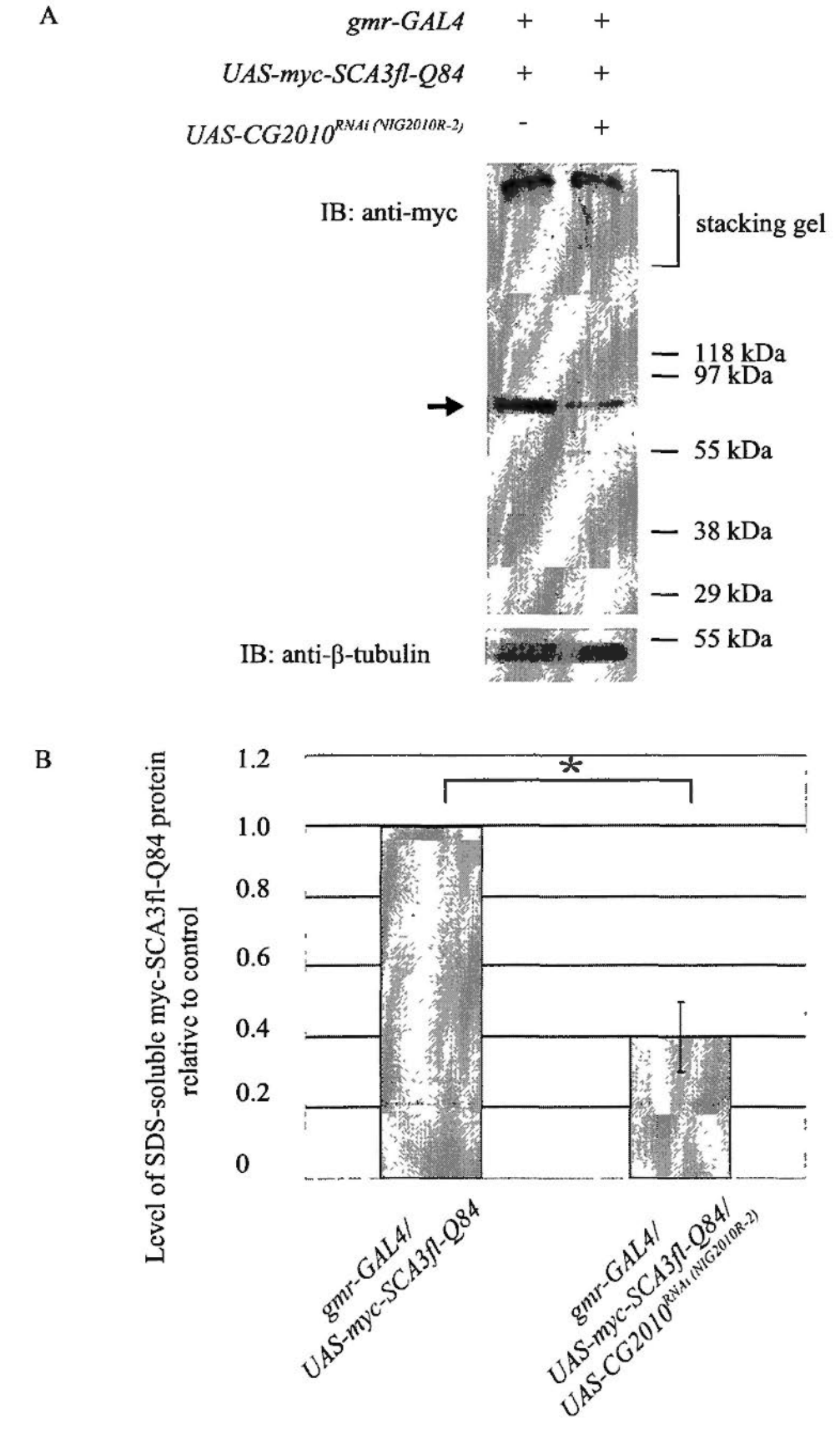
A
gmr-GAL4 + +
UAS-myc-SCA3fl-Q84 + +
UAS-CG2010RNAi (NIG2010R-2) - +
IB: anti-myc
stacking gel
118 kDa
97 kDa
55 kDa
38 kDa
29 kDa
IB: anti-β-tubulin
55 kDa
B
Level of SDS-soluble myc-SCA3fl-Q84 protein relative to control
1.2
1.0
0.8
0.6
0.4
0.2
0
*
gmr-GAL4/ UAS-myc-SCA3fl-Q84
gmr-GAL4/ UAS-myc-SCA3fl-Q84/ UAS-CG2010RNAi (NIG2010R-2)

Figure 4.9. Knock-down of *CG2010* expression reduced the level of SDS-soluble myc-SCA3fl-Q84 protein.

(A) Adult head lysate of *myc-SCA3fl-Q84*-expressing flies with or without knock-down of *CG2010* expression was subjected to immunoblotting. The immunoblot was probed with anti-myc antibody to detect the presence of myc-SCA3fl-Q84 protein. The arrow (→) indicates the monomeric, SDS-soluble myc-SCA3fl-Q84 protein while the signal in stacking gel represents the SDS-insoluble myc-SCA3fl-Q84 protein. Knock-down of *CG2010* expression reduced the level of SDS-soluble myc-SCA3fl-Q84 protein. The immunoblot was stripped and reprobed with anti-β-tubulin antibody to confirm that equal amount of protein was loaded in every lane. **(B)** Quantification of the monomeric, SDS-soluble myc-SCA3fl-Q84 protein. Band intensity was relative to *myc-SCA3fl-Q84*-expressing flies without knock-down of *CG2010* expression. N = 4, * $p < 0.05$ (Student's t-test); error bar represents mean ± SEM from four independent experiments. The flies were raised at 21°C and were assayed at 3 dpe. They were of genotypes:

w; *gmr-GAL4/+*; *UAS-myc-SCA3fl-Q84/+*

w; *gmr-GAL4/UAS-CG2010*$^{RNAi\ (NIG2010R-2)}$; *UAS-myc-SCA3fl-Q84/+*.

Figure 4.10

A

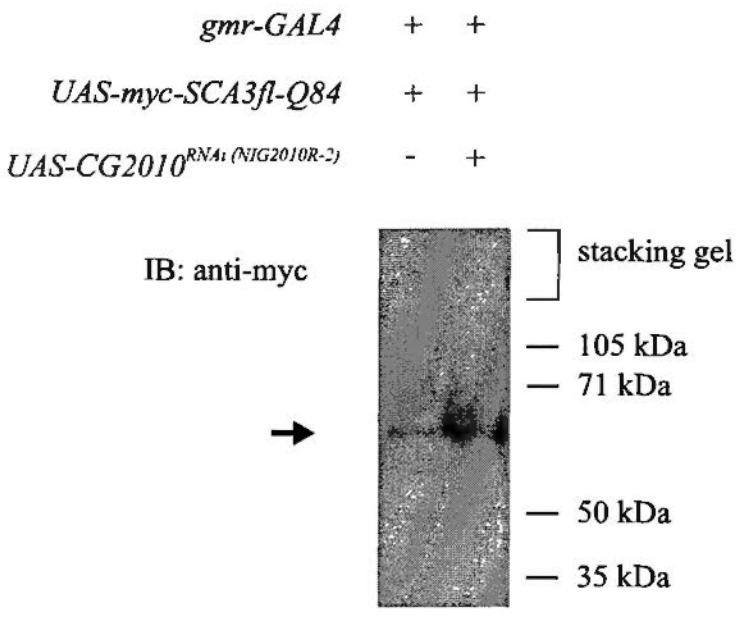

B

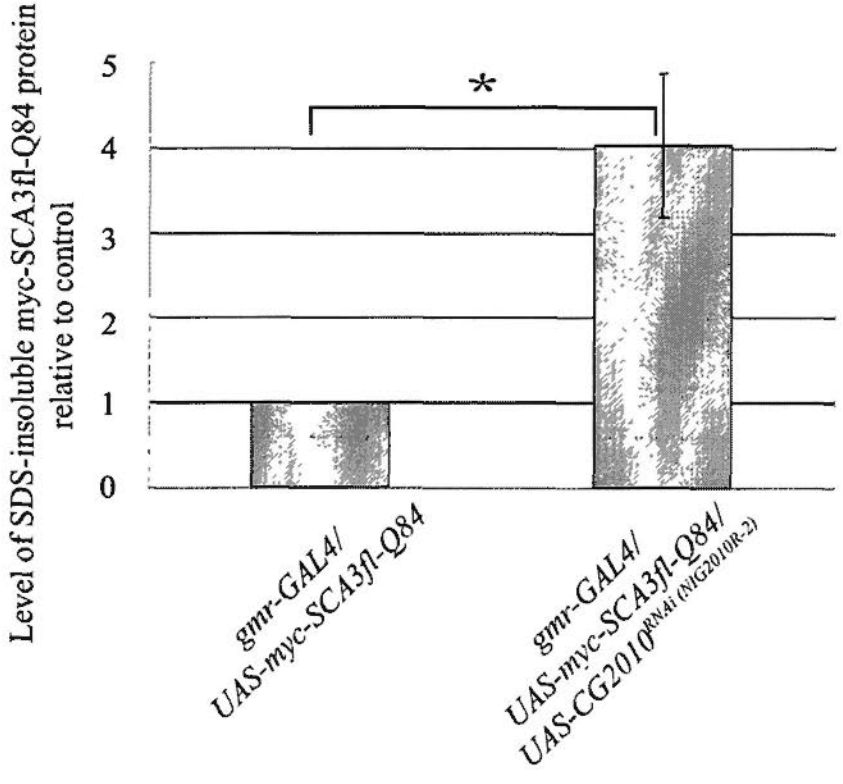

Figure 4.10. Knock-down of *CG2010* expression increased the level of SDS-insoluble myc-SCA3fl-Q84 protein.

(A) Adult head lysate of *myc-SCA3fl-Q84*-expressing flies with or without knock-down of *CG2010* expression was subjected to ultracentrifugation to isolate any SDS-insoluble protein aggregates and to remove the SDS-soluble protein. The resulting pellet was treated with formic acid (100%) to dissociate the aggregates into monomers and then subjected to immunoblotting. The immunoblot was probed with anti-myc antibody to detect the presence of any SDS-insoluble myc-SCA3fl-Q84 protein. The arrow (→) indicates the solubilized insoluble myc-SCA3fl-Q84 protein and the signal intensity represents its level. Knock-down of *CG2010* expression intensified this band. **(B)** Quantification of the solubilized SDS-insoluble myc-SCA3fl-Q84 protein. Band intensity was relative to *myc-SCA3fl-Q84*-expressing flies without knock-down of *CG2010* expression. N = 4, * $p < 0.05$ (Student's t-test); error bar represents mean ± SEM from four independent experiments. The flies were raised at 21°C and were assayed at 3 dpe. They were of genotypes:

w; *gmr-GAL4/+*; *UAS-myc-SCA3fl-Q84/+*

w; *gmr-GAL4/UAS-CG2010*$^{RNAi\ (NIG2010R-2)}$; *UAS-myc-SCA3fl-Q84/+*.

Figure 4.11

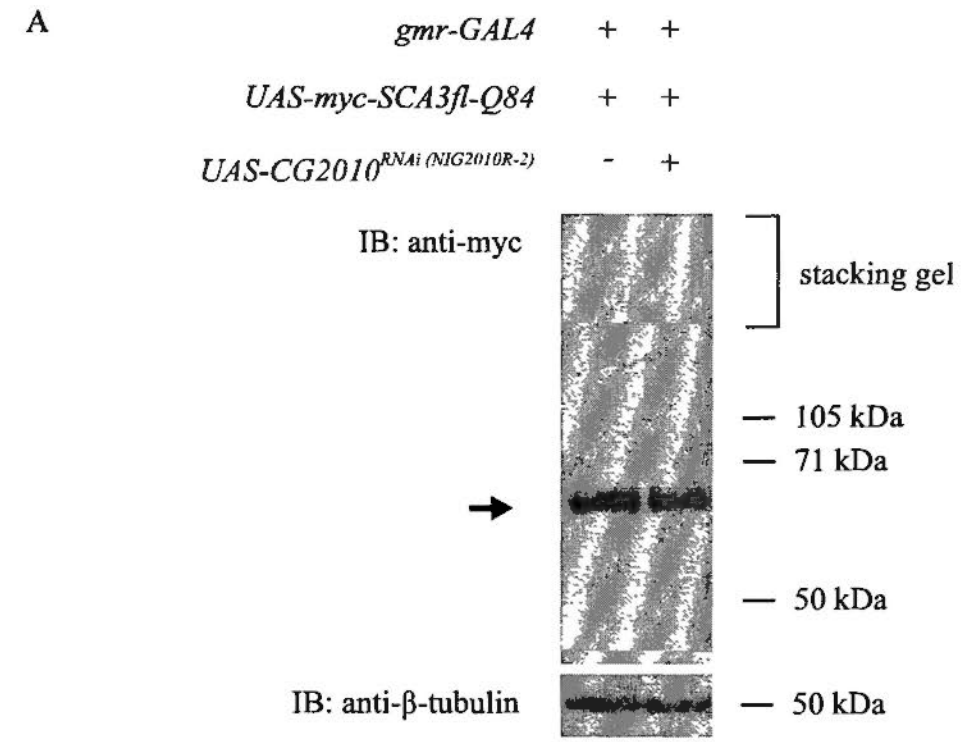
A
gmr-GAL4 + +
UAS-myc-SCA3fl-Q84 + +
UAS-CG2010RNAi (NIG2010R-2) - +
IB: anti-myc
stacking gel
105 kDa
71 kDa
50 kDa
IB: anti-β-tubulin
50 kDa

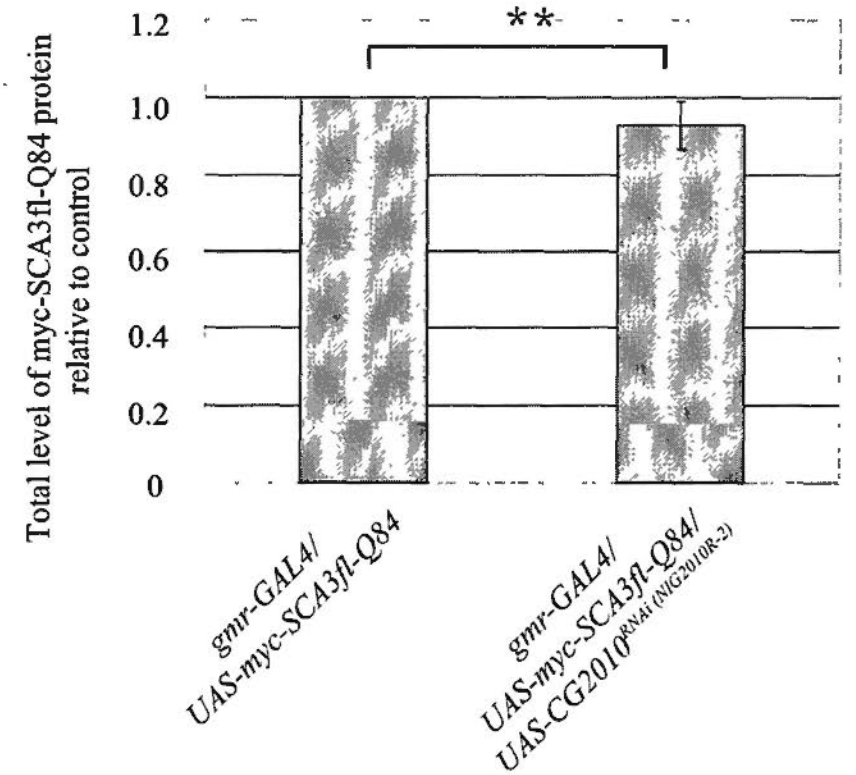
B
Total level of myc-SCA3fl-Q84 protein relative to control
1.2
1.0
0.8
0.6
0.4
0.2
0
**
gmr-GAL4/ UAS-myc-SCA3fl-Q84
gmr-GAL4/ UAS-myc-SCA3fl-Q84/ UAS-CG2010RNAi (NIG2010R-2)

Figure 4.11. Knock-down of *CG2010* expression did not modify the abundance of total myc-SCA3fl-Q84 protein.

(A) Adult head lysate of *myc-SCA3fl-Q84*-expressing flies with or without knock-down of *CG2010* expression was treated with formic acid (100%) to dissociate the aggregates into monomers and then subjected to immunoblotting. The immunoblot was probed with anti-myc antibody to detect the presence of myc-SCA3fl-Q84 protein. The arrow (→) indicates the total level of myc-SCA3fl-Q84 protein. Knock-down of *CG2010* expression did not modify this band. The immunoblot was stripped and reprobed with anti-β-tubulin antibody to confirm that equal amount of protein was loaded in every lane. **(B)** Quantification of **(A)**. Band intensity was relative to *myc-SCA3fl-Q84*-expressing flies without knock-down of *CG2010* expression. N = 3, p = 0.25 (Student's t-test); error bar represents mean ± SEM from three independent experiments. The flies were raised at 21°C and were assayed at 3 dpe. They were of genotypes:

w; *gmr-GAL4/+*; *UAS-myc-SCA3fl-Q84/+*,

w; *gmr-GAL4/UAS-CG2010*$^{RNAi\ (NIG2010R-2)}$; *UAS-myc-SCA3fl-Q84/+*.

4.5 Knock-down of *CG2010* expression reduced ubiquitination of SDS-insoluble expanded polyglutamine protein

As discussed in Chapter 3 (section 3.7), inhibiting ubiquitination of the substrate protein could lead to its accumulation in cells [161]. Since it was found that knock-down of *CG2010* expression led to an increase in the level of SDS-insoluble expanded polyQ protein, it is therefore important to test if this enrichment was accompanied with a reduction in ubiquitination of the SDS-insoluble expanded polyQ protein.

An *in vivo* ubiquitination assay on myc-SCA3fl-Q84 protein was therefore performed in flies expressing *myc-SCA3fl-Q84* transgene with or without knock-down of *CG2010* expression [162, 163]. Firstly, immunoprecipitation was used to capture total myc-SCA3fl-Q84 protein by anti-myc antibody, and the eluate was subjected to immunoblotting (Figure 4.12). The immunoblot was first probed against anti-ubiquitin antibody to detect the presence of ubiquitinated SDS-soluble myc-SCA3fl-Q84 protein in the running gel, and subsequently reprobed with anti-myc antibody to confirm successful immunoprecipitation of myc-SCA3fl-Q84 protein (Figure 4.12). It was found that the level of ubiquitinated SDS-soluble myc-SCA3fl-Q84 protein was similar between the *myc-SCA3fl-Q84*-expressing flies with or without knock-down of *CG2010* expression (Figure 4.12). This implies that *CG2010* does not affect the ubiquitination of the SDS-soluble fraction of expanded polyQ protein.

To examine the effect of *CG2010* on the ubiquitination of the SDS-insoluble

Figure 4.12

A

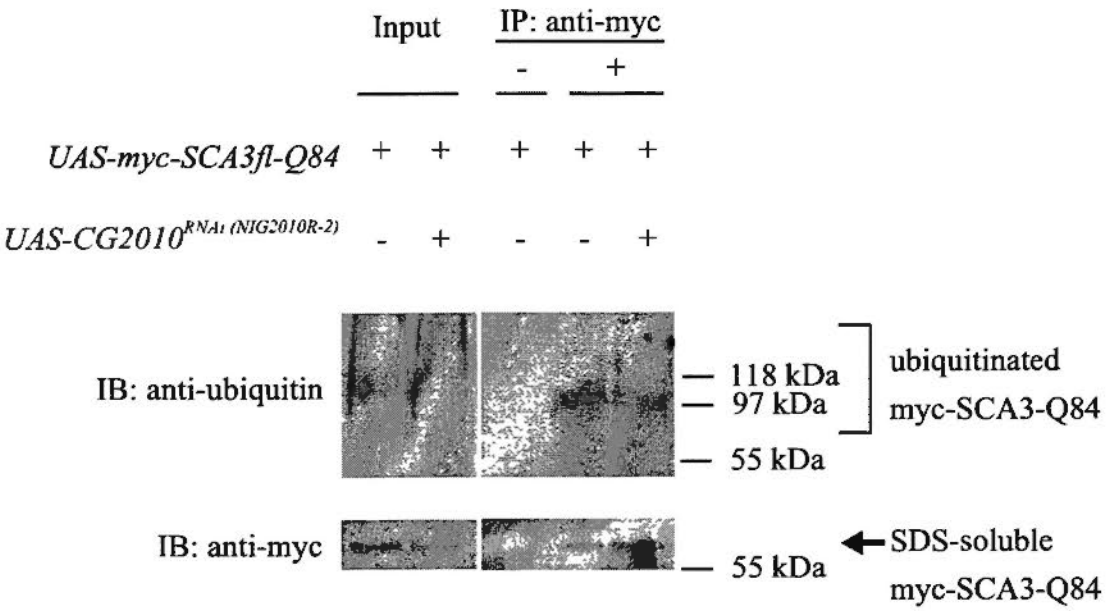

B

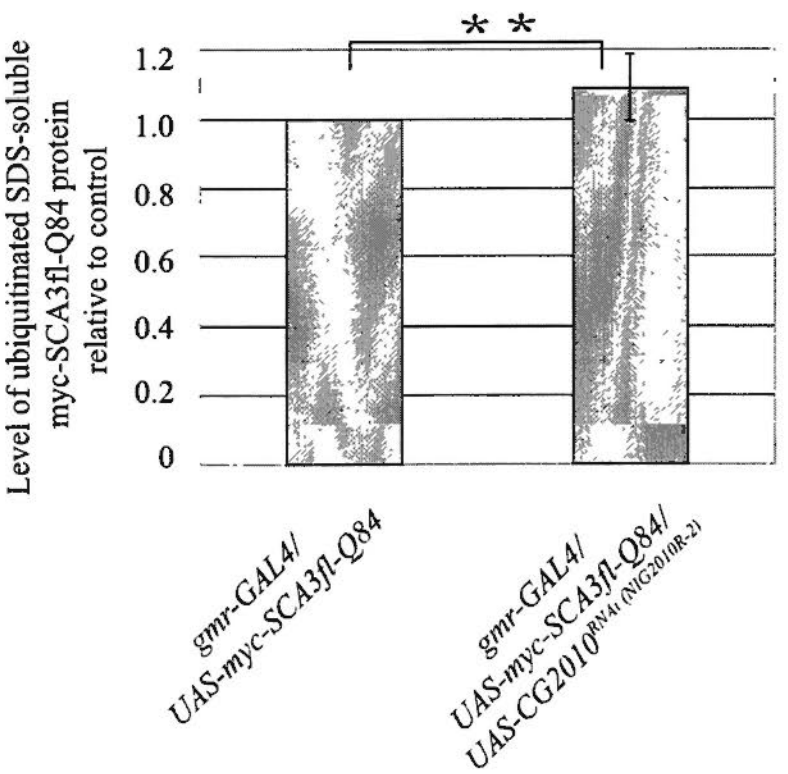

Figure 4.12. Knock-down of *CG2010* expression did not alter the level of ubiquitinated SDS-soluble myc-SCA3fl-Q84 protein.

(A) Adult head lysate of flies expressing myc-SCA3fl-Q84 protein with or without knock-down of *CG2010* expression was subjected to immunoprecipitation using anti-myc antibody to immunoprecipitate myc-SCA3fl-Q84 protein. The input and the eluate were subjected to immunoblotting. Upper row: the immunoblots were probed against anti-ubiquitin antibody to detect the ubiquitinated SDS-soluble protein in the running gel. Lower row: the immunoblots were stripped and reprobed with anti-myc antibody to detect the SDS-soluble myc-SCA3fl-Q84 protein. The input shows the presence of SDS-soluble myc-SCA3fl-Q84 protein in the lysate while positive signal in the eluate confirmed positive immunoprecipitation of SDS-soluble myc-SCA3fl-Q84 protein. Knock-down of *CG2010* expression did not alter the level of ubiquitinated SDS-soluble myc-SCA3fl-Q84 protein. **(B)** Quantification of the ubiquitinated SDS-soluble myc-SCA3fl-Q84 protein in **(A)**. Band intensity was relative to *myc-SCA3fl-Q84*-expressing flies without knock-down of *CG2010* expression. N = 3, ** $p = 0.26$ (Student's t-test); error bar represents mean ± SEM from four independent experiments. The flies were raised at 21°C and were assayed at 3 dpe. They were of genotypes:

w; *gmr-GAL4/+*; *UAS-myc-SCA3fl-Q84/+*,

w; *gmr-GAL4/UAS-CG2010*$^{RNAi\ (NIG2010R-2)}$; *UAS-myc-SCA3fl-Q84/+*.

fraction of myc-SCA3fl-Q84 protein, the above immunoprecipitation was repeated to immunoprecipitate total myc-SCA3fl-Q84 protein by anti-myc antibody. Instead of immunoblotting, the eluate was subjected to filter retardation assay to capture the SDS-insoluble myc-SCA3fl-Q84 protein with size larger than 0.22 μm [146] (Figure 4.13). The signal on the immunoblot obtained upon immunodetection with anti-myc antibody indicates successful immunoprecipitation of the SDS-insoluble myc-SCA3fl-Q84 protein (Figure 4.13A, upper row). The signal on the immunoblot obtained upon immunodetection with anti-ubiquitin antibody indicates the ubiquitinated SDS-insoluble myc-SCA3fl-Q84 protein (Figure 4.13A, lower row). It was found that knock-down of *CG2010* expression reduced the level of ubiquitinated SDS-insoluble myc-SCA3fl-Q84 protein (Figure 4.13).

To exclude the possibility that the above ubiquitin-positive signal came from any ubiquitin recruited to the SDS-insoluble myc-SCA3fl-Q84 protein aggregates rather than from the ubiquitin that was directly conjugated on myc-SCA3fl-Q84 protein, a modified *in vivo* ubiquitination assay (section 2.12.3) was performed. Immunoprecipitation was first used to capture the total myc-SCA3fl-Q84 protein. The eluate was subjected to ultracentrifugation to isolate the SDS-insoluble myc-SCA3fl-Q84 protein [25]. Formic acid (100%) was then used to dissociate aggregated myc-SCA3fl-Q84 proteins into monomers and release any recruited cellular proteins [25, 151]. It is well documented that formic acid cannot break any covalent bonding such as conjugation of ubiquitin on substrates [25, 151]. The formic acid-treated samples were subjected to immunoblotting. Since knock-down of *CG2010* expression led to a 4-fold enrichment of SDS-insoluble myc-SCA3fl-Q84

Figure 4.13

A

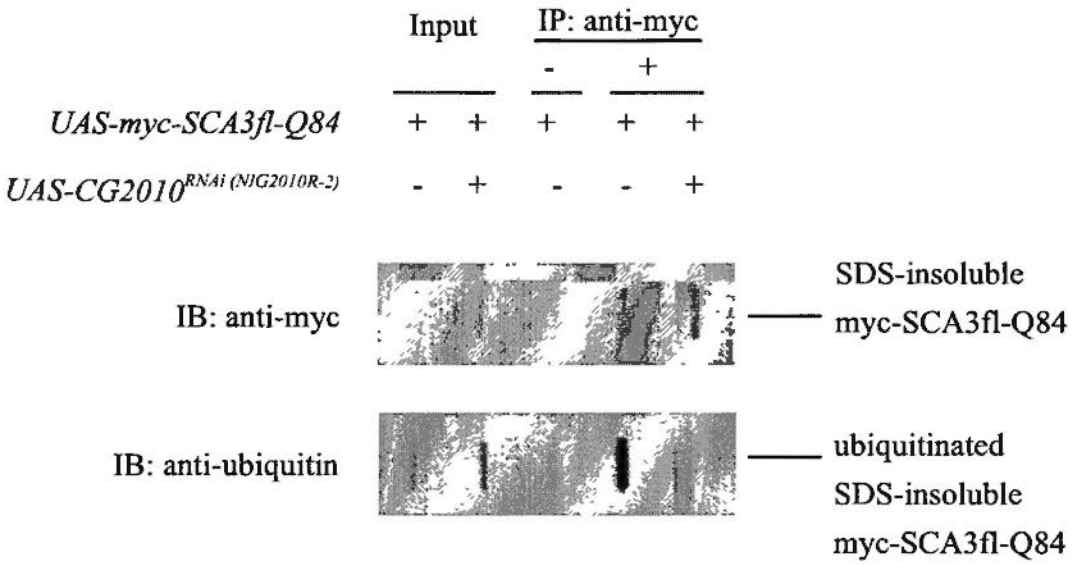

B

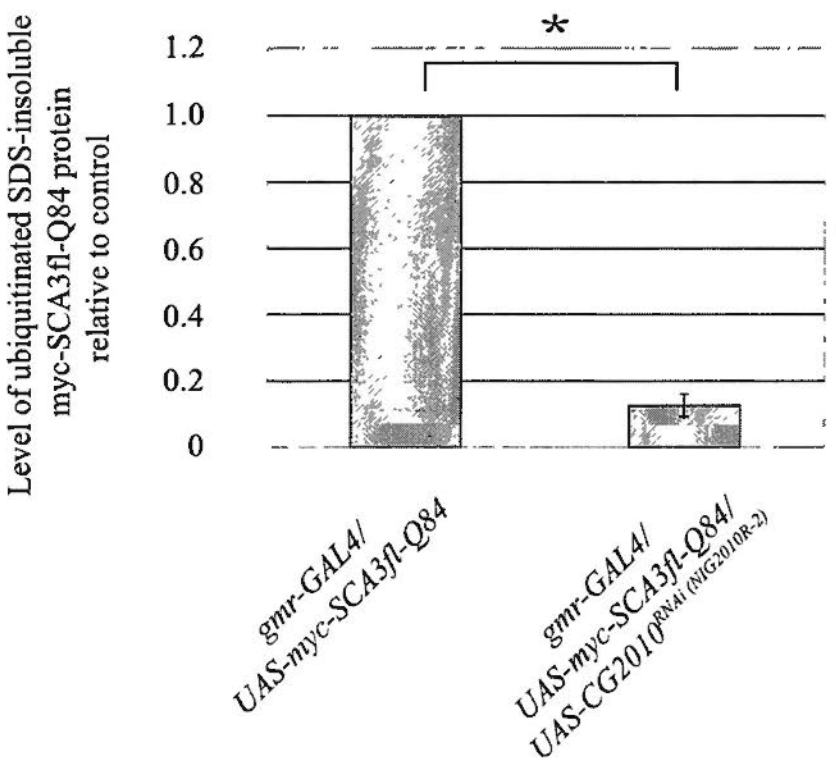

Figure 4.13. Knock-down of *CG2010* expression reduced level of ubiquitinated SDS-insoluble myc-SCA3fl-Q84 protein captured by filter retardation assay.

(A) Adult head lysate of flies expressing myc-SCA3fl-Q84 protein with or without knock-down of *CG2010* expression was subjected to immunoprecipitation using anti-myc antibody to immunoprecipitate myc-SCA3fl-Q84 protein. The input and the eluate were then subjected to filter retardation assay to capture any SDS-insoluble protein aggregates with size larger than 0.22 μm. As both of the antibodies to be used for immunodetection were purified from mice, the samples were divided into two equal halves and loaded into two separate wells. The immunoblot was then cut into two halves for separate immunodetection. Upper row: the half-blot carrying a complete set of samples was probed with anti-myc antibody to detect the SDS-insoluble myc-SCA3fl-Q84 protein aggregates. Positive signal in the input shows the presence of SDS-insoluble myc-SCA3fl-Q84 protein in the lysate. The signal in the eluate confirmed positive immunoprecipitation of the SDS-insoluble myc-SCA3fl-Q84 protein and presence of equal amount of immunoprecipitated SDS-insoluble myc-SCA3fl-Q84 protein in each well. Lower row: the other half-blot carrying a complete set of samples was probed against anti-ubiquitin antibody to detect any ubiquitinated SDS-insoluble protein aggregates. The input indicates the presence of ubiquitinated SDS-insoluble protein aggregates in the lysate. Positive signal in the eluate indicates the ubiquitinated SDS-insoluble myc-SCA3fl-Q84 protein. Knock-down of *CG2010* expression reduced the level of ubiquitinated SDS-insoluble myc-SCA3fl-Q84 protein. **(B)** Quantification of the ubiquitinated SDS-insoluble myc-SCA3fl-Q84 protein in **(A)**. Band intensity was relative to *myc-SCA3fl-Q84*-expressing flies without knock-down of *CG2010* expression. N = 3, * $p < 0.05$ (Student's t-test); error bar represents mean ± SEM from three independent experiments. The flies were raised at 21°C and were assayed at 3 dpe. They were of genotypes:

w; *gmr-GAL4/+*; *UAS-myc-SCA3fl-Q84/+*,

w; *gmr-GAL4/UAS-CG2010*$^{RNAi\ (NIG2010R-2)}$; *UAS-myc-SCA3fl-Q84/+*.

protein (Figure 4.10), the loading ratio of the samples was adjusted accordingly (Figure 4.14). The signal on the immunoblot obtained upon immunodetection with anti-myc antibody confirms successful immunoprecipitation of SDS-insoluble myc-SCA3fl-Q84 protein and presence of equal amount of SDS-insoluble myc-SCA3fl-Q84 protein in the control and CG2010^{RNAi} eluates (Figure 4.14B, lower row). Upon immunodetection with anti-ubiquitin antibody, the ubiquitin conjugated on myc-SCA3fl-Q84 protein contributed to a smear on the immunoblot above the size of monomeric myc-SCA3fl-Q84 protein (Figure 4.14B, upper row). It was found that knock-down of *CG2010* expression reduced the level of ubiquitinated SDS-insoluble myc-SCA3fl-Q84 (Figure 4.14B). Taken together, the data suggest that *CG2010* modifies the ubiquitination of SDS-insoluble myc-SCA3fl-Q84 protein.

To show that not any F-box protein could affect the ubiquitination of SDS-insoluble myc-SCA3fl-Q84 protein, the above experiment was repeated using another F-box protein, CG9461. As previously described, knockdown of *CG9461* expression did not modify polyQ toxicity (Figure 4.1E). Semi-quantitative RT-PCR showed that knock-down of *CG9461* expression by RNAi caused an observable reduction in the transcript level of *CG9461* (Figure 4.15). By performing similar experiment as that in Figure 4.10, it was found that knockdown of *CG9461* expression did not alter the SDS-solubility of myc-SCA3fl-Q84 protein (Figure 4.16A and B). The *in vivo* ubiquitination assay in Figure 4.14B was repeated using this irrelevant F-box protein. It was found that knockdown of *CG9461* expression did not affect the ubiquitination of SDS-insoluble myc-SCA3fl-Q84 protein (Figure 4.16C and D). Taken together, CG2010 is a specific F-box protein that modifies

Figure 4.14

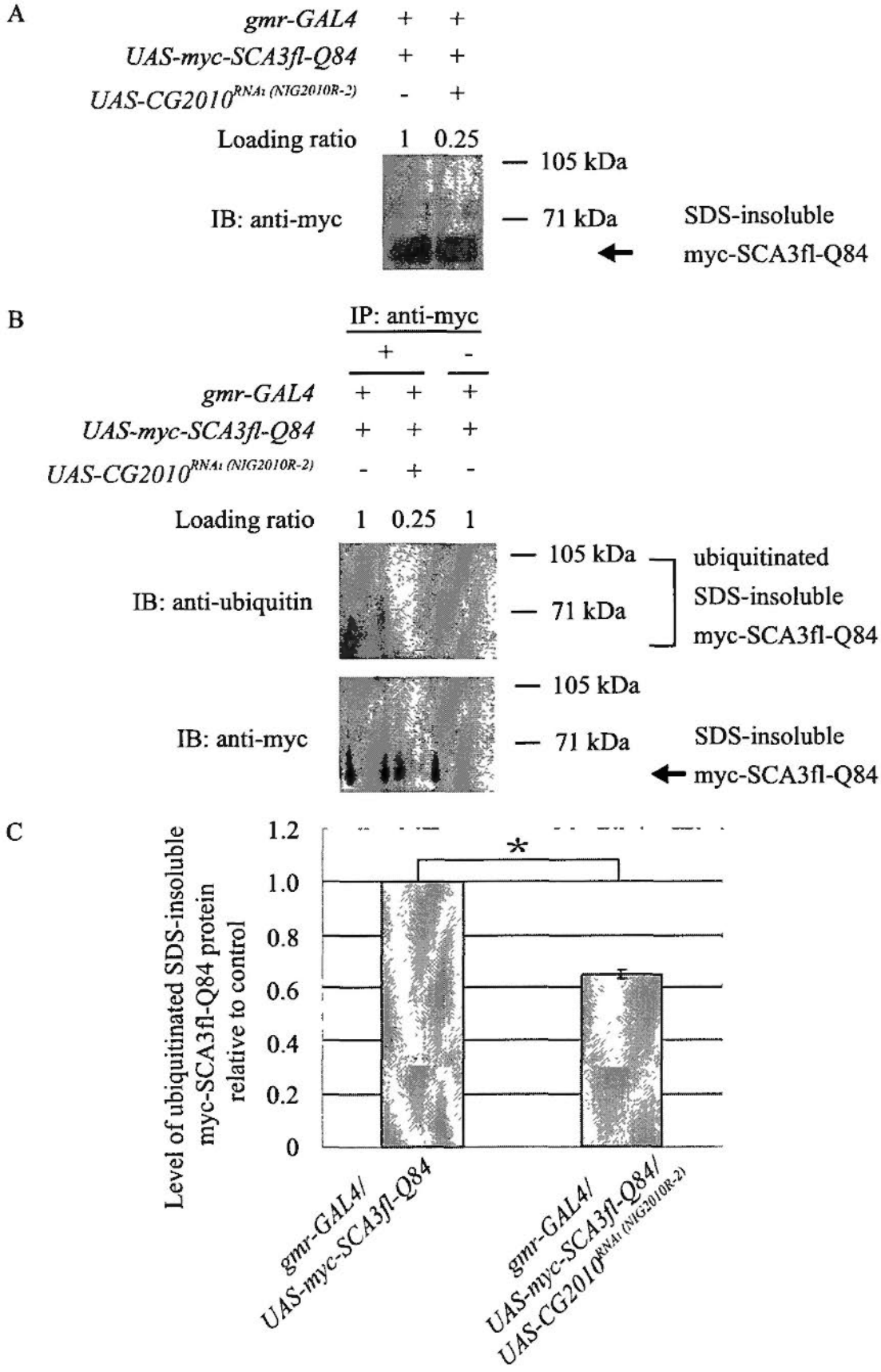
A
gmr-GAL4 + +
UAS-myc-SCA3fl-Q84 + +
UAS-CG2010RNAi (NIG2010R-2) - +
Loading ratio 1 0.25
IB: anti-myc
— 105 kDa
— 71 kDa
SDS-insoluble
myc-SCA3fl-Q84
B
IP: anti-myc
+ -
gmr-GAL4 + + +
UAS-myc-SCA3fl-Q84 + + +
UAS-CG2010RNAi (NIG2010R-2) - + -
Loading ratio 1 0.25 1
IB: anti-ubiquitin
— 105 kDa
— 71 kDa
ubiquitinated
SDS-insoluble
myc-SCA3fl-Q84
IB: anti-myc
— 105 kDa
— 71 kDa
SDS-insoluble
myc-SCA3fl-Q84
C
Level of ubiquitinated SDS-insoluble myc-SCA3fl-Q84 protein relative to control
1.2
1.0
0.8
0.6
0.4
0.2
0
*
gmr-GAL4/ UAS-myc-SCA3fl-Q84
gmr-GAL4/ UAS-myc-SCA3fl-Q84/ UAS-CG2010RNAi (NIG2010R-2)

Figure 4.14. Knock-down of *CG2010* expression reduced the level of ubiquitinated SDS-insoluble myc-SCA3fl-Q84 protein isolated by ultracentrifugation.

(A) Adult head lysate of *myc-SCA3fl-Q84*-expressing flies with or without knock-down of *CG2010* expression was subjected to ultracentrifugation to isolate any SDS-insoluble protein aggregates and to remove the SDS-soluble protein. The resulting pellet was treated with formic acid (100%) to dissociate the aggregates into monomers. The formic acid-treated sample was loaded according to the ratio specified and subjected to immunoblotting. The immunoblot was probed with anti-myc antibody to confirm the presence of equal amount of SDS-insoluble myc-SCA3fl-Q84 protein when the sample was loaded according to the above ratio. **(B)** Adult head lysate from same batch of flies in **(A)** was subjected to immunoprecipitation. Anti-myc antibody was used to immunoprecipitate total myc-SCA3fl-Q84 protein. The eluate was subjected to ultracentrifugation and formic acid (100%) treatment. The resulting eluate was then subjected to immunoblotting according to the loading ratio specified in **(A)**. Upper row: the immunoblot was probed against anti-ubiquitin antibody to detect any ubiquitinated SDS-insoluble myc-SCA3fl-Q84 protein. Signal in the eluate represents the ubiquitinated SDS-insoluble myc-SCA3fl-Q84 protein. Knock-down of *CG2010* expression reduced the level of this ubiquitinated SDS-insoluble myc-SCA3fl-Q84 protein. Lower row: the immunoblot was stripped and reprobed with anti-myc antibody to detect the SDS-insoluble myc-SCA3fl-Q84 protein. Signal in the eluate confirmed positive immunoprecipitation of SDS-insoluble myc-SCA3fl-Q84 protein and equal amount of SDS-insoluble myc-SCA3fl-Q84 protein loaded. **(C)** Quantification of the ubiquitinated SDS-insoluble myc-SCA3fl-Q84 protein **(B)**. Band intensity was relative to *myc-SCA3fl-Q84*-expressing flies without knock-down of *CG2010* expression. N = 4, * $p < 0.05$ (Student's t-test); error bar represents mean ± SEM from four independent experiments. The flies were raised at 21°C and were assayed at 3 dpe. They were of genotypes:

w; *gmr-GAL4/+*; *UAS-myc-SCA3fl-Q84/+*,

w; *gmr-GAL4/UAS-CG2010*$^{RNAi\ (NIG2010R-2)}$; *UAS-myc-SCA3fl-Q84/+*.

ubiquitination of SDS-insoluble myc-SCA3fl-Q84 protein.

4.6 Genetic interaction between *CG2010* and *Cul1* in polyglutamine toxicity

Genetic interaction is useful in studying the functional relationship between two genes in order to test if they are acting on the same pathway [182, 183]. Results from the genetic interaction study between *myc-SCA3fl-Q84* and *Cul1* (Figure 3.3B), and that between *myc-SCA3fl-Q84* and *CG2010* (Figure 4.1D) respectively demonstrated that *Cul1* and *CG2010* are involved in polyQ toxicity. As biochemical data in Chapters 3 and 4 suggest that Cul1 protein act on myc-SCA3fl-Q84 protein through CG2010 protein, genetic interaction between *CG2010* and *Cul1* in polyQ toxicity was examined to test if *CG2010* and *Cul1* act in the same pathway in modifying polyQ toxicity.

In an adult external eye depigmentation assay using the SCA3fl model [129], expression of *myc-SCA3fl-Q84* in the fly eyes by *gmr-GAL4* driver did not have any observable depigmentation (Figure 4.17A). However, knock-down of *Cul1* expression in *myc-SCA3fl-Q84*-expressing flies enhanced degeneration and resulted in depigmentation and formation of small necrotic scars on the eye surface (Figure 4.17B). Similarly, knock-down of *CG2010* expression in *myc-SCA3fl-Q84*-expressing flies enhanced degeneration and resulted in mild depigmentation (Figure 4.17C). Double knock-down of both *Cul1* and *CG2010* expression in *myc-SCA3fl-Q84*-expressing flies did not further enhanced the degenerative phenotype by single knock-down of either *Cul1* or *CG2010* expression (Figure 4.17D). Because there was not any additive effect upon double knock-down

Figure 4.15

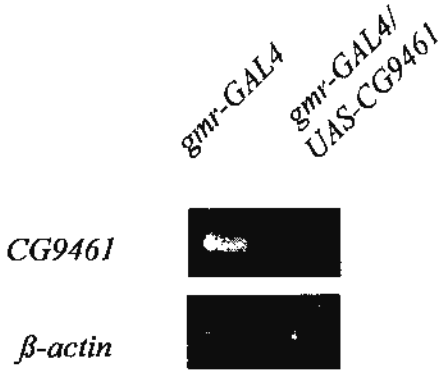

Figure 4.15. Knock-down efficiency of *CG9461* expression.

Transcript level of *CG9461* in *gmr-GAL4* driver control flies and $CG9461^{RNAi}$ flies revealed by RT-PCR. *ß-actin* served as loading control. There is an observable reduction in the transcript level of *CG9461* in $CG9461^{RNAi}$ flies. The experiment was performed twice experiments. The flies were raised at 25°C and were assayed at 3 dpe. They were of genotypes:

w; *gmr-GAL4*/+; +/+,

w; *gmr-GAL4/UAS-CG9461*^{RNAi}; + /+.

Figure 4.16

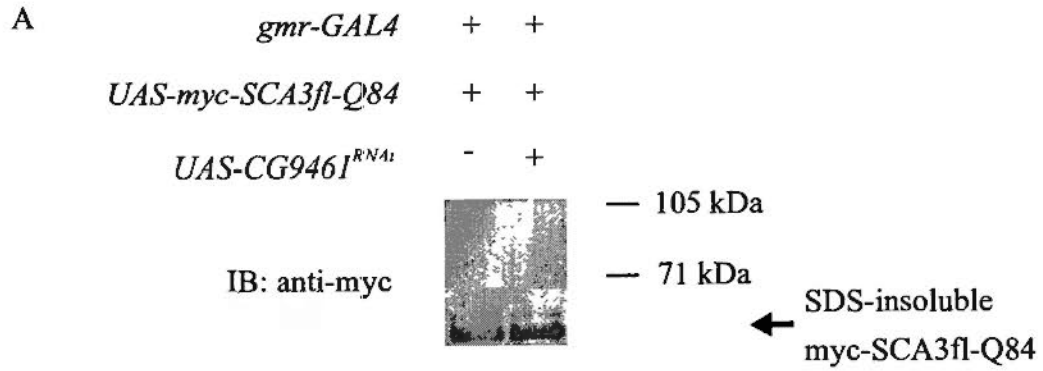
A
gmr-GAL4 + +
UAS-myc-SCA3fl-Q84 + +
UAS-CG9461RNAi - +
IB: anti-myc
— 105 kDa
— 71 kDa
SDS-insoluble
myc-SCA3fl-Q84

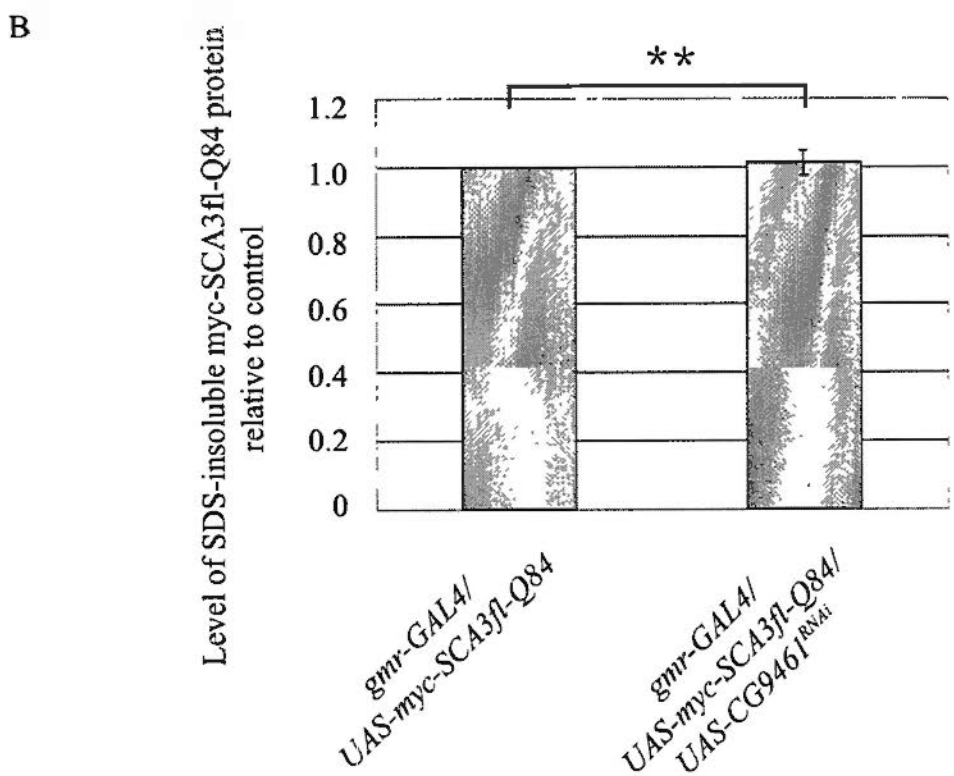
B
**
Level of SDS-insoluble myc-SCA3fl-Q84 protein relative to control
1.2
1.0
0.8
0.6
0.4
0.2
0
gmr-GAL4/ UAS-myc-SCA3fl-Q84
gmr-GAL4/ UAS-myc-SCA3fl-Q84/ UAS-CG9461RNAi

Figure 4.16

C

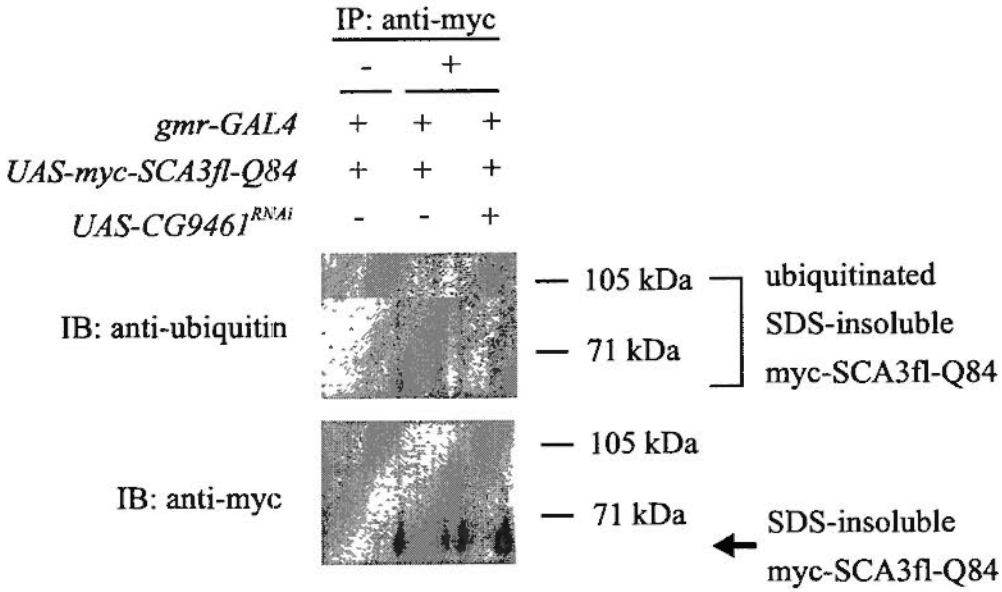

D

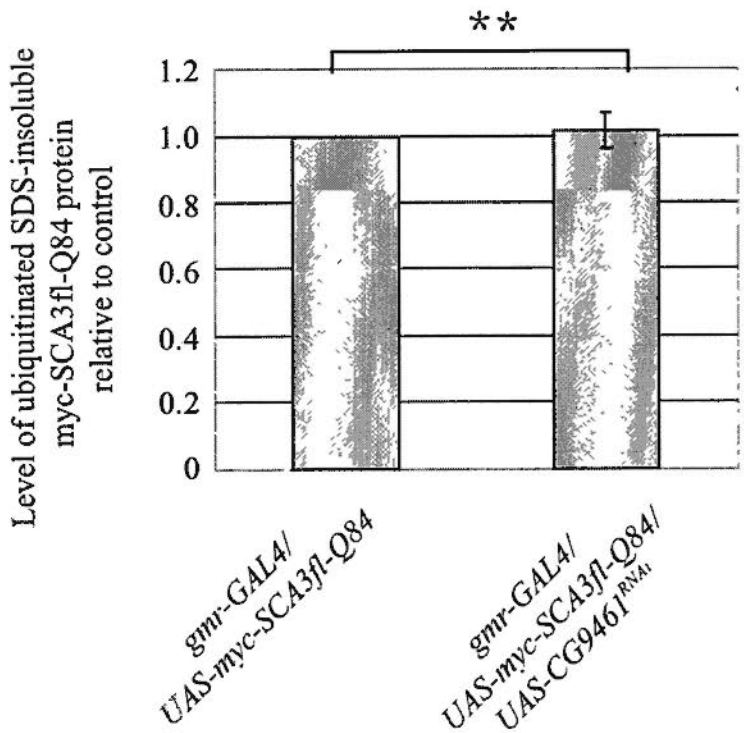

Figure 4.16. Knock-down of *CG9461* expression did not modify SDS-solubility or ubiquitination of SDS-insoluble myc-SCA3fl-Q84 protein.

(**A**) Adult head lysate of *myc-SCA3fl-Q84*-expressing flies with or without knock-down of *CG9461* expression was subjected to ultracentrifugation to isolate any SDS-insoluble protein aggregates and to remove the SDS-soluble protein. The resulting pellet was treated with formic acid (100%) to dissociate the aggregates into monomers. The formic acid treated sample was subjected to immunoblotting. The immunoblot was probed with anti-myc antibody to detect the SDS-insoluble myc-SCA3fl-Q84 protein. (**B**) Quantification of the solubilized, SDS-insoluble myc-SCA3fl-Q84 protein. Band intensity was relative to *myc-SCA3fl-Q84*-expressing flies without knock-down of *CG9461* expression. N = 3, ** $p = 0.79$ (Student's t-test); error bar represents mean ± SEM from three independent experiments. (**C**) Adult head lysate from same batch of flies in (**A**) was subjected to immunoprecipitation. Anti-myc antibody was used to immunoprecipitate total myc-SCA3fl-Q84 protein. The eluate was subjected to ultracentrifugation and formic acid (100%) treatment. The resulting eluate was then subjected to immunoblotting. Upper row: the immunoblot was probed against anti-ubiquitin antibody to detect any ubiquitinated SDS-insoluble myc-SCA3fl-Q84 protein. Signal in the eluate presents the ubiquitinated SDS-insoluble myc-SCA3fl-Q84 protein. Knock-down of *CG9461* expression did not modify the level of this ubiquitinated SDS-insoluble myc-SCA3fl-Q84 protein. Lower row: the immunoblot was stripped and reprobed with anti-myc antibody to detect the SDS-insoluble myc-SCA3fl-Q84 protein. Signal in the eluate confirmed positive immunoprecipitation of SDS-insoluble myc-SCA3fl-Q84 protein. (**D**) Quantification of the ubiquitinated SDS-insoluble myc-SCA3fl-Q84 protein in (**C**). Band intensity was relative to *myc-SCA3fl-Q84*-expressing flies without knock-down of *CG9461* expression. N = 3, ** $p = 0.83$ (Student's t-test); error bar represents mean ± SEM from three independent experiments. The flies were raised at 21°C and were assayed at 3 dpe. They were of genotypes:

w; *gmr-GAL4/+*; *UAS-myc-SCA3fl-Q84/+*,

w; *gmr-GAL4/UAS-CG9461*^{RNAi}; *UAS-myc-SCA3fl-Q84/+*

Figure 4.17

A

gmr-GAL4/ UAS-myc-SCA3fl-Q84

B

gmr-GAL4/ UAS-myc-SCA3fl-Q84/
UAS-Cul1$^{RNAi\ (VDRC42445)}$

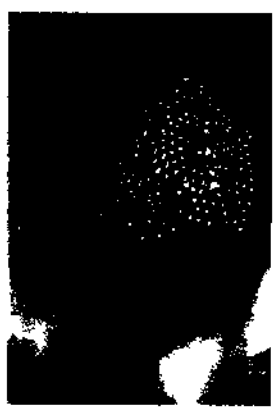

C

gmr-GAL4/ UAS-myc-SCA3fl-Q84/
UAS-CG2010$^{RNAi\ (NIG2010R\ 2)}$

D

gmr-GAL4/ UAS-myc-SCA3fl-Q84/
UAS-Cul1$^{RNAi\ (VDRC42445)}$*/*
UAS-CG2010$^{RNAi\ (NIG2010R\ 2)}$

Figure 4.17 Genetic interaction between *CG2010* and *Cul1* in polyglutamine toxicity.

Adult external eye depigmentation phenotypes of *myc-SCA3fl-Q84*-expressing flies with or without knock-down of *Cul1* and *CG2010* expression are shown. Transgenes were expressed using the *gmr-GAL4* driver. (**A**) At 5 dpe, expression of *myc-SCA3fl-Q84* did not show any observable degenerative phenotype. (**B**) Knock-down of *Cul1* expression enhanced polyQ toxicity and led to loss of pigmentation. (**C**) Knock-down of *CG2010* expression also enhanced polyQ toxicity and led to mild depigmentation. (**D**) Double knock-down of *Cul1* and *CG2010* expression in the *myc-SCA3fl-Q84*-expressing flies showed degenerative phenotype similar to that of single knock-down of either *Cul1* (**B**) or *CG2010* (**C**) expression. The flies were raised at 25°C. They were of genotypes:

(**A**) *w*; *gmr-GAL4/+*; *UAS-myc-SCA3fl-Q84/+*

(**B**) *w*; *gmr-GAL4/+*; *UAS-myc-SCA3fl-Q84 UAS-Cul1*$^{RNAi\ (VDRC42445)}$/+

(**C**) *w*; *gmr-GAL4/UAS-CG2010*$^{RNAi\ (NIG2010R-2)}$; *UAS-myc-SCA3fl-Q84/+*

(**D**) *w*; *gmr-GAL4/ AS-CG2010*$^{RNAi\ (NIG2010R-2)}$; *UAS-myc-SCA3fl-Q84 UAS-Cul1*$^{RNAi\ (VDRC42445)}$/+.

of both *Cul1* and *CG2010* expressions, it is suggested that *Cul1* and *CG2010* are involved in polyQ toxicity through the same pathway.

4.7 Discussion

Cul1-based CRL targets substrate protein using specific F-box protein as substrate receptor [81]. Identifying the F-box protein employed in the targeting of substrate protein is important for the detailed analysis on the ubiquitination of substrate protein mediated by Cul1-based CRL [179, 184, 185]. According to Chapter 3, it is suggested that SDS-insoluble expanded polyQ is a substrate of Cul1-based CRL. Therefore, it is important to identify the F-box protein employed for this substrate targeting.

Although F-box protein is a large protein family with nearly 70 members already identified in humans [178], only 19 of them are conserved in *Drosophila* [175]. Hence, it is likely that Cul1-based CRL targets SDS-insoluble expanded polyQ through at least one of these 19 F-box proteins. Individual knock-down of expression of these 19 F-box proteins was done and the corresponding effect on polyQ toxicity was examined using adult external eye depigmentation assay (section 4.2). Overexpression of *CG11033* was previously reported to enhance polyQ toxicity through unknown mechanisms [140]. Consistently, in the present study it was found that knock-down of *CG11033* expression suppressed degenerative phenotype induced by strong expression of *HA-SCA3tr-Q78* (data not shown). This finding validates the approach employed here to identify F-box proteins that modify polyQ toxicity.

One F-box protein, Slmb protein, resulted in dominant rough eye phenotype upon knock-down of expression (Figure 4.1B). By using the *gmr-GAL4* driver to drive the expression of *UAS-dsRNA*, *Slmb* expression was knocked down since the third-instar larval stage [118]. As discussed in Chapter 3 (section 3.9), *Slmb* is involved in fly eye development by regulating the proteolysis of Cubitus interruptus (Ci) [173]. The dominant phenotype upon knock-down of *Slmb* expression is possibly due to the disturbance of Ci proteolysis during fly eye development.

Two F-box proteins, Rca1 protein (Figure 4.1C) and CG2010 protein (Figure 4.1D), enhanced *HA-SCA3tr-Q78*-induced toxicity upon respective knock-down of expression. Rca1 promotes G1-S phase transition in *Drosophila* [186]. It is reported that cell-cycle arrest enhances toxicity induced by expression of truncated ataxin-3 *in vitro* [187]. Knock-down of *Rca1* expression could induce cell-cycle arrest and thus enhance polyQ toxicity. However, in comparison to the SCA3tr model, it was found that knock-down of *Rca1* expression modified the degenerative phenotype even in the unexpanded control in the SCA3fl model [129] (data not shown). This suggests that *Rca1* has dominant, non-polyQ specific effect on normal ataxin-3 protein. Therefore, *Rca1* is not further investigated in the present study. On the other hand, the enhancement by knock-down of *CG2010* expression was specific to expanded polyQ protein in both the SCA3tr (Figure 4.1D) and SCA3fl models (Figure 4.8). Therefore, *CG2010* was further studied to explore its role in polyQ pathogenesis.

So far, very limited investigation has been performed on CG2010 and the

function of CG2010 is poorly understood. What is known about CG2010 is an F-box protein that carries a conserved F-box domain and a substrate recognition domain. The major function of F-box proteins is to serve as substrate receptors and recruit specific substrates to Cul1-based CRL. However, increasing studies have shown that F-box proteins have other non-CRL related functions [188]. For example, apart from the function in promoting G1-S phase transition, Rca1 protein also prevents premature degradation of cyclin during G2 phase independently of the F-box domain [186, 189]. Therefore, it is possible that CG2010 modifies polyQ toxicity through CRL-irrelevant pathway.

To test if *CG2010* acts on polyQ pathogenesis through the same pathway as *Cul1*, the effect of *CG2010* on the SDS-solubility and ubiquitination of expanded polyQ protein was examined. Similar to *Cul1*, it was found that knock-down of *CG2010* expression reduced ubiquitination of SDS-insoluble (Figures 4.13 and 4.14), but not the SDS-soluble fraction (Figure 4.12), of expanded polyQ protein and increased the level of this SDS-insoluble fraction (Figure 4.10). Besides, data on double knock-down of both *CG2010* and *Cul1* expressions indicate that *CG2010* and *Cul1* act on polyQ toxicity through the same pathway (Figure 4.17). Therefore, it is likely that Cul1-based CRL targets SDS-insoluble expanded polyQ protein using CG2010 protein as substrate receptor. Knock-down of *CG2010* expression would lead to reduced activity of Cul1-based CRL that target SDS-insoluble expanded polyQ protein for ubiquitination and subsequent substrate degradation. Thus SDS-insoluble expanded polyQ protein would accumulate in cells. As mentioned in Chapter 1 (section 1.1.4), SDS-insoluble expanded polyQ protein is neurotoxic [52,

53, 135]. Its accumulation in cells would eventually result in enhanced neurodegeneration.

The above *in vivo* data from *Drosophila* highlight the role of *CG2010* in polyQ pathogenesis. Identifying the human counterpart of *CG2010* might give insight to treatment of polyQ diseases. F-box protein is characterized by the presence of the conserved F-box domain which is usually situated at the N-terminus [175]. In addition to this domain, in an F-box protein there is a variable substrate-binding domain that is responsible for substrate recognition at the C-terminus [175]. Majority of the F-box proteins employ either WD40 repeats or leucine-rich repeats (LRRs) as protein-protein interaction domains [175]. Less common substrate-binding domains include Kelch repeats, CASH domains and proline-rich domains [175]. According to the Structural Classification of Proteins (SCOP) database [190], CG2010 protein carries a RNase inhibitor (RNI)-like domain at the C-terminus. This RNI-like domain is prototypical to LRRs but it does not reach the threshold required to be classified as authentic LRRs based on the sequence [175]. Little study has been done on this RNI-like domain and the function of this domain is largely unknown.

Only three human F-box proteins, namely FBXO33, FBXO38 and FBXO39, carry the RNI-like domain [175]. Little study has been performed on these F-box proteins. According to UniGene from the National Center for Biotechnology Information [191] and the BioGPS [192], *FBXO33* and *FBXO38* are widely expressed in various tissues including brain. Expression of *FBXO39* is less restricted to brain and testis. As F-box proteins recognize substrate proteins through the

substrate-binding domain, it is likely that FBXO33, FBXO38 and FBXO39 proteins which carry the RNI-like domain similarly as CG2010 protein, would target SDS-insoluble expanded polyQ protein for ubiquitination and suppress polyQ toxicity. Therefore, further investigation on the involvement of these three F-box proteins in polyQ pathogenesis might open new opportunities in treating polyQ diseases.

Apart from CG11033, Slmb, Rca1 and CG2010, the remaining 15 F-box proteins investigated in the present study did not modify polyQ toxicity upon individual knock-down of their expressions (Figure 4.1). It is noted that the knock-down efficiency of expression of these F-box proteins, except CG9461, is not confirmed. Therefore, it is not clear whether any of them are also involved in polyQ toxicity.

Moreover, based on the findings that knock-down of endogenous *Cul1* expression modified polyQ toxicity in transgenic *Drosophila* polyQ model, the present study aims at screening out the putative substrate receptor involved in the above modification only from the *Drosophila* homolog of F-box proteins. It is noted that other human F-box proteins that have no homologs in flies are also possible to affect polyQ toxicity. However, due to the large number of human F-box proteins, those that have no homologs in flies were not examined in this study. Large scale siRNA experiment on individual human F-box proteins in mammalian cultured cells such as HEK 293FT could be performed to 1) test the effect of *FBXO33*, *FBXO38* and *FBXO39* on polyQ toxicity and 2) screen for all the F-box proteins that modify

polyQ toxicity.

To sum up, it was found that *CG2010* has similar effect on polyQ pathogenesis as *Cul1* upon knock-down of expression. Hence, it is likely that Cul1-based CRL employs CG2010 protein as substrate receptor for targeting SDS-insoluble expanded polyQ protein for ubiquitination and modify polyQ toxicity.

Chapter 5 Involvement of other components of Cul1-based CRL pathway in polyglutamine pathogenesis

5.1 Introduction

Based on the studies on *Cul* and *CG2010* in Chapters 3 and 4, it is suggested that Cul1-based CRL regulates SDS-solubility of expanded polyQ protein and modulates polyQ toxicity through CG2010 substrate receptor. In addition to Cul1 protein and CG2010 protein, there are other members in the Cul1-based CRL pathway [81, 83, 84]. Firstly, Cul1 binds to Skp1 through its N-terminus and Roc1 through its C-terminus respectively [81]. Secondly, there are regulators such as Nedd8 and CSN5 which would influence the activity of Cul1-based CRL [83, 84, 86]. To have a more complete analysis of the involvement of Cul1-based CRL pathway in polyQ diseases, a preliminary study on the effect of other components of the Cul1-based CRL pathway in polyQ pathogenesis was performed in the SCA3tr model [117].

As described in Chapter 3 (section 3.2), the SCA3tr model expresses a HA-tagged, truncated form of ataxin-3 protein. Expression of the transgene encoding for the truncated ataxin-3 protein with unexpanded polyQ repeats of 27 glutamines (*HA-SCA3tr-Q27*) in the eyes by *gmr-GAL4* driver did not cause any degenerative phenotype even aged for 32 days (Figure 3.2A). Weak expression of the transgene encoding for the truncated ataxin-3 protein with expanded polyQ repeats of 78 glutamines (*HA-SCA3tr-Q78(w)*) induced late-onset progressive degeneration resulting in depigmentation phenotype which could only be observed at 32 dpe but

not at 3 dpe (Figure 3.2B). This transgenic fly line allows identification of any polyQ toxicity enhancers. Stronger expression of *HA-SCA3tr-Q78* transgene (*HA-SCA3tr-Q78(s)*) in another independent transgenic fly line induced more severe degeneration as shown by the extensive loss of pigmentation at 3 dpe already (Figure 3.2C). This transgenic fly line allows identification of any polyQ toxicity suppressors.

As mentioned in Chapter 3 (section 3.1), expansion of the polyQ domain in disease proteins causes accumulation of SDS-insoluble polyQ protein in neurons which results in neurotoxicity [52, 53, 135]. HA-SCA3tr-Q78 protein is largely SDS-insoluble [117]. Modification on SDS solubility of HA-SCA3tr-Q78 protein was also examined so as to define the role of the toxicity modifiers, if any, in polyQ diseases.

5.2 Roc1a

The Roc1 protein is responsible for recruiting ubiquitin-loaded E2 to the CRL complex [81, 83, 84]. It carries a variable N-terminal β-strand domain and a conserved RING domain [193]. Both of these two domains are required for binding to the C-terminus of cullins [193]. In *Drosophila*, there are three Roc proteins (Roc1a, Roc1b and Roc2) which share 57-70% amino acid identity among each other [132, 194]. They are functionally different [132] and demonstrate specificity towards different cullins, e.g. Roc1a binds Cul1 and Cul4, Roc 1b binds Cul3 while Roc2 binds Cul5 [193].

To test the effect of *Roc1a*, which is employed by Cul1-based CRL, on polyQ toxicity, expression of *Roc1a* was knocked down by RNAi [134] in the SCA3tr model [117]. It was found that knock-down of *Roc1a* expression did not modify degenerative phenotype induced by weak or strong expression of *HA-SCA3tr-Q78* transgene (Figure 5.1). Overexpression of *Roc1a* was also performed to test its effect on polyQ toxicity. Two independent transgenic lines [132] were employed so as to exclude the possibility of positional effect due to insertion of transgene on chromosome [138]. It was found that overexpression of *Roc1a* did not modify the degenerative phenotype induced by both weak and strong expression of *HA-SCAtr-Q78* transgene (Figure 5.2).

To test the effect of *Roc1a* on SDS-solubility of expanded polyQ protein, filter retardation assay was employed [146]. As mentioned in Chapter 3 (section 3.3), this assay detects SDS-insoluble protein aggregates with size larger than 0.22 μm [146]. It was shown that overexpression of *Roc1a* did not alter the level of SDS-insoluble HA-SCAtr-Q78 protein (Figure 5.3). Combining with the above data, it is suggested that altering expression level of *Roc1a* does not affect both polyQ toxicity and SDS-solubility of expanded polyQ protein.

5.3 SkpA

Skp1 is the adaptor subunit that recruits the substrate receptor to the CRL complex [81, 83, 84]. It carries a POZ (Poxvirus and zinc finger) domain [195] and a Skp1-dimerization domain [196, 197]. It binds to the N-terminus of cullins through the Skp1-dimerization domain [196]. In *Drosophila*, there are six *Skp1*-related genes

Figure 5.1

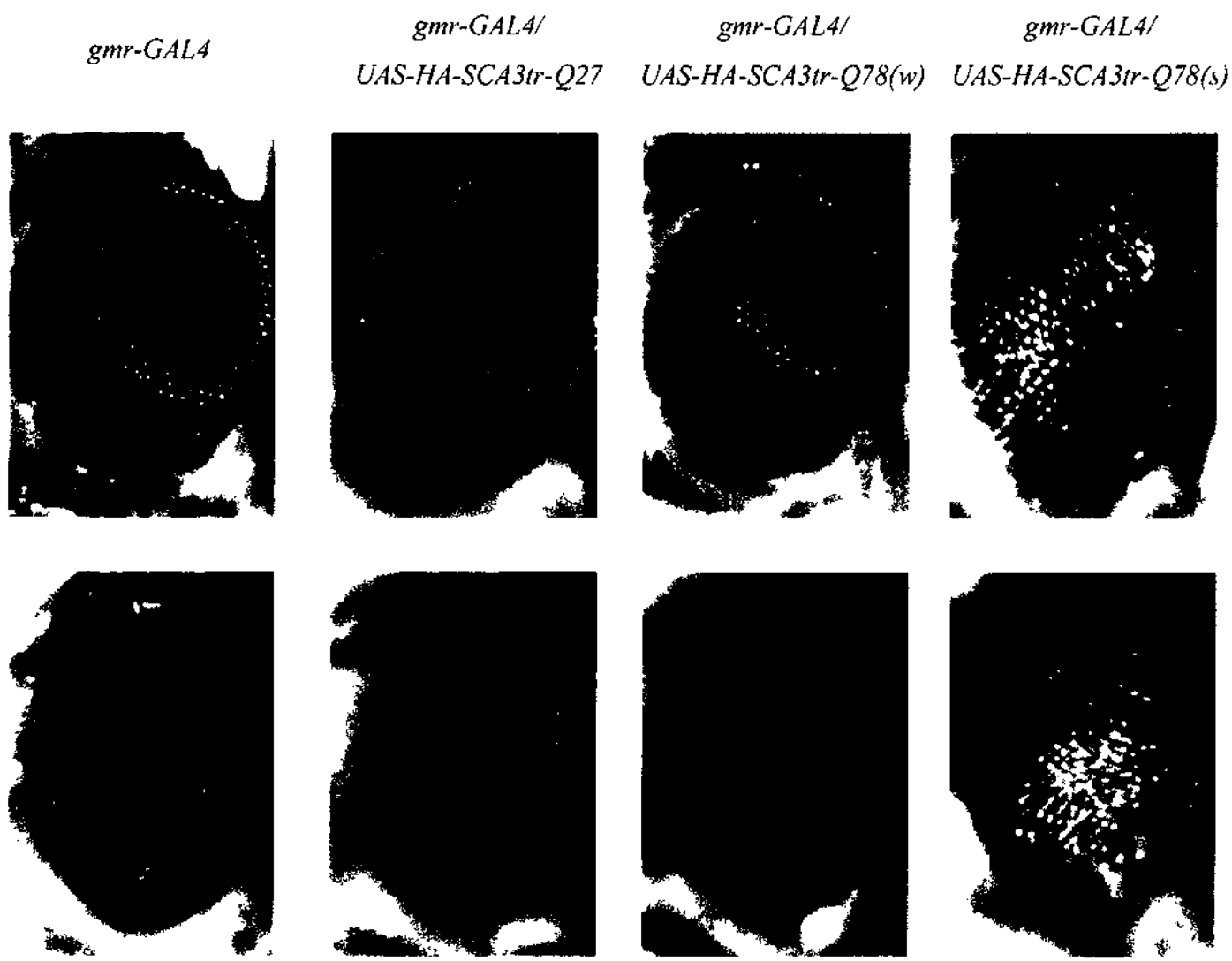
gmr-GAL4
gmr-GAL4/ UAS-HA-SCA3tr-Q27
gmr-GAL4/ UAS-HA-SCA3tr-Q78(w)
gmr-GAL4/ UAS-HA-SCA3tr-Q78(s)
A
B
UAS-Roc1

Figure 5.1. Knock-down of *Roc1a* expression did not modify degeneration induced by *HA-SCA3tr-Q78* expression in adult fly eyes.

Adult external eye depigmentation phenotypes of *gmr-GAL4* driver-only control flies and flies expressing *truncated ataxin-3* transgenes (*HA-SCA3tr-Q27* or *HA-SCA3tr-Q78)* with or without (indicated by "-") knock-down of *Roc1a* expression are shown. Transgenes were expressed using the *gmr-GAL4* driver. (**A**) At 3 dpe, expression of *HA-SCA3tr-Q27* transgene did not cause any degenerative phenotype. Weak expression of *HA-SCA3tr-Q78* (*HA-SCA3tr-Q78(w)*) transgene did not cause any observable depigmentation while strong expression of *HA-SCA3tr-Q78* (*HA-SCA3tr-Q78(s)*) transgene caused severe depigmentation. (**B**) Knock-down of *Roc1a* expression did not modify degenerative phenotype induced by *HA-SCA3tr-Q78(w)* or *HA-SCA3tr-Q78(s)*. The experiment was performed once. The flies were raised at 25°C. They were of genotypes:

(**A**) *w*; *gmr-GAL4*/+; +/+,

w; *gmr-GAL4 UAS-HA-SCA3tr-Q27*/+; +/+,

w; *gmr-GAL4*/+; *UAS-HA-SCA3tr-Q78(w)*/+,

w; *gmr-GAL4 UAS-HA-SCA3tr-Q78(s)*/+; +/+

(**B**) *w*; *gmr-GAL4/UAS-Roc1a*^{RNAi}; +/+,

w; *gmr-GAL4 UAS-HA-SCA3tr-Q27/UAS-Roc1a*^{RNAi}; +/+,

w; *gmr-GAL4/UAS-Roc1a*^{RNAi}; *UAS-HA-SCA3tr-Q78(w)*/+,

w; *gmr-GAL4 UAS-HA-SCA3tr-Q78(s)/UAS-Roc1a*^{RNAi}; +/+.

Figure 5.2

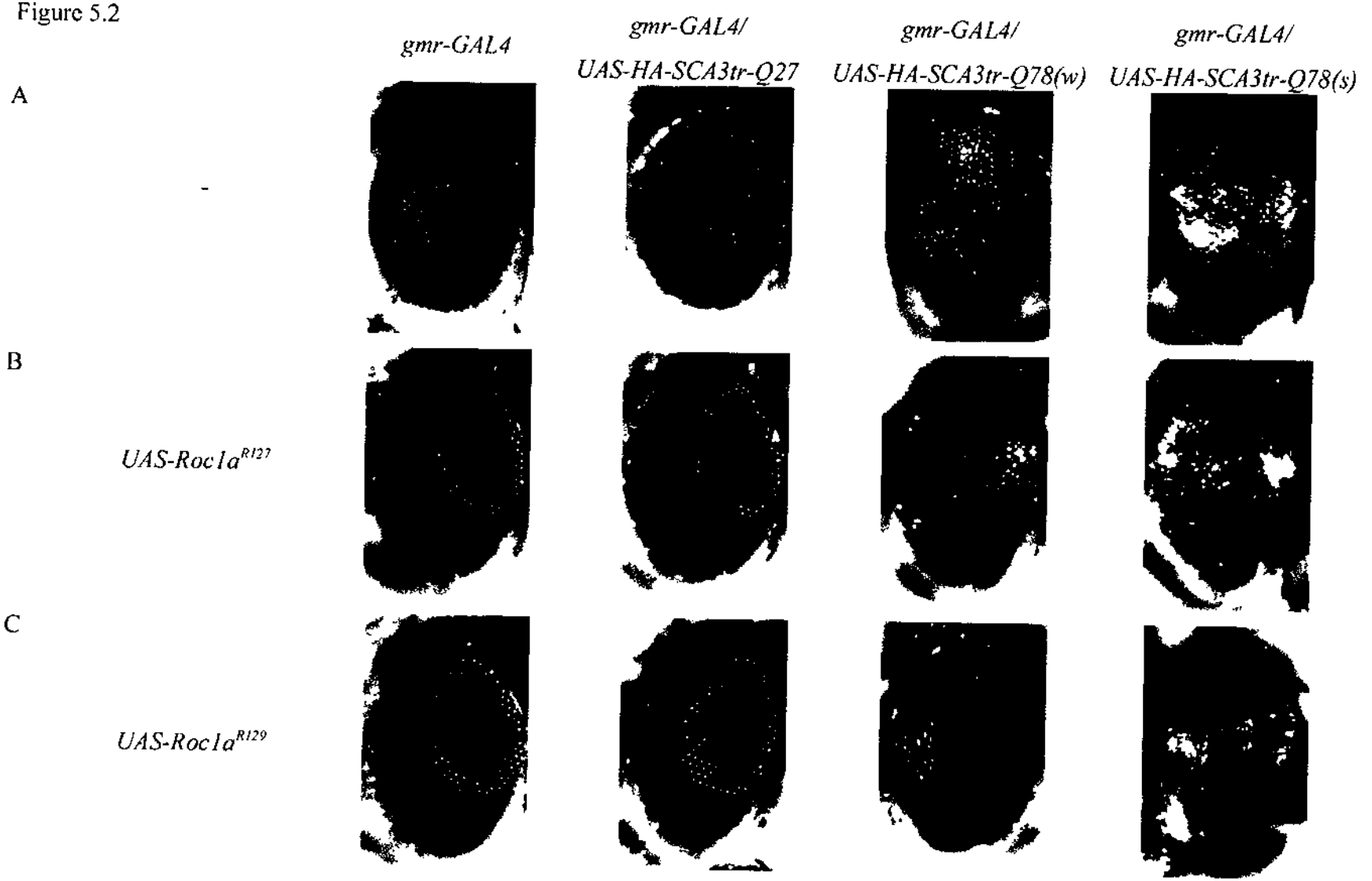
gmr-GAL4
gmr-GAL4/
UAS-HA-SCA3tr-Q27
gmr-GAL4/
UAS-HA-SCA3tr-Q78(w)
gmr-GAL4/
UAS-HA-SCA3tr-Q78(s)
A
B
UAS-Roc1a^R127
C
UAS-Roc1a^R129

Figure 5.2. Overexpression of *Roc1a* did not modify degeneration induced by *HA-SCA3tr-Q78* expression in adult fly eyes.

Adult external eye depigmentation phenotypes of *gmr-GAL4* driver-only control flies and flies expressing *truncated ataxin-3* transgenes (*HA-SCA3tr-Q27* or *HA-SCA3tr-Q78)* with or without (indicated by "-") overexpression of *Roc1a* are shown. Transgenes were expressed using the *gmr-GAL4* driver. (**A**) At 3 dpe, expression of *HA-SCA3tr-Q27* transgene did not cause any degenerative phenotype. Weak expression of *HA-SCA3tr-Q78* (*HA-SCA3tr-Q78(w)*) transgene induced slight depigmentation while strong expression of *HA-SCA3tr-Q78* (*HA-SCA3tr-Q78(s)*) transgene caused extensive loss of pigmentation and formation of necrotic scars. Overexpression of *Roc1a* using neither *UAS-Roc1a*^{R127} transgenic line (**B**) nor *UAS-Roc1a*^{R129} transgenic line (**C**) modified degenerative phenotype induced by *HA-SCA3tr-Q78(w)* or *HA-SCA3tr-Q78(s)* expression. The experiment was performed once. The flies were raised at 25°C. They were of genotypes:

(**A**) *w*; *gmr-GAL4*/+; +/+,

w; *gmr-GAL4 UAS-HA-SCA3tr-Q27*/+; +/+,

w; *gmr-GAL4*/+; *UAS-HA-SCA3tr-Q78(w)*/+,

w; *gmr-GAL4 UAS-HA-SCA3tr-Q78(s)*/+; +/+

(**B**) *w*; *gmr-GAL4/UAS-Roc1a*^{R127}; +/+,

w; *gmr-GAL4 UAS-HA-SCA3tr-Q27/UAS-Roc1a*^{R127}; +/+,

w; *gmr-GAL4/UAS-Roc1a*^{R127}; *UAS-HA-SCA3tr-Q78(w)*/+,

w; *gmr-GAL4 UAS-HA-SCA3tr-Q78(s)/UAS-Roc1a*^{R127}; +/+

(**C**) *w*; *gmr-GAL4*/+; *UAS-Roc1a*^{R129}/+,

w; *gmr-GAL4 UAS-HA-SCA3tr-Q27*/+; *UAS-Roc1a*^{R129}/+,

w; *gmr-GAL4*/+; *UAS-HA-SCA3tr-Q78(w)/UAS-Roc1a*^{R129},

w; *gmr-GAL4 UAS-HA-SCA3tr-Q78(s)*/+; *UAS-Roc1a*^{R129}/+.

Figure 5.3

gmr-GAL4	+	+	+	+
UAS-HA-SCA3tr-Q78(w)	-	+	+	+
UAS-Roc1a^{R129}	-	-	+	-
UAS-Roc1a^{R157}	-	-	-	+

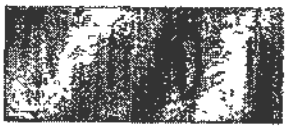

IB: anti-HA

Figure 5.3. Overexpression of *Roc1a* did not alter SDS-solubility of HA-SCA3tr-Q78 protein.

Adult head lysate of *gmr-GAL4* driver-only control flies and *HA-SCA3tr-Q78(w)*-expressing flies with or without *Roc1a* overexpression was subjected to filter retardation assay to capture SDS-insoluble protein aggregates with size larger than 0.22 μm for immunodetection. The immunoblot was probed with anti-HA antibody to detect the SDS-insoluble HA-SCA3tr-Q78 protein. The signal intensity represents the level of SDS-insoluble HA-SCA3tr-Q78 protein. Overexpression of *Roc1a* using neither *UAS-Roc1a*^{R127} transgenic line nor *UAS-Roc1a*^{R129} transgenic line altered the level of SDS-insoluble HA-SCA3tr-Q78 protein. The experiment was performed once. The flies were raised at 25°C and were assayed at 3 dpe. They were of genotypes:

w; *gmr-GAL4*/+; +/+,

w; *gmr-GAL4*/+; *UAS-HA-SCA3tr-Q78(w)*/+,

w; *gmr-GAL4*/+; *UAS-HA-SCA3tr-Q78(w)/UAS-Roc1a*^{R129},

w; *gmr-GAL4/UAS-Roc1a*^{R127}; *UAS-HA-SCA3tr-Q78(w)*/+.

which are named from *SkpA* through *SkpF* [198]. Among them, *SkpA* is chosen for the present study because 1) it shares the highest homology with human *Skp1* [198], and 2) the SkpA protein has been demonstrated to directly interact with Cul1 protein by yeast-two-hybrid analysis and *in vitro* interaction study [199, 200].

To test the effect of *SkpA* on polyQ toxicity, expression of *SkpA* was knocked down by RNAi [134] in the SCA3tr model [117]. It was found that knock-down of *SkpA* expression showed no effect on the degenerative phenotype conferred by both weak and strong expression of *HA-SCA3tr-Q78* transgenes (Figure 5.4). This piece of preliminary data suggests that lowering expression level of *SkpA* would not affect polyQ toxicity.

5.4 Nedd8

Nedd8 is an ubiquitin-like protein which is highly conserved from *Drosophila* to humans [85]. It promotes CRL activity upon conjugation to a conserved lysine residue on cullin [81, 83, 84, 86].

To test the effect of *Nedd8* on polyQ toxicity, expression of *Nedd8* was knocked down by RNAi [134] in the SCA3tr model [117]. It was found that knock-down of *Nedd8* expression showed no effect on the degenerative phenotype conferred by both weak and strong expression of *HA-SCA3tr-Q78* transgene (Figure 5.5). Overexpression of a transgene encoding for Nedd8 fused to a Yellow Fluorescent Protein (YFP; *YFP-Nedd8*) was also performed to test its effect on polyQ toxicity. Two independent transgenic lines [86] were employed so as to exclude the possibility

Figure 5.4

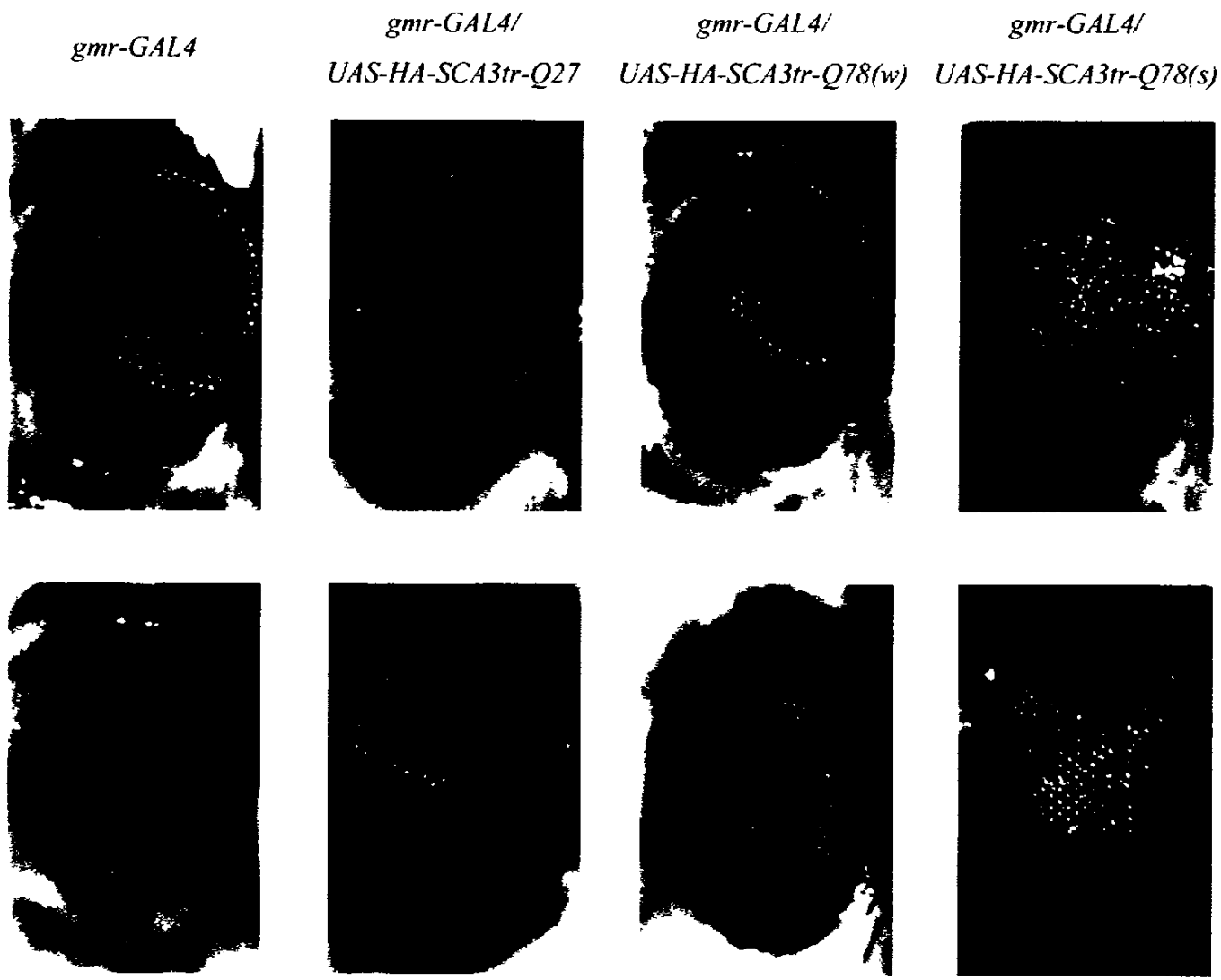
gmr-GAL4
gmr-GAL4/
UAS-HA-SCA3tr-Q27
gmr-GAL4/
UAS-HA-SCA3tr-Q78(w)
gmr-GAL4/
UAS-HA-SCA3tr-Q78(s)
A
B
UAS-SkpA^RNAi

Figure 5.4. Knock-down of *SkpA* expression did not modify degeneration induced by *HA-SCA3tr-Q78* expression in adult fly eyes.

Adult external eye depigmentation phenotypes of *gmr-GAL4* driver-only control flies and flies expressing truncated ataxin-3 transgenes (*HA-SCA3tr-Q27* or *HA-SCA3tr-Q78)* with or without (indicated by "-") knock-down of *SkpA* expression are shown. Transgenes were expressed using the *gmr-GAL4* driver. **(A)** At 3 dpe, expression of *HA-SCA3tr-Q27* transgene did not cause any degenerative phenotype. Weak expression of *HA-SCA3tr-Q78* (*HA-SCA3tr-Q78(w)*) transgene did not cause any observable depigmentation while strong expression of *HA-SCA3tr-Q78* (*HA-SCA3tr-Q78(s)*) transgene caused extensive loss of pigmentation. **(B)** Knock-down of *SkpA* expression did not modify degenerative phenotype induced by *HA-SCA3tr-Q78(w)* or *HA-SCA3tr-Q78(s)* expression. The experiment was performed once. The flies were raised at 25°C. They were of genotypes:

(A) *w*; *gmr-GAL4*/+; +/+,

w; *gmr-GAL4 UAS-HA-SCA3tr-Q27*/+; +/+,

w; *gmr-GAL4*/+; *UAS-HA-SCA3tr-Q78(w)*/+,

w; *gmr-GAL4 UAS-HA-SCA3tr-Q78(s)*/+; +/+

(B) *w*; *gmr-GAL4*/+; $UAS\text{-}SkpA^{RNAi}$/+,

w; *gmr-GAL4 UAS-HA-SCA3tr-Q27*/+; $UAS\text{-}SkpA^{RNAi}$/+,

w; *gmr-GAL4*/+; *UAS-HA-SCA3tr-Q78(w)*/$UAS\text{-}SkpA^{RNAi}$,

w; *gmr-GAL4 UAS-HA-SCA3tr-Q78(s)*/+; $UAS\text{-}SkpA^{RNAi}$/+.

Figure 5.5

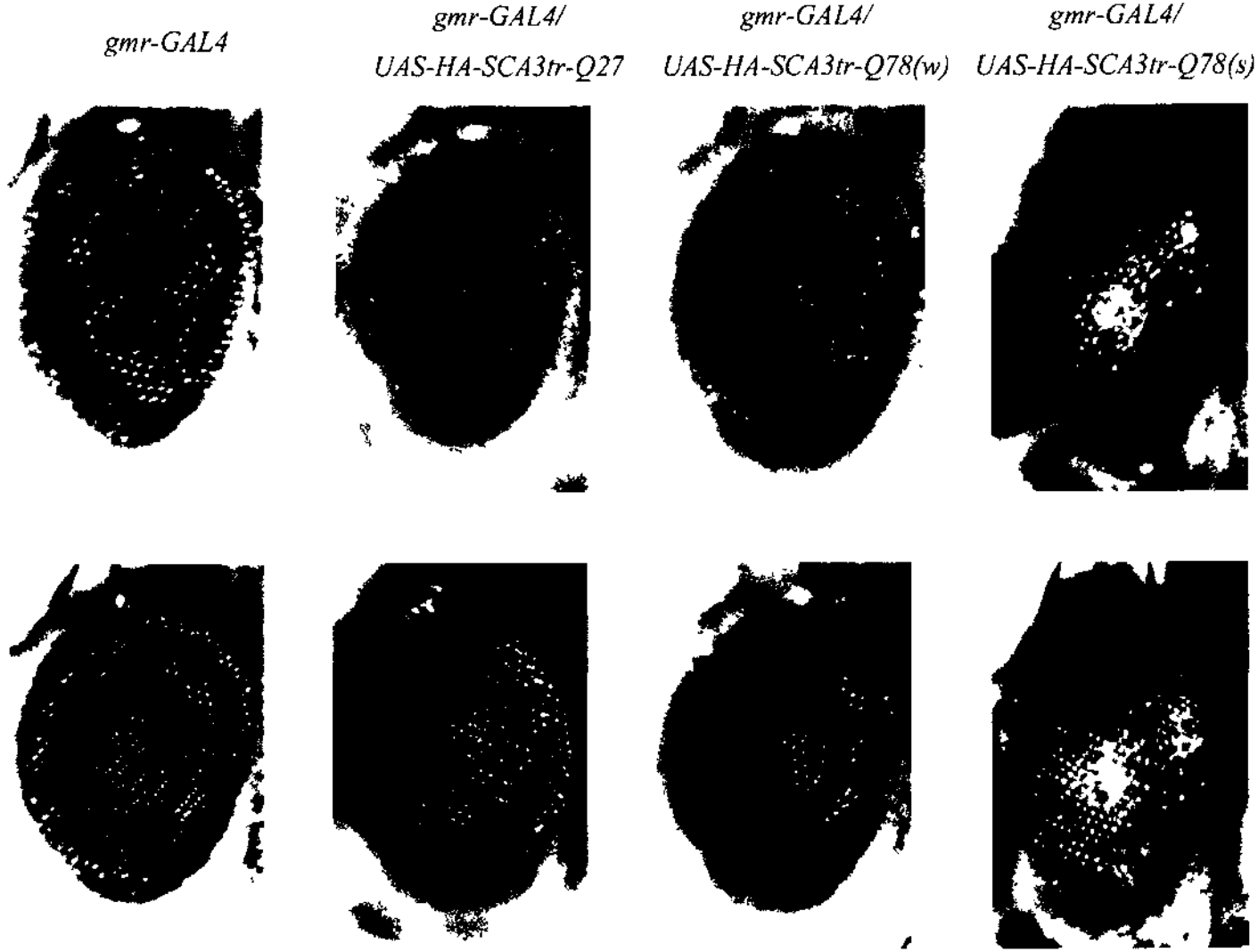
gmr-GAL4
gmr-GAL4/
UAS-HA-SCA3tr-Q27
gmr-GAL4/
UAS-HA-SCA3tr-Q78(w)
gmr-GAL4/
UAS-HA-SCA3tr-Q78(s)
A
B
UAS-Nedd8

Figure 5.5. Knock-down of *Nedd8* expression did not modify degeneration induced by *HA-SCA3tr-Q78* expression in adult fly eyes.

Adult external eye depigmentation phenotypes of *gmr-GAL4* driver-only control flies and flies expressing *truncated ataxin-3* transgenes (*HA-SCA3tr-Q27* or *HA-SCA3tr-Q78)* with or without (indicated by "-") knock-down of *Nedd8* expression are shown. Transgenes were expressed using the *gmr-GAL4* driver. **(A)** At 3 dpe, expression of *HA-SCA3tr-Q27* transgene did not cause any degenerative phenotype. Weak expression of *HA-SCA3tr-Q78* (*HA-SCA3tr-Q78(w)*) transgene did not cause any observable depigmentation while strong expression of *HA-SCA3tr-Q78* (*HA-SCA3tr-Q78(s)*) transgene caused extensive loss of pigmentation. **(B)** Knock-down of *Nedd8* expression did not modify degenerative phenotype induced by *HA-SCA3tr-Q78(w)* or *HA-SCA3tr-Q78(s)* expression. The experiment was performed once. The flies were raised at 25°C. They were of genotypes:

(A) *w*; *gmr-GAL4/+*; *+/+*,

w; *gmr-GAL4 UAS-HA-SCA3tr-Q27/+*; *+/+*,

w; *gmr-GAL4/+*; *UAS-HA-SCA3tr-Q78(w)/+*,

w; *gmr-GAL4 UAS-HA-SCA3tr-Q78(s)/+*; *+/+*

(B) *w*; *gmr-GAL4/UAS-Nedd8*^{RNAi}; *+/+*,

w; *gmr-GAL4 UAS-HA-SCA3tr-Q27/UAS-Nedd8*^{RNAi}; *+/+*,

w; *gmr-GAL4/UAS-Nedd8*^{RNAi}; *UAS-HA-SCA3tr-Q78(w)/+*,

w; *gmr-GAL4 UAS-HA-SCA3tr-Q78(s)/UAS-Nedd8*^{RNAi}; *+/+*.

of positional effect due to insertion of transgene on chromosomes [138]. It was found that overexpression of *YFP-Nedd8* did not modify the degenerative phenotype induced by both weak and strong expression of *HA-SCA3tr-Q78* transgene in these two independent transgenic lines (Figure 5.6).

To test the effect of *Nedd8* on SDS-solubility of expanded polyQ protein, filter retardation assay was employed [146]. As mentioned in Chapter 3 (section 3.3), this assay detects SDS-insoluble protein aggregates with size larger than 0.22 μm [146]. It was shown that overexpression of *YFP-Nedd8* in two independent transgenic lines did not alter the level of SDS-insoluble HA-SCA3tr-Q78 protein (Figure 5.7). Combining with the above data, it is suggested that altering expression level of *Nedd8* does not affect polyQ toxicity and SDS-solubility of expanded polyQ protein.

5.5 CSN5

The COP9 signalosome (CSN) is composed of eight subunits (CSN1-8) [92]. One of the subunits, CSN5, bears a Nedd8-isopeptidase activity [92]. CSN5 regulates CRL activity by removing Nedd8 conjugated on cullins via its Nedd8-isopeptidase activity [81, 83, 84, 92].

To test the effect of *CSN5* on polyQ toxicity, overexpression of wild-type *CSN5* was performed in the SCA3tr model [117]. Two independent transgenic lines [132] were employed so as to exclude the possibility of positional effect due to insertion of transgene on chromosomes [138]. It was found that overexpressing wild-type *CSN5* in both independent transgenic lines did not modify degeneration induced by both

Figure 5.6

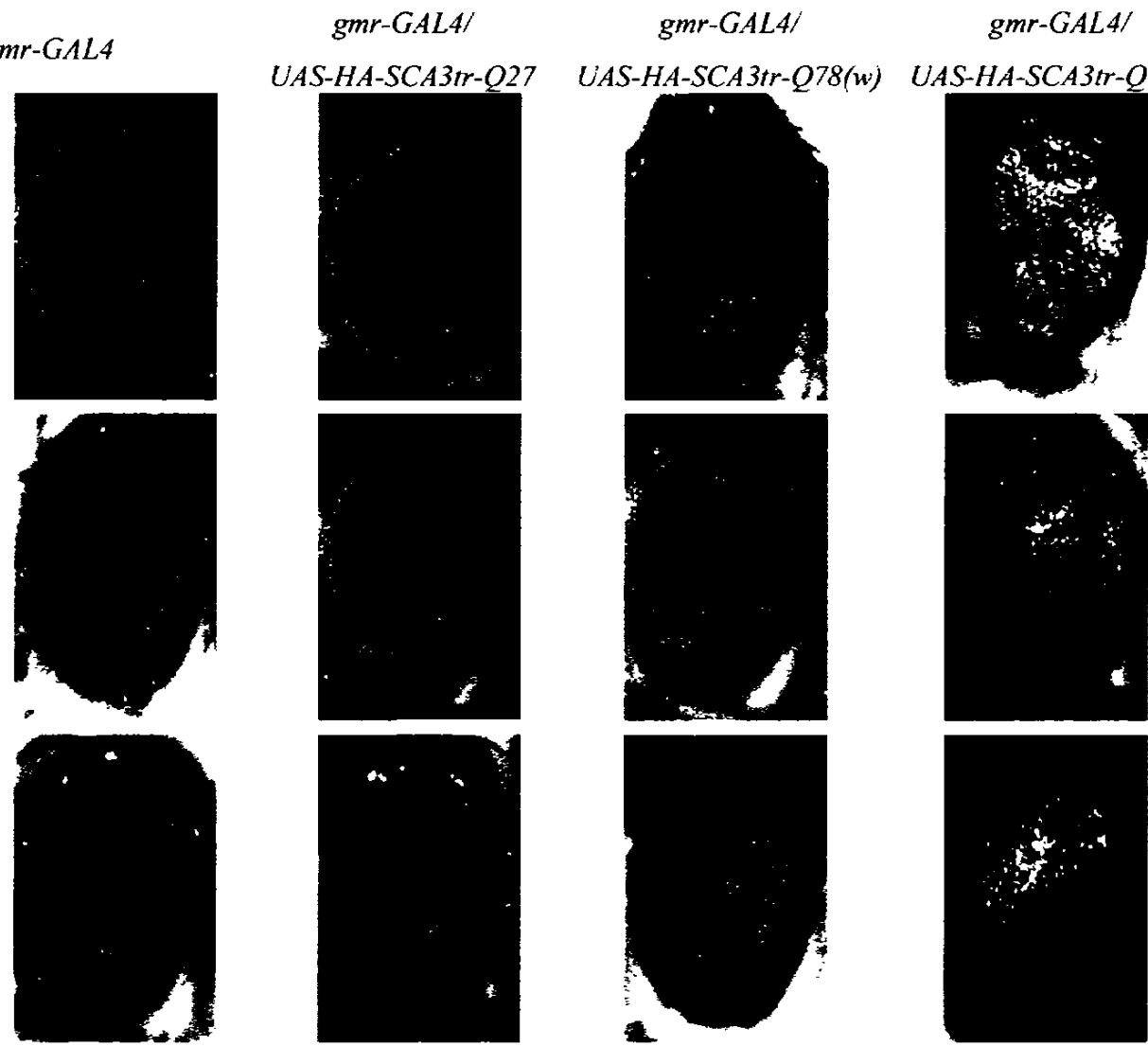
gmr-GAL4
gmr-GAL4/
UAS-HA-SCA3tr-Q27
gmr-GAL4/
UAS-HA-SCA3tr-Q78(w)
gmr-GAL4/
UAS-HA-SCA3tr-Q78(s)
A
B
UAS-YFP-Nedd8(II)
C
UAS-YFP-Nedd8(III)

Figure 5.6. Overexpression of *YFP-Nedd8* did not modify degeneration induced by *HA-SCA3tr-Q78* expression in adult fly eyes.

Adult external eye depigmentation phenotypes of *gmr-GAL4* driver-only control flies and flies expressing *truncated ataxin-3* transgenes (*HA-SCA3tr-Q27* or *HA-SCA3tr-Q78)* with or without (indicated by "-") overexpression of *YFP-Nedd8* are shown. Transgenes were expressed using the *gmr-GAL4* driver. (**A**) At 3 dpe, expression of *HA-SCA3tr-Q27* transgene did not cause any degenerative phenotype. Weak expression of *HA-SCA3tr-Q78* (*HA-SCA3tr-Q78(w)*) transgene did not cause any observable degenerative phenotype while strong expression of *HA-SCA3tr-Q78* (*HA-SCA3tr-Q78(s)*) transgene caused extensive loss of pigmentation. Overexpression of *YFP-Nedd8* in neither *UAS-YFP-Nedd8*$^{(II)}$ transgenic line (**B**) nor *UAS-YFP-Nedd8*$^{(III)}$ line (**C**) modified degenerative phenotype induced by expression of *HA-SCA3tr-Q78(w)* or *HA-SCA3tr-Q78(s)* transgene. The experiment was performed once. The flies were raised at 25°C. They were of genotypes:

(**A**) *w*; *gmr-GAL4/+*; *+/+*,

w; *gmr-GAL4 UAS-HA-SCA3tr-Q27/+*; *+/+*,

w; *gmr-GAL4/+*; *UAS-HA-SCA3tr-Q78(w)/+*,

w; *gmr-GAL4 UAS-HA-SCA3tr-Q78(s)/+*; *+/+*

(**B**) *w*; *gmr-GAL4/UAS-YFP-Nedd8*$^{(II)}$; *+/+*,

w; *gmr-GAL4 UAS-HA-SCA3tr-Q27/UAS-YFP-Nedd8*$^{(II)}$; *+/+*,

w; *gmr-GAL4/UAS-YFP-Nedd8*$^{(II)}$; *UAS-HA-SCA3tr-Q78(w)/+*,

w; *gmr-GAL4 UAS-HA-SCA3tr-Q78(s)/UAS-YFP-Nedd8*$^{(II)}$; *+/+*

(**C**) *w*; *gmr-GAL4/+*; *UAS-YFP-Nedd8*$^{(III)}$*/+*,

w; *gmr-GAL4 UAS-HA-SCA3tr-Q27/+*; *UAS-YFP-Nedd8*$^{(III)}$*/+*,

w; *gmr-GAL4/+*; *UAS-HA-SCA3tr-Q78(w)/UAS-YFP-Nedd8*$^{(III)}$,

w; *gmr-GAL4 UAS-HA-SCA3tr-Q78(s)/+*; *UAS-YFP-Nedd8*$^{(III)}$*/+*.

Figure 5.7

A

gmr-GAL4	+	+	+
UAS-HA-SCA3tr-Q78(w)	-	+	+
UAS-YFP-Nedd8$^{(II)}$	-	-	+

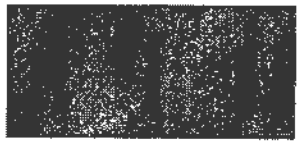

IB: anti-HA

B

gmr-GAL4	+	+	+
UAS-HA-SCA3tr-Q78(s)	-	+	+
UAS-YFP-Nedd8$^{(III)}$	-	-	+

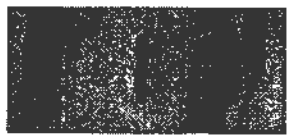

IB: anti-HA

Figure 5.7. Overexpression of *YFP-Nedd8* did not alter the SDS-solubility of HA-SCA3tr-Q78 protein.

(A) Adult head lysate of *gmr-GAL4* driver-only control flies and *HA-SCA3tr-Q78(w)*-expressing flies with or without overexpression of *YFP-Nedd8* was subjected to filter retardation assay to capture SDS-insoluble protein aggregates with size larger than 0.22 μm. The immunoblot was probed with anti-HA antibody to detect the SDS-insoluble HA-SCA3tr-Q78 protein. The signal intensity represents the level of SDS-insoluble HA-SCA3tr-Q78 protein. Overexpression of *YFP-Nedd8* in *UAS-YFP-Nedd8$^{(II)}$* transgenic line did not alter the level of SDS-insoluble HA-SCA3tr-Q78 protein. **(B)** The above experiment was repeated on *gmr-GAL4* driver control flies and *HA-SCA3tr-Q78(s)*-expressing flies with or without overexpression of *YFP-Nedd8*. Overexpression of *YFP-Nedd8* in *UAS-YFP-Nedd8$^{(III)}$* transgenic line did not alter the level of SDS-insoluble HA-SCA3tr-Q78 protein. The above experiments were performed once. The flies were raised at 25°C and were assayed at 3 dpe. They were of genotypes:

(A) *w*; *gmr-GAL4/+*; *UAS-HA-SCA3tr-Q78(w)/+*,

w; *gmr-GAL4/UAS-YFP-Nedd8$^{(II)}$*; *UAS-HA-SCA3tr-Q78(w)/+*

(B) *w*; *gmr-GAL4 UAS-HA-SCA3tr-Q78(s)/+*; *+/+*,

w; *gmr-GAL4 UAS-HA-SCA3tr-Q78(s)/+*; *UAS-YFP-Nedd8$^{(III)}$/+*.

weak and strong expression of *HA-SCA3tr-Q78* transgene (Figure 5.8B and C). $CSN5^{D148N}$ is a dominant-negative mutant protein with the Nedd8-isopeptidase activity abolished [86]. Similar to wild-type *CSN5*, overexpressing of $CSN5^{D148N}$ did not modify degeneration induced by both weak and strong expression of *HA-SCA3tr-Q78* (Figure 5.8D). These data suggest that neither increasing CSN5 level nor reducing its activity (by the use of dominant negative mutant) affects polyQ toxicity.

To test the effect of *CSN5* on SDS-solubility of expanded polyQ protein, ultracentrifugation was performed to isolate the SDS-insoluble protein aggregates and to remove the SDS-soluble protein [25]. This resulting pellet was treated by formic acid (100%) to solubilize the isolated SDS-insoluble protein aggregates into protein monomers [25, 151] for subsequent immunodetection. It was found that overexpressing wild-type *CSN5* did not alter the level of SDS-insoluble SCA3tr-Q78 protein (Figure 5.9). These data show that increasing expression level of *CSN5* does not affect SDS-solubility of expanded polyQ protein.

5.6 Discussion

According to Chapters 3 and 4, Cul1-based CRL might be involved in polyQ pathogenesis using CG2010 as substrate receptor. Apart from Cul1 and CG2010, there are other subunits (i.e. Roc1 and SkpA) in the Cul1-based CRL complex and there are regulators (i.e. Nedd8 and CSN5) which would influence the activity of Cul1-based CRL in the pathway [81, 83, 84].

Figure 5.8

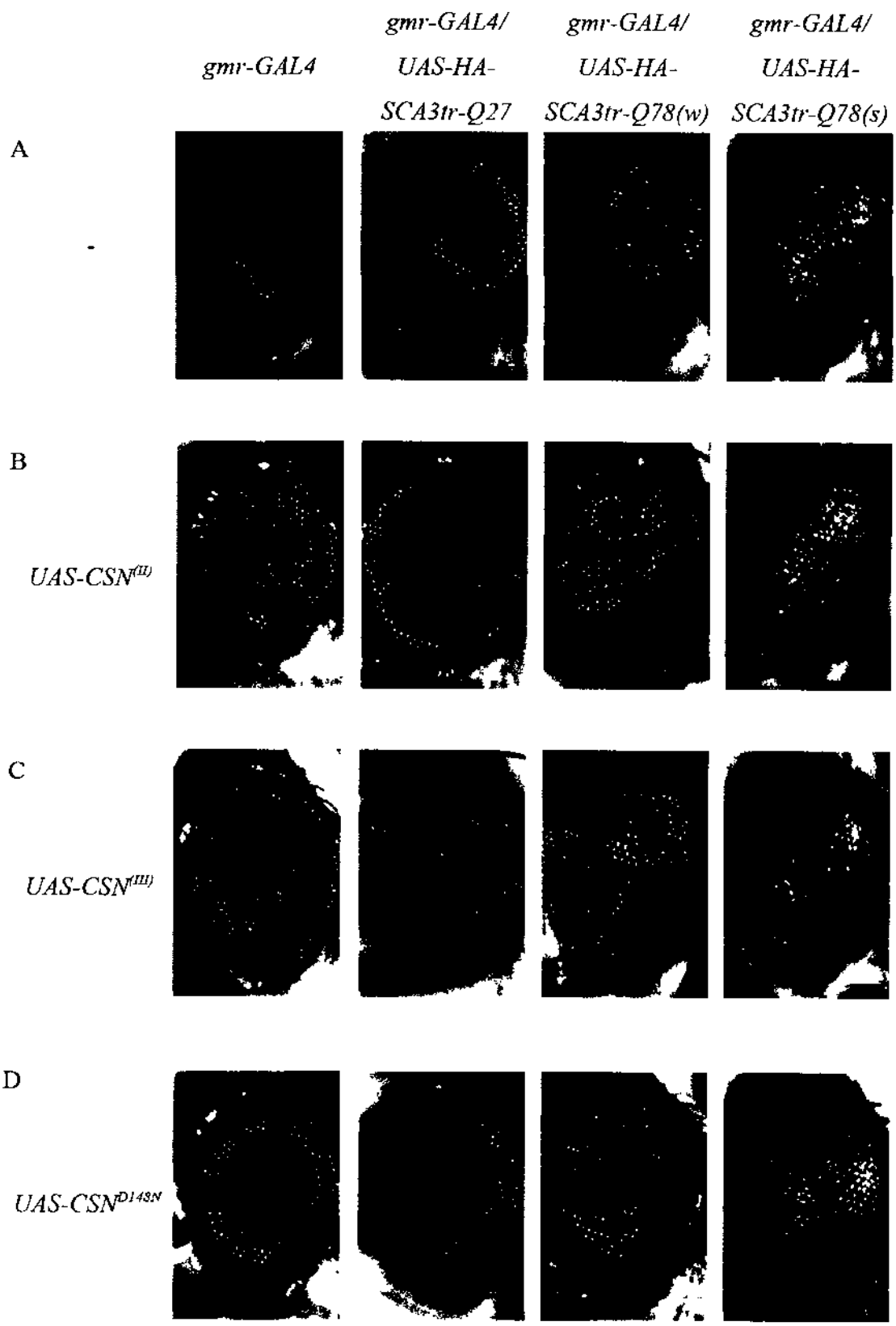
gmr-GAL4
gmr-GAL4/ UAS-HA-SCA3tr-Q27
gmr-GAL4/ UAS-HA-SCA3tr-Q78(w)
gmr-GAL4/ UAS-HA-SCA3tr-Q78(s)
A
B
UAS-CSN(II)
C
UAS-CSN(III)
D
UAS-CSND148N

Figure 5.8. Overexpression of *CSN5* did not modify degeneration induced by *HA-SCA3tr-Q78* expression in adult fly eyes.

Adult external eye depigmentation phenotypes of *gmr-GAL4* driver-only control flies and flies expressing *truncated ataxin-3* transgenes (*HA-SCA3tr-Q27* or *HA-SCA3tr-Q78)* with or without (indicated by "-") overexpression of wild-type or mutant *CSN5* are shown. Transgenes were expressed using the *gmr-GAL4* driver. **(A)** At 3 dpe, expression of *HA-SCA3tr-Q27* transgene did not cause any degenerative phenotype. Weak expression of *HA-SCA3tr-Q78* (*HA-SCA3tr-Q78(w)*) transgene did not cause any observable degenerative phenotype while strong expression of *HA-SCA3tr-Q78* (*HA-SCA3tr-Q78(s)*) transgene caused extensive loss of pigmentation. Overexpression of wild-type *CSN5* using neither *UAS-CSN5$^{(II)}$* transgenic line **(B)** nor *UAS-CSN5$^{(III)}$* transgenic line **(C)** modified degenerative phenotype induced by *HA-SCA3tr-Q78(w)* or *HA-SCA3tr-Q78(s)* expression. **(D)** Overexpression of dominant negative mutant *CSN5^{D148N}* did not modify degenerative phenotype induced by *HA-SCA3tr-Q78(w)* or *HA-SCA3tr-Q78(s)* expression. The experiment was performed once. The flies were raised at 25°C. They were of genotypes:

(A) *w*; *gmr-GAL4/+*; *+/+*,
w; *gmr-GAL4 UAS-HA-SCA3tr-Q27/+*; *+/+*,
w; *gmr-GAL4/+*; *UAS-HA-SCA3tr-Q78(w)/+*,
w; *gmr-GAL4 UAS-HA-SCA3tr-Q78(s)/+*; *+/+*
(B) *w*; *gmr-GAL4/UAS-CSN5$^{(II)}$*; *+/+*,
w; *gmr-GAL4 UAS-HA-SCA3tr-Q27/UAS-CSN5$^{(II)}$*; *+/+*,
w; *gmr-GAL4/UAS-CSN5$^{(II)}$*; *UAS-HA-SCA3tr-Q78(w)/+*,
w; *gmr-GAL4 UAS-HA-SCA3tr-Q78(s)/UAS-CSN5$^{(II)}$*; *+/+*
(C) *w*; *gmr-GAL4/+*; *UAS-CSN5$^{(III)}$/+*,
w; *gmr-GAL4 UAS-HA-SCA3tr-Q27/+*; *UAS-CSN5$^{(III)}$/+*,
w; *gmr-GAL4/+*; *UAS-HA-SCA3tr-Q78(w)/UAS-CSN5$^{(III)}$*,
w; *gmr-GAL4 UAS-HA-SCA3tr-Q78(s)/+*; *UAS-CSN5$^{(III)}$/+*
(D) *w*; *gmr-GAL4/UAS-CSN5^{D148N}*; *+/+*,
w; *gmr-GAL4 UAS-HA-SCA3tr-Q27/UAS-CSN5^{D148N}*; *+/+*,
w; *gmr-GAL4/UAS-CSN5^{D148N}*; *UAS-HA-SCA3tr-Q78(w)/+*,
w; *gmr-GAL4 UAS-HA-SCA3tr-Q78(s)/UAS-CSN5^{D148N}*; *+/+*.

Figure 5.9

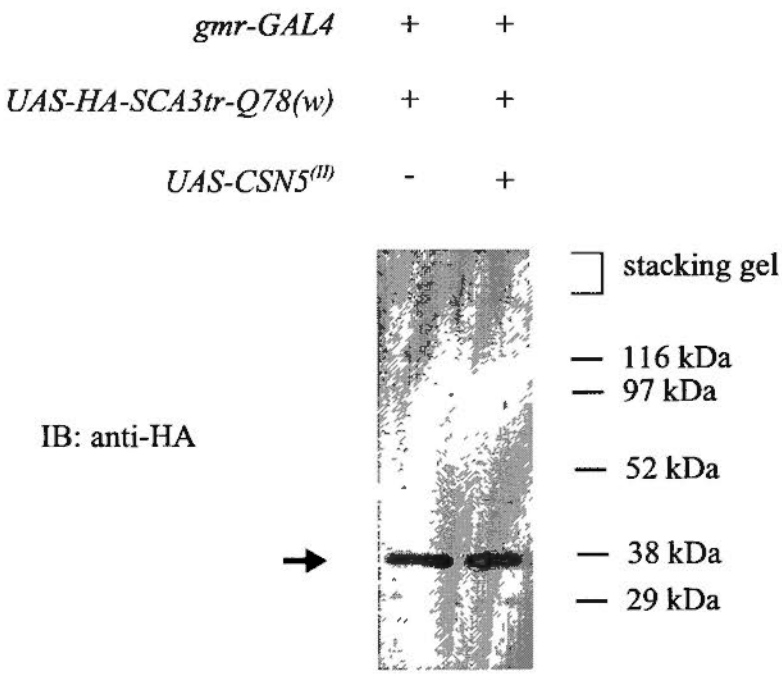
gmr-GAL4 + +
UAS-HA-SCA3tr-Q78(w) + +
UAS-CSN5(II) - +
IB: anti-HA
stacking gel
116 kDa
97 kDa
52 kDa
38 kDa
29 kDa

Figure 5.9. Overexpression of *CSN5* did not alter the SDS-solubility of HA-SCA3tr-Q78 protein.

Adult head lysate of *HA-SCA3tr-Q78(w)*-expressing flies with or without overexpression of wild-type *CSN5* was subjected to ultracentrifugation to isolate the SDS-insoluble protein aggregates and remove the SDS-soluble protein. The resulting pellet was treated with formic acid (100%) to solubilize the SDS-insoluble protein aggregates for subsequent immunoblotting. The immunoblot was probed with anti-HA antibody to detect the solubilized SDS-insoluble HA-SCA3tr-Q78 protein. The arrow (→) indicates the solubilized SDS-insoluble HA-SCA3tr-Q78 protein. Overexpression of wild-type *CNS5* did not alter the level of SDS-insoluble HA-SCA3tr-Q78 protein. The experiment was performed once. The flies were raised at 25°C and were assayed at 3 dpe. They were of genotypes:

w; *gmr-GAL4/+*; *UAS-HA-SCA3tr-Q78(w)/+*,

w; *gmr-GAL4/UAS-CSN5*$^{(II)}$; *UAS-HA-SCA3tr-Q78(w)/+*.

Several lines of evidence have suggested the involvement of *Roc1a*, *SkpA* and *Nedd8* in polyQ pathogenesis. From the RNAi screen performed by Mehta *et al.* (2009), it was found that *rbx1*, the worm homolog of *Roc1a*, and *skr1*, the worm homolog of *SkpA*, enhanced polyQ toxicity upon knock-down of expression in *C. elegans* [95]. Nedd8 was found in protein aggregates in various neurodegenerative diseases including polyQ disease [201]. Later, it was demonstrated *in vitro* by immunofluorescence analysis that Nedd8 interacted with the Josephin domain of ataxin-3 [202]. All these suggest that Roc1a, SkpA, Nedd8 and possibly other components of the CRL pathway such as CSN5 may affect polyQ pathogenesis.

To have a more complete analysis on the involvement of Cul1-based CRL pathway in polyQ pathogenesis, a preliminary study on the effect of *Roc1a*, *SkpA*, *Nedd8* and *CSN5* on polyQ toxicity and SDS-solubility of expanded polyQ protein was performed individually using the SCA3tr model [117]. It was found that none of the components of Cul1-based CRL pathway under investigation modified polyQ toxicity or SDS-solubility of expanded polyQ protein.

This finding seems to be contradictory to the speculation that Cul1-based CRL affects polyQ pathogenesis. However, two things have to be noted. Firstly, the difference in findings on *Roc1a* and *SkpA* from Mehta *et al.* (2009) and those from the present study may be due to the difference in polyQ model and the phenotype assays used. As discussed in Chapter 3 (section 3.10), Mehta *et al.* (2009) employed a *C. elegans* model expressing an YFP fused with 35 residues of glutamine [95]. Among the nine currently found polyQ diseases, 35 residues of glutamine are only

around the threshold for disease development [168]. The low number of glutamine repeats and the lack of an unexpanded control lead to query about whether the effect by *rbx1* and *skr1* is specific to expanded polyQ protein. Besides, the stringency and detection sensitivity between two studies may also be different and therefore make it difficult to compare directly. Secondly, the expression levels of the proteins under investigation were not confirmed in the present study. Therefore, confirmation of the expression levels of these proteins by methods such as semi-quantitative RT-PCR has to be performed before any conclusion can be made.

To sum up, the involvement of Roc1a, SkpA, Nedd8 and CSN5 in polyQ is not confirmed in this preliminary study.

Chapter 6 Effect of expanded polyglutamine protein on CRL activity

6.1 Introduction

As reviewed in Chapter 1 (section 1.1.4), expansion of the polyQ domain in the polyQ protein gives rise to a gain-of-function toxicity in polyQ diseases [38]. This gain-of-function toxicity negatively affects various cellular pathways including gene transcription, protein degradation and mitochondrion functioning [38, 168]. It is likely that polyQ protein interferes with CRL pathways and deregulates CRL activity upon expansion of the polyQ domain. To test this speculation, the effect of expanded polyQ protein on the accumulation of CRL specific substrates was examined (section 6.2). As neddylation is important for the activity of CRLs [83], the effect of expanded polyQ protein on neddylation of cullins was also studied using Cul1 as a model (section 6.3). The possible mechanisms behind and the consequences of the effect of expanded polyQ protein on CRL activity will be discussed as well (section 6.4).

6.2 Effect of polyQ expansion on the stability of CRL substrates

Under normal circumstances, CRL targets specific substrates for degradation [81]. Accumulation of CRL substrates implies impairment of CRL activity. To test the effect of expanded polyQ protein on CRL activity, CRL specific degron reporters previously prepared from our laboratory (unpublished data by C. C. Wu and H. Y. E. Chan, unpublished observations) were employed.

Degron refers to the protein degradation signal located at either the N- or C-terminus of a protein [203, 204]. It is responsible for the specific recognition by the specific E3 ubiquitin ligases [205]. Beta-catenin (β-cat) is a specific substrate of human Cul1-based CRL [206]. Its amino acid residues at positions 33 and 37 are essential for β-cat phosphorylation and subsequent recognition by Cul1-based CRL using Beta Transducin repeat containing protein (β-TrCP) as the substrate receptor [207]. A truncated form of β-cat carrying the first 73 amino acids was generated as the β-cat degron reporter (C. C. Wu and H. Y. E. Chan, unpublished observations). NF-E2-related factor-2 (Nrf2) is a specific substrate of human Cul3-based CRL with Kelch-like ECH-associated protein 1 (Keap1) substrate receptor [208]. Its Neh2 (Nrf2-ECH homology 2) domain was used as the Nrf2 degron reporter [209, 210] (C. C. Wu and H. Y. E. Chan, unpublished observations). c-Jun is a specific substrate of human Cul4A-based CRL with de-etiolated-1 substrate receptor [211]. Full-length c-Jun was used as the c-Jun degron reporter (C. C. Wu and H. Y. E. Chan, unpublished observations). A *myc* tag was added at the 5' end of these *degron reporter* transgenes for imrnunodetection. Normally, in cells transfected with these *degron reporter* transgenes, degron reporters translated are kept at low steady-state level as they are constitutively targeted by the corresponding CRLs for degradation (unpublished data by C. C. Wu and H. Y. E. Chan (2008)).

The effect of expanded polyQ protein on the accumulation of these degron reporters were examined using the eGFP-polyQ model [25] in HEK 293FT cells. This model has been described in Chapter 3 (section 3.5). It expresses an *eGFP* transgene fused to either an unexpanded *CAG*-repeat of 27 *CAGs* (*eGFP-Q27)* or an

expanded *CAG*-repeat of 75 *CAG*s (*eGFP-Q75).* This model recapitulates the aggregating property of expanded polyQ protein (Figure 3.18B). It was found that β-cat degron reporter accumulated when *β-cat degron reporter* transgene was co-transfected with *eGFP-Q75* transgene as compared to *eGFP-Q27* transgene (Figure 6.1). Similarly, there was an increased level of Nrf2 degron reporter when *Nrf2 degron reporter* transgene was co-transfected with *eGFP-Q75* transgene as compared to *eGFP-Q27* control (Figure 6.2). However, there was no observable difference in the level of c-Jun degron reporter when *c-Jun degron reporter* transgene was co-transfected with either *eGFP-Q27* or *eGFP-Q75* transgene (Figure 6.3). This suggests that expanded polyQ protein specifically induces accumulation of Cul1 and Cul3-based CRL substrates.

6.3 Effect of expanded polyQ protein on neddylation of Cul1

Nedd8 is a 6 kDa, ubiquitin-like protein [85]. Neddylation refers to the conjugation of Nedd8 on the neddylation substrate [85]. Cullins are the well-known neddylation substrates [212] . Neddylation of cullins promotes recruitment of ubiquitin-loaded E2s to the CRL complexes and is essential to the activity of CRLs [84, 212]. Wu *et al.* (2005) demonstrated that by performing immunoblotting on third-instar larvae lysate using antibodies against the unneddylated cullin, two bands with several kDa difference in molecular weight could be obtained [86]. The band with lower molecular weight represented the unneddylated cullin protein while the band with higher molecular weight represented the neddylated cullin protein.

Figure 6.1

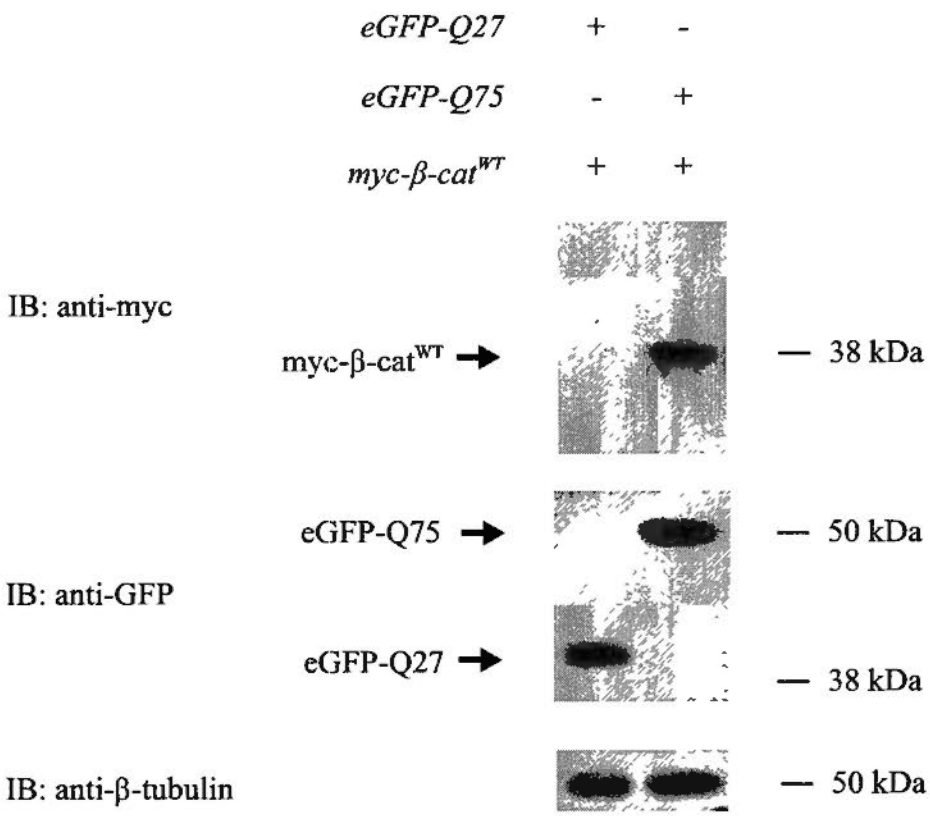
eGFP-Q27 + -
eGFP-Q75 - +
myc-β-cat^WT + +
IB: anti-myc
myc-β-cat^WT
— 38 kDa
eGFP-Q75
— 50 kDa
IB: anti-GFP
eGFP-Q27
— 38 kDa
IB: anti-β-tubulin
— 50 kDa

Figure 6.1. Expanded eGFP-polyQ protein induced accumulation of β-cat degron reporter in HEK 293FT cells.

Cells were transiently co-transfected with the constructs carrying the *β-cat degron reporter* transgene and *eGFP-Q27* or *eGFP-Q75*. At 96 hpt, cells were harvested and the lysate was subjected to immunoblotting. The immunoblot was probed against anti-myc antibody to detect the β-cat degron reporter. There was an increased level of β-cat degron reporter in cells co-transfected with *eGFP-Q75* transgene as compared to those co-transfected with *eGFP-Q27* transgene. The immunoblot was stripped and reprobed against anti-GFP antibody to confirm comparable expression level between the *eGFP-Q27* or *eGFP-Q75* transgene. The immunoblot was then stripped and reprobed with anti-β-tubulin antibody to confirm that equal amount of protein was loaded in every lane. The experiment was performed once.

Figure 6.2

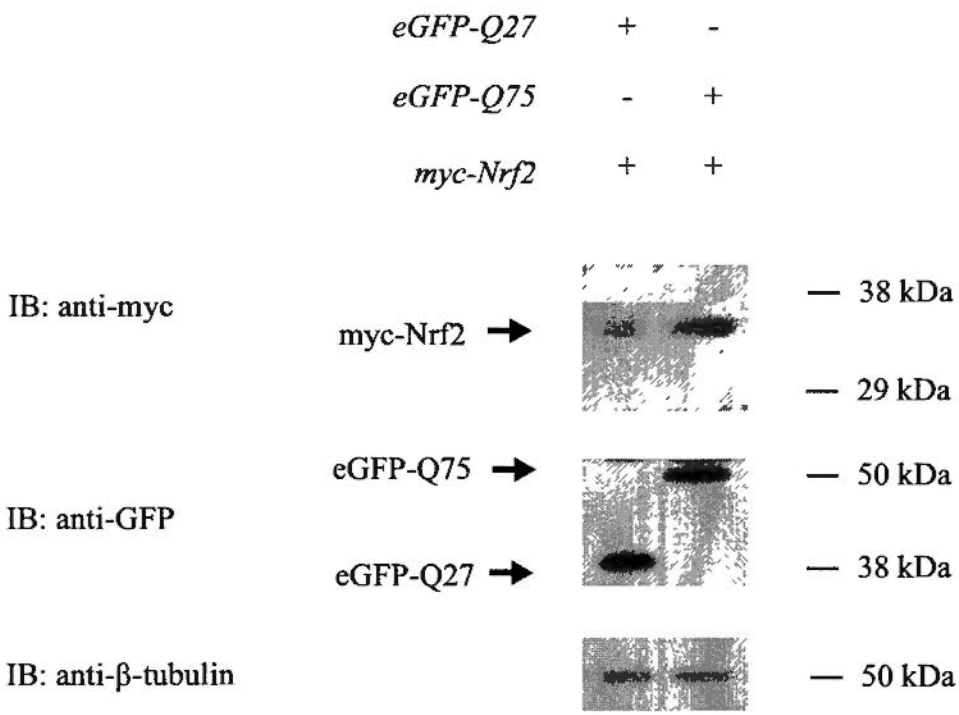
eGFP-Q27 + -
eGFP-Q75 - +
myc-Nrf2 + +
IB: anti-myc
myc-Nrf2
— 38 kDa
— 29 kDa
IB: anti-GFP
eGFP-Q75
eGFP-Q27
— 50 kDa
— 38 kDa
IB: anti-β-tubulin
— 50 kDa

Figure 6.2. Expanded eGFP-polyQ protein induced accumulation of Nrf2 degron reporter in HEK 293FT cells.

Cells were transiently co-transfected with the constructs carrying the *Nrf2 degron reporter* transgene and *eGFP-Q27* or *eGFP-Q75*. At 96 hpt, cells were harvested and the lysate was subjected to immunoblotting. The immunoblot was probed against anti-myc antibody to detect the Nrf2 degron reporter. There was an increased level of Nrf2 degron reporter in cells co-transfected with *eGFP-Q75* transgene as compared to those co-transfected with *eGFP-Q27* transgene. The immunoblot was stripped and reprobed against anti-GFP antibody to confirm comparable expression level between the *eGFP-Q27* or *eGFP-Q75* transgene. The immunoblot was then stripped and reprobed with anti-β-tubulin antibody to confirm that equal amount of protein was loaded in every lane. The experiment was performed once.

Figure 6.3

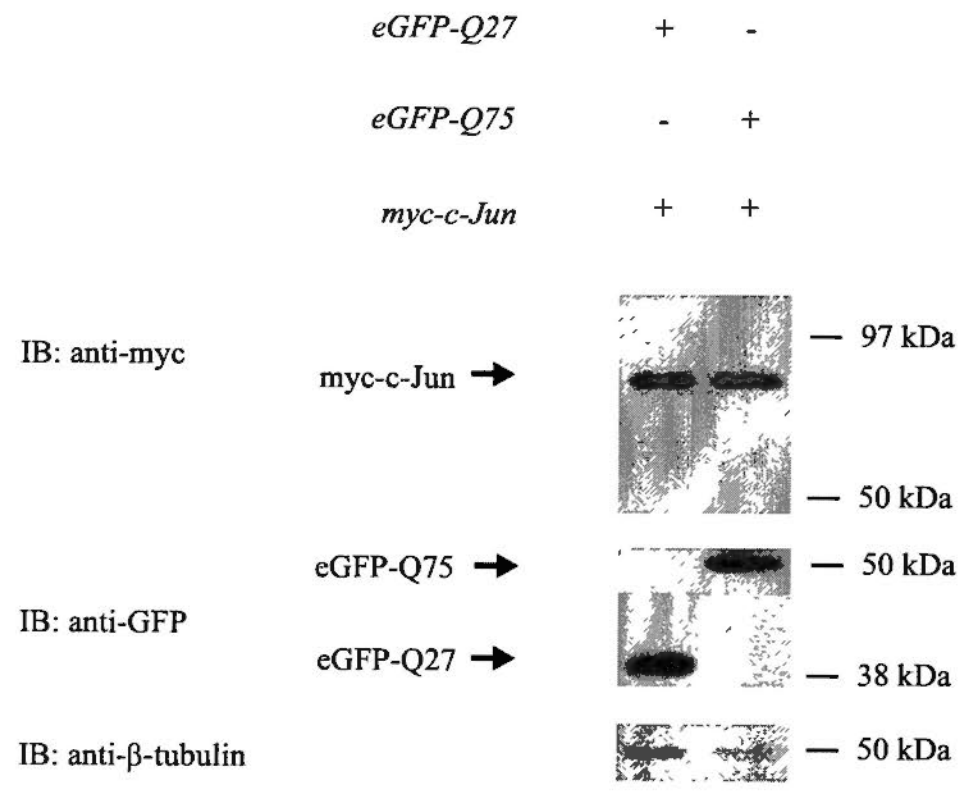
eGFP-Q27 + -
eGFP-Q75 - +
myc-c-Jun + +
IB: anti-myc
myc-c-Jun
97 kDa
50 kDa
eGFP-Q75
50 kDa
IB: anti-GFP
eGFP-Q27
38 kDa
IB: anti-β-tubulin
50 kDa

Figure 6.3. Expanded eGFP-polyQ protein did not alter the level of c-Jun degron reporter in HEK 293FT cells.

Cells were transiently co-transfected with the constructs carrying the *c-Jun degron reporter* transgene and *eGFP-Q27* or *eGFP-Q75*. At 96 hpt, cells were harvested and the lysate was subjected to immunoblotting. The immunoblot was probed against anti-myc antibody to detect the c-Jun degron reporter. The level of c-Jun degron reporter in cells co-transfected with *eGFP-Q75* transgene was similar to that in cells co-transfected with *eGFP-Q27* transgene. The immunoblot was stripped and reprobed against anti-GFP antibody to confirm comparable expression level between the *eGFP-Q27* or *eGFP-Q75* transgene. The immunoblot was then stripped and reprobed with anti-β-tubulin antibody to confirm that equal amount of protein was loaded in every lane. The experiment was performed once.

In the present study, the effect by expanded polyQ protein on neddylation of cullins using Cul1 as an example was examined in the SCA3fl transgenic *Drosophila* model [129]. As described in Chapter 3 (section 3.3), in this model a *myc*-tagged, full-length *ataxin-3* transgene with either an unexpanded *CAG*-repeat of 27 *CAG*s (*myc-SCA3fl-Q27*) or an expanded *CAG*-repeat of 84 *CAG*s (*myc-SCA3fl-Q84*) was expressed. By performing immunoblotting on adult fly head lysate in flies expressing *myc-SCA3fl-Q27* transgene, two bands with several kDa difference in molecular weight were obtained in the running gel upon immunodetection using anti-Cul1 antibody (Figure 6.4). The lower band represents the unneddylated Cul1 while the upper band represents the neddylated Cul1 [86]. As compared to the *myc-SCA3fl-Q27*-expressing flies, the level of neddylated Cul1 was reduced in flies expressing *myc-SCA3fl-Q84* transgene (Figure 6.4).

To test if neddylated Cul1 was recruited to the SDS-insoluble myc-SCA3fl-Q84 protein aggregates, the adult fly head lysate was treated with formic acid (100%) to solubilize the SDS-insoluble myc-SCA3fl-Q84 protein aggregates into monomers [151] and to release any cellular proteins originally recruited to the aggregates [25]. The sample treated with buffer only (0% formic acid control) and that treated with formic acid (100%) were subjected to immunoblotting (Figure 6.5). Comparing to the buffer-treated control, there was an increased level of monomeric myc-SCA3fl-Q84 protein in the formic acid (100%)-treated sample (Figure 6.5). This indicates successful solubilization of SDS-insoluble protein aggregates upon formic acid (100%) treatment. However, there was no increase in the level of neddylated Cul1 in the running gel after formic acid (100%) treatment. This suggests

Figure 6.4

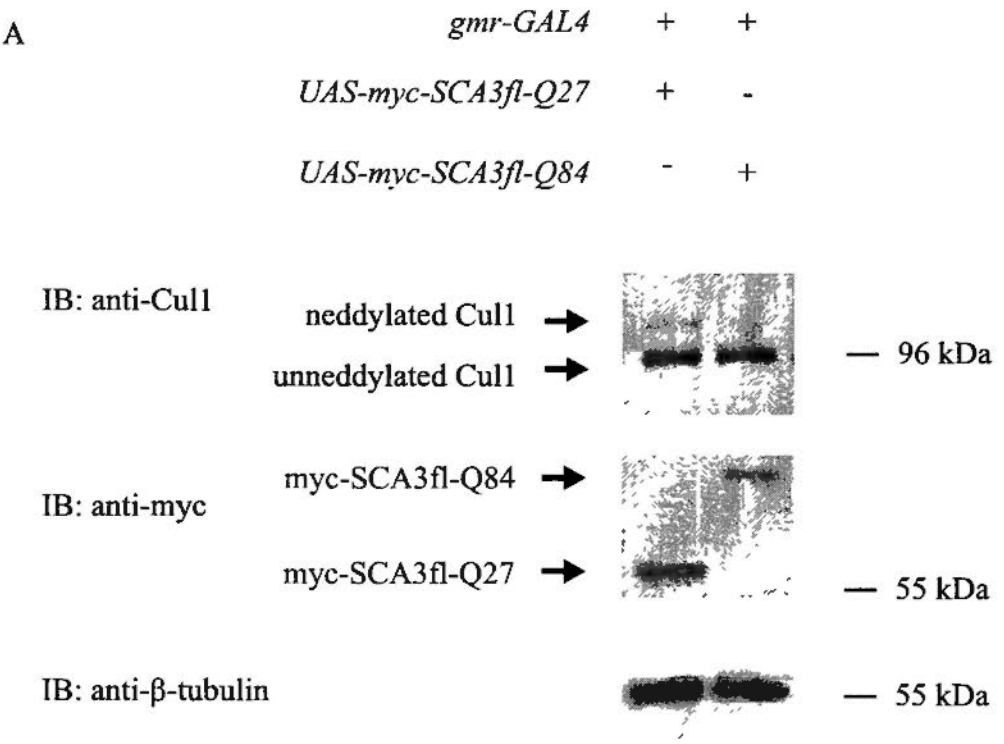
A
gmr-GAL4 + +
UAS-myc-SCA3fl-Q27 + -
UAS-myc-SCA3fl-Q84 - +
IB: anti-Cul1
neddylated Cul1
unneddylated Cul1
— 96 kDa
IB: anti-myc
myc-SCA3fl-Q84
myc-SCA3fl-Q27
— 55 kDa
IB: anti-β-tubulin
— 55 kDa

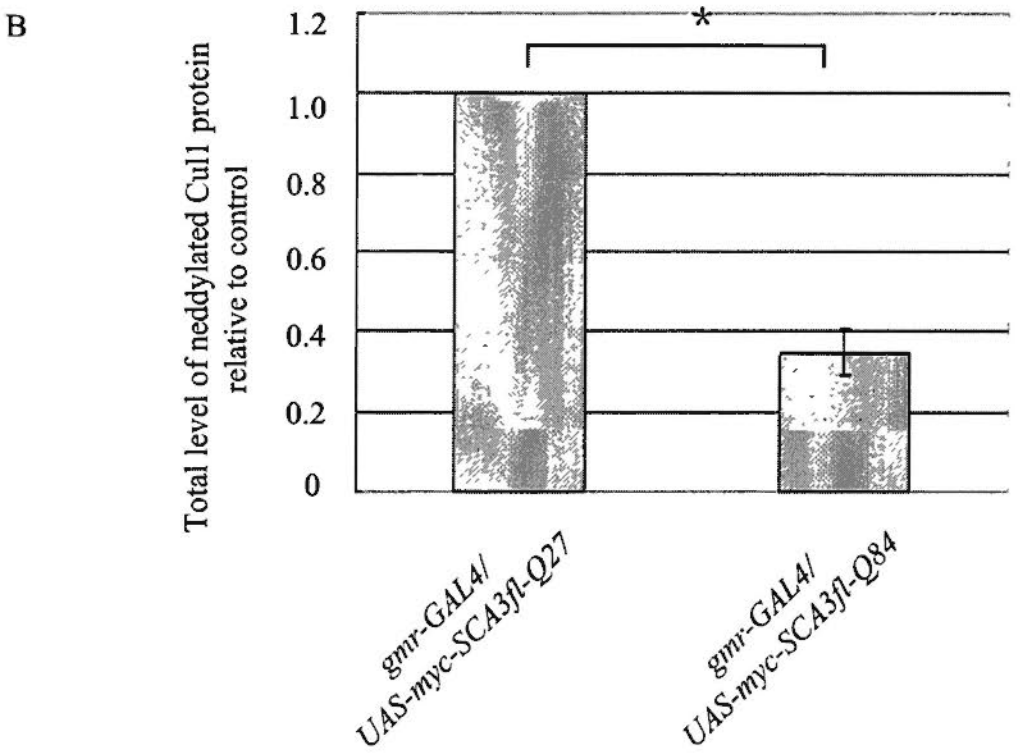
B
Total level of neddylated Cul1 protein relative to control
1.2
1.0
0.8
0.6
0.4
0.2
0
*
gmr-GAL4/ UAS-myc-SCA3fl-Q27
gmr-GAL4/ UAS-myc-SCA3fl-Q84

Figure 6.4. Expanded full-length ataxin-3 protein reduced level of neddylated Cul1.

Adult head lysate of flies expressing *myc-SCA3fl-Q27* or *myc-SCA3fl-Q84* transgene by *gmr-GAL4* driver was subjected to immunoblotting. The immunoblot was probed with anti-Cul1 antibody to detect the Cul1 protein (both the unneddylated form and the neddylated form). The lower band represents the unneddylated Cul1 while the upper band represents the neddylated Cul1. In flies expressing *myc-SCA3fl-Q84* transgene, there was a reduced level of neddylated Cul1 protein in the running gel as compared to the *myc-SCA3fl-Q27*-expressing flies. The immunoblot was stripped and reprobed with anti-myc antibody to confirm the presence of myc-SCA3fl-Q27 and myc-SCA3fl-Q84 proteins. The immunoblot was then stripped and reprobed with anti-β-tubulin antibody to confirm that equal amount of protein was loaded in every lane. (**B**) Quantification of the upper band (for neddylated Cul1) of (**A**). Band intensity was relative to the upper band from *myc-SCA3fl-Q27*-expressing flies. N = 4, $p < 0.05$ (Student's t-test); error bar represents mean ± SEM from four independent experiments. The flies were raised at 21°C and were assayed at 3 dpe. They were of genotypes:

w; *gmr-GAL4 UAS-myc-SCA3fl-Q27*/+; +/+,

w; *gmr-GAL4*/+; *UAS-myc-SCA3fl-Q84*/+.

Figure 6.5

A

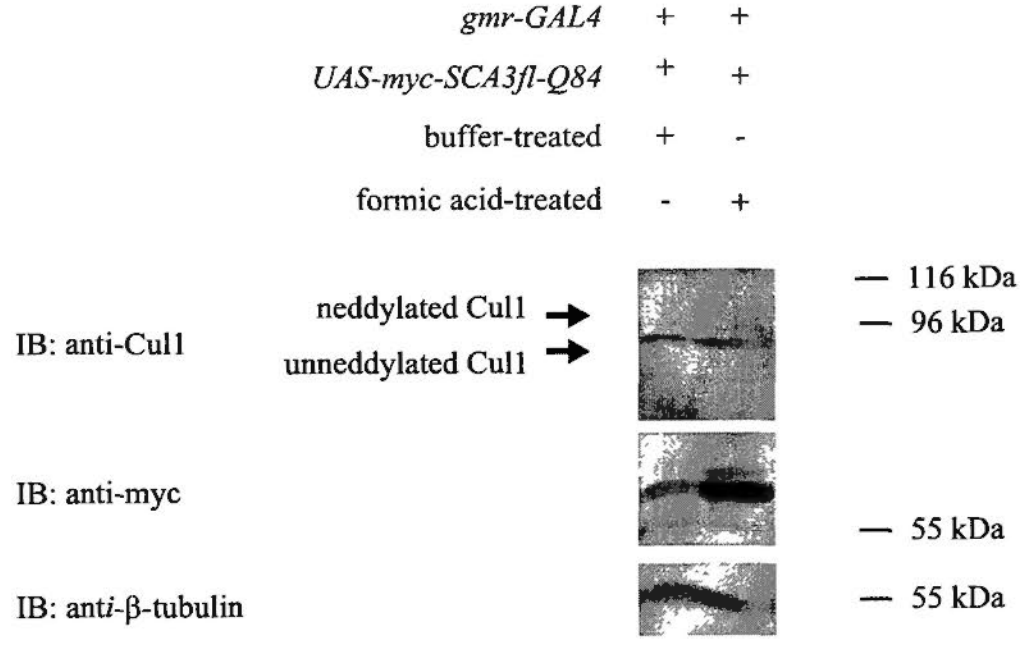
gmr-GAL4 + +
UAS-myc-SCA3fl-Q84 + +
buffer-treated + -
formic acid-treated - +
IB: anti-Cul1
neddylated Cul1
unneddylated Cul1
116 kDa
96 kDa
IB: anti-myc
55 kDa
IB: anti-β-tubulin
55 kDa

B

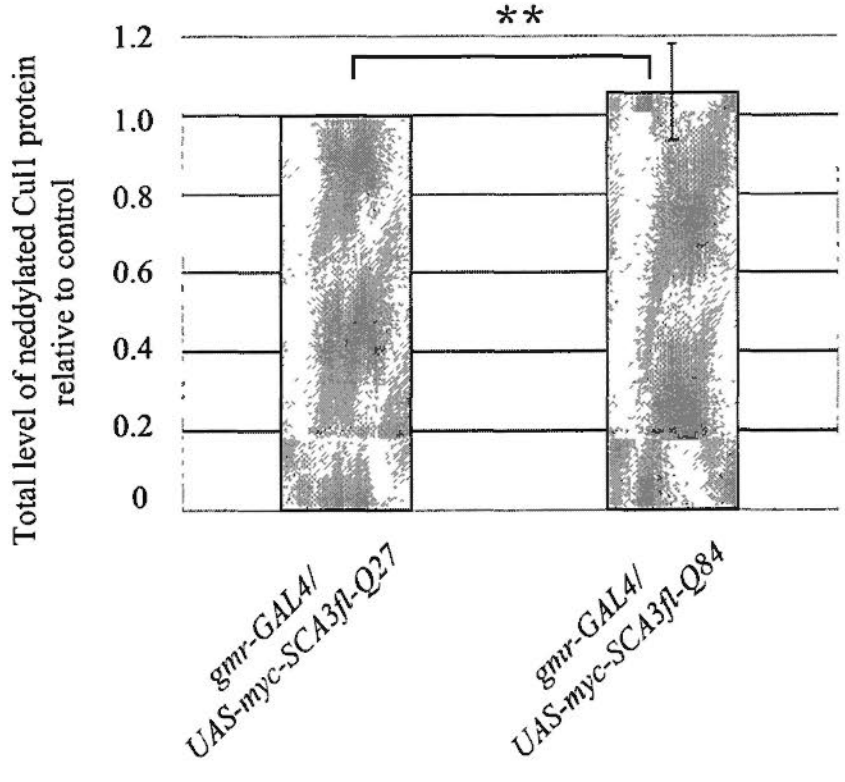
**
Total level of neddylated Cul1 protein relative to control
1.2
1.0
0.8
0.6
0.4
0.2
0
gmr-GAL4/ UAS-myc-SCA3fl-Q27
gmr-GAL4/ UAS-myc-SCA3fl-Q84

Figure 6.5. Neddylated Cul1 was not recruited to the SDS-insoluble expanded full-length ataxin-3 protein aggregates.

Adult head lysate of flies expressing *myc-SCA3fl-Q84* transgene by *gmr-GAL4* driver was treated with buffer only or formic acid (100%) to solubilize the protein aggregates and to release any recruited cellular proteins in the SDS-insoluble aggregates. The sample was then subjected to immunoblotting. The immunoblot was probed with anti-Cul1 antibody to detect the Cul1 protein (both the unneddylated form and the neddylated form). The lower band represents the unneddylated Cul1 while the upper band represents the neddylated Cul1. There was no significant difference in the level of neddylated Cul1 protein in the running gel between the buffer-treated control and the formic acid-treated sample. The immunoblot was stripped and reprobed with anti-myc antibody to confirm successful solubilization of myc-SCA3fl-Q84 protein aggregates as indicated by the increase in the level of monomeric myc-SCA3fl-Q84 protein upon formic acid treatment. The immunoblot was then stripped and reprobed with anti-β-tubulin antibody to confirm that equal amount of protein was loaded in every lane. (**B**) Quantification of the upper band (for neddylated Cul1) of (**A**). Band intensity was relative to the upper band of the buffer-treated control. N = 3, $p = 0.74$ (Student's t-test); error bar represents mean ± SEM from three independent experiments. The flies were raised at 21°C and were assayed at 3 dpe. They were of genotype:

w; *gmr-GAL4/+*; *UAS-myc-SCA3fl-Q84/+*.

that neddylated Cul1 is not recruited to the SDS-insoluble myc-SCA3fl-Q84 protein aggregates.

Taken together, these data suggest that polyQ protein reduces neddylation of Cul1 upon expansion of polyQ domain. The reduction in the level of neddylated Cul1 is not likely to be due to the recruitment of neddylated Cul1 to the expanded polyQ protein aggregates.

6.4 Discussion

As reviewed in Chapter 1 (section 1.1.4), expanded polyQ protein interferes with various cellular pathways [38]. In this chapter, the effect of expanded polyQ protein on CRL activity was investigated.

Accumulation of CRL substrates is an indication of impairment of CRL activity [159, 213, 214]. In the present study using the eGFP-polyQ model [25] in HEK 293FT cells, it was found that upon expansion of polyQ domain, polyQ protein induced accumulation of β-cat (Figure 6.1) and Nrf2 degron reporters (Figure 6.2) but not c-Jun degron reporter (Figure 6.3). This result is consistent to a previous study in our laboratory using another polyQ model, the truncated SCA3 (SCA3tr) model, in HEK 293FT cells (C. C. Wu and H. Y. E. Chan, unpublished observations). It was reported that expression of a *FLAG*-tagged, *truncated ataxin-3* transgene with an expanded *CAG*-repeat of 76 *CAG*s caused accumulation of β-cat and Nrf2 degron reporters, but not c-Jun degron reporter, as compared to the unexpanded control with 27 *CAG*s (C. C. Wu and H. Y. E. Chan, unpublished observations). β-cat, Nrf2 and

c-Jun degron reporters are the specific degron reporters of Cul1-, Cul3- and Cul4-based CRLs respectively. This suggests that expanded polyQ protein specifically impairs activity of Cul1- and Cul3 based CRLs.

One way expanded polyQ protein may impair CRL activity is through deregulating neddylation of cullins. Neddylation refers to the conjugation of Nedd8 to the neddylation substrate [215]. Similar to ubiquitination, neddylation requires E1, E2 and E3 [83, 215, 216]: APP-BP-1/ Uba3 heterodimeric E1 activates Nedd8 [216]; Ubc12 E2 conjugates Nedd8 to the cullin [216]; DCN1 and Roc1 act as a multi-subunit E3 that facilitates loading of Nedd8-loaded Ubc12 to the cullin for neddylation [217-220]. Upon neddylation, Nedd8 interacts with ubiquitin-loaded E2 and thus recruits E2 to the CRL complex upon conjugation to the cullin [221, 222]. It was demonstrated that neddylation of cullin promoted CRL activity *in vitro* [223-226] and were essential to the function of CRLs in fission yeast and several metazoan species *in vivo* [173, 227-230]. As reviewed in Chapter 1 (section 1.5), neddylation is reversed by a process called "deneddylation" through the isopeptidase activity of CSN5 [86, 92].

In the present study, it was found that ataxin-3 reduced the level of neddylated Cul1 upon expansion of the polyQ domain (Figure 6.4). This reduction in the level of neddylated Cul1 was not likely to be due to the recruitment of neddylated Cul1 to expanded ataxin-3 protein aggregates (Figure 6.5). Previously, it was reported that Nedd8 co-localized with protein aggregates in a number of neurodegenerative diseases including polyQ diseases such as SCA3 [201]. In addition, it was

demonstrated that Nedd8 interacted with the Josephin domain of ataxin-3 [202]. This may contribute to an active targeting of Nedd8 to ataxin-3 aggregates in SCA3. It is possible that ataxin-3 protein recruits Nedd8 to the protein aggregates upon expansion of polyQ domain which subsequently reduces the level of free Nedd8 for conjugation to Cul1 in cells.

In addition to limiting the level of free Nedd8 in cells, expanded polyQ protein may interfere with the components in the neddylation and deneddylation pathways by unknown mechanisms and thus hinder Cul1 neddylation. As neddylation is essential to Cul1-based CRL activity [227, 228], reducing Cul1 neddylation would inhibit Cul1-based CRL activity and lead to accumulation of Cul1-based CRL substrates.

Cul4 is also a neddylation substrate. Neddylation and deneddylation pathways are similar in Cul4 as well [83, 84, 173]. The finding that expanded polyQ protein did not modify the level of Cul4-based CRL specific degron reporter implies that reduction in cullin neddylation by expanded polyQ protein *per se* is not sufficient to impair CRL activity. It is therefore likely that expanded polyQ deregulates CRL activity, at least in the case of Cul1-based CRL, through other concerted unknown mechanisms in addition to reducing cullin neddylation. Recently, it was reported that polyQ domain-expanded huntingtin protein induced accumulation of β-cat, a specific substrate of Cul1-based CRL, through reducing the association between β-cat and its corresponding substrate receptor, β-TrCP [231]. This interference on association between β-cat and β-TrCP may be a general effect by expanded polyQ protein and

may apply to β-cat degron reporter used in the present study as well. Different types of CRLs employ different adaptor proteins and substrate receptors [81]. Expanded polyQ protein may recruit specific adaptor proteins or substrate receptors of Cul1- and Cul3-based CRLs, but not those of Cul4-based CRL, to the aggregate and therefore specifically affect the activity of Cul1- and Cul3-based CRL.

The impairment of the activity of Cul1- and Cul3-based CRLs could exert negative impacts on cells. Cul1- and Cul3-based CRLs regulate degradation of a number of important effectors in various cellular pathways from DNA replication, cell cycle, signal transduction to development [81, 179]. The impairment of the activity of Cul1- and Cul3-based CRLs would imbalance these pathways and result in cytotoxicity. It was reported that expanded huntingtin protein induced accumulation of β-cat in neurons. This accumulation was neurotoxic while reducing β-cat level suppressed the toxic phenotype [231].

To sum up, the above data suggest that expanded polyQ protein may impair the activity of Cul1- and Cul3-based CRLs through reducing neddylation of cullins and other unknown mechanisms. The impairment of the activity of Cul1- and Cul3-based CRLs would eventually lead to neurotoxicity.

Chapter 7 Distinct effects of ubiquitin on polyglutamine diseases and Parkinson's disease toxicity

7.1 Introduction

Polyglutamine diseases and a number of other neurodegenerative diseases, including PD, are collectively called protein misfolding diseases as they are caused by misfolding and aggregation of the corresponding disease proteins [10, 53, 232-235]. In protein misfolding diseases, protein quality control by UPS-mediated degradation is of utmost importance to the cell homeostasis [59, 236, 237]. In UPS, E3 ubiquitin ligases target specific substrate proteins for ubiquitin conjugation [160, 238, 239]. Ubiquitinated substrates are then recognized by the proteasome for degradation [160, 238, 239]. Ubiquitin and other UPS components are commonly found in protein aggregates of polyQ diseases and PD in both experimental disease models and patient tissues [59, 240, 241]. This suggests that UPS is associated with the pathogenesis of polyQ diseases and PD.

In previous chapters, the role of a type of E3 ubiquitin ligases called CRLs in polyQ diseases was investigated (Chapters 3-5). The possible involvement of CRLs in PD was also tested (Figure 3.12). In this chapter, the roles of ubiquitin in PD (section 7.2) and polyQ diseases (section 7.3) were examined, and the differential roles of ubiquitin in PD and polyQ diseases will be discussed (section 7.4).

7.2 Effect of *ubiquitin* overexpression on Parkinson's disease

Presence of intraneuronal protein aggregates designated as Lewy bodies and

selective degeneration of DA neurons in substantial nigra par compacta are the hallmarks of PD [242, 243]. Lewy bodies are composed of α-synuclein and many other cellular proteins [149]. Various animal models have been used to study *α-synuclein*-induced toxicity in PD [244]. In *Drosophila* model of PD, it was demonstrated that expression of *α-synuclein*^{WT} induced toxicity that resulted in PD-like symptoms such as deposition of α-synuclein aggregates and degeneration of DA neurons [245].

In the present study, the effect of overexpressing *ubiquitin* on *α-synuclein*^{WT}-induced toxicity was examined using a transgene encoding for a HA-tagged, wild-type ubiquitin (HA-Ub^{WT}). The expression of *HA-Ub*^{WT} transgene was confirmed by immunoblotting (Figure 7.1). In deep pseudopupil assay, expression of a transgene encoding for human α-synuclein^{WT} in the fly eyes by *gmr-GAL4* driver induced retinal degeneration. On average, only 2 rhabdomeres per ommatidium could be observed (Figure 7.2A). Expression of *HA-Ub*^{WT} transgene suppressed the degeneration induced by *α-synuclein*^{WT} expression and raised the number of rhabdomeres per ommatidium to about 3 (an average of 2.9; Figure 7.2B). This shows that increasing cellular level of ubiquitin mitigates *α-synuclein*^{WT}-induced toxicity.

To test if proteasome was involved in the suppression on *α-synuclein*^{WT}-induced toxicity by expression of *HA-Ub*^{WT} transgene, a dominant negative proteasome mutant termed *Pros26*^{1} was employed [246]. In *Pros26*^{1} mutant, there is a missense mutation in the 20S proteasome subunit β6 [246]. Genetic and biochemical studies have demonstrated that this mutation interferes with proteasome function in a dominant

Figure 7.1

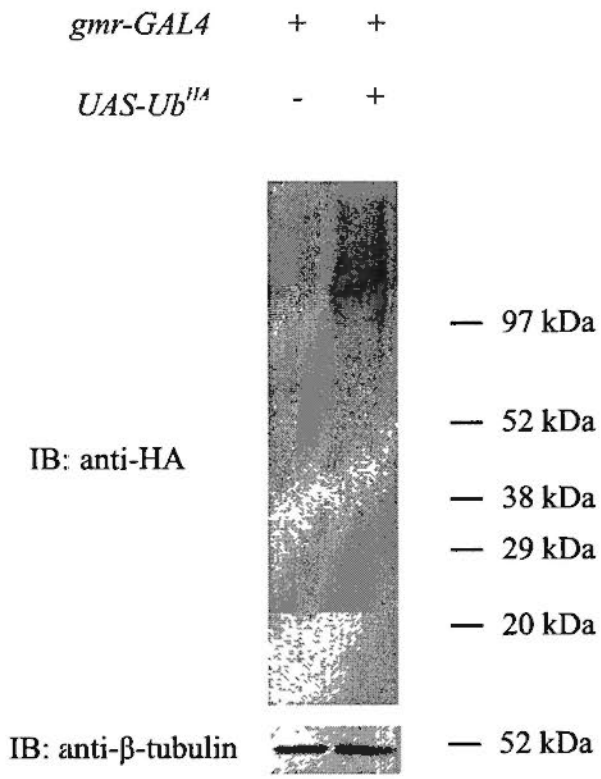
gmr-GAL4 + +
UAS-Ub^HA - +
IB: anti-HA
IB: anti-β-tubulin
97 kDa
52 kDa
38 kDa
29 kDa
20 kDa
52 kDa

Figure 7.1. Expression of *HA-Ub^{WT}* transgene.

Adult head lysate of *gmr-GAL4* driver control flies and flies expressing *HA-Ub^{WT}* transgene by *gmr-GAL4* driver was subjected to immunoblotting. The immunoblot was probed with anti-HA antibody to detect the HA-Ub^{WT} protein. The immunoblot was then stripped and reprobed with anti-β-tubulin antibody to confirm that equal amount of protein was loaded onto every lane. The experiment was performed once. The flies were raised at 25°C and were assayed at 3 dpe. They were of genotypes:

w; *gmr-GAL4*/+; +/+,

w; *gmr-GAL4*/+; *UAS-HA-Ub^{WT}*/+.

Figure 7.2

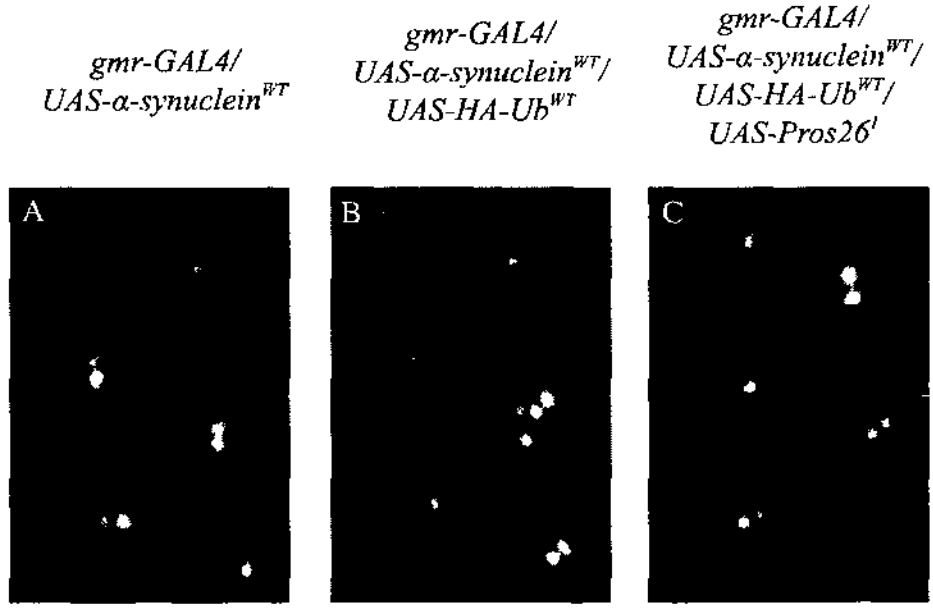
gmr-GAL4/ UAS-α-synuclein^WT
gmr-GAL4/ UAS-α-synuclein^WT/ UAS-HA-Ub^WT
gmr-GAL4/ UAS-α-synuclein^WT/ UAS-HA-Ub^WT/ UAS-Pros26^1
A
B
C

D

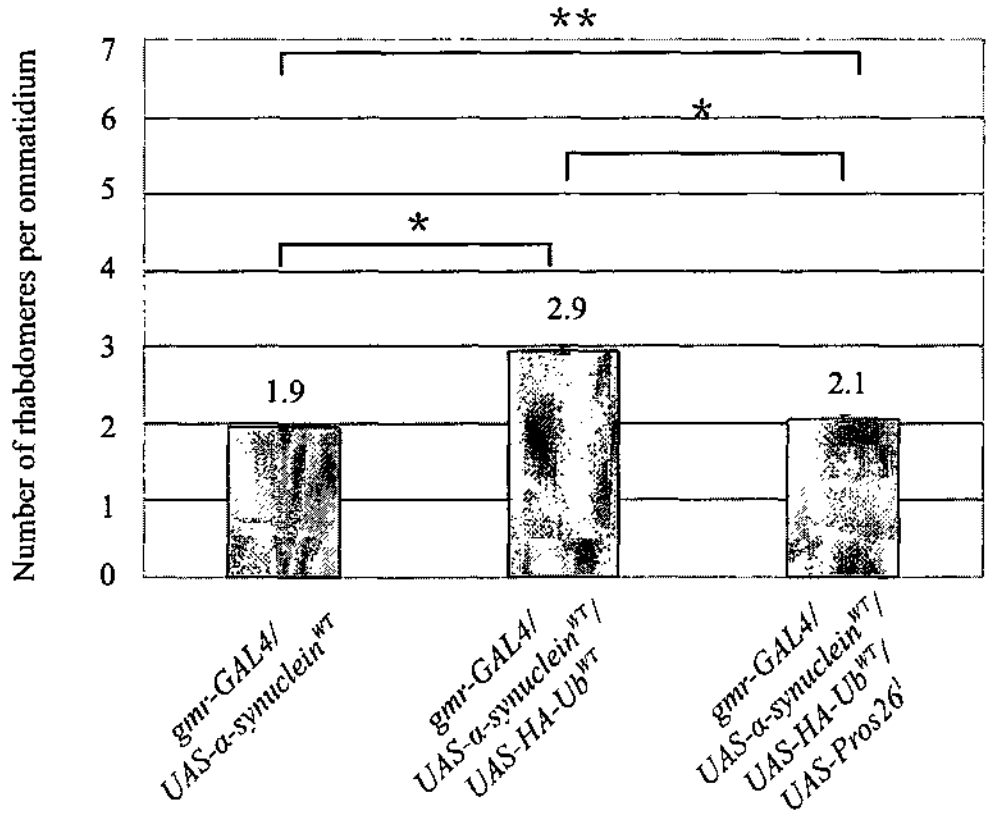
Number of rhabdomeres per ommatidium
0
1
2
3
4
5
6
7
**
*
*
1.9
2.9
2.1
gmr-GAL4/ UAS-α-synuclein^WT
gmr-GAL4/ UAS-α-synuclein^WT/ UAS-HA-Ub^WT
gmr-GAL4/ UAS-α-synuclein^WT/ UAS-HA-Ub^WT/ UAS-Pros26^1

Figure 7.2. Expression of *HA-Ub^{WT}* transgene suppressed *α-synuclein^{WT}*-induced retinal degeneration in adult flies.

(**A** - **C**) Deep pseudopupil images of *α-synuclein^{WT}*-expressing flies are shown. On average, 1.9 rhabdomeres per ommatidium were observed under microscope (**A**). Expression of *HA-Ub^{WT}* transgene in *α-synuclein^{WT}*-expressing flies increased the rhabdomere score to an average of 2.9 (**B**). Additional expression of *Pros26^{1}* transgene reduced the above rhabdomere score to an average of 2.1 (**C**). Transgenes were expressed using the *gmr-GAL4* driver. (**D**) Quantification of (**A** - **C**). N = 22, * $p < 0.05$ while ** $p = 1.94$ (Mann-Whitney Rank Sum Test); error bars represent mean ± SEM from at least 22 flies collected from three independent experiments. At least 330 ommatidia were scored per group. The flies were raised at 25°C and were assayed at 2 dpe. They were of genotypes:

w; *gmr-GAL4/+*; *UAS-α-synuclein^{WT}/+*,

w; *gmr-GAL4/+*; *UAS-α-synuclein^{WT}/UAS-HA-Ub^{WT}*,

w; *gmr-GAL4/UAS-Pros26^{1}*; *UAS-α-synuclein^{WT}/UAS-HA-Ub^{WT}*.

negative manner [247-249]. It was found that expression of *Pros26*^{1} transgene in *α-synuclein*^{WT}-expressing flies with *HA-Ub*^{WT} expression abolished the suppression of *α-synuclein*^{WT}-induced toxicity upon expressing *HA-Ub*^{WT} transgene and reduced the rhabdomere score to back to 2 (an average of 2.1; Figure 7.2C). This implies that normal functioning of proteasome is essential for the suppressive effect conferred by ubiquitin overexpression against *α-synuclein*^{WT}-induced toxicity.

The effect of *HA-Ub*^{WT} expression on *α-synuclein*^{WT}-induced toxicity was double confirmed by examination of DA neurons in DM1 clusters in fly brains. By directing the expression of a transgene encoding for eGFP in DA neurons using the *ddc-GAL4* driver, the number of DA neurons could be counted upon whole-mount dissection of the adult fly brain and subsequent confocal microscopic observation. It was found that on average, there were 14 DA neurons in *ddc-GAL4* driver control flies (Figure 7.3A and B). Expression of *α-synuclein*^{WT} transgene induced DA degeneration and reduced the number of DA neurons to around 10 (an average of 9.5; Figure 7.3C). Expression of *HA-Ub*^{WT} transgene suppressed the neurodegeneration induced by *α-synuclein*^{WT} expression and restored the number of DA neurons to nearly 14 (an average of 13.5; Figure 7.3D). This confirms that ubiquitin overexpression helps mitigates *α-synuclein*^{WT}-induced toxicity.

Notably, in collaboration with Dr. K. K. K. Chung's laboratory (Department of Biochemistry, Hong Kong University of Science and Technology), it was found that the expression level of *α-synuclein*^{WT} was not affected by co-expression of *HA-Ub*^{WT} transgene [130]. This indicates that the suppressive effect by enhancing

Figure 7 3

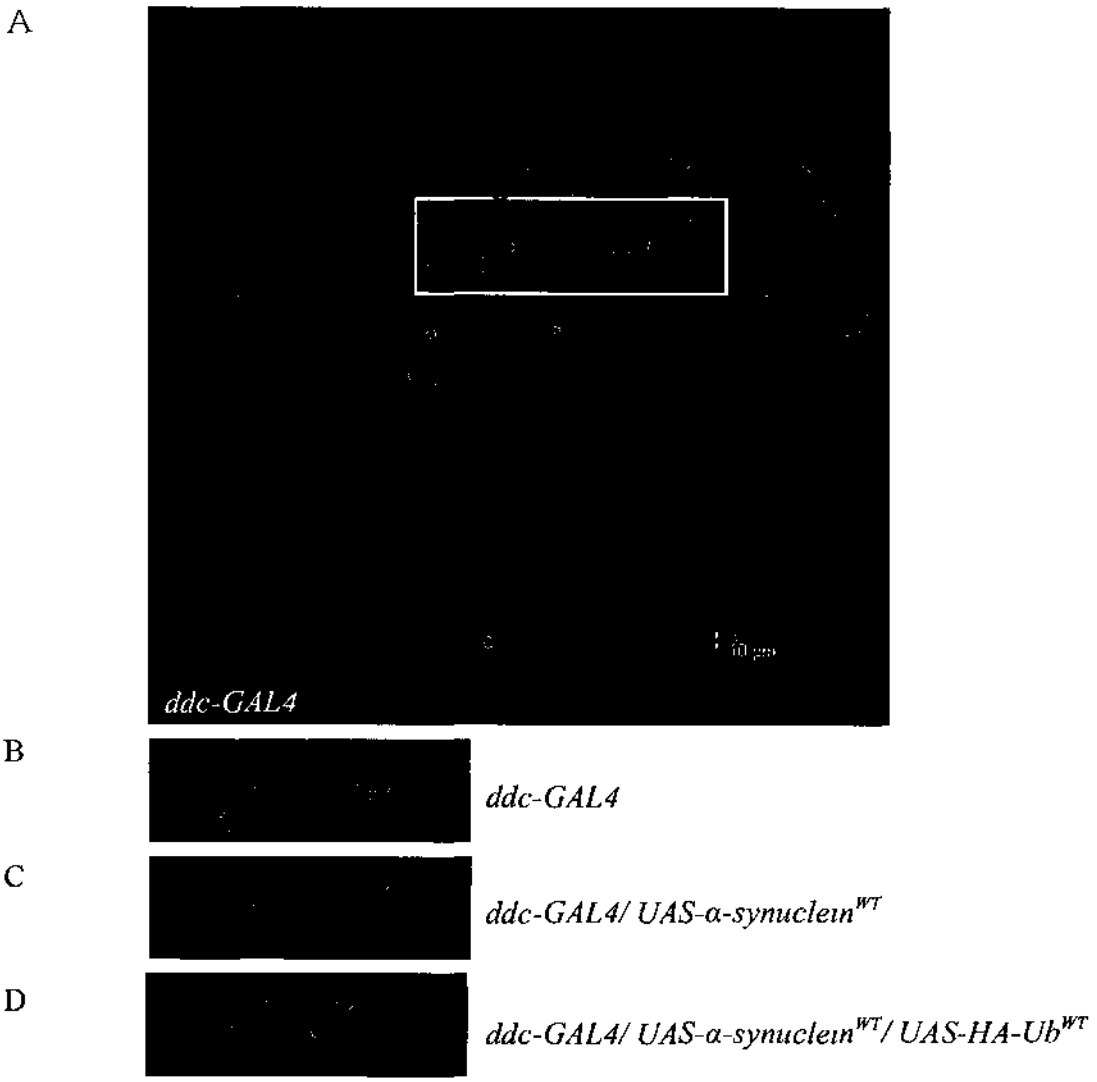
A
ddc-GAL4
B
ddc-GAL4
C
ddc-GAL4/ UAS-α-synuclein^WT
D
ddc-GAL4/ UAS-α-synuclein^WT/ UAS-HA-Ub^WT
E
Number of DA neurons in DM1 clusters
16
12
8
4
0
*
*
ddc-GAL4
ddc-GAL4/ UAS-α-synuclein^WT
ddc-GAL4/ UAS-α-synuclein^WT / UAS-HA-Ub^WT

Figure 7.3. Expression of *HA-Ub^{WT}* transgene suppressed *α-synuclein^{WT}*-induced DA neurons degeneration in adult flies.

(**A** - **D**) Confocal images of whole-mount adult brains of flies with eGFP-positive DA neurons are shown. White rectangle encircles the DM1 clusters. On average, 14 DA neurons were observed in *ddc-GAL4* driver control flies (**A** and **B**). Expression of *α-synuclein^{WT}* transgene reduced the number of DA neurons to an average of 9.5 (**C**). Co-expression with *HA-Ub^{WT}* transgene in *α-synuclein^{WT}*-expressing flies restored the above number of DA neurons to an average of 13.5 (**D**). Scale bar in (**A**) indicates a distance of 10 μm. All images are of the same magnification. (**E**) Quantification of (**B** - **C**). N = 3, * $p < 0.01$ (Student *t*-test); error bars represent mean ± SEM from three independent experiments. At least 5 brains were scored per genotype per experiment. The flies were raised at 25°C and were assayed at 25 dpe. They were of genotypes:

(**A** and **B**) *w*; *ddc-GAL4/+*; *+/+*,

(**C**) *w*; *ddc-GAL4/+*; *UAS-α-synuclein^{WT}/+*,

(**D**) *w*; *ddc-GAL4/+*; *UAS-α-synuclein^{WT}/UAS-HA-Ub^{WT}*.

ubiquitin level is not due to any modification on the protein level of α-synuclein.

7.3 Effect of *ubiquitin* overexpression on polyglutamine diseases

The adult external eye depigmentation phenotype assay was used as a direct and reliable method to test if enhancing the level of ubiquitin would suppress polyQ toxicity [137]. As described in Chapter 3 (section 3.2), the SCA3tr transgenic *Drosophila* model which expresses a HA-tagged, truncated form of ataxin-3 protein was used in this study [117]. At 3 dpe, expression of the transgene encoding for the truncated ataxin-3 protein with unexpanded polyQ repeats of 27 glutamines (*HA-SCA3tr-Q27*) in the eyes by *gmr-GAL4* driver did not cause any degenerative phenotype (Figure 7.4A). Weak expression of the transgene encoding for the truncated ataxin-3 protein with expanded polyQ repeats of 78 glutamines (*HA-SCA3tr-Q78(w)*) induced mild depigmentation while strong expression of *HA-SCA3tr-Q78* transgene (*HA-SCA3tr-Q78(s)*) in another independent transgenic fly line led to extensive loss of pigmentation (Figure 7.4A). It was found that overexpression of *HA-Ub*^{WT} transgene did not modify the depigmentation phenotype induced by expression of *HA-SCA3tr-Q78(w)* or *HA-SCA3tr-Q78(s)* transgene (Figure 7.4B).

To test if *HA-Ub*^{WT} expression indeed modified *HA-SCA3tr-Q78*-induced degeneration but such modification was too mild to be observed through external eye depigmentation phenotype assay, deep pseudopupil assay was employed as a more sensitive method to examine the effect of *HA-Ub*^{WT} overexpression on

Figure 7.4

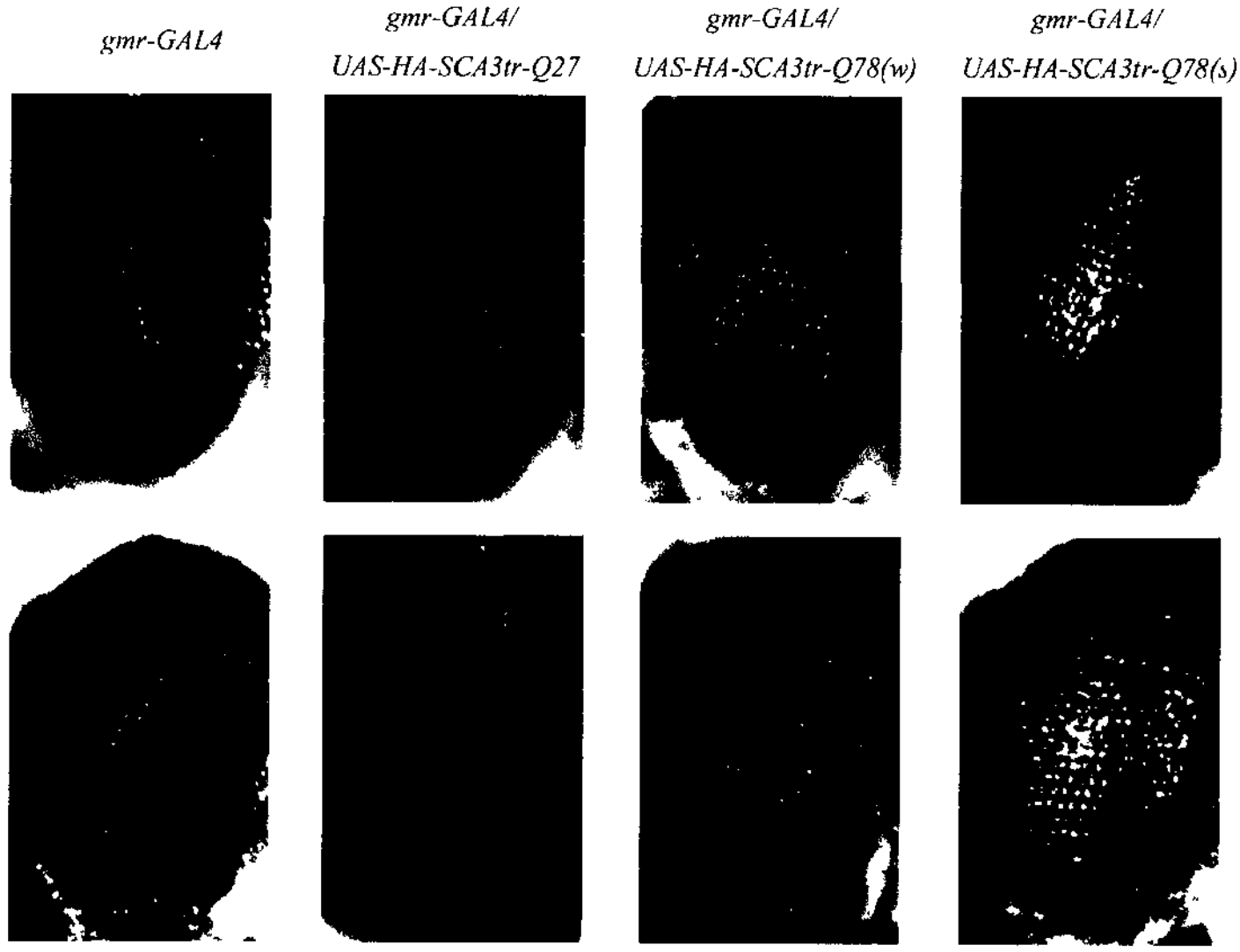
gmr-GAL4
gmr-GAL4/
UAS-HA-SCA3tr-Q27
gmr-GAL4/
UAS-HA-SCA3tr-Q78(w)
gmr-GAL4/
UAS-HA-SCA3tr-Q78(s)
A
B
UAS-HA-Ub^WT

Figure 7.4. Expression of *HA-Ub^{WT}* transgene did not modify external eye depigmentation phenotype resulted from expression of *HA-SCA3tr-Q78* transgene in adult flies.

Adult external eye depigmentation phenotypes of *gmr-GAL4* driver-only control flies and flies expressing *truncated ataxin-3* transgenes (*HA-SCA3tr-Q27* or *HA-SCA3tr-Q78)* with or without (indicated by "-") expression of *HA-Ub^{WT}* transgene are shown. Transgenes were expressed using the *gmr-GAL4* driver. (**A**) At 3 dpe, expression of *HA-SCA3tr-Q27* transgene did not cause any degenerative phenotype. Weak expression of *HA-SCA3tr-Q78* (*HA-SCA3tr-Q78(w)*) transgene induced mild depigmentation while strong expression of *HA-SCA3tr-Q78* (*HA-SCA3tr-Q78(s)*) transgene caused extensive loss of pigment. (**B**) Expression of *HA-Ub^{WT}* transgene did not modify degenerative phenotype induced by *HA-SCA3tr-Q78(w)* or *HA-SCA3tr-Q78(s)*. Consistent results were obtained from three independent experiments. The flies were raised at 25°C. They were of genotypes:

(**A**) *w*; *gmr-GAL4*/+; +/+,

w; *gmr-GAL4 UAS-HA-SCA3tr-Q27*/+; +/+,

w; *gmr-GAL4*/+; *UAS-HA-SCA3tr-Q78(w)*/+,

w; *gmr-GAL4 UAS-HA-SCA3tr-Q78(s)*/+; +/+

(**B**) *w*; *gmr-GAL4*/+; *UAS-HA-Ub^{WT}*/+,

w; *gmr-GAL4 UAS-HA-SCA3tr-Q27*/+; *UAS-HA-Ub^{WT}*/+,

w; *gmr-GAL4*/+; *UAS-HA-SCA3tr-Q78(w)/UAS-HA-Ub^{WT}*,

w; *gmr-GAL4 UAS-HA-SCA3tr-Q78(s)*/+; *UAS-HA-Ub^{WT}*/+.

HA-SCA3tr-Q78-induced retinal degeneration. In an inducible SCA3tr model [52], the *HA-SCA3tr-Q78* expression was delayed until adulthood by the use of the temperature-sensitive GAL80 ($GAL80^{ts}$) system [250]. Before the induction of *HA-SCA3tr-Q78* expression (i.e. at 0 day post-induction (0 dpi)), *HA-SCA3tr-Q78* transgenic flies displayed intact retinal structure and nearly 7 (an average of 6.9; Figure 7.5A) rhabdomeres per ommatidium could be observed. However, at 12 dpi, *HA-SCA3tr-Q78* expression led to retinal degeneration and reduced the rhabdomere score to around 4 (an average of 4.1; Figure 7.5B). Expression of $HA\text{-}Ub^{WT}$ transgene in *HA-SCA3tr-Q78*-expressing flies did not rescue the above retinal degeneration as indicated by the similar rhabdomere score calculated (an average of 4.2; Figure 7.15C). Combining with the above data, it is suggested that enhancing cellular level of ubiquitin shows no protective effect against polyQ toxicity.

7.5 Discussion

Efficient degradation of misfolded proteins by UPS is desirable to protein misfolded diseases including polyQ diseases and PD [59, 236, 237]. It was reported that sufficient level of free ubiquitin in cells helped against physiological stress mediated by misfolded proteins [251-253]. In the present study, the differential effects of ubiquitin in PD and polyQ diseases were examined.

The link between UPS and PD has been extensively reviewed [254-257]. In particular, several studies have reported that protein misfolding could initiate formation of Lewy bodies and caused DA degeneration [242, 243]. In the present study, it was found that increasing cellular level of ubiquitin suppressed

Figure 7.5

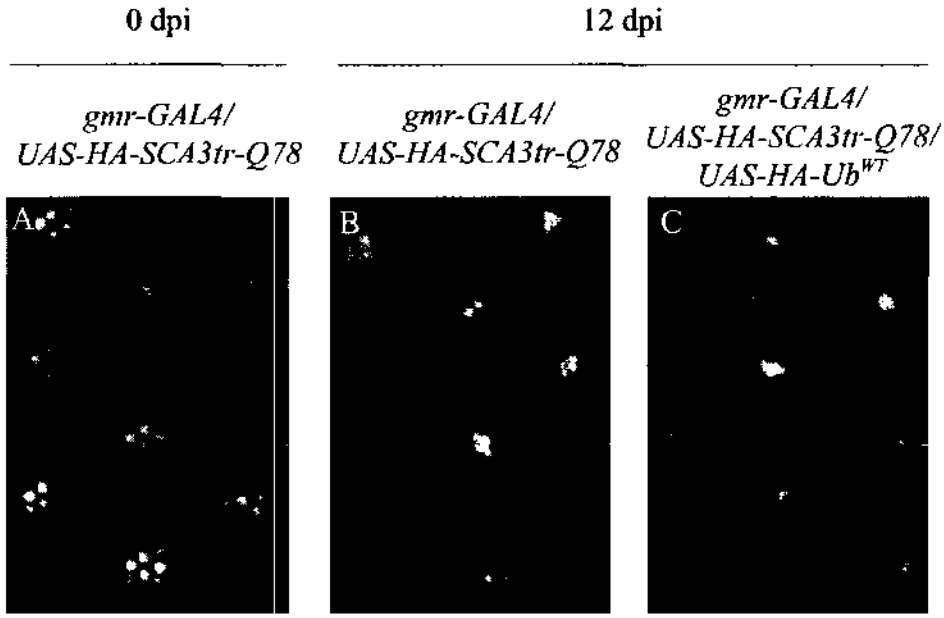
0 dpi
12 dpi
gmr-GAL4/
UAS-HA-SCA3tr-Q78
gmr-GAL4/
UAS-HA-SCA3tr-Q78
gmr-GAL4/
UAS-HA-SCA3tr-Q78/
UAS-HA-Ub^WT
A
B
C

D

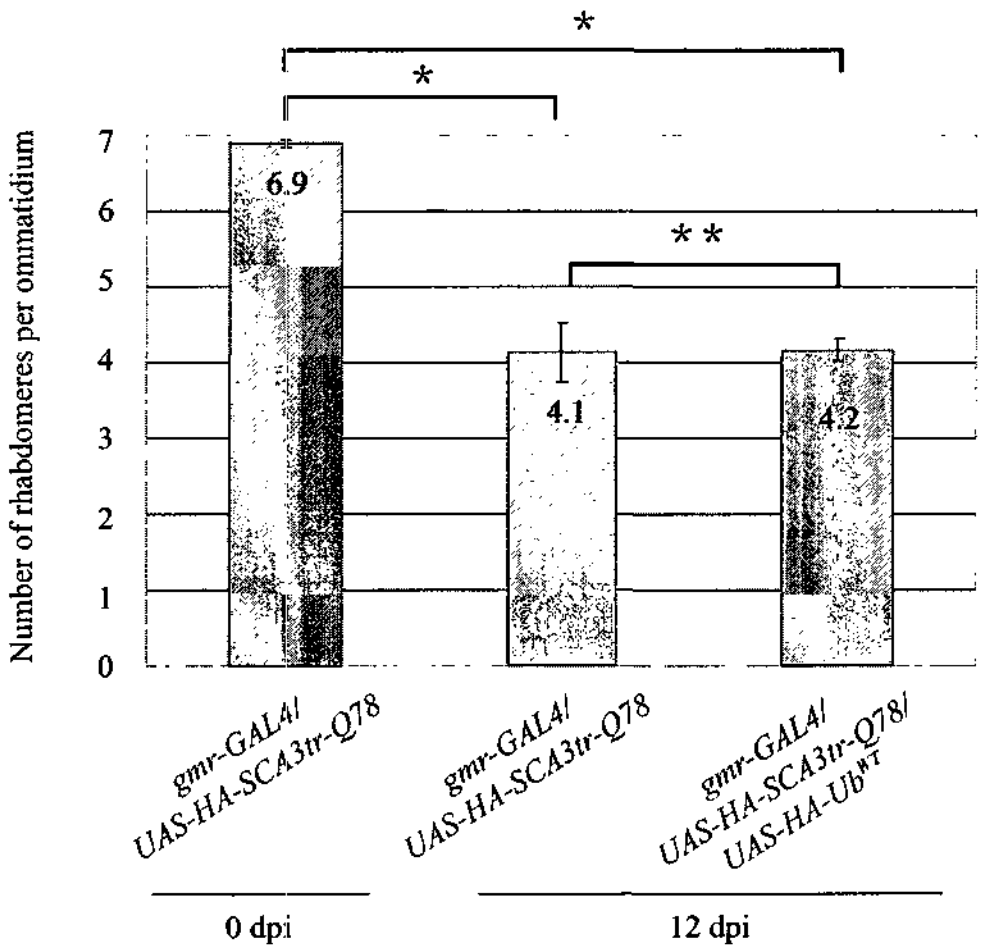
*
*
**
Number of rhabdomeres per ommatidium
7
6
5
4
3
2
1
0
6.9
4.1
4.2
gmr-GAL4/
UAS-HA-SCA3tr-Q78
gmr-GAL4/
UAS-HA-SCA3tr-Q78
gmr-GAL4/
UAS-HA-SCA3tr-Q78/
UAS-HA-Ub^WT
0 dpi
12 dpi

Figure 7.5. Expression of *HA-Ub^{WT}* transgene did not modify retinal degeneration resulted from induced expression of *HA-SCA3tr-Q78* transgene in adult flies.

(**A** - **C**) Deep pseudopupil images of *HA-SCA3tr-Q78*-expressing flies with or without expression of *HA-Ub^{WT}* transgene are shown. Transgenes were expressed using the *gmr-GAL4* driver. (**A**) At 0 dpi of *HA-SCA3tr-Q78* expression, on average 6.9 rhabdomeres per ommatidium were observed. (**B**) At 12 dpi, expression of *HA-SCA3tr-Q78* transgene reduced the rhabdomere score to an average of 4.1. (**C**) Co-expression with *HA-Ub^{WT}* transgene in these *HA-SCA3tr-Q78*-expressing flies did not modify the above degenerative phenotype as indicated by the similar rhabdomere score (an average of 4.2). (**D**) Quantification of (**A** - **C**). N = 31, * $p < 0.01$ while ** $p = 0.51$ (Mann-Whitney Rank Sum Test); error bars represent mean ± SEM from at least 31 flies collected from four independent experiments. At least 465 ommatidia were scored per group. The flies were raised at 25°C since 0 dpi. They were assayed at 0 and 12 dpi. They were of genotypes:

(**A** and **B**) *w*; *gmr-GAL4 UAS-HA-SCA3tr-Q78/+*; *tubP-GAL80^{ts}/+*,

(**C**) *w*; *gmr-GAL4 UAS-HA-SCA3tr-Q78/+*; *tubP-GAL80^{ts}/UAS-HA-Ub^{WT}*.

α-synuclein^{WT}-induced toxicity (Figure 7.2). This suppression required normal functioning of the proteasome (Figure 7.2C) and was not due to any modification on α-synuclein level [130]. Instead, in the collaboration mentioned above, Dr. K. K. K. Chung's group found that enhancing ubiquitin level indeed promoted degradation of general misfolded proteins [130]. These data suggest that although enhancing cellular level of ubiquitin could not reduce the level of toxic α-synuclein, it could facilitate degradation of misfolded proteins in general. The reduction in level of general misfolded proteins protects against *α-synuclein*^{WT}-induced toxicity, possibly through two mechanisms. Firstly, reduced level of misfolded proteins in cells disfavors the formation of toxic Lewy bodies [242, 243]. Secondly, reducing level of misfolded proteins lowers the physiological stress to neurons. As a result, it is likely that the neurons become less susceptible to *α-synuclein*^{WT}-induced toxicity.

Unlike PD, in the present study it was found that enhancing cellular level of ubiquitin did not modify polyQ toxicity (Figures 7.4 and 7.5). This suggests that merely enhancing degradation of general misfolded proteins is not enough to suppress polyQ toxicity.

In short, there are differential effects of ubiquitin on PD and polyQ diseases. This indicates that although PD and polyQ diseases are both protein misfolding diseases, there is fundamental difference in the basics of pathogenesis between these two diseases.

Chapter 8 General Discussion and Conclusion

It is now commonly accepted that expanded polyQ proteins are misfolded, insoluble and accumulate as toxic aggregates in cells [53, 233]. Over a decade, mechanisms to promote degradation of insoluble expanded polyQ proteins have been hot areas of research [53, 233]. Since the discovery on the involvement of E3 ubiquitin ligase E6-AP in polyQ protein aggregation [258], increasing number of E3 ubiquitin ligases have been reported to promote degradation of polyQ proteins and suppressed toxicity [77, 80, 169, 170, 259, 260]. These findings suggest redundancy of E3 ubiquitin ligases in degradation of expanded polyQ proteins [261]. The present study aims to study previously unidentified E3 ubiquitin ligases that are involved in polyQ pathogenesis. In particular, the present study targets at investigating the role of CRLs in polyQ diseases in two directions: **1)** the modifying effects of CRLs on polyQ toxicity and expanded polyQ protein solubility properties, and **2)** the interfering effect of expanded polyQ protein on CRL E3 ligase activities.

It is suggested that Cul1-based CRL is one E3 ubiquitin ligase that specifically modifies polyQ toxicity, but not α-synuclein toxicity. It modifies the SDS-solubility of expanded polyQ protein (Chapter 3). Data indicate that the polyQ specificity of Cul1-based CRL replies on the selective recognition of SDS-insoluble expanded polyQ protein by CG2010 substrate receptor (Chapter 4). Therefore, identifying human neuronal-specific F-box proteins with conserved substrate recognition domain as CG2010 is of great therapeutic interest against polyQ diseases.

Moreover, the study on the distinct effects of ubiquitin on polyQ diseases and α-synuclein toxicity indicates that enhancing degradation of general misfolded proteins does not help much in suppressing polyQ toxicity. This also highlights the importance of targeting degradation of expanded polyQ protein through specific E3 ubiquitin ligases.

On the other hand, it was found that expanded polyQ protein impaired the activity of Cul1-and Cul3-based CRLs. This result implies a novel mechanism by which expanded polyQ protein confers toxicity in neurons. Apart from understanding the substrate receptors that are involved in E3 ligase specificity, investigations on how expanded polyQ protein impairs CRLs activity may give further directions on the therapeutic approach against polyQ toxicity.

Taken together, the present study identifies Cul1-based CRL as a novel E3 ubiquitin ligase involved in polyQ pathogenesis and demonstrates a novel mechanism by which expanded polyQ protein confers toxicity. These findings allow better understanding of polyQ pathogenesis and provide a new direction for therapeutic development against polyQ diseases.

References

1. Palop, J.J., J. Chin, and L. Mucke, *A network dysfunction perspective on neurodegenerative diseases.* Nature, 2006. **443**(7113): p. 768-73.
2. Bredesen, D.E., R.V. Rao, and P. Mehlen, *Cell death in the nervous system.* Nature, 2006. **443**(7113): p. 796-802.
3. Wenk, G.L., *Neuropathologic changes in Alzheimer's disease.* J Clin Psychiatry, 2003. **64 Suppl 9**: p. 7-10.
4. Savica, R., W.A. Rocca, and J.E. Ahlskog, *When does Parkinson disease start?* Arch Neurol. **67**(7): p. 798-801.
5. Wijesekera, L.C. and P.N. Leigh, *Amyotrophic lateral sclerosis.* Orphanet J Rare Dis, 2009. **4**: p. 3.
6. Tatzelt, J. and H.M. Schatzl, *Molecular basis of cerebral neurodegeneration in prion diseases.* Febs J, 2007. **274**(3): p. 606-11.
7. La Spada, A.R. and J.P. Taylor, *Repeat expansion disease: progress and puzzles in disease pathogenesis.* Nat Rev Genet. **11**(4): p. 247-258.
8. Gao, H.M. and J.S. Hong, *Why neurodegenerative diseases are progressive: uncontrolled inflammation drives disease progression.* Trends Immunol, 2008. **29**(8): p. 357-65.
9. Fearnley, J.M. and A.J. Lees, *Ageing and Parkinson's disease: substantia nigra regional selectivity.* Brain, 1991. **114 (Pt 5)**: p. 2283-301.
10. Ross, C.A. and M.A. Poirier, *Protein aggregation and neurodegenerative disease.* Nat Med, 2004. **10 Suppl**: p. S10-7.
11. Rubinsztein, D.C., *The roles of intracellular protein-degradation pathways in neurodegeneration.* Nature, 2006. **443**(7113): p. 780-6.
12. DiMauro, S. and E.A. Schon, *Mitochondrial disorders in the nervous system.* Annu Rev Neurosci, 2008. **31**: p. 91-123.
13. De Vos, K.J., et al., *Role of axonal transport in neurodegenerative diseases.* Annu Rev Neurosci, 2008. **31**: p. 151-73.
14. Zoghbi, H.Y. and H.T. Orr, *Glutamine repeats and neurodegeneration.* Annu Rev Neurosci, 2000. **23**: p. 217-47.
15. Gatchel, J.R. and H.Y. Zoghbi, *Diseases of unstable repeat expansion: mechanisms and common principles.* Nat Rev Genet, 2005. **6**(10): p. 743-55.
16. Truant, R., et al., *Canadian Association of Neurosciences Review: polyglutamine expansion neurodegenerative diseases.* Can J Neurol Sci, 2006. **33**(3): p. 278-91.
17. Zoghbi, H. and H. Orr, *Glutamine repeats and neurodegeneration.* Annu Rev Neurosci, 2000. **23**: p. 217-247.
18. Michalik, A. and C. Van Broeckhoven, *Pathogenesis of polyglutamine disorders: aggregation revisited.* Hum Mol Genet, 2003. **12 Spec No 2**: p. R173-86.
19. Hands, S., C. Sinadinos, and A. Wyttenbach, *Polyglutamine gene function and dysfunction in the ageing brain.* Biochim Biophys Acta, 2008. **1779**(8): p. 507-21.
20. Reiner, A., et al., *Wild-type huntingtin plays a role in brain development and neuronal survival.* Mol Neurobiol, 2003. **28**: p. 259-276.

21. Cattaneo, E., *Dysfunction of wild-type huntingtin in Huntington disease.* News Physiol Sci, 2003. **18**: p. 34-37.
22. Cattaneo, E., et al., *Loss of normal huntingtin function: new developments in Huntington's disease research.* Trends Neurosci, 2001. **24**(3): p. 182-8.
23. Warrick, J.M., et al., *Suppression of polyglutamine-mediated neurodegeneration in Drosophila by the molecular chaperone HSP70.* Nat Genet, 1999. **23**(4): p. 425-8.
24. Chan, H.Y., et al., *Genetic modulation of polyglutamine toxicity by protein conjugation pathways in Drosophila.* Hum Mol Genet, 2002. **11**(23): p. 2895-904.
25. Lam, W., et al., *Human receptor for activated protein kinase C1 associates with polyglutamine aggregates and modulates polyglutamine toxicity.* Biochem Biophys Res Commun, 2008. **377**(2): p. 714-9.
26. Chan, W.M., P.C. Shaw, and H.Y.E. Chan, *The influence of protein nucleocytoplasmic transport on expanded polyglutamine-induced neurodegeneration.* FASEB J., 2008. **22**(1_MeetingAbstracts): p. 1013.6-.
27. Ordway, J.M., et al., *Ectopically expressed CAG repeats cause intranuclear inclusions and a progressive late onset neurological phenotype in the mouse.* Cell, 1997. **91**(6): p. 753-63.
28. Shao, J. and M. Diamond, *Polyglutamine diseases: emerging concepts in pathogenesis and therapy.* Human Molecular Genetics, 2007. **16**(Review Issue 2): p. R115-R123.
29. Huen, N.Y., S.L. Wong, and H.Y. Chan, *Transcriptional malfunctioning of heat shock protein gene expression in spinocerebellar ataxias.* Cerebellum, 2007. **6**(2): p. 111-7.
30. Brignull, H.R., J.F. Morley, and R.I. Morimoto, *The stress of misfolded proteins: C. elegans models for neurodegenerative disease and aging.* Adv Exp Med Biol, 2007. **594**: p. 167-89.
31. Duennwald, M.L., et al., *A network of protein interactions determines polyglutamine toxicity.* Proc Natl Acad Sci U S A, 2006. **103**(29): p. 11051-6.
32. Chai, Y., et al., *The role of protein composition in specifying nuclear inclusion formation in polyglutamine disease.* J Biol Chem, 2001. **276**(48): p. 44889-97.
33. Riley, B.E. and H.T. Orr, *Polyglutamine neurodegenerative diseases and regulation of transcription: assembling the puzzle.* Genes Dev, 2006. **20**(16): p. 2183-92.
34. Butler, R. and G.P. Bates, *Histone deacetylase inhibitors as therapeutics for polyglutamine disorders.* Nat Rev Neurosci, 2006. **7**(10): p. 784-96.
35. Lin, M.T. and M.F. Beal, *Mitochondrial dysfunction and oxidative stress in neurodegenerative diseases.* Nature, 2006. **443**(7113): p. 787-95.
36. Gunawardena, S., et al., *Disruption of axonal transport by loss of huntingtin or expression of pathogenic polyQ proteins in Drosophila.* Neuron, 2003. **40**(1): p. 25-40.
37. Matsuyama, Z., et al., *Polyglutamine repeats of spinocerebellar ataxia 6 impair the cell-death-preventing effect of CaV2.1 Ca2+ channel--loss-of-function cellular model of SCA6.* Neurobiol Dis, 2004. **17**(2): p. 198-204.
38. Takahashi, T., S. Katada, and O. Onodera, *Polyglutamine Diseases: Where*

Does Toxicity Come From? What Is Toxicity? Where Are We Going? J Mol Cell Biol: p. mjq005.

39. Qi, M.L., et al., *Proteome analysis of soluble nuclear proteins reveals that HMGB1/2 suppress genotoxic stress in polyglutamine diseases.* Nat Cell Biol, 2007. **9**(4): p. 402-14.
40. Li, L.B., et al., *RNA toxicity is a component of ataxin-3 degeneration in Drosophila.* Nature, 2008. **453**(7198): p. 1107-11.
41. Todd, P.K. and H.L. Paulson, *RNA-mediated neurodegeneration in repeat expansion disorders.* Ann Neurol. **67**(3): p. 291-300.
42. Li, L.B. and N.M. Bonini, *Roles of trinucleotide-repeat RNA in neurological disease and degeneration.* Trends Neurosci. **33**(6): p. 292-8.
43. Bates, G., *History of genetic disease: the molecular genetics of Huntington disease—a history.* Nat Rev Genet, 2005. **6**: p. 766-773.
44. Perutz, M.F., et al., *Glutamine repeats as polar zippers: their possible role in inherited neurodegenerative diseases.* Proc Natl Acad Sci U S A, 1994. **91**(12): p. 5355-8.
45. Michalik, A. and C. Broeckhoven, *Pathogenesis of polyglutamine disorders: aggregation revisited.* Human Molecular Genetics, 2003. **12**(Review Issue 2): p. R173-16.
46. Poirier, M.A., et al., *Huntingtin spheroids and protofibrils as precursors in polyglutamine fibrilization.* J Biol Chem, 2002. **277**(43): p. 41032-7.
47. Kim, S., et al., *Polyglutamine protein aggregates are dynamic.* Nat Cell Biol, 2002. **4**(10): p. 826-31.
48. Nagai, Y., et al., *A toxic monomeric conformer of the polyglutamine protein.* Nat Struct Mol Biol, 2007. **14**(4): p. 332-40.
49. Li, M., et al., *Soluble androgen receptor oligomers underlie pathology in a mouse model of spinobulbar muscular atrophy.* J Biol Chem, 2007. **282**(5): p. 3157-64.
50. Ehrnhoefer, D.E., et al., *Green tea (-)-epigallocatechin-gallate modulates early events in huntingtin misfolding and reduces toxicity in Huntington's disease models.* Hum Mol Genet, 2006. **15**(18): p. 2743-51.
51. Diaz-Hernandez, M., et al., *Biochemical, ultrastructural, and reversibility studies on huntingtin filaments isolated from mouse and human brain.* J Neurosci, 2004. **24**(42): p. 9361-71.
52. Wong, S.L., W.M. Chan, and H.Y. Chan, *Sodium dodecyl sulfate-insoluble oligomers are involved in polyglutamine degeneration.* Faseb J, 2008. **22**(9): p. 3348-57.
53. Williams, A.J. and H.L. Paulson, *Polyglutamine neurodegeneration: protein misfolding revisited.* Trends Neurosci, 2008. **31**(10): p. 521-8.
54. Meriin, A.B. and M.Y. Sherman, *Role of molecular chaperones in neurodegenerative disorders.* Int J Hyperthermia, 2005. **21**(5): p. 403-19.
55. Voisine, C., J.S. Pedersen, and R.I. Morimoto, *Chaperone networks: Tipping the balance in protein folding diseases.* Neurobiol Dis.
56. Jana, N.R., et al., *Polyglutamine length-dependent interaction of Hsp40 and Hsp70 family chaperones with truncated N-terminal huntingtin: their role in suppression of aggregation and cellular toxicity.* Hum Mol Genet, 2000. **9**(13): p. 2009-18.
57. Cummings, C.J., et al., *Chaperone suppression of aggregation and altered*

subcellular proteasome localization imply protein misfolding in SCA1. Nat Genet, 1998. **19**(2): p. 148-54.
58. Chai, Y., et al., *Analysis of the role of heat shock protein (Hsp) molecular chaperones in polyglutamine disease.* J Neurosci, 1999. **19**(23): p. 10338-47.
59. Ardley, H.C., C.C. Hung, and P.A. Robinson, *The aggravating role of the ubiquitin-proteasome system in neurodegeneration.* FEBS Lett, 2005. **579**(3): p. 571-6.
60. Cummings, C.J., et al., *Over-expression of inducible HSP70 chaperone suppresses neuropathology and improves motor function in SCA1 mice.* Hum Mol Genet, 2001. **10**(14): p. 1511-8.
61. Adachi, H., et al., *Heat shock protein 70 chaperone overexpression ameliorates phenotypes of the spinal and bulbar muscular atrophy transgenic mouse model by reducing nuclear-localized mutant androgen receptor protein.* J Neurosci, 2003. **23**(6): p. 2203-11.
62. Hershko, A. and A. Ciechanover, *The ubiquitin system.* Annu Rev Biochem, 1998. **67**: p. 425-479.
63. Glickman, M. and A. Ciechanover, *The ubiquitin-proteasome proteolytic pathway: destruction for the sake of construction.* Physiol Rev, 2002. **82**: p. 373-428.
64. Pickarta, C. and M. Eddins, *Ubiquitin: structures, functions, mechanisms.* Biochimica et Biophysica Acta, 2004. **1695**: p. 55-72.
65. Scheffner, M., U. Nuber, and J.M. Huibregtse, *Protein ubiquitination involving an E1-E2-E3 enzyme ubiquitin thioester cascade.* Nature, 1995. **373**(6509): p. 81-3.
66. Pickart, C. and D. Fushman, *Polyubiquitin chains: polymeric protein signals.* Current Opinion in Chemical Biology, 2004. **8**(6): p. 610-616.
67. Berke, S. and H. Paulsony, *Protein aggregation and the ubiquitin proteasome pathway: gaining the UPPer hand on neurodegeneration.* Current Opinion in Genetics & Development, 2003. **13**: p. 253-261.
68. Pickart, C. and D. Fushman, *Polyubiquitin chains: polymeric protein signals.* Current Opinion in Chemical Biology 2004. **8**(6): p. 610-616.
69. Dikshit, P. and N.R. Jana, *Role of Ubiquitin Protein Ligases in the Pathogenesis of Polyglutamine Diseases.* Neurochem Res, 2007.
70. Ballinger, C., et al., *Identification of CHIP, a novel tetratricopeptide repeat-containing protein that interacts with heat shock proteins and negatively regulates chaperone functions.* Mol Cell Biol 1999. **19**: p. 4535-4545.
71. Jiang, J., et al., *CHIP is a U-box-dependent E3 ubiquitin ligase: identification of Hsc70 as a target for ubiquitylation.* J Biol Chem, 2001. **276**: p. 42938-42944.
72. Connell, P., et al., *CHIP is a chaperone-dependent E3 ligase that ubiquitylates unfolded protein.* Nat Cell Biol 2001. **3**: p. 93-96.
73. McDonough, H. and C. Patterson, *CHIP: a link between the chaperone and proteasome systems.* Cell Stress Chaperones 2003. **8**: p. 303-308.
74. Al-Ramahi, I., et al., *CHIP protects from the neurotoxicity of expanded and wild-type ataxin-1 and promotes their ubiquitination and degradation.* J Biol Chem 2006. **281**: p. 26714-26724.
75. Miller, V., et al., *CHIP suppresses polyglutamine aggregation and toxicity in*

vitro and in vivo. J Neurosci 2005. **25**: p. 9152-9166.
76. Huibregtse, J.M., et al., *A family of proteins structurally and functionally related to the E6-AP ubiquitin-protein ligase.* Proc Natl Acad Sci U S A, 1995. **92**(7): p. 2563-7.
77. Mishra, A., et al., *E6-AP promotes misfolded polyglutamine proteins for proteasomal degradation and suppresses polyglutamine protein aggregation and toxicity.* J Biol Chem, 2008. **283**(12): p. 7648-56.
78. Cookson, M.R., *Neurodegeneration: how does parkin prevent Parkinson's disease?* Curr Biol, 2003. **13**(13): p. R522-4.
79. Imai, Y., M. Soda, and R. Takahashi, *Parkin suppresses unfolded protein stress-induced cell death through its E3 ubiquitin-protein ligase activity.* J Biol Chem, 2000. **275**(46): p. 35661-4.
80. Tsai, Y.C., et al., *Parkin facilitates the elimination of expanded polyglutamine proteins and leads to preservation of proteasome function.* J Biol Chem, 2003. **278**(24): p. 22044-55.
81. Petroski, M.D. and R.J. Deshaies, *Function and regulation of cullin-RING ubiquitin ligases.* Nat Rev Mol Cell Biol, 2005. **6**(1): p. 9-20.
82. Willems, A.R., M. Schwab, and M. Tyers, *A hitchhiker's guide to the cullin ubiquitin ligases: SCF and its kin.* Biochim Biophys Acta, 2004. **1695**(1-3): p. 133-70.
83. Bosu, D.R. and E.T. Kipreos, *Cullin-RING ubiquitin ligases: global regulation and activation cycles.* Cell Div, 2008. **3**: p. 7.
84. Merlet, J., et al., *Regulation of cullin-RING E3 ubiquitin-ligases by neddylation and dimerization.* Cell Mol Life Sci, 2009. **66**(11-12): p. 1924-38.
85. Kamitani, T., et al., *Characterization of NEDD8, a developmentally down-regulated ubiquitin-like protein.* J Biol Chem, 1997. **272**(45): p. 28557-62.
86. Wu, J.T., et al., *Neddylation and deneddylation regulate Cul1 and Cul3 protein accumulation.* Nat Cell Biol, 2005. 7(10): p. 1014-20.
87. Kipreos, E.T., *Ubiquitin-mediated pathways in C. elegans.* WormBook, 2005: p. 1-24.
88. Wu, J.T., Y.R. Chan, and C.T. Chien, *Protection of cullin-RING E3 ligases by CSN-UBP12.* Trends Cell Biol, 2006. **16**(7): p. 362-9.
89. Galan, J.M. and M. Peter, *Ubiquitin-dependent degradation of multiple F-box proteins by an autocatalytic mechanism.* Proc Natl Acad Sci U S A, 1999. **96**(16): p. 9124-9.
90. Zhou, P. and P.M. Howley, *Ubiquitination and degradation of the substrate recognition subunits of SCF ubiquitin-protein ligases.* Mol Cell, 1998. **2**(5): p. 571-80.
91. Cope, G.A. and R.J. Deshaies, *Targeted silencing of Jab1/Csn5 in human cells downregulates SCF activity through reduction of F-box protein levels.* BMC Biochem, 2006. **7**: p. 1.
92. Schwechheimer, C., *The COP9 signalosome (CSN): an evolutionary conserved proteolysis regulator in eukaryotic development.* Biochim Biophys Acta, 2004. **1695**(1-3): p. 45-54.
93. Marin, I., *Diversification of the cullin family.* BMC Evol Biol, 2009. **9**: p. 267.

94. Manfiolli, A.O., et al., *FBXO25-associated nuclear domains: a novel subnuclear structure.* Mol Biol Cell, 2008. **19**(5): p. 1848-61.
95. Mehta, R., et al., *Proteasomal regulation of the hypoxic response modulates aging in C. elegans.* Science, 2009. **324**(5931): p. 1196-8.
96. Kuazi, A., et al., *NEDD8 protein is involved in ubiquitinated inclusion bodies.* J Pathol, 2003. **199**: p. 259-266.
97. Mori, F., et al., *Accumulation of NEDD8 in neuronal and glial inclusions of neurodegenerative disorders.* Neuropathol Appl Neurobiol, 2005. **31**: p. 53-61.
98. Bence, N.F., E.J. Bennett, and R.R. Kopito, *Application and analysis of the GFPu family of ubiquitin-proteasome system reporters.* Methods Enzymol, 2005. **399**: p. 481-90.
99. Menendez-Benito, V., S. Heessen, and N.P. Dantuma, *Monitoring of ubiquitin-dependent proteolysis with green fluorescent protein substrates.* Methods Enzymol, 2005. **399**: p. 490-511.
100. Marsh, J.L., T. Lukacsovich, and L.M. Thompson, *Animal models of polyglutamine diseases and therapeutic approaches.* J Biol Chem, 2009. **284**(12): p. 7431-5.
101. van Ham, T.J., et al., *Neurodegenerative diseases: Lessons from genome-wide screens in small model organisms.* EMBO Mol Med, 2009. **1**(8-9): p. 360-70.
102. Bilen, J. and N.M. Bonini, *Drosophila as a model for human neurodegenerative disease.* Annu Rev Genet, 2005. **39**: p. 153-71.
103. Cauchi, R. and M. Heuvel, *The Fly as a Model for Neurodegenerative Diseases: Is It Worth the Jump?* Neurodegenerative Dis, 2006. **3**: p. 338-356.
104. Marsh, J.L. and L.M. Thompson, *Drosophila in the study of neurodegenerative disease.* Neuron, 2006. **52**(1): p. 169-78.
105. Sang, T.K. and G.R. Jackson, *Drosophila models of neurodegenerative disease.* NeuroRx, 2005. **2**(3): p. 438-46.
106. Shulman, J.M., et al., *From fruit fly to bedside: translating lessons from Drosophila models of neurodegenerative disease.* Curr Opin Neurol, 2003. **16**(4): p. 443-9.
107. Chan, H., Bonini, NM, *Drosophila models of polyglutamine diseases.* Neurogenetics: Methods and Protocols, 2003. **217**: p. 241-251.
108. Lu, B., *Recent advances in using Drosophila to model neurodegenerative diseases.* Apoptosis, 2009. **14**(8): p. 1008-20.
109. Ryder, E. and S. Russell, *Transposable elements as tools for genomics and genetics in Drosophila.* Brief Funct Genomic Proteomic, 2003. **2**(1): p. 57-71.
110. Venken, K.J. and H.J. Bellen, *Emerging technologies for gene manipulation in Drosophila melanogaster.* Nat Rev Genet, 2005. **6**(3): p. 167-78.
111. Rubin, G.M., et al., *Comparative genomics of the eukaryotes.* Science, 2000. **287**(5461): p. 2204-15.
112. Yoshihara, M., A.W. Ensminger, and J.T. Littleton, *Neurobiology and the Drosophila genome.* Funct Integr Genomics, 2001. **1**(4): p. 235-40.
113. Reiter, L.T., et al., *A systematic analysis of human disease-associated gene sequences in Drosophila melanogaster.* Genome Res, 2001. **11**(6): p. 1114-25.
114. Brand, A.H. and N. Perrimon, *Targeted gene expression as a means of altering cell fates and generating dominant phenotypes.* Development, 1993. **118**(2): p. 401-15.

115. McGuire, S.E., G. Roman, and R.L. Davis, *Gene expression systems in Drosophila: a synthesis of time and space.* Trends Genet, 2004. **20**(8): p. 384-91.
116. Phelps, C.B. and A.H. Brand, *Ectopic gene expression in Drosophila using GAL4 system.* Methods, 1998. **14**(4): p. 367-79.
117. Warrick, J.M., et al., *Expanded polyglutamine protein forms nuclear inclusions and causes neural degeneration in Drosophila.* Cell, 1998. **93**(6): p. 939-49.
118. Ellis, M.C., E.M. O'Neill, and G.M. Rubin, *Expression of Drosophila glass protein and evidence for negative regulation of its activity in non-neuronal cells by another DNA-binding protein.* Development, 1993. **119**(3): p. 855-65.
119. Jackson, G.R., et al., *Polyglutamine-expanded human huntingtin transgenes induce degeneration of Drosophila photoreceptor neurons.* Neuron, 1998. **21**(3): p. 633-42.
120. Charroux, B., et al., *Atrophin contributes to the negative regulation of epidermal growth factor receptor signaling in Drosophila.* Dev Biol, 2006. **291**(2): p. 278-90.
121. Takeyama, K., et al., *Androgen-dependent neurodegeneration by polyglutamine-expanded human androgen receptor in Drosophila.* Neuron, 2002. **35**(5): p. 855-64.
122. Fernandez-Funez, P., et al., *Identification of genes that modify ataxin-1-induced neurodegeneration.* Nature, 2000. **408**(6808): p. 101-6.
123. Satterfield, T.F. and L.J. Pallanck, *Ataxin-2 and its Drosophila homolog, ATX2, physically assemble with polyribosomes.* Hum Mol Genet, 2006. **15**(16): p. 2523-32.
124. Latouche, M., et al., *A conditional pan-neuronal Drosophila model of spinocerebellar ataxia 7 with a reversible adult phenotype suitable for identifying modifier genes.* J Neurosci, 2007. **27**(10): p. 2483-92.
125. Mutsuddi, M., et al., *The spinocerebellar ataxia 8 noncoding RNA causes neurodegeneration and associates with staufen in Drosophila.* Curr Biol, 2004. **14**(4): p. 302-8.
126. Young, M.W., *The tick-tock of the biological clock.* Sci Am, 2000. **282**(3): p. 64-71.
127. Wu, J.S. and L. Luo, *A protocol for dissecting Drosophila melanogaster brains for live imaging or immunostaining.* Nat Protoc, 2006. **1**(4): p. 2110-5.
128. Warrick, J., et al., *Expanded polyglutamine protein forms nuclear inclusions and causes neural degeneration in Drosophila.* Cell, 1998. **93**: p. 939-949.
129. Warrick, J.M., et al., *Ataxin-3 suppresses polyglutamine neurodegeneration in Drosophila by a ubiquitin-associated mechanism.* Mol Cell, 2005. **18**(1): p. 37-48.
130. Lee, F.K., et al., *The role of ubiquitin linkages on alpha-synuclein induced-toxicity in a Drosophila model of Parkinson's disease.* J Neurochem, 2009. **110**(1): p. 208-19.
131. Heriche, J.K., et al., *Involvement of an SCFSlmb complex in timely elimination of E2F upon initiation of DNA replication in Drosophila.* BMC Genet, 2003. **4**: p. 9.
132. Donaldson, T.D., et al., *Targeted disruption of Drosophila Roc1b reveals functional differences in the Roc subunit of Cullin-dependent E3 ubiquitin*

ligases. Mol Biol Cell, 2004. **15**(11): p. 4892-903.
133. Kaneko, M. and J.C. Hall, *Neuroanatomy of cells expressing clock genes in Drosophila: transgenic manipulation of the period and timeless genes to mark the perikarya of circadian pacemaker neurons and their projections.* J Comp Neurol, 2000. **422**(1): p. 66-94.
134. Dietzl, G., et al., *A genome-wide transgenic RNAi library for conditional gene inactivation in Drosophila.* Nature, 2007. **448**(7150): p. 151-6.
135. Chan, H.Y., et al., *Mechanisms of chaperone suppression of polyglutamine disease: selectivity, synergy and modulation of protein solubility in Drosophila.* Hum Mol Genet, 2000. **9**(19): p. 2811-20.
136. Duennwald, M.L., *Chaperones and Polyglutamine Expansion Disorders* 1st ed. Heat Shock Proteins, ed. I.R.B. Alexzander A.A. Asea. Vol. 3. 2008, MA, USA: Springer Netherlands. 3-23.
137. Chan, H.Y. and N.M. Bonini, *Drosophila models of polyglutamine diseases.* Methods Mol Biol, 2003. **217**: p. 241-51.
138. Spradling, A.C. and G.M. Rubin, *The effect of chromosomal position on the expression of the Drosophila xanthine dehydrogenase gene.* Cell, 1983. **34**(1): p. 47-57.
139. Merry, D.E., et al., *Cleavage, aggregation and toxicity of the expanded androgen receptor in spinal and bulbar muscular atrophy.* Hum Mol Genet, 1998. **7**(4): p. 693-701.
140. Bilen, J. and N.M. Bonini, *Genome-wide screen for modifiers of ataxin-3 neurodegeneration in Drosophila.* PLoS Genet, 2007. **3**(10): p. 1950-64.
141. Agrawal, N., et al., *Identification of combinatorial drug regimens for treatment of Huntington's disease using Drosophila.* Proc Natl Acad Sci U S A, 2005. **102**(10): p. 3777-81.
142. Wolfgang, W.J., et al., *Suppression of Huntington's disease pathology in Drosophila by human single-chain Fv antibodies.* Proc Natl Acad Sci U S A, 2005. **102**(32): p. 11563-8.
143. Boeddrich, A., et al., *An arginine/lysine-rich motif is crucial for VCP/p97-mediated modulation of ataxin-3 fibrillogenesis.* Embo J, 2006. **25**(7): p. 1547-58.
144. Slepko, N., et al., *Normal-repeat-length polyglutamine peptides accelerate aggregation nucleation and cytotoxicity of expanded polyglutamine proteins.* Proc Natl Acad Sci U S A, 2006. **103**(39): p. 14367-72.
145. Rosenbaum, E.E., R.C. Hardie, and N.J. Colley, *Calnexin is essential for rhodopsin maturation, Ca2+ regulation, and photoreceptor cell survival.* Neuron, 2006. **49**(2): p. 229-41.
146. Wanker, E.E., et al., *Membrane filter assay for detection of amyloid-like polyglutamine-containing protein aggregates.* Methods Enzymol, 1999. **309**: p. 375-86.
147. La Spada, A.R., et al., *Androgen receptor gene mutations in X-linked spinal and bulbar muscular atrophy.* Nature, 1991. **352**(6330): p. 77-9.
148. Polymeropoulos, M.H., et al., *Mutation in the alpha-synuclein gene identified in families with Parkinson's disease.* Science, 1997. **276**(5321): p. 2045-7.
149. Spillantini, M.G., et al., *Alpha-synuclein in Lewy bodies.* Nature, 1997. **388**(6645): p. 839-40.
150. Auluck, P.K., et al., *Chaperone suppression of alpha-synuclein toxicity in a*

Drosophila model for Parkinson's disease. Science, 2002. **295**(5556): p. 865-8.
151. Hazeki, N., et al., *Formic acid dissolves aggregates of an N-terminal huntingtin fragment containing an expanded polyglutamine tract: applying to quantification of protein components of the aggregates.* Biochem Biophys Res Commun, 2000. **277**(2): p. 386-93.
152. Sen, N., et al., *Nitric oxide-induced nuclear GAPDH activates p300/CBP and mediates apoptosis.* Nat Cell Biol, 2008. **10**(7): p. 866-73.
153. Banerjee, S., et al., *Modulation of SCF beta-TrCP-dependent I kappaB alpha ubiquitination by hydrogen peroxide.* J Biol Chem. **285**(4): p. 2665-75.
154. Lovly, C.M., et al., *Regulation of Chk2 ubiquitination and signaling through autophosphorylation of serine 379.* Mol Cell Biol, 2008. **28**(19): p. 5874-85.
155. Hiramatsu, Y., et al., *Degradation of Tob1 mediated by SCFSkp2-dependent ubiquitination.* Cancer Res, 2006. **66**(17): p. 8477-83.
156. Friedman, M.J., et al., *Polyglutamine domain modulates the TBP-TFIIB interaction: implications for its normal function and neurodegeneration.* Nat Neurosci, 2007. **10**(12): p. 1519-28.
157. Zheng, N., et al., *Structure of the Cul1-Rbx1-Skp1-F boxSkp2 SCF ubiquitin ligase complex.* Nature, 2002. **416**(6882): p. 703-9.
158. Wu, K., et al., *The SCF(HOS/beta-TRCP)-ROC1 E3 ubiquitin ligase utilizes two distinct domains within CUL1 for substrate targeting and ubiquitin ligation.* Mol Cell Biol, 2000. **20**(4): p. 1382-93.
159. Piva, R., et al., *In vivo interference with Skp1 function leads to genetic instability and neoplastic transformation.* Mol Cell Biol, 2002. **22**(23): p. 8375-87.
160. Pickart, C.M. and M.J. Eddins, *Ubiquitin: structures, functions, mechanisms.* Biochim Biophys Acta, 2004. **1695**(1-3): p. 55-72.
161. Kaganovich, D., R. Kopito, and J. Frydman, *Misfolded proteins partition between two distinct quality control compartments.* Nature, 2008. **454**(7208): p. 1088-95.
162. Mimnaugh, E.G., P. Bonvini, and L. Neckers, *The measurement of ubiquitin and ubiquitinated proteins.* Electrophoresis, 1999. **20**(2): p. 418-28.
163. Ohlmeyer, J.T. and T. Schupbach, *Encore facilitates SCF-Ubiquitin-proteasome-dependent proteolysis during Drosophila oogenesis.* Development, 2003. **130**(25): p. 6339-49.
164. Novoselova, T.V., et al., *Treatment with extracellular HSP70/HSC70 protein can reduce polyglutamine toxicity and aggregation.* J Neurochem, 2005. **94**(3): p. 597-606.
165. Kadener, S., et al., *Neurotoxic protein expression reveals connections between the circadian clock and mating behavior in Drosophila.* Proc Natl Acad Sci U S A, 2006. **103**(36): p. 13537-42.
166. Morton, A.J., et al., *Disintegration of the sleep-wake cycle and circadian timing in Huntington's disease.* J Neurosci, 2005. **25**(1): p. 157-63.
167. Higa, L.A. and H. Zhang, *Stealing the spotlight: CUL4-DDB1 ubiquitin ligase docks WD40-repeat proteins to destroy.* Cell Div, 2007. **2**: p. 5.
168. Shao, J. and M.I. Diamond, *Polyglutamine diseases: emerging concepts in pathogenesis and therapy.* Hum Mol Genet, 2007. **16 Spec No. 2**: p. R115-23.
169. Yang, H., et al., *Ubiquitin ligase Hrd1 enhances the degradation and*

suppresses the toxicity of polyglutamine-expanded huntingtin. Exp Cell Res, 2007. **313**(3): p. 538-50.
170. Ying, Z., et al., *Gp78, an ER associated E3, promotes SOD1 and ataxin-3 degradation.* Hum Mol Genet, 2009. **18**(22): p. 4268-81.
171. Adachi, H., et al., *CHIP overexpression reduces mutant androgen receptor protein and ameliorates phenotypes of the spinal and bulbar muscular atrophy transgenic mouse model.* J Neurosci, 2007. **27**: p. 5115-5126.
172. Ou, C.Y., H. Pi, and C.T. Chien, *Control of protein degradation by E3 ubiquitin ligases in Drosophila eye development.* Trends Genet, 2003. **19**(7): p. 382-9.
173. Ou, C.Y., et al., *Distinct protein degradation mechanisms mediated by Cul1 and Cul3 controlling Ci stability in Drosophila eye development.* Genes Dev, 2002. **16**(18): p. 2403-14.
174. Grima, B., et al., *The F-box protein slimb controls the levels of clock proteins period and timeless.* Nature, 2002. **420**(6912): p. 178-82.
175. Jin, J., et al., *Systematic analysis and nomenclature of mammalian F-box proteins.* Genes Dev, 2004. **18**(21): p. 2573-80.
176. Kipreos, E.T. and M. Pagano, *The F-box protein family.* Genome Biol, 2000. **1**(5): p. REVIEWS3002.
177. Skaar, J.R., J.K. Pagan, and M. Pagano, *SnapShot: F box proteins I.* Cell, 2009. **137**(6): p. 1160-1160 e1.
178. Skaar, J.R., et al., *SnapShot: F Box Proteins II.* Cell, 2009. **137**(7): p. 1358, 1358 e1.
179. Ho, M.S., et al., *The utility F-box for protein destruction.* Cell Mol Life Sci, 2008. **65**(13): p. 1977-2000.
180. Altschul, S.F., et al., *Gapped BLAST and PSI-BLAST: a new generation of protein database search programs.* Nucleic Acids Res, 1997. **25**(17): p. 3389-402.
181. Berger, Z., et al., *Lithium rescues toxicity of aggregate-prone proteins in Drosophila by perturbing Wnt pathway.* Hum Mol Genet, 2005. **14**(20): p. 3003-11.
182. Treier, M., D. Bohmann, and M. Mlodzik, *JUN cooperates with the ETS domain protein pointed to induce photoreceptor R7 fate in the Drosophila eye.* Cell, 1995. **83**(5): p. 753-60.
183. Whitworth, A.J., et al., *Rhomboid-7 and HtrA2/Omi act in a common pathway with the Parkinson's disease factors Pink1 and Parkin.* Dis Model Mech, 2008. **1**(2-3): p. 168-74; discussion 173.
184. Ho, M.S., P.I. Tsai, and C.T. Chien, *F-box proteins: the key to protein degradation.* J Biomed Sci, 2006. **13**(2): p. 181-91.
185. Okabe, H., et al., *A critical role for FBXW8 and MAPK in cyclin D1 degradation and cancer cell proliferation.* PLoS One, 2006. **1**: p. e128.
186. Zielke, N., et al., *Molecular dissection of the APC/C inhibitor Rca1 shows a novel F-box-dependent function.* EMBO Rep, 2006. **7**(12): p. 1266-72.
187. Yoshizawa, T., et al., *Cell cycle arrest enhances the in vitro cellular toxicity of the truncated Machado-Joseph disease gene product with an expanded polyglutamine stretch.* Hum Mol Genet, 2000. **9**(1): p. 69-78.
188. Hermand, D., *F-box proteins: more than baits for the SCF?* Cell Div, 2006. **1**: p. 30.

189. Grosskortenhaus, R. and F. Sprenger, *Rca1 inhibits APC-Cdh1(Fzr) and is required to prevent cyclin degradation in G2.* Dev Cell, 2002. **2**(1): p. 29-40.
190. Gough, J., et al., *Assignment of homology to genome sequences using a library of hidden Markov models that represent all proteins of known structure.* J Mol Biol, 2001. **313**(4): p. 903-19.
191. Wheeler, D.L., et al., *Database resources of the National Center for Biotechnology.* Nucleic Acids Res, 2003. **31**(1): p. 28-33.
192. Wu, C., et al., *BioGPS: an extensible and customizable portal for querying and organizing gene annotation resources.* Genome Biol, 2009. **10**(11): p. R130.
193. Reynolds, P.J., J.R. Simms, and R.J. Duronio, *Identifying determinants of cullin binding specificity among the three functionally different Drosophila melanogaster Roc proteins via domain swapping.* PLoS One, 2008. **3**(8): p. e2918.
194. Ohta, T., et al., *ROC1, a homolog of APC11, represents a family of cullin partners with an associated ubiquitin ligase activity.* Mol Cell, 1999. **3**(4): p. 535-41.
195. Bardwell, V.J. and R. Treisman, *The POZ domain: a conserved protein-protein interaction motif.* Genes Dev, 1994. **8**(14): p. 1664-77.
196. Nye, T.M., et al., *Statistical analysis of domains in interacting protein pairs.* Bioinformatics, 2005. **21**(7): p. 993-1001.
197. Schulman, B.A., et al., *Insights into SCF ubiquitin ligases from the structure of the Skp1-Skp2 complex.* Nature, 2000. **408**(6810): p. 381-6.
198. Murphy, T.D., *Drosophila skpA, a component of SCF ubiquitin ligases, regulates centrosome duplication independently of cyclin E accumulation.* J Cell Sci, 2003. **116**(Pt 11): p. 2321-32.
199. Bocca, S.N., et al., *Occurrence of a putative SCF ubiquitin ligase complex in Drosophila.* Biochem Biophys Res Commun, 2001. **286**(2): p. 357-64.
200. Raj, L., et al., *Targeted localized degradation of Paired protein in Drosophila development.* Curr Biol, 2000. **10**(20): p. 1265-72.
201. Mori, F., et al., *Accumulation of NEDD8 in neuronal and glial inclusions of neurodegenerative disorders.* Neuropathol Appl Neurobiol, 2005. **31**(1): p. 53-61.
202. Ferro, A., et al., *NEDD8: a new ataxin-3 interactor.* Biochim Biophys Acta, 2007. **1773**(11): p. 1619-27.
203. Varshavsky, A., *The N-end rule: functions, mysteries, uses.* Proc Natl Acad Sci U S A, 1996. **93**(22): p. 12142-9.
204. Sen, N., A. Sen, and E.R. Mackow, *Degrons at the C terminus of the pathogenic but not the nonpathogenic hantavirus G1 tail direct proteasomal degradation.* J Virol, 2007. **81**(8): p. 4323-30.
205. Pickart, C.M., *Back to the future with ubiquitin.* Cell, 2004. **116**(2): p. 181-90.
206. Hart, M., et al., *The F-box protein beta-TrCP associates with phosphorylated beta-catenin and regulates its activity in the cell.* Curr Biol, 1999. **9**(4): p. 207-10.
207. Sadot, E., et al., *Regulation of S33/S37 phosphorylated beta-catenin in normal and transformed cells.* J Cell Sci, 2002. **115**(Pt 13): p. 2771-80.
208. Zhang, D.D., et al., *Keap1 is a redox-regulated substrate adaptor protein for a Cul3-dependent ubiquitin ligase complex.* Mol Cell Biol, 2004. **24**(24): p.

10941-53.
209. Itoh, K., et al., *Keap1 represses nuclear activation of antioxidant responsive elements by Nrf2 through binding to the amino-terminal Neh2 domain.* Genes Dev, 1999. **13**(1): p. 76-86.
210. McMahon, M., et al., *Redox-regulated turnover of Nrf2 is determined by at least two separate protein domains, the redox-sensitive Neh2 degron and the redox-insensitive Neh6 degron.* J Biol Chem, 2004. **279**(30): p. 31556-67.
211. Wertz, I.E., et al., *Human De-etiolated-1 regulates c-Jun by assembling a CUL4A ubiquitin ligase.* Science, 2004. **303**(5662): p. 1371-4.
212. Pan, Z.Q., et al., *Nedd8 on cullin: building an expressway to protein destruction.* Oncogene, 2004. **23**(11): p. 1985-97.
213. Benmaamar, R. and M. Pagano, *Involvement of the SCF complex in the control of Cdh1 degradation in S-phase.* Cell Cycle, 2005. **4**(9): p. 1230-2.
214. Bondar, T., et al., *Cul4A and DDB1 associate with Skp2 to target p27Kip1 for proteolysis involving the COP9 signalosome.* Mol Cell Biol, 2006. **26**(7): p. 2531-9.
215. Liakopoulos, D., et al., *A novel protein modification pathway related to the ubiquitin system.* Embo J, 1998. **17**(8): p. 2208-14.
216. Gong, L. and E.T. Yeh, *Identification of the activating and conjugating enzymes of the NEDD8 conjugation pathway.* J Biol Chem, 1999. **274**(17): p. 12036-42.
217. Kurz, T., et al., *The conserved protein DCN-1/Dcn1p is required for cullin neddylation in C. elegans and S. cerevisiae.* Nature, 2005. **435**(7046): p. 1257-61.
218. Kurz, T., et al., *Dcn1 functions as a scaffold-type E3 ligase for cullin neddylation.* Mol Cell, 2008. **29**(1): p. 23-35.
219. Kamura, T., et al., *The Rbx1 subunit of SCF and VHL E3 ubiquitin ligase activates Rub1 modification of cullins Cdc53 and Cul2.* Genes Dev, 1999. **13**(22): p. 2928-33.
220. Furukawa, M., et al., *The CUL1 C-terminal sequence and ROC1 are required for efficient nuclear accumulation, NEDD8 modification, and ubiquitin ligase activity of CUL1.* Mol Cell Biol, 2000. **20**(21): p. 8185-97.
221. Sakata, E., et al., *Direct interactions between NEDD8 and ubiquitin E2 conjugating enzymes upregulate cullin-based E3 ligase activity.* Nat Struct Mol Biol, 2007. **14**(2): p. 167-8.
222. Kawakami, T., et al., *NEDD8 recruits E2-ubiquitin to SCF E3 ligase.* Embo J, 2001. **20**(15): p. 4003-12.
223. Podust, V.N., et al., *A Nedd8 conjugation pathway is essential for proteolytic targeting of p27Kip1 by ubiquitination.* Proc Natl Acad Sci U S A, 2000. **97**(9): p. 4579-84.
224. Read, M.A., et al., *Nedd8 modification of cul-1 activates SCF(beta(TrCP))-dependent ubiquitination of IkappaBalpha.* Mol Cell Biol, 2000. **20**(7): p. 2326-33.
225. Morimoto, M., et al., *Modification of cullin-1 by ubiquitin-like protein Nedd8 enhances the activity of SCF(skp2) toward p27(kip1).* Biochem Biophys Res Commun, 2000. **270**(3): p. 1093-6.
226. Wu, K., A. Chen, and Z.Q. Pan, *Conjugation of Nedd8 to CUL1 enhances the ability of the ROC1-CUL1 complex to promote ubiquitin polymerization.* J

Biol Chem, 2000. **275**(41): p. 32317-24.
227. Osaka, F., et al., *Covalent modifier NEDD8 is essential for SCF ubiquitin-ligase in fission yeast.* Embo J, 2000. **19**(13): p. 3475-84.
228. Ohh, M., et al., *An intact NEDD8 pathway is required for Cullin-dependent ubiquitylation in mammalian cells.* EMBO Rep, 2002. **3**(2): p. 177-82.
229. Pintard, L., et al., *Neddylation and deneddylation of CUL-3 is required to target MEI-1/Katanin for degradation at the meiosis-to-mitosis transition in C. elegans.* Curr Biol, 2003. **13**(11): p. 911-21.
230. Jia, S., R. Kobayashi, and S.I. Grewal, *Ubiquitin ligase component Cul4 associates with Clr4 histone methyltransferase to assemble heterochromatin.* Nat Cell Biol, 2005. **7**(10): p. 1007-13.
231. Godin, J.D., et al., *Mutant huntingtin-impaired degradation of beta-catenin causes neurotoxicity in Huntington's disease.* Embo J: p. emboj.2010.117.
232. Nakamura, T. and S.A. Lipton, *Cell death: protein misfolding and neurodegenerative diseases.* Apoptosis, 2009. **14**(4): p. 455-68.
233. Saunders, H.M. and S.P. Bottomley, *Multi-domain misfolding: understanding the aggregation pathway of polyglutamine proteins.* Protein Eng Des Sel, 2009. **22**(8): p. 447-51.
234. Winklhofer, K.F., J. Tatzelt, and C. Haass, *The two faces of protein misfolding: gain- and loss-of-function in neurodegenerative diseases.* Embo J, 2008. **27**(2): p. 336-49.
235. Gundersen, V., *Protein aggregation in Parkinson's disease.* Acta Neurologica Scandinavica. **122**(s190): p. 82-87.
236. Tai, H.C. and E.M. Schuman, *Ubiquitin, the proteasome and protein degradation in neuronal function and dysfunction.* Nat Rev Neurosci, 2008. **9**(11): p. 826-38.
237. Schwartz, A.L. and A. Ciechanover, *Targeting proteins for destruction by the ubiquitin system: implications for human pathobiology.* Annu Rev Pharmacol Toxicol, 2009. **49**: p. 73-96.
238. Kerscher, O., R. Felberbaum, and M. Hochstrasser, *Modification of proteins by ubiquitin and ubiquitin-like proteins.* Annu Rev Cell Dev Biol, 2006. **22**: p. 159-80.
239. Nandi, D., et al., *The ubiquitin-proteasome system.* J Biosci, 2006. **31**(1): p. 137-55.
240. DiFiglia, M., et al., *Aggregation of huntingtin in neuronal intranuclear inclusions and dystrophic neurites in brain.* Science, 1997. **277**(5334): p. 1990-3.
241. Layfield, R., J.R. Cavey, and J. Lowe, *Role of ubiquitin-mediated proteolysis in the pathogenesis of neurodegenerative disorders.* Ageing Res Rev, 2003. **2**(4): p. 343-56.
242. Savitt, J.M., V.L. Dawson, and T.M. Dawson, *Diagnosis and treatment of Parkinson disease: molecules to medicine.* J Clin Invest, 2006. **116**(7): p. 1744-54.
243. Thomas, B. and M.F. Beal, *Parkinson's disease.* Hum Mol Genet, 2007. **16 Spec No. 2**: p. R183-94.
244. Maries, E., et al., *The role of alpha-synuclein in Parkinson's disease: insights from animal models.* Nat Rev Neurosci, 2003. **4**(9): p. 727-38.
245. Feany, M.B. and W.W. Bender, *A Drosophila model of Parkinson's disease.*

Nature, 2000. **404**(6776): p. 394-8.
246. Belote, J.M. and E. Fortier, *Targeted expression of dominant negative proteasome mutants in Drosophila melanogaster.* Genesis, 2002. **34**(1-2): p. 80-2.
247. Huang, Y., R.T. Baker, and J.A. Fischer-Vize, *Control of cell fate by a deubiquitinating enzyme encoded by the fat facets gene.* Science, 1995. **270**(5243): p. 1828-31.
248. Schweisguth, F., *Dominant-negative mutation in the beta2 and beta6 proteasome subunit genes affect alternative cell fate decisions in the Drosophila sense organ lineage.* Proc Natl Acad Sci U S A, 1999. **96**(20): p. 11382-6.
249. Covi, J.A., J.M. Belote, and D.L. Mykles, *Subunit compositions and catalytic properties of proteasomes from developmental temperature- sensitive mutants of Drosophila melanogaster.* Arch Biochem Biophys, 1999. **368**(1): p. 85-97.
250. McGuire, S.E., Z. Mao, and R.L. Davis, *Spatiotemporal gene expression targeting with the TARGET and gene-switch systems in Drosophila.* Sci STKE, 2004. **2004**(220): p. pl6.
251. Hanna, J., D.S. Leggett, and D. Finley, *Ubiquitin depletion as a key mediator of toxicity by translational inhibitors.* Mol Cell Biol, 2003. **23**(24): p. 9251-61.
252. Osaka, H., et al., *Ubiquitin carboxy-terminal hydrolase L1 binds to and stabilizes monoubiquitin in neuron.* Hum Mol Genet, 2003. **12**(16): p. 1945-58.
253. Anderson, C., et al., *Loss of Usp14 results in reduced levels of ubiquitin in ataxia mice.* J Neurochem, 2005. **95**(3): p. 724-31.
254. Olanow, C.W. and K.S. McNaught, *Ubiquitin-proteasome system and Parkinson's disease.* Mov Disord, 2006. **21**(11): p. 1806-23.
255. Betarbet, R., T.B. Sherer, and J.T. Greenamyre, *Ubiquitin-proteasome system and Parkinson's diseases.* Exp Neurol, 2005. **191 Suppl 1**: p. S17-27.
256. Lim, K.L. and J.M. Tan, *Role of the ubiquitin proteasome system in Parkinson's disease.* BMC Biochem, 2007. **8 Suppl 1**: p. S13.
257. Cook, C. and L. Petrucelli, *A critical evaluation of the ubiquitin-proteasome system in Parkinson's disease.* Biochim Biophys Acta, 2009. **1792**(7): p. 664-75.
258. Cummings, C.J., et al., *Mutation of the E6-AP ubiquitin ligase reduces nuclear inclusion frequency while accelerating polyglutamine-induced pathology in SCA1 mice.* Neuron, 1999. **24**(4): p. 879-92.
259. Miller, V.M., et al., *CHIP suppresses polyglutamine aggregation and toxicity in vitro and in vivo.* J Neurosci, 2005. **25**(40): p. 9152-61.
260. Matsumoto, M., et al., *Molecular clearance of ataxin-3 is regulated by a mammalian E4.* Embo J, 2004. **23**(3): p. 659-69.
261. Morishima, Y., et al., *CHIP deletion reveals functional redundancy of E3 ligases in promoting degradation of both signaling proteins and expanded glutamine proteins.* Hum Mol Genet, 2008. **17**(24): p. 3942-52.